

University of Nevada, Reno

**GEOCHEMISTRY OF NATURALLY
OCCURRING ARSENIC IN THE HUMBOLDT
RIVER BASIN, NEVADA**

A dissertation submitted in partial fulfillment of the
requirement for the degree of Doctor of Philosophy in
Hydrogeology

by

Shahnewaz Mohammad

Dr. Regina N. Tempel/Dissertation Advisor

December, 2013

Copyright by Shahnewaz Mohammad 2013

All Rights Reserved



University of Nevada, Reno
Statewide • Worldwide

THE GRADUATE SCHOOL

We recommend that the dissertation
prepared under our supervision by

SHAHNEWAZ MOHAMMAD

entitled

**Geochemistry Of Naturally Occurring Arsenic In The Humboldt
River Basin, Nevada**

be accepted in partial fulfillment of the
requirements for the degree of

DOCTOR OF PHILOSOPHY

Regina N. Tempel, Ph.D., Advisor

Clay A. Cooper, Ph.D., Committee Member

David E. Prudic, Ph.D., Committee Member

Scott W. Tyler, Ph.D., Committee Member

Paul J. Lechler, Ph.D., Graduate School Representative

Marsha H. Read, Ph. D., Dean, Graduate School

December, 2013

Abstract

The geochemistry of naturally occurring arsenic (As) has been investigated in the surface waters and ground waters of the shallow alluvial aquifers of the Humboldt River Basin (HRB) in northern Nevada using laboratory experiments, geochemical reaction path modeling, and statistical analysis methods. A total of 15 surface water samples and 19 sediment samples were obtained from the Humboldt River and river-bottom sediments in the field in September, 2007. The ground water data from 72 wells, selected from a total of 47,500 samples from 18,800 springs and wells, in the HRB and northern Nevada were obtained from a public domain database provided by the Nevada Bureau of Mines and Geology. Concentrations of dissolved As in the waters of the Humboldt River (HR) range from 0.012 to 0.066 mg/L, with an average of 0.032 mg/L. The concentrations of As in shallow alluvial ground waters range up to 0.55 mg/L with an average of 0.06 mg/L. The current Environmental Protection Agency (EPA) maximum contaminant level (MCL) of As is 0.01 mg/L. The study of the distribution, sources, and processes controlling As in the Quaternary alluvial aquifers of the HRB and northern Nevada has found that the distribution of high As concentrations can be correlated with local and regional geology and geomorphology. The highest concentrations of As in the ground waters occur in the mineralized zones of metallic-sulfides around Boulder Valley, followed by the Quaternary playa deposits around Lovelock Valley and the Humboldt Sink, where evaporation predominates. Bivariate correlations and factor analyses of the dissolved components in the ground water suggest that the sources of dissolved As are likely from dissolution of As-bearing sulfides, iron-oxyhydroxides, weathering of ferromagnesian silicates, and mixing with geothermal waters, where oxidation of As-bearing sulfides is a

local source of As in the Boulder valley area. The statistical and geochemical analyses of the HR bed sediments suggest that oxidation of As-bearing sulfide minerals is the source for high dissolved As in the upstream area. Concentrations of dissolved As and other trace elements are affected by mixing with ground water inflows occurring as river base flows in the upper HR and middle HR areas. Mixing with high-As geothermal waters locally enriches As near known areas of geothermal hot springs. Evaporation further enriches As in lower reaches of the river. Sequential extraction analyses of the river sediments demonstrate that As is mostly (83%) bound to the residual fraction which contains silicate minerals, and a lesser amount of As (13%) is held by Fe-oxy-hydroxides. The results of geochemical reaction path modeling indicate that oxidation of As-bearing sulfide minerals plays the most important role for source of As and sulfate in the upstream region with approximately 3.75 mmoles (449 ppm) of pyrite and 6.88×10^{-4} mmoles (0.11 ppm) of arsenopyrite oxidized per liter of river water. The acidity produced by the oxidation of sulfide minerals is buffered by carbonate equilibria as a result of dissolution of Pre-Cenozoic carbonate rocks in the country rocks of the upstream region. Modeling results demonstrate that the source of As from oxidation of sulfide minerals is less significant in the downstream, where mixing with shallow ground water inflows and local geothermal spring water control the enrichment of dissolved As. The effects of evapotranspiration further control the dissolved As concentrations in the lower HR waters. The process of sorption-desorption, which is pH-dependent, is less significant in the HR unlike many other similar semi-arid environments, and needs further evaluation.

For my family, whose love, support,
and patience helped to make this possible.

Acknowledgements

This research was partially supported by the funding from Student Research Grants from Geological Society of America, Sigma Xi, and University of Nevada, Reno (UNR)-International Grant. Support was also provided by the University of Nevada, Reno through teaching and research assistantships from the graduate program of Hydrologic Sciences and Department of Geological Sciences and Engineering.

First and foremost, I would like to express my special thanks to my advisor, Dr. Regina N. Tempel, for providing me support, advice, valuable inputs in conducting this research project and writing dissertation manuscripts. I would also like to convey my heartfelt thanks to my committee members, Dr. Clay Cooper, Dr. Paul Lechler, Dr. Dave Prudic, Dr. Scott Tyler, and Dr. Alan Wallace for their valuable suggestions and guidance in writing this dissertation.

Thanks to Dr. Simon Poulson and Chris Sladek for isotope analysis of water samples in the Stable Isotope Laboratory at the Mackay School of Earth Sciences and Engineering at UNR. Special thanks to Mario Desilets, and Dr. Paul Lechler for XRD and sequential extraction analysis at the Geochemistry Laboratory in the Nevada Bureau of Mines and Geology. Thanks to Dr. Mo Ahmadian for SEM analysis of the sediment samples at the Chemical and Materials and Engineering Department at UNR.

Thanks to Francisco Suarez, Reda Ibrahim, and Mark Hausner for their support throughout my time at the University of Nevada. Field assistance from Francisco Suarez was invaluable in collecting data.

Finally, I would like to thank my family for their patience and encouragement.

Table of Contents

1: Chapter 1: Introduction	1
2: Chapter 2: Previous Work and Background	4
2.1: Regional occurrences of arsenic	4
2.2: Study area	5
2.2.1: Geologic setting	8
2.2.2: Hydrogeologic setting	10
2.2.3: Ore deposits, mining and geothermal activities	13
2.3: Source and occurrence of arsenic	16
2.4: Aqueous geochemistry of arsenic	18
3: Chapter 3: Study goals, materials and methods	21
3.1: Study goals and components	22
3.2: Materials and methods	22
4: Chapter 4: Occurrence of arsenic in ground waters in the Humboldt River Basin, North-Central Nevada	23
4.1: Introduction	24
4.2: Study area and background	26
4.2.1: Geologic and hydrogeologic framework	26
4.3: Methods	28
4.3.1: Ground water data collection and compilation	28
4.3.2: Analytical methods of the samples in database	29
4.3.3: Data analysis	29
4.3.4: Factor analysis	40
4.4: Results	42
4.4.1: Spatial distribution of arsenic	42
4.4.2: Chemical composition of water samples	44
4.4.3: Relationship of arsenic and chemical parameters	48
4.4.4: Factor analyses results	50

4.5: Discussion	57
4.5.1: Relationship of arsenic and geochemical parameters	57
4.5.2: Conceptual release mechanism of arsenic	60
4.6: Conclusions and future studies	62
5: Chapter 5: Statistical and geochemical analyses of arsenic distribution in the waters and sediments of the Humboldt River System, North-Central Nevada	64
5.1: Introduction	65
5.2: Study area	67
5.2.1: Humboldt River System	67
5.2.2: Ground water movement and interaction	72
5.2.3: Morphology and geologic setting	75
5.2.4: ore deposits, mining and geothermal activities	78
5.3: Methods	79
5.3.1: Water analyses	80
5.3.2: Analytical methods for river sediments	82
5.3.3: Data analyses	84
5.4: Results	85
5.4.1: Chemistry of water	85
5.4.2: Mineralogy and chemistry of river-bed sediments	89
5.4.3: Relationship of arsenic with chemical parameters	98
5.5: Discussion	106
5.5.1: Arsenic in river sediments	106
5.5.2: Arsenic in river waters	107
5.5.3: Processes in the Upper Humboldt River	110
5.5.4: Processes in the Lower Humboldt River	116
5.5.5: Conceptual model	122
5.6: Conclusions	123

6: Chapter 6: Geochemical modeling of processes controlling arsenic enrichment in the waters of the Humboldt River, Northern Nevada	125
6.1: Introduction	126
6.2: Background	128
6.2.1: Study area	128
6.2.2: Geology and mineralogy	128
6.2.3: Hydrology of the Humboldt River Basin	133
6.2.4: Hydrogeochemistry of the Humboldt River	135
6.3: Modeling methods	135
6.3.1: Conceptual model	137
6.3.2: Thermodynamic modeling calculations	151
6.3.3: Model constraints	152
6.3.4: Modeling assumptions	158
6.4: Modeling Results	161
6.4.1: Speciation and mineral saturation calculations	161
6.4.2: Sensitivity analysis	162
6.5: Modeling discussion	169
6.5.1: Pathway 1	169
6.5.2: Pathway 2	174
6.5.3: Pathway 3	176
6.5.4: Pathway 4	177
6.5.5: Pathway 5	178
6.5.6: Pathway 6	181
6.6: Conclusions	182
7: Chapter 7: Conclusions and Recommendations	184
7.1: Summary of results	184
7.2: Recommendations for future studies	185
7.3: Global Significance	187
8: References	188

List of Tables

Table 2.1:	Generalized summary of hydrogeologic units at HRB, northern Nevada.	11
Table 2.2:	Types of mineral deposits in the Humboldt River Basin	15
Table 2.3:	Major arsenic minerals occurring in nature	17
Table 4.1:	Summarized physical and important chemical components of ground water samples included in this study.	32
Table 4.2:	Descriptive statistics of physical parameters of the ground water data used in this study.	36
Table 4.3:	Spearman's rho correlation coefficients for dissolved As and chemical parameters of the ground waters used in this study.	49
Table 4.4:	Factor analyses results of total elemental concentrations of the ground water data for group-I.	51
Table 4.5:	Factor analyses results of total elemental concentrations of the ground water data for group-II.	53
Table 4.6:	Factor analyses results of total elemental concentrations of the ground water data for group-III.	56
Table 5.1:	Average daily discharge of the Humboldt River during September, 2007 recorded at various stream gages.	70
Table 5.2:	Generalized summary of hydrologic sub-units of the Humboldt River Basin with schematic geologic settings in northern Nevada	77
Table 5.3:	Summarized physical parameters and some important chemical components of waters from the Humboldt River.	81
Table 5.4:	Concentrations (mg/kg) of As, and other elements in the river-bed sediment samples in different fractions obtained from sequential extraction analyses.	93
Table 5.5:	A) Factor analyses results of total elemental concentrations of the upper Humboldt River-bed sediments (samples from 001 to 003) that were digested in aqua-regia.	99

Table 5.5:	B) Factor analyses results of total elemental concentrations of the lower Humboldt River-bed sediments (samples from 007 to 019) that were digested in aqua-regia.	100
Table 5.6:	A) Factor analyses results of total elemental concentrations of the upper Humboldt River-waters (samples from 001 to 004) that were digested in aqua-regia.	102
Table 5.6:	B) Factor analyses results of total elemental concentrations of lower Humboldt River-waters (samples from 007 to 019) that were digested in aqua-regia.	103
Table 5.7:	Water quality data from Golconda hot spring system.	104
Table 5.8:	Water quality data of the Humboldt River waters at various stations for the year of 2007.	108
Table 6.1:	Summarized physical parameters and some important chemical components of waters from the Humboldt River.	136
Table 6.2:	Average daily base flow of the Humboldt River during August - September, 2007 recorded at various stream gages.	140
Table 6.3:	Groundwater quality data for groups-I, II, and III corresponding to Upper Humboldt, Middle Humboldt, and Lower Humboldt River basins, respectively.	141
Table 6.4:	Average evaporation data (inches) of various stations in northern Nevada.	142
Table 6.5:	Average annual and September precipitation data of northern Nevada.	143
Table 6.6:	Water chemistry data that were used in the simulations for different pathways along the flow-path of the Humboldt River.	146
Table 6.7:	Values used to calculate the amounts of reactant minerals titrated into the fluid over the course of the reaction path when modeling reaction of rainwater with country rocks.	154
Table 6.8:	Kinetics rates used in mineral dissolution in the water-rock reaction simulation in EQ3/6.	155
Table 6.9:	Surface parameters of ferrihydrite (HFO) and equilibrium constants used in the desorption modeling.	159

Table 6.10: Speciation results showing dominant species resulted from EQ3 speciation modeling for Humboldt River sample waters.	163
Table 6.11: Saturation Indices calculated from water samples of the Humboldt River using EQ3/6 computer codes.	165
Table 6.12: Simulation results for various parameters and As concentrations for all modeled pathways.	166

List of Figures

Figure 1.1: Shaded relief map of northern Nevada showing the location of Humboldt River Basin (Source of data: Nevada Bureau of Mines and Geology).	3
Figure 2.1: Shaded relief map of northern Nevada showing the location of Humboldt River Basin (HRB).	7
Figure 2.2: Schematic surface geology of northern Nevada and HRB.	9
Figure 2.3: Schematic hydrogeologic cross section showing different hydrogeologic features controlling ground water flow and discharge in the Humboldt River Basin.	12
Figure 2.4: The Eh-pH stability diagram of arsenic species in the As-O ₂ -H ₂ O system at 25 °C and 1 bar total pressure	19
Figure 4.1: Shaded relief map of northern Nevada showing the location of Humboldt River Basin (HRB).	25
Figure 4.2: Map of Humboldt River Basin and Northern Nevada illustrating the locations of ground water samples that have been used in this study.	31
Figure 4.3: A) Histograms illustrating variations of As concentrations and other chemical parameters in the ground water samples from Group-I.	37
Figure 4.3: B) Histograms illustrating variations of As concentrations and other chemical parameters in the ground water samples from Group-II.	38
Figure 4.3: C) Histograms illustrating variations of As concentrations and other chemical parameters in the ground water samples from Group-III.	39
Figure 4.4: Map illustrating spatial distribution of dissolved As concentrations in ground water in mg/L in the HRB area.	43
Figure 4.5: Piper diagrams for different groups of ground water illustrating ground water types.	47
Figure 5.1: Map of the Humboldt River Basin (HRB) in northern Nevada showing the Humboldt River and locations of	66

sampling points of river water and sediments.

Figure 5.2:	Histograms showing average of monthly mean discharge in 2007 of the Humboldt River at different stations.	69
Figure 5.3:	Top: Map illustrating contours of ground water elevation (meters above sea-level) and movement indicated by arrows around the HRB flood plains; bottom: 3-D schematic diagram showing ground water elevation with contours.	74
Figure 5.4:	Schematic geologic map of HRB and northern Nevada.	76
Figure 5.5:	Piper diagram showing hydrochemical phases for river waters of the upper, middle and the lower Humboldt River.	86
Figure 5.6:	Stiff diagrams of river water samples (sample numbers on right of each diagram) showing differences in major chemical composition.	87
Figure 5.7:	Relationship between oxygen and hydrogen isotope data of surface water samples collected from the Humboldt River and its tributaries.	88
Figure 5.8:	A) Photomicrographs of river-bed sediments (sample 006), illustrating typical detrital smectite clay (Sm) on the surface quartz (Qtz) grains.	90
Figure 5.8	B) Photomicrographs of river-bed sediments (sample 007), illustrating typical flaky nature of smectite (Sm) clay minerals on the surface of quartz (Qtz) grains.	90
Figure 5.8:	C) Photomicrographs of river-bed sediments (sample 012), illustrating smectite-illite (Sm/Ill).	91
Figure 5.8:	D) Photomicrographs of river-bed sediments (sample 015), illustrating typical flaky nature of smectite (Sm) clay minerals on the surface of partially dissolved feldspar.	91
Figure 5.8:	E) Photomicrographs of river-bed sediments (sample 016), illustrating detrital flaky smectite clays (Sm) on the surface of feldspar (Fd).	92
Figure 5.8:	F) Photomicrographs of river-bed sediments (sample 019), illustrating typical flaky nature of smectite (Sm) clay minerals on the surface of partially dissolved feldspar (Fd).	92

Figure 5.9: Elemental concentrations (%) of some key-elements in the river-bed sediments obtained from sequential extraction analyses.	96
Figure 5.10: Sulfate concentrations (in mmol/L) vs. Cl concentrations (mmol/L) for the water samples from the Humboldt River.	112
Figure 5.11: Ratio of dissolved sulfate to chloride in the waters along the flow-path of the Humboldt River.	120
Figure 5.12: Relationship of pH with As concentrations in the Humboldt River waters.	120
Figure 5.13: Schematic conceptual model showing arsenic mobilization and transportation pathways along the Humboldt River waters and its sediments from upper to lower reaches.	121
Figure 6.1: Location map of the Humboldt River Basin (HRB) in northern Nevada showing the locations of active mines, hot springs and hot wells and sampling points of stream water and sediments used in this study.	130
Figure 6.2: Schematic generalized geologic map of the HRB and northern Nevada illustrating broad lithologic distribution of major rock formations.	131
Figure 6.3: Flow chart showing procedure used to combine reaction path calculations with mineral and water chemistry data in EQ3/6 computer codes.	144
Figure 6.4: Schematic diagram showing different path-ways used in the conceptual model.	145
Figure 6.5: Location of samples used in modeled pathways 1 and 2 (sample 001, and 003 to 004) in the Upper Humboldt River.	148
Figure 6.6: Location of samples used in modeled pathway 3 (sample 007 to 008) in the Middle Humboldt River.	149
Figure 6.7: Location of samples used in modeled pathways 4, 5 and 6 (sample 012 to 01; 015 to 016; and 017 to 019) in the Lower Humboldt River.	150
Figure 6.8: Concentrations of dissolved As released as a result of desorption simulations for different concentrations of As in the sediments.	180

CHAPTER 1

1. Introduction

Arsenic (As) is a ubiquitous metalloid that ranks twentieth in crustal abundance, with average concentrations of 2 mg/kg, and is found in the atmosphere, soils and rocks, natural water, and organisms (Bhumbla and Keefer, 1994). Elevated level of dissolved As in drinking water is linked to increased risks of cancer, diabetes, and heart disease (National Research Council, 2001), and contamination of groundwater by naturally occurring arsenic is considered as one of the greatest environmental disasters and one of the prominent causes of skin-cancer mortality in the world (Smith et al., 2006).

Regional occurrences of As in ground water and surface water in the western United States and other regions have been reported by several workers (Stauffer and Thompson, 1984; Welch et al., 1988; 2000; Welch and Lico, 1998; Robertson, 1989; Jones et al., 1999; Savage et al., 2000). Elevated levels of As exceeding the U.S. EPA maximum contaminant level (MCL) of 0.01mg/L, or 10 ppb (EPA, 2009) have been found in western Nevada (Welch et al, 2000). In one study, up to 2.6 mg/L As has been reported in the ground water from Holocene alluvial and lacustrine aquifers in Nevada (Welch and Lico, 1998). Arsenic concentrations in the stream sediments of the Humboldt River Basin (HRB) have been reported up to as high as 1785 mg/kg in (Folger, 2000).

The Humboldt River Basin (HRB) is a naturally occurring internally draining river basin that covers approximately 43,700 km² (Figure 1.1), and forms a substantial part of the larger Great Basin (Yager and Folger, 2003). It includes the upper reaches of

the Little Humboldt River in Elko County, the Reese River in Lander County, and the main Humboldt River and its many tributaries that flow mainly westward and south-westward into the Humboldt sink and Carson sink respectively. The basin contains a wide variety of metallic and nonmetallic mineral deposits, and the area has been considered as one of the Nation's leading producers for gold, silver, copper, mercury and tungsten (Wallace et al., 2004).

The Humboldt River system plays an important role in maintaining wildlife habitats and wetlands, irrigation, and water storage in Rye Patch reservoir, and Humboldt Sink, where it terminates. Because of the importance of the Humboldt River and the shallow groundwater of the HRB in supporting agriculture, mining industries, geothermal power plants, wildlife habitats, and domestic uses, assessment of arsenic behavior and cycling in the river water and groundwater is essential.

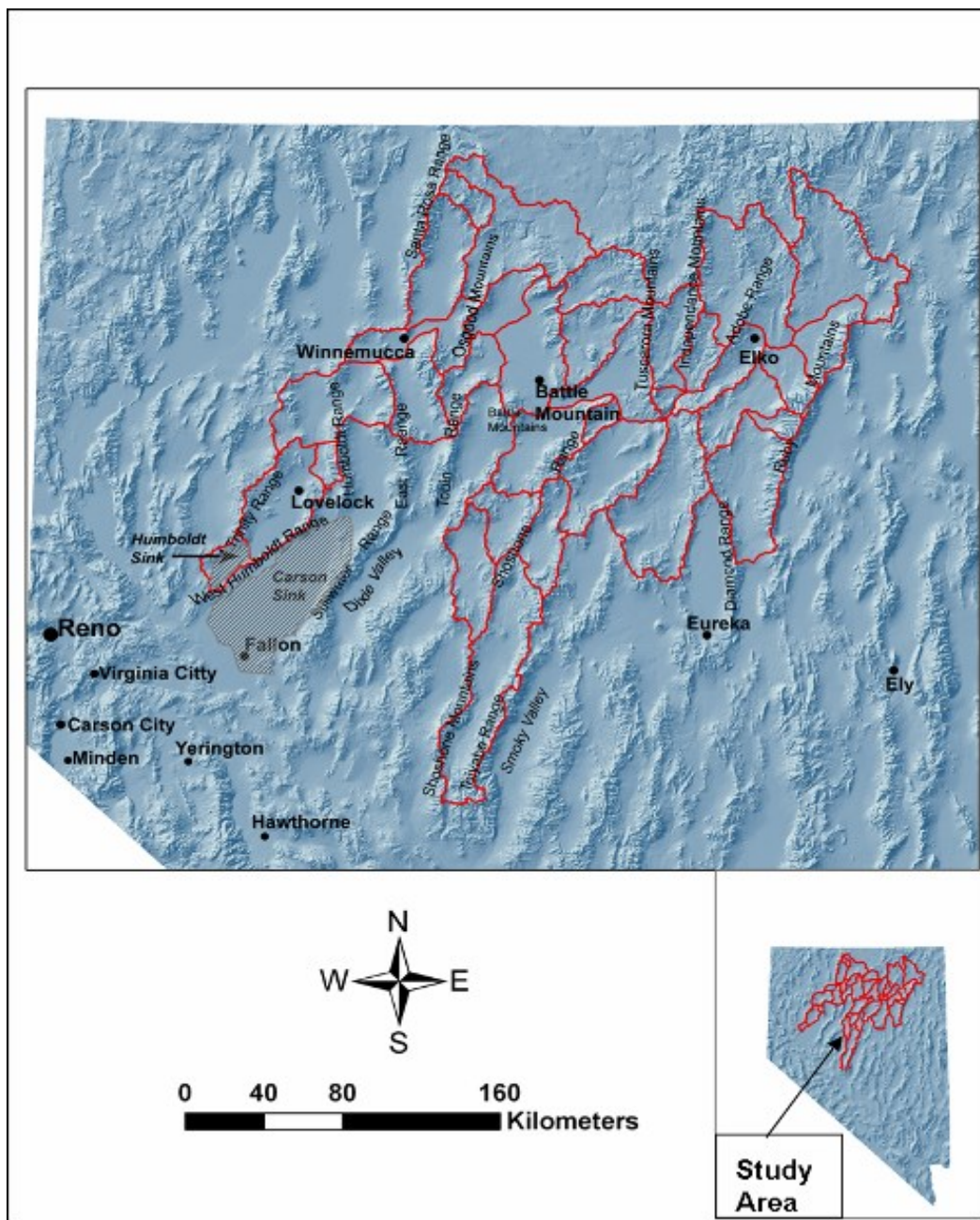


Figure 1.1: Shaded relief map of northern Nevada showing the location of Humboldt River Basin (Source of data: Nevada Bureau of Mines and Geology).

The dissertation is divided into 7 chapters. Chapter 2 provides a summary of previous research characterizing the occurrence and distribution of naturally occurring As in waters and sediments in different geologic settings, an overview of aquatic geochemistry of As, an overview of the hydrogeologic and geochemical factors that controls the distribution and cycling of naturally occurring As between water and sediments. Chapter 3 presents the overall goals of the study and an overview of the methods used in the course of the project. Chapter 4, Chapter 5 and Chapter 6 are preliminary form of manuscripts to be submitted to peer-reviewed journals. Finally, Chapter 7 provides a synthesis of the research presented in this dissertation, with a focus on future studies and recommendation.

CHAPTER 2

2. Previous work and background

This chapter provides a summary of previous research characterizing the occurrence and distribution of naturally occurring As in waters and sediments in different geologic settings, an overview of aquatic geochemistry of As, an overview of the geologic and hydrogeologic settings of the study area.

2.1. Regional occurrences of arsenic

Based on currently available information, it is currently recognized that various factors control the occurrence of As in both groundwater and surface waters. For example, three major hydrogeologic settings have been identified for widespread As-groundwater in “redox-mixed” environments: 1) alluvial aquifers in river flood plains: West-Bengal of India, Bangladesh (Zheng et al., 2004); 2) fluvial-glacial deposits: Mahomet and Glasford aquifers of Lower Illinois River Basin (Kelly et al., 2005); New England, Nova Scotia glaciated bedrock and drift aquifers (Peters et al., 2008); and 3) deltas: Vietnam (Berg et al., 2001). In these environments, occurrence of As in groundwater is mainly controlled by redox-biogeochemical reactions (Saunders et. al., 2005A, B). On the other hand, in semi-arid environment, distribution of dissolved As is mainly controlled by oxidation of As-bearing sulfide minerals, evaporation, and pH-dependent sorption-desorption, along with mixing with geothermal waters (e.g., Western Nevada, Arizona, Wyoming, Mexico, Chile, Southern High Plain Aquifers of Texas) cited in Stauffer (1984), Robertson (1989), Schreiber et al. (2000), Tempel et.al. (2000), Welch et al. (2000), Smedley and Kinniburgh (2002), Romero et al. (2003), and Scanlon et al. (2009). The HRB region

represents an example of semi-arid geographical setting with mixed alluvial-flood plain in a topographical high area, where the intermountain basin-fills form shallow alluvial aquifers with recharge from stream base flows. Hydrogeologic settings in the river flood-plain typically have very low hydraulic gradients due to their low topographic relief, and therefore, As-rich fluids are not quickly flushed out of the system. On the other hand, in topographical high areas with enclosed valleys in semi-arid environment, As concentrations are likely controlled by the amount of recharge and discharge, mixing and dilution, and evaporation in. As a result As can build up to toxic levels in the groundwater and surface waters. Very little is known about As occurrence in semi-arid regions with topographically high relief and inland basins like HRB in northern Nevada, where very low rates of precipitation with high rates of evaporation and weathering are significant. High concentrations of As in the waters with similar hydrogeologic settings have been found in the Rio Loa River Basin in Chile, where evaporation, geothermal mixing and mining activities are the major controls. Similar conditions exist elsewhere, and as global population increases and water supplies dwindle, the natural As contamination problem is likely to grow in significance.

2.2. Study area

The HRB is a natural, internally drained river basin that covers approximately 43,700 km² (Figure 2.1). It forms a substantial part of the Basin and Range physiographic province, which is the one of the most arid areas in the U.S.A. (Yager and Folger, 2003). The tributaries of the Humboldt River (HR) originate in the

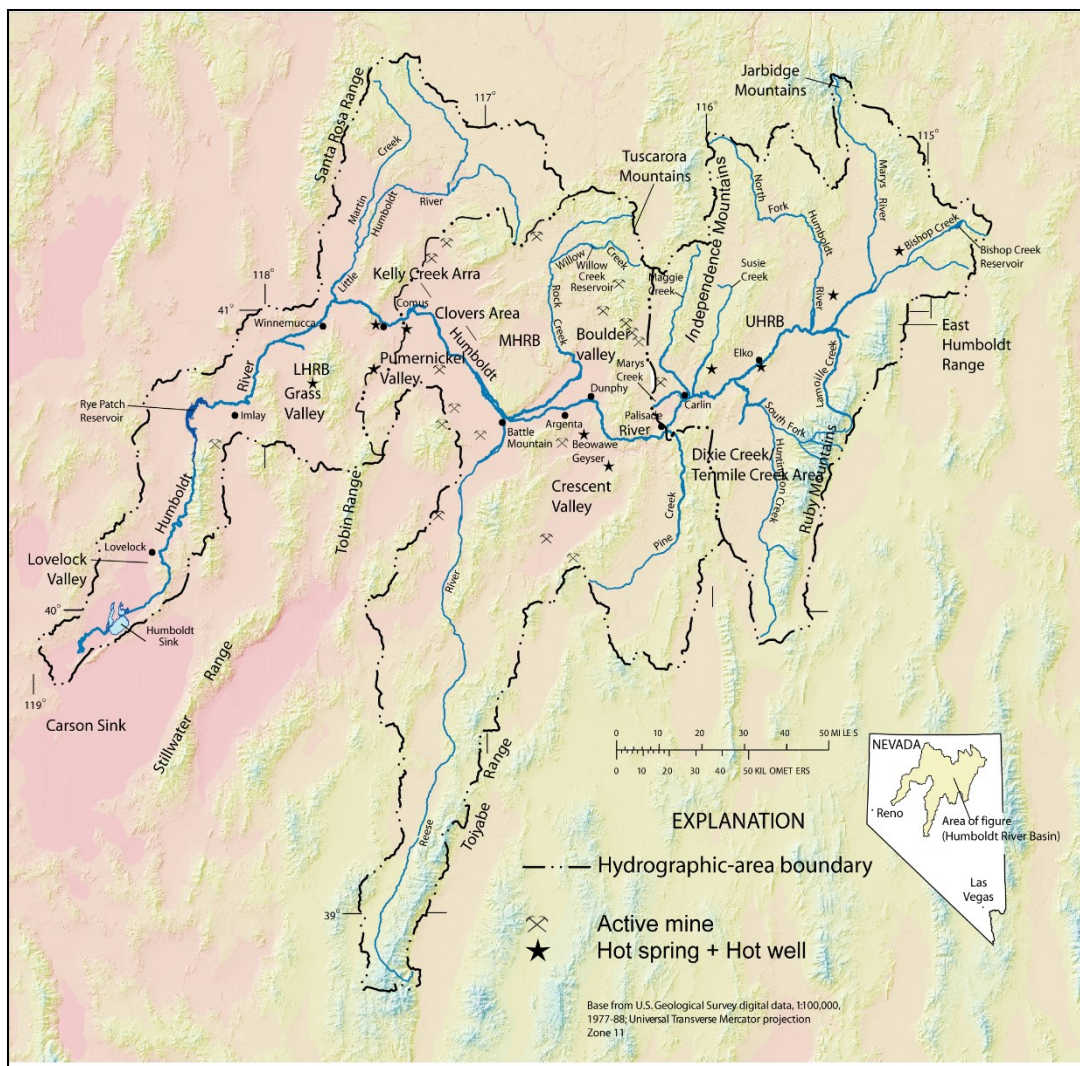


Figure 2.1: Shaded relief map of northern Nevada showing the location of Humboldt River Basin (HRB) (modified after Prudic et al., 2006). Note: UHRB: Upper Humboldt River Basin; MHRB: Middle Humboldt River Basin; LHRB: Lower Humboldt River Basin.

mountains of northeastern Nevada and the river flows from east to west and then southwest towards the Humboldt Sink. The HRB includes the upper reaches of the Little Humboldt River in Elko County, the north-flowing Reese River in Lander and Nye Counties, and the main Humboldt River and its many tributaries that flow westward into the Humboldt Sink. It is a significant source of water for municipal uses, irrigation, and mining-related activities. The basin and its surrounding areas is one of the leading producers of gold, silver, copper, mercury, and tungsten in the U.S. since the mid-1800s (Wallace et al., 2004).

2.2.1. Geologic setting

Figure 2.2 illustrates the schematic geologic map of Northern Nevada with the HRB. The complex geologic landscape of northern Nevada was affected by multiple east-directed orogenic events in the Paleozoic and Mesozoic that produced a complex tectono-stratigraphic package by the end of the Mesozoic. Most of the clastic and carbonate strata that were produced during the Mesozoic sedimentation were removed by erosion in the eastern part of the basin. The arc-related magmatic activities during the late Mesozoic era produced plutonic rocks throughout the HRB, which in turn produced various metallic mineral deposits including gold, silver and other metallic ore deposits. During the early Cenozoic era, the area was subjected to widespread erosion (Henry 2008; Wallace et al., 2008).

During the late Eocene through early Miocene, volcanic activity was widespread in Nevada, and Eocene and Oligocene volcanic activities blanketed the low-relief topography with flow and ash-flow tuff units. Miocene volcanic activities produced a bimodal suite of volcanic rocks from andesitic to rhyolitic in composition.

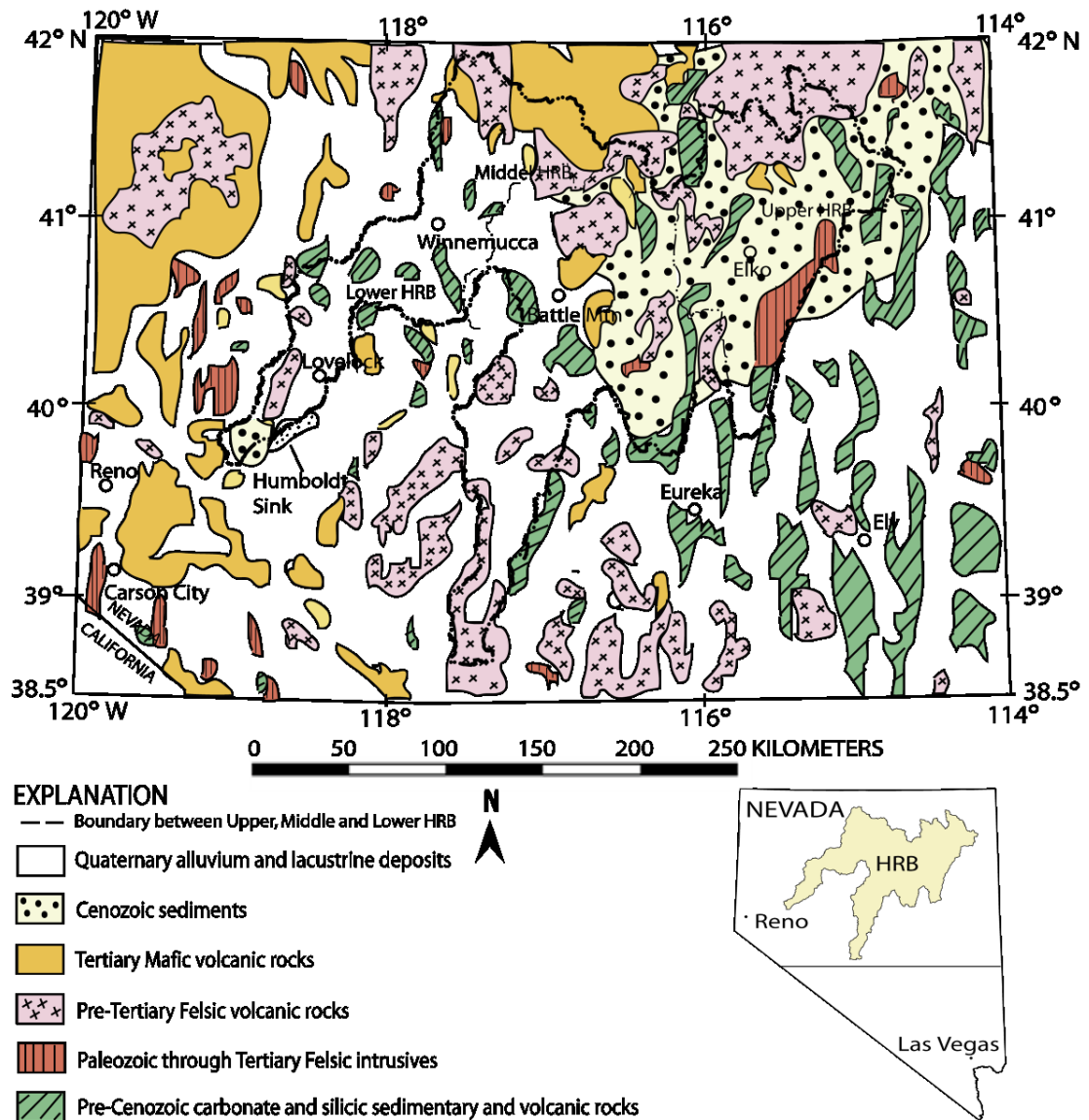


Figure 2.2: Schematic surface geology of northern Nevada and HRB. Source of GIS database: Great Basin Geoscience Database.

(<http://keck.library.unr.edu/data/gbgeosci/gbgdb.htm>).

Crustal extension beginning at about 15 Ma eventually produced the modern horst and graben (basin and range) physiography, and compartmentalized the strata with faulting. Arsenic-bearing metal sulfide (e.g., gold) deposits formed (Arehart et al., 1993) throughout the area during each period of volcanic activities. The sediments derived from erosion of adjacent horsts were deposited as alluvium and lacustrine valley-fill deposits.

2.2.2. Hydrogeologic setting

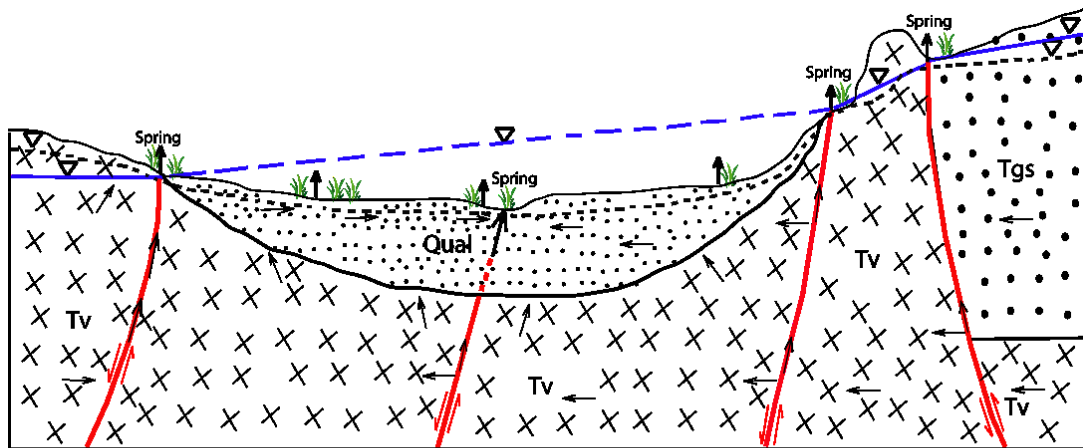
Table 2.1 lists the hydrogeologic units in northern Nevada including the HRB area. Much of the Great Basin is underlain by consolidated to semi-consolidated sedimentary deposits ranging in age from Proterozoic to Cenozoic. Among these units, carbonate rocks constitute deeper regional aquifers, whereas the overlying clastic sedimentary rocks of Tertiary and Quaternary constitute shallow alluvial aquifers ranging only tens to few hundreds of meters in depth (Plume, 1996).

Figure 2.3 illustrates the schematic hydrogeologic cross section showing the aquifers of interest for this study. In general, the aquifers of this study consist primarily of basin-fill sediments with some volcanic rocks that were deposited in individual alluvial basins. The older basin-fill deposits consist of consolidated to semi-consolidated deposits of conglomerate, sandstone, siltstone, claystone, freshwater limestone, and evaporites (Yager and Folger, 2003). The younger basin-fill deposits consist of mostly unconsolidated to semi-consolidated and unsorted to poorly sorted clay, silt, sand, gravel, and boulders that make up the uppermost part of the basin-fill stratigraphy. Numerous extensional faulting have compartmentalized many of the Tertiary volcanic rocks (e.g., welded and non-welded tuffs), which constitute the confined aquifers in the HRB. These aquifers are relatively at deeper level

Table 2.1: Generalized summary of hydrogeologic units at HRB, northern Nevada (modified after Plume 1995; and Maurer et al. 1996).

Geologic age	Hydro-geologic unit	Lithology	Thickness ¹ (meters)	Water-bearing characteristics (K ²)
Basin-fill deposits				
Quaternary	Flood-plain deposits	Sorted to poorly sorted boulders, gravel, sand, silt, and clay.	Few meters to hundreds of meters along Humboldt River. 0 at basin margins to hundreds of meters.	K~ 0.1 to 600 m/d, frequently between 0.85 and 22.5 m/d.
	Alluvial-fan Deposits	Boulders, gravel, sand, silt, clay, and intermittent beds of limestone and rhyolitic ash.		K~ 5 to 30 m/d with average 40 m/d.
Tertiary and Cretaceous	Older basin-filled deposits	Interbedded sediments and volcanic rocks deposited in lakes and streams including siltstone, claystone, shale, limestone, conglomerate, and sandstone, with some tuff, and ash.	~ 300-2400	K ranges from about 0.3 to 2 m/d.
Bedrock				
Tertiary and Jurassic	Volcanic rocks	Felsic flows, domes, and ash-flow tuffs; intermediate lava flows, pyroclastic rocks, and air-fall tuffs; mafic volcanic rocks; and ash.	~ 60-150	K ranges from 3X10 ⁻³ to 3 m/d with average of ~ 0.6 m/d.
Tertiary and Jurassic	Intrusive igneous rocks	Felsic to intermediate, plutons, dikes, and minor plugs (solidified lava that fills the conduit of a volcano).	Not determined	
Devonian to Ordovician	Clastic Sedimentary Rocks	Quartzite, chert, shale, mudstone, sandstones, and calcareous siltstones with some intermediate and mafic volcanic rocks.	~ 450-700	K ~ 4X10 ⁻⁴ to 30 m/d, frequently between 3 X10 ⁻⁴ and 0.15 m/d.
Permian to Mississippian		Mudstone, siltstone, quartzite, limestone, shale, and sandstone.	~ 750-7000	
Devonian to Cambrian	Carbonate Rocks	Limestone, dolomite, limy siltstone, sandy dolomite, claystone, chert, and quartzite.	~ 2100-5700	K ~ 3X10 ⁻² to 45 m/d, most values from 6X10 ⁻² to 3 m/d.

¹Combined thickness of all stratigraphic units. Listed total thickness probably not present at any single locality. ²Hydraulic conductivity in m/d.



Not to scale; vertical exaggerated.

EXPLANATION


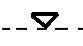


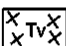



- | | | | |
|---|---|---|--|
|  | Valley-fill deposits: Alluvial aquifer.
Qual: Quaternary sand, silt, and gravel. |  | Water table: Defines upper bound of alluvial and welded-tuff aquifer |
|  | Valley-fill deposits: Alluvial aquifer.
Tgs: Tertiary sand, and gravel. |  | Potentiometric surface of regional welded-tuff aquifer:
Solid where below land surface. Dotted where above land surface |
|  | Volcanic rocks: welded-tuff aquifer and non-welded tuff confining unit.
Tv: tertiary welded tuffs, lava flows, and bedded tuffs |  | Area of evapotranspiration |
|  | Fault: Solid where faults form conduits for upward regional groundwater flow to surface. Dashed where fault forms conduit for upward flow in alluvial aquifer |  | General direction of ground water-flow |

Figure 2.3: Schematic hydrogeologic cross section showing different hydrogeologic features controlling ground water flow and discharge in the Humboldt River Basin (modified after Reiner et al., 2002).

underlying the basin-fill deposits of the Quaternary alluvial aquifers (Yager and Folger, 2003).

Faults and related fractures can act as enhanced conduits for ground water flow, but also can act as barriers and impede flow where hydrogeologic units of differing permeability (e.g., carbonate against clastic sedimentary rocks) are juxtaposed or where the fault-plane is filled by fault gouge (Reiner et al., 2002).

In general, the ground water in the HRB moves from recharge areas along the mountain fronts to discharge as seepage to stream channels, and evapotranspiration on the valley floors. Recharge also occurs in mountainous areas underlain by carbonate rocks. The main discharge area in the Humboldt River Basin is the river flood plain, which can be as much as a mile wide (Plume, 1995).

The precipitation ranges from 15 to 110 cm annually and most frequently in the range of 15 to 30 cm in the valleys and floodplain areas. Precipitation generally is greater at higher elevations in the mountains than in the adjacent valleys and occurs mostly during the wet season from late November to May (Prudic et al., 2006). The average annual precipitation map prepared by the Division of Water Resources (NDWR) of State of Nevada-Department of Conservation and Natural Resources (<http://water.nv.gov/index.cfm>) indicates annual average precipitation with a range of 10-20 cm in the lower Humboldt River Basin area with a low annual average of less than 10 cm near Humboldt Sink area. Shevenell (1996) reported potential evaporation exceedingly higher than precipitation in much of the regions in HRB.

2.2.3. Ore deposits, mining and geothermal activities

The types of ore deposits in the HRB area are summarized in Table 2.2. There are three major classes of mineral deposits in the HRB: 1) pluton-related polymetallic

deposits; 2) sedimentary rock-hosted gold-silver deposits (including Carlin-type and distal-disseminated gold-silver deposits); and 3) gold-silver deposits that formed in relatively shallow, epithermal environments (Wallace et al., 2004). The mining activities for both pluton-related and sedimentary rock-hosted metal deposits occur at Battle Mountain, Carlin, and Copper Canyon in the Upper and Middle HRB. Many of these deposits are mined from deep, extremely large open pits, and exploitation of these deep ores has required extensive dewatering of adjacent aquifers (Wallace et al., 2004), and in many cases, the fluids produced by dewatering are put back into the Humboldt River after treatment (Prudic et al., 2006).

Because of the increased mining activities with the increased development of large open pit mines and associated increase in populations, ground water use in the HRB increased in the last two decades. A report of Nevada Division of Water Planning indicated that mine water withdrawals in the HRB alone accounted for about 70% of the state total mine water withdrawals (Nevada Division of Water Planning, 1995) and have been increased in the recent (Yager and Folger, 2005). Based on the demand and conditions of mining, a significant portion of dewatered water is re-injected into nearby aquifers, infiltrated to underlying aquifers from storage reservoirs, evaporated in lined ponds, discharged to surface water bodies, or used for irrigation. The remaining portion of water is consumptively used by mining operations (Nevada Division of Water Planning, 1995). Pumping of large volumes of ground water for mining use and dewatering has resulted in water-level declines of tens to hundreds of meters in areas of dewatering (Crompton, 1995; Plume, 1996). The HRB region also contains a number of geothermal hot springs and hot wells that have

Table 2.2: Types of mineral deposits in the Humboldt River Basin (modified after Wallace et al., 2004).

Type of Mineral Deposit	Examples
Pluton-related polymetallic	Battle Mountain, Majuba Hill, McCoy-Cove.
Sedimentary rock-hosted gold-silver	Carlin type: Carlin Trend, Getchell Trend, Independence, Alligator Ridge, Cortez.
	Distal-disseminated: Lone Tree, Marigold, Trenton Canyon, bald Mountain, Toiyabe.
Sedimentary rock-hosted gold-silver	Midas, Mule Canyon, Florida Canyon.
Epithermal gold-silver	

been exploited for geothermal power plants (Shevenell and Garside, 2005; Shevenell et al., 2008). A significant portion of ground water is also used for irrigation and livestock.

2.3. Source and occurrence of arsenic

Arsenic naturally occurs in more than 200 different mineral forms (Onishi, 1969). Most of these minerals occur in metalliferous ore deposits, or their alteration products. Table 2.3 lists some of the most common As-minerals.

Arsenic is commonly associated with many types of hydrothermal ore deposits. It is best known for its association in a variety of gold deposits, including volcanic-hosted and sediment-hosted “carlin-type” gold deposits in northern Nevada (Arehart et al., 1993). Arsenic also occurs variably in rock forming minerals, and ferromagnesian (Fe-Mg-bearing) minerals, and biotite and amphibole appear to be the most As-enriched in high temperature (igneous) minerals. Biotite has been found as one of the most likely source of As due to weathering of typical igneous and metamorphic rocks (Saunders et al., 2000). Biotite not only contains significant amounts of As (Table 2.3), but it is one of the fastest weathering silicate minerals. Thus As-flux to hydrosphere is enhanced by weathering kinetics as well as As-contents.

Table 2.3: Major arsenic minerals occurring in nature (WHO, 2001).

Minerals	Chemical composition	Occurrence
Realgar	AsS	Vein deposits, often associated with orpiment, clays and limestone, also deposits from hot springs
Orpiment	As ₂ S ₃	Hydrothermal veins, hot springs, volcanic sublimation products
Cobaltite	CoAsS	High temperature deposits, metamorphic rocks
Arsenopyrite	FeAsS	The most abundant As-mineral, dominantly mineral veins
Tennantite	(Cu,Fe) ₁₂ As ₄ S ₁₃	Hydrothermal veins
Enargite	Cu ₃ AsS ₄	Hydrothermal veins
Arsenolite	As ₂ O ₃	Secondary mineral formed by oxidation of arsenopyrite, native As and other As minerals
Scorodite	FeAsO ₄ .2H ₂ O	Secondary mineral
Rammelsbergite	NiAs ₂	Commonly in mesothremal veins
Safflorite	(Co,Fe)As ₂	Commonly in mesothremal veins
Seligmannite	PbCuAsS ₃	Hydrothermal veins
Annabergite	(Ni,Co) ₃ (AsO ₄) ₂ .8H ₂ O	Secondary mineral
Hoernesite	Mg ₃ (AsO ₄) ₂ .8H ₂ O	Secondary mineral, smelter wastes
Conichalcite	CaCu(AsO ₄)(OH)	Secondary mineral
Adamite	Zn ₂ (OH)(AsO ₄)	Secondary mineral
Loellingite	FeAs	Found in mesothremal vein deposits
Pharmacosiderite	Fe ₃ (AsO ₄) ₂ (OH).5H ₂ O	Oxidation product of arsenopyrite and other As minerals

2.4. Aqueous geochemistry of arsenic

The geochemistry of As in water depends on many factors such as redox state, pH, presence of iron, manganese and aluminum oxides, sulfate or clay minerals in the aquifer. The aqueous chemistry of As is very complex due to multiple oxidation states and organo-metallic reactions. Inorganic arsenic may exist in +5, +3, 0, and -3 oxidation states. In natural water, only +5 (arsenate) and +3 (arsenite) oxidation states are common, and arsenite is biologically more active and toxic than arsenate (Smedley and Kinniburgh, 2002). In oxygenated fresh and marine water of near neutral pH, inorganic arsenic mainly occurs as As(V) or arsenate species [H_2AsO_4^- and HAsO_4^{2-}]. In mildly reducing water such as geothermal hot springs and groundwater, arsenic occurs mostly as dissolved As (III) or arsenite species [H_3AsO_3^0 : arsenious acid]. The pH and Eh are two of the important factors controlling the occurrence of dissolved arsenic in water (Figure 2.4).

In oxygenated environment, As can be released to water because of oxidation of As-bearing sulfide minerals as a result of water-rock reactions (Schreiber et al., 2000; Lengke and Tempel, 2005). In arid and semi-arid environments, As can be enriched secondarily due to evaporation, pH-dependent desorption, competition among oxyanions for sorption sites and/or counter-ion effects associated with the change in water chemistry from Ca- to Na-rich water (Welch et al., 2000; Robertson, 1989; Scanlon et al., 2009). In the river-flood plains, iron, manganese, and aluminum form solid oxides as either individual particles or as coatings on other grains under oxidizing conditions. These minerals have high adsorption capacities with an average surface area of $200 \text{ m}^2/\text{g}$ (Drever, 1997). Among these minerals, the solid surfaces of hydrous iron oxides (HFO)

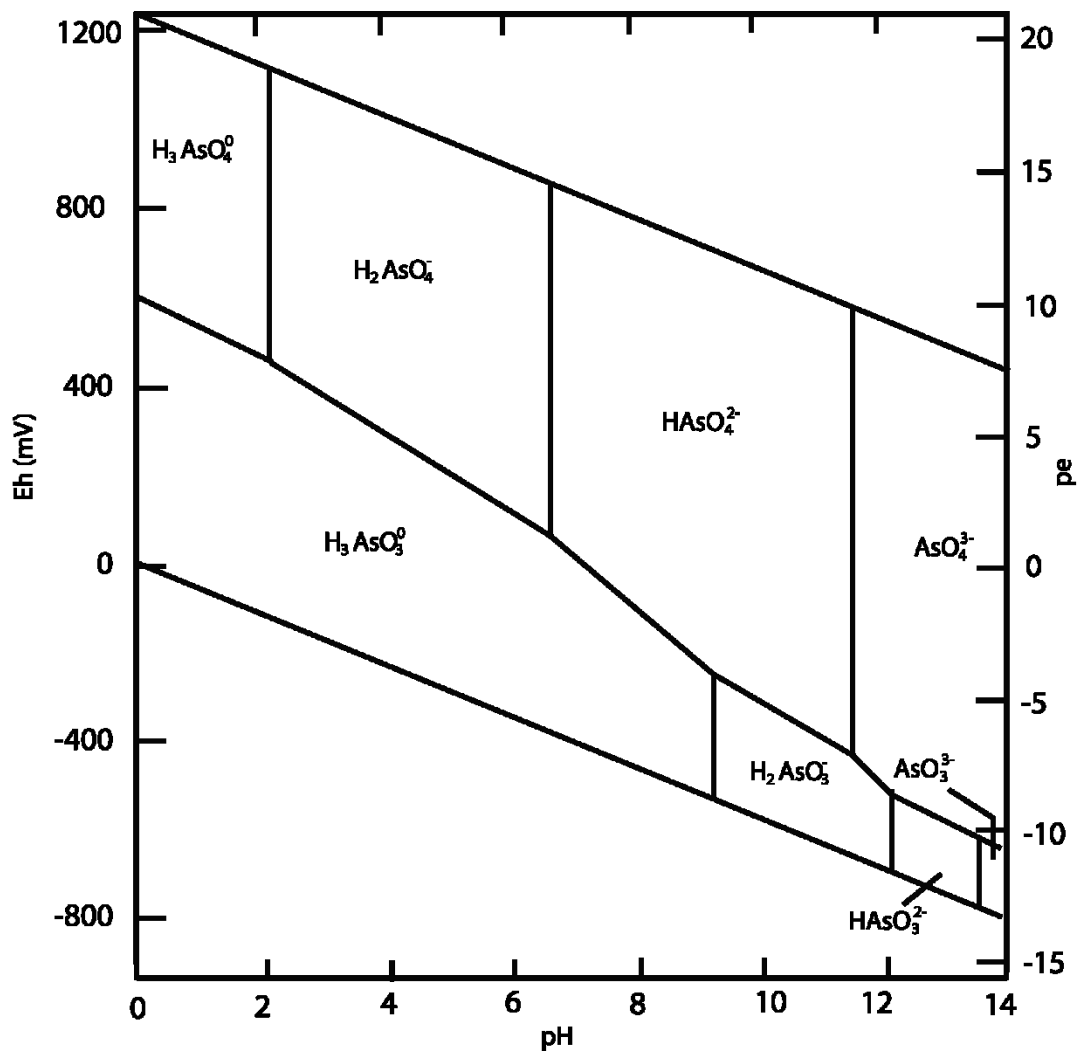


Figure 2.4: The Eh-pH stability diagram of arsenic species in the As-O₂-H₂O system at 25 °C and 1 bar total pressure (modified from Brookins, 1988).

can adsorb large quantities of positively charged cations due to their high negative charges on the surfaces (Hem, 1985). This high adsorption capacity of iron oxyhydroxides and their affinity for co-precipitation with other ions (metals and oxyanions including As) control the trace element and metal geochemistry of water. In iron-rich aquifers, hydrous ferric oxides (HFO) play the dominant role in trace element-groundwater geochemistry by sorption onto HFO at circum-neutral pH (Le Guern, et al., 2003).

In highly reducing conditions, sulfate can be reduced to produce hydrogen sulfide (H_2S) or aqueous complex of H_2S , which in turn can co-precipitate to metal sulfides (Saunders et al., 2005). However, reduction of sulfate and co-precipitation to metals depend on the availability of substantial amount of sulfate and iron in the groundwater. Huerta-Diaz and Morse (1992) studied pyrite in marine sediments and observed that trace metals and metalloids such as arsenic, cobalt (Co), nickel (Ni) were the most strongly associated elements with pyrite. Upon oxidation, pyrite is unstable and the above reaction reverses releasing iron and sulfate along with associated arsenic to the solution.

CHAPTER 3

3. Study goals, materials and methods

This chapter describes the overall goals of the study and presents an overview of the methods and materials used in the course of the project.

3.1. Study goals and components

This dissertation links the physical hydrologic processes at work in the HRB, in conjunction with the geochemical processes affecting the distribution and occurrence of naturally occurring dissolved As in waters. Although the HRB has not been extensively studied previously with respect to dissolved As, it has a significant impact on the use of water for municipal, industries, aquifer management and storage, and wetland management. The HRB region represents a large-scale example of an “ideal” hydrogeochemical setting for As-cycling from source to sink with As release, transport, deposition into sediments and enrichment into both surface and groundwater. Arsenic concentrations are likely to be controlled by the amount of recharge and discharge, mixing and/or dilution, and evaporation in enclosed valleys in a semi-arid environment, where very low rates of precipitation with high rates of evaporation and weathering are significant. Therefore, the broad objective of this study was to investigate the cycling of naturally occurring arsenic by studying As behavior and geochemistry in the sediments and surface water of the Humboldt River and shallow groundwater of the alluvial aquifers within the HRB region. To achieve this objective, the study was divided into three different phases: 1) identify the processes controlling distribution and occurrence of

As in ground water in the HRB; 2) geochemical and statistical analyses of the sediment and water samples from the Humboldt River flood-plain; and 3) develop a conceptual model for arsenic cycling based on the processes identified in phase one and two, and quantify and determine the relative importance of the processes using geochemical and reaction path modeling techniques

3.2. Materials and methods

The methodologies used in these studies fall into three different categories: 1) ground water data (water elevation, quality, etc.) collection from the published public domain, and analyses of the data using various statistical and computation techniques; 2) sample collection for river water and river bed sediments, field data collection for physical characterization of the samples, and laboratory analysis of the samples for petrographic and geochemical characterization; 3) geochemical reaction path modeling and simulations of various processes identified for dissolved As distribution along the flow path of the HRB.

These methodologies are described in details in the following respective chapters (Chapter 4, Chapter 5, and Chapter 6) that present each of the components of this dissertation mentioned above.

CHAPTER 4

Occurrence of Arsenic in Ground Waters in the Humboldt River Basin, North-central Nevada.

ABSTRACT: Elevated ground water arsenic (As) levels are widespread in the shallow alluvial aquifers in the northern part of the Nevada and Humboldt River Basin (HRB), with up to 0.55 mg/L with an average of 0.04 mg/L (mean = 0.018, median = 0.015), exceeding the current EPA maximum contaminant level (MCL) of 0.01 mg/L. The objective of this study was to evaluate the distribution, sources and mobilization mechanisms of As in the shallow alluvial aquifers of the HRB using available public domain database from USGS, Nevada Bureau of Mines and Geology, and Nevada Department of Conservation and Natural Resources. Distribution of As concentrations illustrate spatial relationship with high concentrations in the mineralized zones of metallic-sulfides in Boulder valley, and surrounding areas, and in playa deposits and terminal sink of the Humboldt River, where annual evaporation predominates over precipitation. The regional source of dissolved As concentrations in ground water is likely to appear from dissolution of As-bearing ferromagnesian silicates (e.g., biotite) from the Tertiary volcanic rocks and dissolution of As-bearing iron-oxyhydroxides in the Quaternary alluvial aquifers. Oxidation of As-bearing sulfides appears to be a localized source of As in the mineralized zones in Boulder Valley. Secondary enrichment of As by mixing with geothermal waters on a localized scale have been inferred from the statistical correlations and qualitative geochemical analyses of waters. The HRB ground water case study has a similar As occurrence to those of other semi-arid oxidizing systems with high alkalinity and salinity, and high rates of evaporation.

Key Words: Arsenic, Ground water, Hydrogeochemistry, Humboldt River Basin, Nevada.

4.1 Introduction

Elevated levels of dissolved arsenic (As) have been found in ground water of the Humboldt River Basin (HRB) and surrounding areas in Northern Nevada.

Concentrations of As have been found up to 0.55 mg/L with an average concentration of 0.043 mg/L (mean = 0.018, median = 0.015), which is 4 times more than the World Health Organization (WHO) and U.S. Environmental Protection Agency (EPA) maximum contaminant level (MCL) drinking water standard of 0.01 mg/L (WHO, 2001; EPA, 2009).

Previous studies with respect to As in ground water have focused largely on the ground water from Quaternary alluvial aquifers of the western Nevada from Carson Sink and Carson Desert (Welch et al., 1988; 1998, 2000). Because of the importance of ground water in irrigation and for mining and geothermal industries in and around the HRB area, understanding the processes that control As-enrichment in ground water is critical. This study is a reconnaissance study on the occurrence and distribution of arsenic in shallow ground water of the HRB and surrounding areas of northern Nevada (Figure 4.1) based on the available public-domain database from Nevada Bureau of Mines and Geology. The study area has been selected because of wide-ranging variability in As concentrations with a semi-arid climate that have been observed in many other regions including Chile, Mongolia, Mexico, and southwest USA (Robertson, 1989; Smedely and Kinniburgh, 2002; Romero et. al., 2003). Assessment of arsenic enrichment is also a critical issue because of the rapid growth of mining industries and geothermal power plants along with higher demands for water supplies by municipalities and agriculture in northern Nevada.

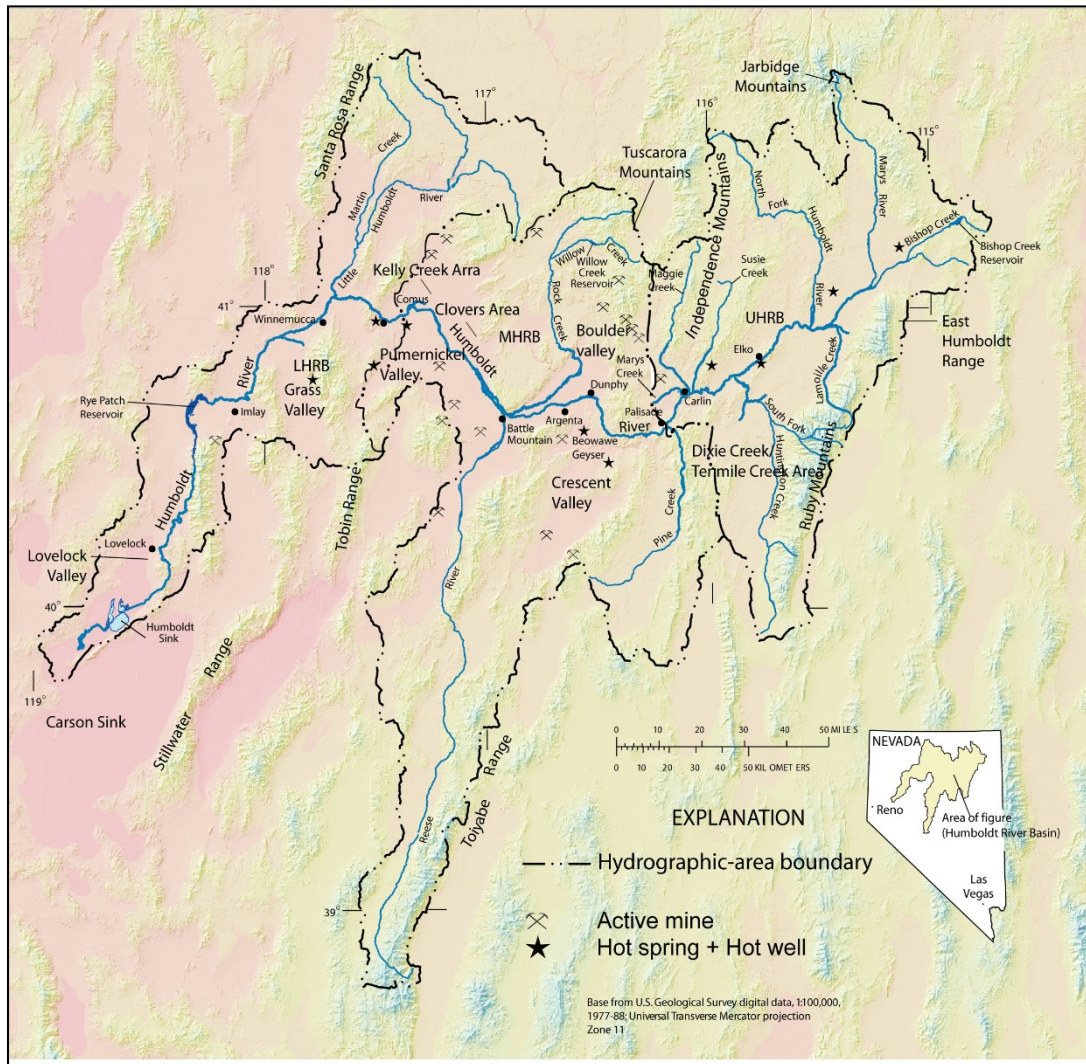


Figure 4.1: Shaded relief map of northern Nevada showing the location of Humboldt River Basin (HRB) (modified after Prudic et al., 2006). Note: UHRB: Upper Humboldt River Basin; MHRB: Middle Humboldt River Basin; LHRB: Lower Humboldt River Basin.

4.2. Study area and background

The HRB is a natural, internally drained river basin that covers approximately 43,700 km² (Figure 4.1). It forms a substantial part of the Basin and Range physiographic province, which is the one of the most arid areas in the U.S.A. (Yager and Folger, 2003). The basin is formed by a number of streams and tributaries that originate in the mountains of north-central and north-eastern Nevada. The HR (Humboldt River) river flows from east to west and then southwest towards the Humboldt Sink. The HRB includes the upper reaches of the Little Humboldt River in Elko County, the north-flowing Reese River in Lander and Nye Counties, and the main Humboldt River and its many tributaries that flow westward into the Humboldt Sink. It is a significant source of water for municipal uses, irrigation, and mining-related activities. The basin and its surrounding areas is one of the leading producers of gold, silver, copper, mercury, and tungsten in the U.S. since the mid-1800s (Wallace et al., 2004).

4.2.1. Geologic and hydrogeologic framework

The geologic and hydrogeologic settings of the study area is described in details in Chapter 2. Figure 2.2 in Chapter 2 illustrates schematic surface geology of northern Nevada and HRB. Table 2.1 in Chapter 2 lists the hydrogeologic units in northern Nevada including the HRB area. Much of the Great Basin is underlain by consolidated to semi-consolidated sedimentary deposits ranging in age from Proterozoic to Cenozoic. Among these units, carbonate rocks constitute deeper regional aquifers, whereas the overlying clastic sedimentary rocks of Tertiary and Quaternary constitute

shallow alluvial aquifers ranging only tens to few hundreds of meters in depth (Plume, 1996).

Figure 2.3 in Chapter 2 illustrates the schematic hydrogeologic cross section showing the aquifers of interest for this study. In general, the aquifers of this study consist primarily of basin-fill sediments with some volcanic rocks that were deposited in individual alluvial basins. The older basin-fill deposits consist of consolidated to semi-consolidated deposits of conglomerate, sandstone, siltstone, claystone, freshwater limestone, and evaporites (Yager and Folger, 2003). The younger basin-fill deposits consist of mostly unconsolidated to semi-consolidated and unsorted to poorly sorted clay, silt, sand, gravel, and boulders that make up the uppermost part of the basin-fill stratigraphy. Numerous extensional faulting have compartmentalized many of the Tertiary volcanic rocks (e.g., welded and non-welded tuffs), which constitute the confined aquifers in the HRB. These aquifers are relatively at deeper level underlying the basin-fill deposits of the Quaternary alluvial aquifers (Yager and Folger, 2003).

Faults and related fractures can act as enhanced conduits for ground water flow, but also can act as barriers and impede flow where hydrogeologic units of differing permeability (e.g., carbonate against clastic sedimentary rocks) are juxtaposed or where the fault-plane is filled by fault gouge (Reiner et al., 2002).

In general, the ground water in the HRB moves from recharge areas along the mountain fronts to discharge as seepage to stream channels, and evapotranspiration on the valley floors. Recharge also occurs in mountainous areas underlain by carbonate rocks. The main discharge area in the Humboldt River Basin is the river flood plain, which can be as much as a mile wide (Plume, 1995).

4.3. Methods

4.3.1. Ground water data collection and compilation

In this study, we used the most recently updated water quality data available in the public domain from the Great Basin Center for Geothermal Research (GBCGR) at the Nevada Bureau of Mines and Geology (NBMG) (<http://www.unr.edu/Geothermal/GeochemDB.htm>). The database contains more than 47,500 samples of thermal and non-thermal ground waters from 18,800 springs and wells throughout the Great Basin. This geochemical database of water samples, including all ground water samples, both hot or cold, have been integrated with the U.S. Geological Survey-NWIS (National Water Information System) database (<http://water.usgs.gov/nv/nwis/qw>). Additional ground water quality data from the Bureau of Mining Regulation & Reclamation of Nevada Division of Environmental Protection (NDEP; www.ndep.nv.gov) were incorporated in this study. This combined database contains geochemical information that includes major ions (HCO_3^- , SO_4^{2-} , Cl^- , Ca^{2+} , Mg^{2+} , Na^+ , K^+), minor and trace elements (including total As) of ground water samples in the Great Basin by geographic coordinates and sampling date. The data were processed and selected using the following criteria: 1) data that had complete suite of chemical constituents including major ions and trace elements with dissolved As, pH, electrical conductivity, and TDS; 2) data that were within the $\pm 5\%$ error margin of charge balance; 3) the wells that were located within the HRB boundary; and 4) the wells that were within the Tertiary Valley-fill aquifers and Quaternary Alluvial aquifers. For multiple data from a single well, the median of the data were selected to prevent duplication.

The wells that have been used in this study were installed as part of the U.S. Geological Survey-ground water level monitoring program for the shallow ground water within the Quaternary and Tertiary alluvial aquifers in the valley-fill deposits (Maurer et al., 1996; Plume, 1995; 1996). The water data from NDEP were part of ground water monitoring programs for the mining industries in the Maggie Creek Basin, Boulder Valley, and the Pumpernickel Valley areas. The ground water from the monitoring wells in Maggie Creek and Boulder Valley area are from Tertiary Volcanic Valley-fill deposits, whereas the ground water from monitoring wells in the Pumpernickel Valley and Clover Valley/Kelley Creek Basin are mostly from the Quaternary Alluvial aquifers.

4.3.2. Analytical methods of the samples in database

All of the ground water samples were collected following the standard sampling protocol of EPA. Samples from NWIS were analyzed in the USGS-National Water Quality Laboratory of Denver, Colorado, and samples from the NBMG were analyzed in the Nevada State Health Laboratory (<http://www.unr.edu/Geothermal/GeochemDB.htm>). Analytical results were reported in mg/L for the major- and trace-element chemistry. Only few data contained isotope data in the database, and therefore were not used in this study.

4.3.3. Data analysis

In order to assess the ground water geochemistry and arsenic enrichment, we investigated the data by using two approaches. First, we investigated data to determine the geochemistry and evolved water chemistry by applying qualitative geochemical tools such as Piper diagrams and various qualitative techniques such as source-rock deduction (Hounslow, 1995) and correlations between As and

geochemical parameters. Second, we investigated the relationship of As with various geochemical parameters by applying statistical factor analysis. To achieve these goals, the data were subdivided into three groups based on the geographical distribution of data in different sub-catchment basins (Figure 4.2). The three groups are:

- 1) Group I: Samples distributed between Carlin and Battle Mountain which includes Maggie Creek Basin, Willow Creek and Rock Creek Basin, Boulder Valley in the north of the HR, and Argenta and Crescent Valley in the south of the HR.
- 2) Group II: Samples distributed in the Clover Valley/Kelly Creek Basin bounded by Little Humboldt River in the north, and areas around Golconda and Pumpnickel Valley in the south of the HR.
- 3) Group III: Samples distributed between Rye Patch Reservoir and the Humboldt Sink which includes the Lovelock Valley, and surrounding areas of the lower HRB region northwest of Carson Sink.

Table 4.1 summarizes the ground water quality data that were used in this study, and Table 4.2 summarizes descriptive statistics of these data. Figure 4.3 illustrates the histograms of various chemical parameters and dissolved As in the waters.

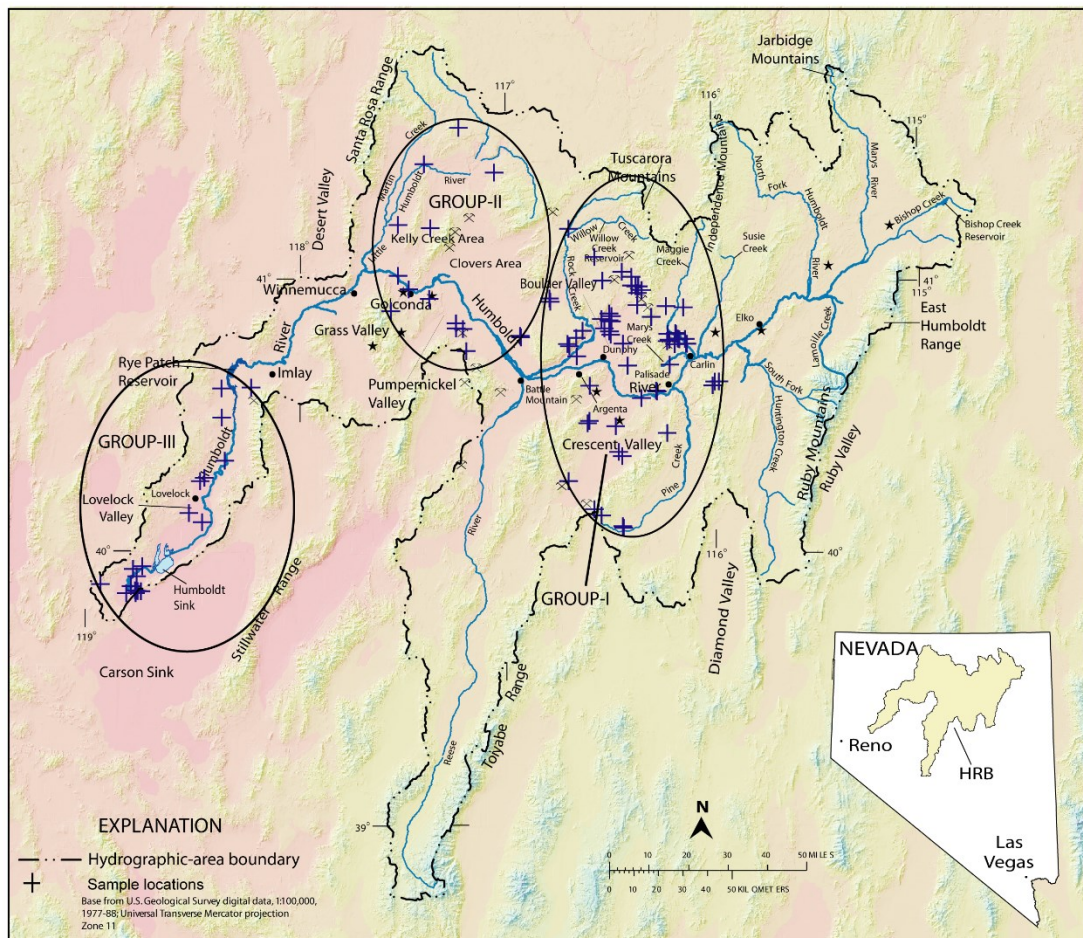


Figure 4.2: Map of Humboldt River Basin and Northern Nevada illustrating the locations of ground water samples that have been used in this study. The samples have been grouped into three groups as Group-I, II, and III (see text for information about the geographic locations).

Table 4.1: Summarized physical and important chemical components of ground water samples included in this study. Concentrations are in mg/L unless otherwise stated. Source: U.S. Geological Survey, <http://waterdata.usgs.gov/nwis>; NDEP. TEMP: Temperature (°C); COND: Conductivity (µS/cm); n.d.: No Data.

Group	TEMP	COND	pH	TDS	K	Na	Ca	Mg	SiO ₂	As	B	Ba	Br	Cl	F	Fe	HCO ₃	Li	Mn	SO ₄
	n.d.	86	7.1	56	1.51	9.8	6.3	1.7	41.2	0.017	n.d.	0.11	n.d.	4.5	0.19	0.45	34	n.d.	0.008	6.7
	n.d.	970	7.1	630	3.45	36.5	108	59.2	43	0.004	n.d.	0.11	n.d.	33.7	0.19	3.37	338	n.d.	0.53	183
	n.d.	447	6.8	290	3.10	27.3	18	4.8	46	0.013	n.d.	0.07	n.d.	17.3	0.11	1.1	86	n.d.	0.317	91.4
	12	466	7.3	303	8.80	30	43	12.0	50	0.012	n.d.	0.11	n.d.	19	0.5	0.004	196	0.05	0.001	51
	14.5	495	7.5	345	15	35	45	13.0	50	0.012	n.d.	0.08	n.d.	27	0.5	0.02	205	0.05	0.009	56
	14.5	495	7.1	497	15	35	45	13.0	50	0.012	n.d.	0.08	n.d.	27	0.5	0.02	205	0.05	0.009	56
	13.5	610	7.7	368	23	41	44	14.0	44	0.01	n.d.	0.09	n.d.	25	0.5	0.04	210	0.06	0.03	65
	13.5	610	7.7	396	23	41	44	14.0	44	0.052	n.d.	0.09	n.d.	25	0.5	0.04	210	0.06	0.03	65
	14	382	6.9	233	4.3	34	27	9.8	38	0.015	n.d.	0.1	n.d.	23	0.3	0.02	116	0.01	0.001	46
	n.d.	385	7.4	250	6.12	34.7	56.3	12.0	41	0.183	n.d.	0.09	n.d.	14.5	0.42	0.06	133	n.d.	0.004	28.6
Group-I	n.d.	354	7.1	230	5.48	37.9	48.6	10.4	46	0.072	n.d.	0.18	n.d.	19.9	0.4	0.06	125	n.d.	0.004	28.5
	n.d.	385	7.1	250	6.41	36.2	54.2	11.2	38	0.073	n.d.	0.09	n.d.	22.8	0.47	0.06	130	n.d.	0.004	30.8
	n.d.	370	7.5	240	5.14	39.5	41.5	10.6	39	0.076	n.d.	0.08	n.d.	15.3	0.47	0.06	133	n.d.	0.017	27.6
	n.d.	770	7.3	500	12.5	64.6	112.4	22.7	37	0.043	n.d.	0.2	n.d.	98.2	0.33	0.06	126	n.d.	0.004	44.2
	n.d.	385	7.4	250	4.65	31.3	52.3	9.0	41	0.089	n.d.	0.05	n.d.	18.4	0.48	0.06	112	n.d.	0.004	25.5
	n.d.	277	7.2	180	5.12	32.5	37.5	5.9	42	0.087	n.d.	0.1	n.d.	13.3	0.48	0.06	90	n.d.	0.004	19.7
	10.5	510	7.7	331	1.48	13.3	72.4	7.1	26.4	0.012	0.01	n.d.	0.04	8.9	0.07	0.01	273	n.d.	0.002	9.7
	n.d.	431	7.7	280	4.26	26.4	43.8	9.8	38	0.072	n.d.	0.08	n.d.	27	0.52	0.06	129	n.d.	0.013	31.5
	29	476	7.3	445	8.70	32	48	16.0	19	0.052	n.d.	0.11	n.d.	11	1.2	0.02	244	0.11	0.06	46
	12	370	8.0	240	5.32	24.7	30.8	7.7	51.1	0.008	0.01	n.d.	0.13	25.1	0.33	0.01	133	n.d.	0.002	24.2
	n.d.	616	7.2	400	6.54	34.2	56.2	16.5	37	0.058	n.d.	0.12	n.d.	46	0.39	0.06	121	n.d.	0.02	49.8
	14	382	7.2	337	4.30	34	27	9.8	38	0.015	n.d.	0.1	n.d.	23	0.3	0.02	116	0.01	0.001	46

Continued to next page

	TEMP	COND	pH	TDS	K	Na	Ca	Mg	SiO ₂	As	B	Ba	Br	Cl	F	Fe	HCO ₃	Li	Mn	SO ₄
	10	504	7.7	327	2.48	36.1	69.0	8.0	47.7	0.003	0.058	n.d.	0.050	8.4	1.98	0.07	304	n.d.	0.06	23.6
	17.8	662	7.4	430	1.85	25.8	93.8	18.2	50.3	0.003	0.079	0.003	0.250	39.9	0.20	0.008	310	0.015	0.001	23.6
	16	379	7.4	230	2.1	24.0	34.0	18	47.0	0.007	n.d.	0.1	n.d.	7.3	0.20	0.02	226	0.013	0.001	6.3
	16	379	7.4	246	2.1	24.0	34.0	18	47.0	0.032	n.d.	0.1	n.d.	7.3	0.20	0.02	226	0.013	0.001	6.3
	18	389	7.2	413	5.5	27.0	37.0	14	51.0	0.086	n.d.	0.03	n.d.	18.0	0.40	0.09	152	0.015	0.049	57
	19.5	336	6.8	218	6.0	26.0	30.0	10	56.0	0.070	n.d.	0.03	n.d.	18.0	0.40	0.38	131	0.006	0.051	40
	22.5	339	7.5	192	3.6	14.0	29.0	18	19.0	0.070	n.d.	0.08	n.d.	9.8	0.40	0.05	160	0.023	0.002	34
	22.5	339	7.9	307	3.6	14.0	29.0	18	19.0	0.070	n.d.	0.08	n.d.	9.8	0.40	0.05	160	0.023	0.002	34
	28	860	6.7	559	12	58.0	95.0	26	36.0	0.400	n.d.	0.08	n.d.	32.0	0.60	0.11	381	0.150	0.03	100
	49	1000	6.8	611	23	81.0	94.0	23	37.0	0.030	n.d.	0.15	n.d.	16.0	1.30	0.54	525	0.350	0.06	73
	22	682	7.8	443	2.9	32.0	48.0	42	5.3	0.007	n.d.	0.05	n.d.	38.0	0.50	0.005	299	0.020	0.16	75
	17.5	418	7.6	290	7.7	40.0	30.0	7.4	60.0	0.007	n.d.	0.06	n.d.	23.0	0.60	0.02	168	0.024	0.004	31
	17.5	418	7.6	271	7.7	40.0	30.0	7.4	60.0	0.011	n.d.	0.06	n.d.	23.0	0.60	0.02	168	0.024	0.004	31
Group-I	45	981	6.4	582	22	77.0	100	25.0	34.0	0.002	n.d.	0.17	n.d.	14.0	1.10	0.18	537	0.330	0.01	64
	26	554	7.3	379	13	47.0	56.0	11.0	51.0	0.003	n.d.	0.05	n.d.	19.0	0.50	0.01	234	0.088	0.11	84
	11.5	343	7.9	223	5.69	48.4	20.2	8.7	50.3	0.004	0.04	n.d.	0.030	10.1	0.29	0.01	180	n.d.	0.03	42.1
	12.5	360	8.1	234	1.68	10.1	39.4	15.1	17.6	0.005	0.03	n.d.	0.020	2.9	0.08	0.01	206	n.d.	0.001	10.9
	35	948	7.0	917	21	72.0	100	27.0	23.0	0.011	n.d.	0.11	n.d.	14.0	1.00	0.32	573	0.290	0.03	62
	13.2	340	7.9	221	1.37	14.4	45.2	13.5	18.0	0.003	0.04	n.d.	0.040	7.2	0.29	0.01	210	n.d.	0.002	16
	13.7	330	7.9	214	3.98	15.8	30.2	11.2	44.7	0.008	0.06	0.10	0.09	11.9	0.20	0.21	145	0.008	0.02	17.9
	15	567	7.1	357	9.6	39.0	54.0	13.0	57.0	0.006	n.d.	0.09	n.d.	35.0	1.00	0.005	239	0.067	0.001	41
	15.5	624	7.5	559	11	39.0	56.0	12.0	60.0	0.006	n.d.	0.08	n.d.	24.0	1.70	0.005	251	0.081	0.001	44
	15	567	7.1	368	9.6	39.0	54.0	13.0	57.0	0.022	n.d.	0.09	n.d.	35.0	1.00	0.005	239	0.067	0.001	41
	n.d.	359	7.7	232	6	23.1	32.9	8.8	52.0	0.010	n.d.	0.08	n.d.	11.3	0.60	0.02	150	n.d.	0.003	30.5
	14.5	1030	7.4	662	12	110	74.0	19.0	58.0	0.022	n.d.	0.03	n.d.	92.0	1.00	0.004	268	0.082	0.001	180

Continued to next page

	TEMP	COND	pH	TDS	K	Na	Ca	Mg	SiO ₂	As	B	Ba	Br	Cl	F	Fe	HCO ₃	Li	Mn	SO ₄
	14.5	1030	7.7	872	12.0	110.0	74.0	19.0	58.0	0.022	n.d.	0.03	n.d.	92	1.0	0.004	268	0.08	0.001	180
	n.d.	722	7.8	469	10.9	57.8	74.6	18.0	41.2	0.04	n.d.	0.06	n.d.	19.1	1.0	0.02	318	n.d.	0.006	67.3
	n.d.	290	7.8	212	5.50	17.7	28.6	6.1	51.0	0.01	n.d.	0.08	n.d.	9.6	0.60	0.02	118	n.d.	0.004	26.4
	20	418	6.9	310	12.0	32.0	39.0	4.0	73.0	0.002	n.d.	0.03	n.d.	38	0.40	0.14	150	0.02	0.04	21.0
	20	418	6.9	271	12.0	32.0	39.0	4.0	73.0	0.11	n.d.	0.10	n.d.	38	0.40	0.14	150	0.02	0.04	21.0
	11.5	310	8.0	201	0.87	5.1	31.7	18.5	13.4	0.02	0.04	n.d.	0.02	2.1	0.10	0.01	188	n.d.	0.002	7.9
	n.d.	452	7.9	305	4.40	53.4	35.0	9.1	15.0	0.01	n.d.	0.06	n.d.	22.1	0.90	0.02	189	n.d.	0.005	28.8
	28.5	682	6.9	513	5.30	37.0	83.0	14.0	14.0	0.11	n.d.	0.03	n.d.	16	1.90	2.00	95	0.100	0.34	230
	12.2	432	7.7	281	2.00	8.2	67.5	13.4	19.1	0.001	0.05	0.04	0.04	5.8	0.20	0.06	248	0.006	0.006	19.9
	16	1040	7.7	675	24.4	144.0	59.4	40.5	49.6	0.004	0.04	n.d.	0.66	114	1.21	2.62	237	n.d.	0.08	300
	32.2	593	7.4	385	5.84	28.5	62.1	19.3	28.2	0.005	0.14	0.12	0.07	8.1	0.60	0.24	315	0.07	0.06	45.5
Group-I	n.d.	492	8.2	274	8.50	50.9	31.4	9.9	28.5	0.01	n.d.	0.10	n.d.	34.9	1.40	0.02	231	n.d.	0.05	61.2
	14.5	610	7.3	362	6.80	46.0	61.0	12.0	30.0	0.005	n.d.	0.15	n.d.	34	0.40	0.03	273	0.04	0.03	49.0
	14.5	610	7.8	542	6.80	46.0	61.0	12.0	30.0	0.005	n.d.	0.15	n.d.	34	0.40	0.03	273	0.04	0.03	49.0
	n.d.	559	7.1	349	10.1	39.7	55.2	12.9	31.2	0.01	n.d.	0.07	n.d.	16.8	1.40	0.02	237	n.d.	0.006	50.6
	n.d.	493	8.5	298	9.40	52.2	38.2	7.7	52.0	0.02	n.d.	0.07	n.d.	16.6	1.90	0.02	229	n.d.	0.03	30.7
	10	259	7.6	200	3.90	22.0	22.0	4.9	52.0	0.006	n.d.	0.07	n.d.	15	0.30	0.007	107	0.02	0.001	26.0
	10	259	7.6	305	3.90	22.0	22.0	4.9	52.0	0.006	n.d.	0.07	n.d.	15	0.30	0.007	107	0.02	0.001	26.0
	n.d.	431	7.5	280	7.41	38.4	61.2	13.2	52.3	0.147	n.d.	0.13	n.d.	20.5	0.58	0.06	142	n.d.	0.004	35.0
	21	405	7.3	263	7.10	38.0	33.0	5.9	54.0	0.016	n.d.	0.05	n.d.	36	0.50	0.54	143	0.03	0.14	28.0
	21	405	7.3	273	7.10	38.0	33.0	5.9	54.0	0.003	n.d.	0.05	n.d.	36	0.50	0.54	143	0.03	0.14	28.0
	19	419	7.9	292	8.90	43.0	27.0	6.4	63.0	0.016	n.d.	0.07	n.d.	30	1.50	0.01	152	0.08	0.001	34.0
	19	419	8.0	429	8.90	43.0	27.0	6.4	63.0	0.016	n.d.	0.07	n.d.	30	1.50	0.01	152	0.08	0.001	34.0
	9.5	523	8.1	491	4.00	34.0	46.0	15.0	58.0	0.07	0.10	n.d.	n.d.	48	0.20	0.04	177	n.d.	0.03	51.0
Group-II	n.d.	339	8.5	220	2.48	25.8	32.8	10.9	56.7	0.009	n.d.	0.06	n.d.	17.8	0.30	0.06	129	n.d.	0.007	38.9
	n.d.	653	7.9	424	10.8	67.3	41.9	11.7	54.6	0.007	n.d.	0.08	n.d.	35.5	0.56	0.06	229	n.d.	0.007	48.5

Continued to next page

	TEMP	COND	pH	TDS	K	Na	Ca	Mg	SiO ₂	As	B	Ba	Br	Cl	F	Fe	HCO ₃	Li	Mn	SO ₄
Group-II	11	3220	8.1	1940	1.30	530	100	22.0	52.0	0.011	0.72	n.d.	n.d.	730	0.60	0.04	182	n.d.	0.14	270
	n.d.	519	8.0	337	8.70	60.0	26.7	6.2	51.3	0.012	n.d.	0.07	n.d.	20.7	0.51	0.06	174	n.d.	0.006	41.0
	n.d.	561	8.2	364	6.60	57.3	42.8	13.1	48.2	0.006	n.d.	0.06	n.d.	20.8	0.72	0.06	243	n.d.	0.003	47.3
	14	1000	7.7	695	13.0	120	51.0	14.0	48.0	0.003	0.30	n.d.	n.d.	210	0.60	0.31	155	n.d.	0.94	34.0
	13	411	7.5	390	4.00	26.0	38.0	11.0	39.0	0.010	0.09	n.d.	n.d.	24.0	0.20	0.006	183	n.d.	0.001	26.0
	14	720	7.5	681	10.0	150	22.0	7.7	21.0	0.022	0.35	n.d.	n.d.	42.0	0.50	0.09	308	n.d.	0.27	98.0
	8.5	690	8.0	616	13.0	100	25.0	7.1	67.0	0.010	0.46	n.d.	n.d.	90.0	0.50	0.16	216	n.d.	0.24	30.0
	14	1680	8.0	1179	16.0	240	64.0	19.0	55.0	0.029	1.10	n.d.	n.d.	270	0.40	0.09	259	n.d.	0.34	200
	14	737	8.1	614	8.40	100	40.0	11.0	31.0	0.025	0.60	n.d.	n.d.	76.0	0.50	0.09	227	n.d.	0.002	89.0
	6.0	1970	7.7	1294	3.20	210	75.0	72.0	21.0	0.003	0.48	n.d.	n.d.	370	0.30	0.01	201	n.d.	0.001	320
Group-III	16	628	7.9	408	34.0	82.0	19.0	11.0	50.0	0.058	n.d.	0.04	0.05	16.0	0.60	0.003	320	n.d.	0.001	27.0
	16	779	7.9	506	3.40	140	23.0	6.8	32.0	0.002	0.73	0.02	0.08	44.0	0.40	0.013	266	0.04	0.001	100
	20	833	8.5	541	5.97	181	4.6	2.1	57.3	0.046	n.d.	n.d.	0.46	94.9	1.00	1.23	279	n.d.	0.16	24.0
	n.d.	1494	8.2	970	22.0	320	21.0	2.5	55.2	0.011	n.d.	0.58	n.d.	360	0.90	0.05	300	n.d.	0.07	14.0
	15.5	1460	8.1	948	12.0	220	69.0	17.0	65.0	0.042	0.98	n.d.	n.d.	140	0.5		510	n.d.	0.001	130
	13	785	7.8	510	7.00	120	37.0	6.4	24.0	0.024	0.61	0.06	n.d.	46.0	0.40	0.003	249	0.05	0.001	110
	12.8	1350	8.5	877	10.0	270	14.0	3.5	32.0	0.019	0.96	0.009	n.d.	77.0	0.50	0.012	461	0.17	0.002	170
	12.9	1850	7.7	1201	19.0	260	110	18.0	27.0	0.033	n.d.	0.12	0.04	140	0.80	0.003	490	n.d.	0.50	290
	17	573	9.0	372	2.50	120	0.4	0.1	29.0	0.423	n.d.	n.d.	0.02	7.4	1.40	0.154	237	n.d.	0.03	42.8
	21	1080	8.7	701	8.69	244	2.3	0.7	49.8	0.023	n.d.	n.d.	0.21	109	1.40	0.015	407	n.d.	0.007	18.3
	15	2450	8.0	1591	8.10	590	2.4	3.3	41.0	0.550	n.d.	0.03	0.29	170	2.50	0.031	1280	n.d.	0.14	4.6
	14	1190	7.6	773	10.0	200	41.0	11.0	42.0	0.100	n.d.	0.04	0.03	33.0	1.00	0.003	483	n.d.	0.60	160
	13	1380	7.2	896	8.10	140	110	30.0	31.0	0.031	1.20	0.15	0.05	58.0	0.30	0.003	508	0.08	1.00	220
	20	444	8.6	288	5.15	93.9	1.6	0.1	50.8	0.029	n.d.	n.d.	0.01	8.0	0.80	0.04	209	n.d.	0.015	32.6
	13.5	1250	7.5	812	5.80	190	47.0	14.0	33.0	0.140	1.20	0.09	0.01	110	1.00	0.23	429	0.05	1.00	130
	21	1440	8.2	935	7.62	253	23.8	1.6	47.5	0.046	n.d.	n.d.	0.66	317	0.50	0.01	108	n.d.	0.06	94.0
	13.2	920	7.2	597	7.70	72.0	86.0	20.0	21.0	0.008	n.d.	0.19	0.05	63.0	0.30	0.003	282	n.d.	0.17	140
	15	418	7.6	271	1.70	27.0	41.0	11.0	52.0	0.065	n.d.	0.03	0.02	15.0	0.90	0.003	182	n.d.	0.05	39.0
21	367	7.0	238	2.50	27.0	32.0	7.7	28.0	0.005	n.d.	0.05	0.02	16.0	0.40	0.003	120	n.d.	0.001	52.0	

Table 4.2: Descriptive statistics of physical parameters of the ground water data used in this study.

	Group-I					Group-II					Group-III				
	Min.	Max.	Mean	Median	Std. Dev.	Min.	Max.	Mean	Median	Std. Dev.	Min.	Max.	Mean	Median	Std. Dev.
TEMP	10	49	17.27	16	8.04	6	19	11.76	13.50	3.66	12.80	21.00	15.87	15.50	3.02
COND	86.24	1040	466.4	431.6	206.8	338.8	3220	762.89	671.48	806.09	367	2450	963.08	1080	537.2
pH	6.40	8.50	7.42	7.41	0.40	7.50	8.45	7.94	8	0.26	7	9	7.94	7.90	0.55
TDS _c	56	916.7	319.5	297.1	155.4	220	1940.1	580.8	552.6	472.09	238.3	1590.9	625.4	701.3	348.8
K	0.87	24.4	5.98	5.92	5.64	1.30	16	6.43	8.55	4.47	1.70	34	7.31	7.7	7.86
Na	5.11	144	32.04	34.43	23.19	25.80	530	85.36	83.65	133.92	27	590	146.5	181	128.8
Ca	6.28	112.4	43.74	44	22.72	22	100	41.15	40.95	21.75	0.36	110	17.19	23.8	34.76
Mg	1.74	59.2	11.97	12.45	9.12	6.16	72	12.67	11.35	16.70	0.11	30	4.30	6.80	8.13
SiO ₂	5.30	73	38.27	44	14.51	21	67	44.94	51.65	14.43	21	65	38.42	41	12.87
As	0.001	0.40	0.02	0.01	0.06	0.003	0.07	0.01	0.01	0.02	0.002	0.55	0.04	0.03	0.15
B	0.01	0.14	0.04	0.05	0.03	0.09	1.10	0.36	0.46	0.32	0.61	1.20	0.92	0.97	0.24
Ba	0.003	0.20	0.07	0.08	0.04	0.06	0.09	0.07	0.07	0.01	0.01	0.58	0.06	0.05	0.15
Br	0.02	0.66	0.06	0.05	0.17	n.d.	n.d.	n.d.	n.d.	n.d.	0.01	0.66	0.05	0.05	0.18
Cl	2.06	114	18.38	18.7	20.86	17.80	730	67.57	45	201.39	7.36	360	56.31	63	98.68
F	0.07	1.98	0.49	0.5	0.45	0.20	1.50	0.46	0.50	0.32	0.30	2.50	0.70	0.80	0.53
Fe	0.004	3.37	0.04	0.04	0.55	0.01	0.31	0.05	0.06	0.08	0.003	1.23	0.01	0.01	0.29
HCO ₃	34	573	188.3	192.5	99.8	129	308	197.4	192	47.98	108	1280	318.8	300	254.5
Li	0.01	0.35	0.03	0.03	0.08	0.09	0.09	0.09	0.09	n.d.	0.04	0.17	0.07	0.05	0.05
Mn	0.0002	0.53	0.01	0.01	0.08	0.001	0.94	0.02	0.01	0.26	0.001	1	0.03	0.06	0.33
SO ₄	6.30	300	38.19	37.50	50.16	26	320	65.25	47.90	96.55	4.60	290	61.31	94	78.21

Note: TEMP: Temperature (°C); COND: Conductivity (μS/cm); Min: Minimum; Max: Maximum; Std. Dev: Standard Deviation.

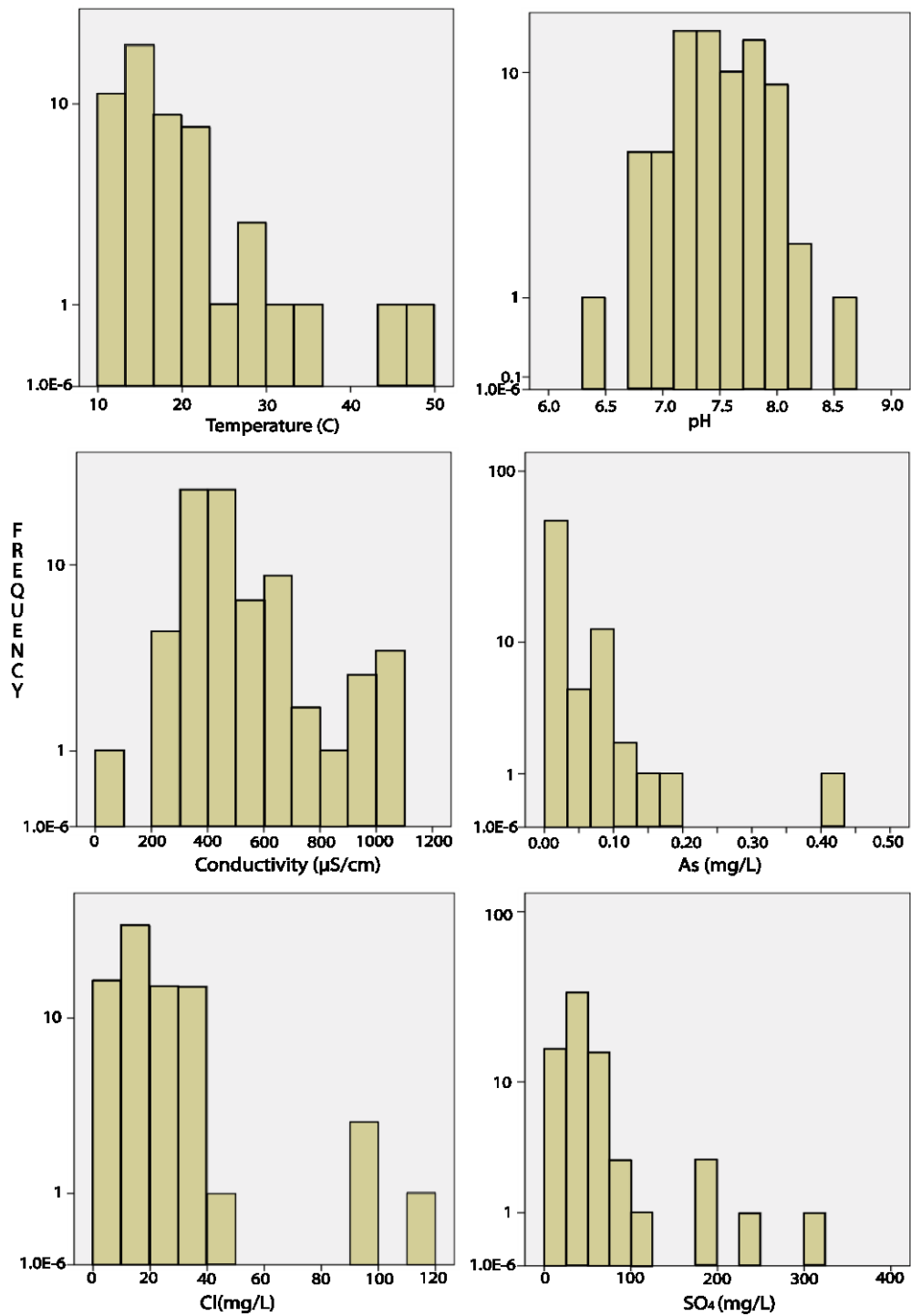


Figure 4.3A: Histograms illustrating variations of As concentrations and other chemical parameters in the ground water samples from Group-I.

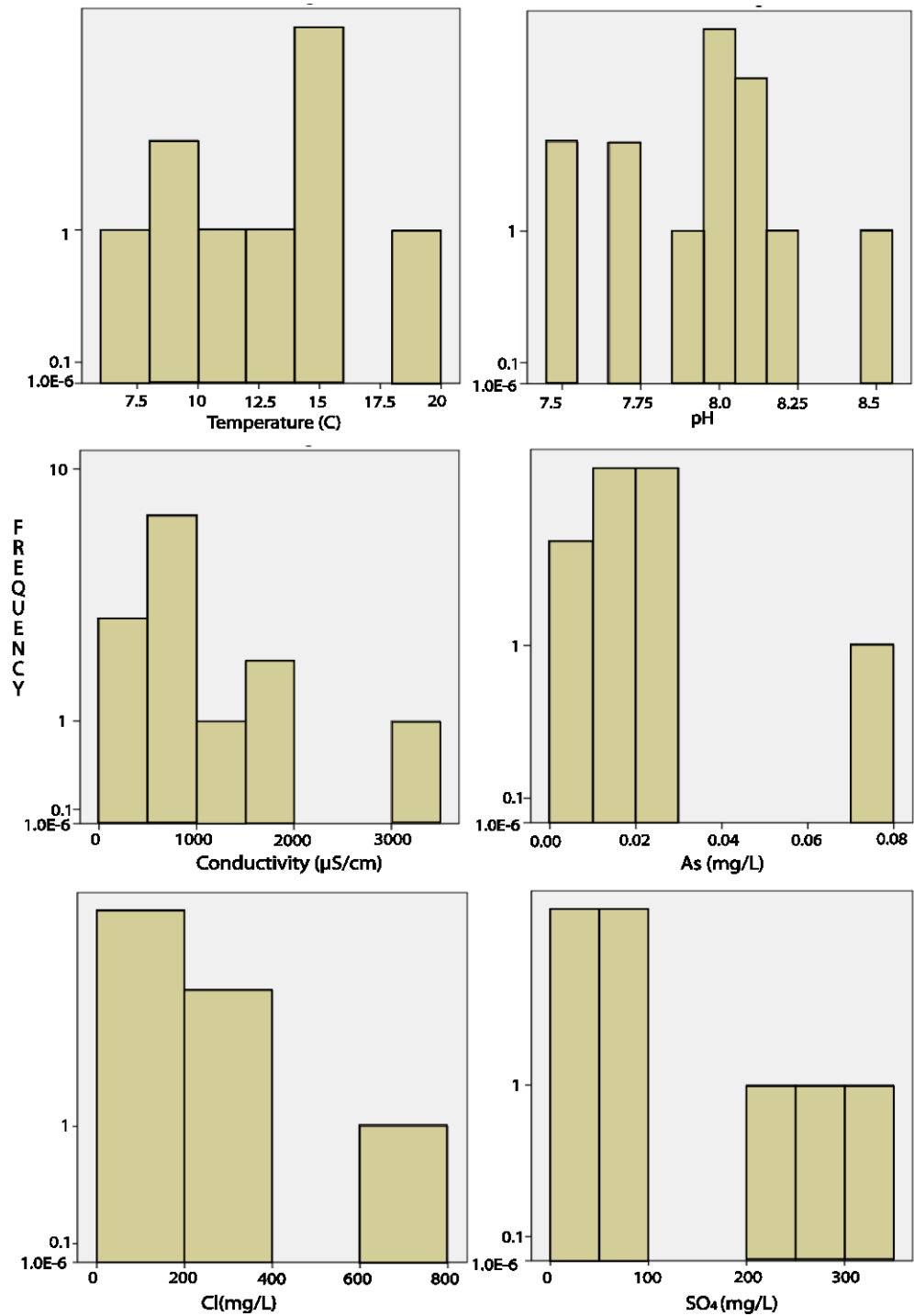


Figure 4.3B: Histograms illustrating variations of As concentrations and other chemical parameters in the ground water samples from Group-II.

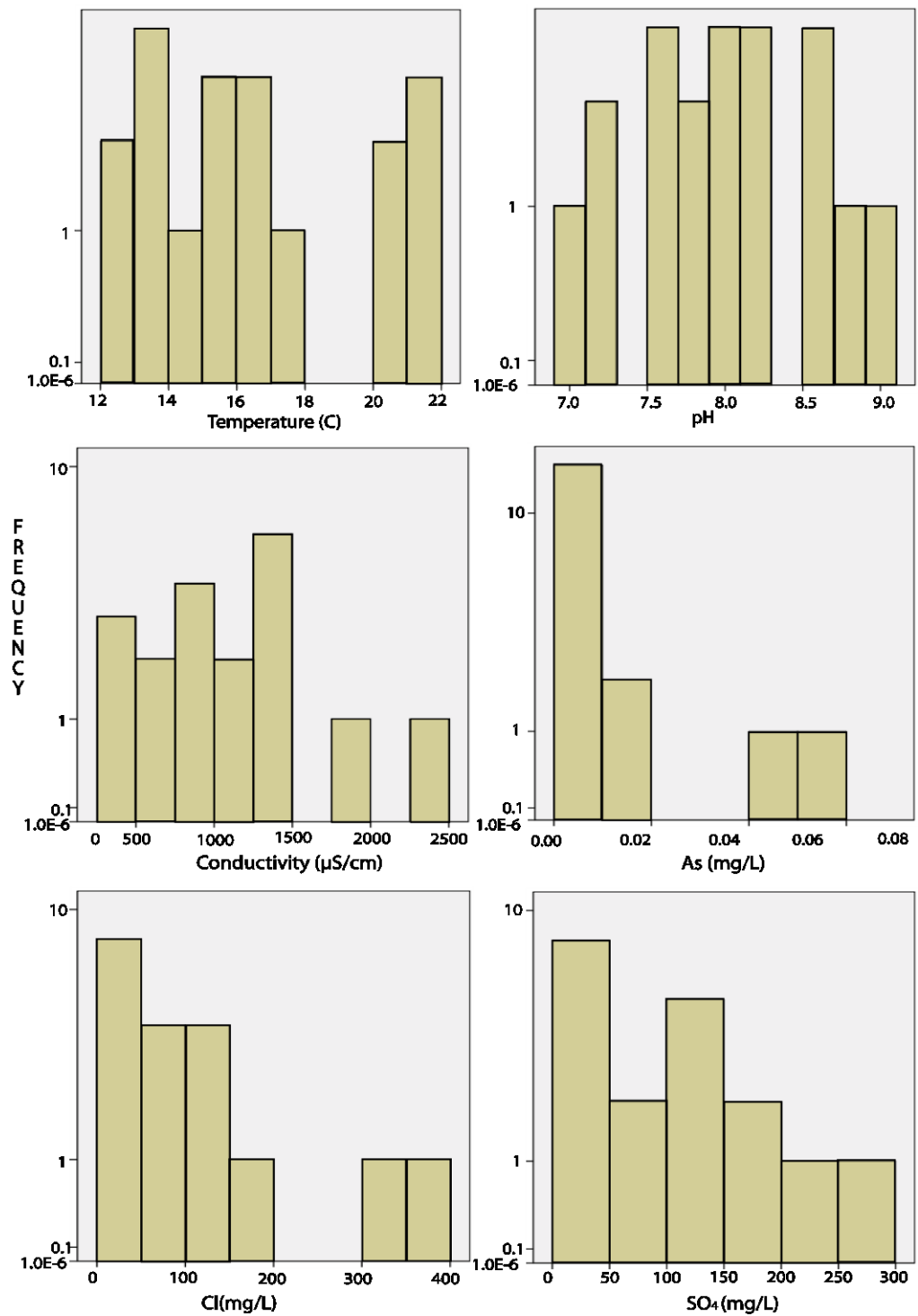


Figure 4.3C: Histograms illustrating variations of As concentrations and other chemical parameters in the ground water samples from Group-III.

4.3.4. Factor analysis

The water data in each group were analyzed using factor analysis to identify simple correlations between chemical parameters. Factor analysis is a method of sorting and displaying complex relationships among many variables (Usunoff and Guzman, 1989; Guler et al. 2002); in our case, the variables are chemical parameters. The method is useful in determining the geographical distribution of resulting factors as well as in determining the major processes that may control the distribution of hydrochemical variables (Stuben et al., 2003; Wang et al., 2007; Dongarra et al., 2009; Jang, 2010). These analyses were performed applying Principal Component Analysis (PCA) extraction method by using Statistical Package for Social Sciences (SPSS 16.0, 2007) software package. The PCA method computes the data in a linear combination of variables by extracting the maximum variance (Factor 1) from the chemical parameters. The computation is repeated to obtain additional factors that explain the rest of the variance (Factor 2, 3 and so on) of the chemical parameters. The resulting factor loadings, also known as component loadings in PCA, are the correlation coefficients between the variables and factors. Analogous to Pearson's r , the squared factor loading is the percent of variance in that indicator variable (i.e., chemical parameters) explained by the factor. The performance of these factor models can be assessed by the communalities, where the communality is the sum of the squared factor loadings for all factors for a given variable (row). In other words, it measures the percent of variance in a given variable explained by all the factors together and may be interpreted as the reliability of the indicator (Child, 2006). The individual communalities indicate how well the model is working for the individual variables, and the total communality gives an overall assessment of performance.

Assumptions and limitations

The basic assumptions in factor analysis are that the variables are linearly related and the multivariate normal distribution exists. Because the factor analysis method is based on the covariance or correlation matrix, the results are influenced by the similarities between samples, and consequently can be affected by extreme outliers or inadequate data sets (Davis, 2002).

One of the primary limitations of the factor analysis method is that it is often difficult to determine which solution is optimal and thus how many factors to retain in the final solution. Therefore, a more philosophical assumption is required that the underlying factors extracted from the data set represent physically meaningful processes. In practice, the simplest rule is to retain only factors whose eigenvalues are greater than one, because the sums of squares are normalized to unit variance; the magnitude of the eigenvalues provides a measure of their importance relative to the original variables (Davis, 2002).

In our study, the first step of factor analyses involved standardizing the raw data by converting them into dimensionless variables. Then the data were transformed into factors followed by determination of correlation matrix, eigenvalues and eigenvectors to yield the covariance matrix. Only factors with eigenvalues that exceed one were retained in this work (Reyment and Joreskog, 1993). In this study, the absolute value of factor loading 0.5 is used as a cutoff value (Wang et al., 2007). The terms, “strong” “moderate” and “weak” as applied to factor loadings, refer to absolute values of >0.75 , $0.75-0.5$, and $0.5-0.3$ respectively. Factor analyses for ground water were performed on the analytical results of water-chemistry and physical parameters that include pH, temperature, and electrical conductivity (EC).

4.4. Results

4.4.1. *Spatial distribution of arsenic*

A simplified spatial distribution of As is illustrated in Figure 4.4, where it is evident that samples with relatively high concentrations of As occur in the Group-I waters located in the Boulder Valley, Maggie Creek Basin, bounded by the Tuscarora Mountains and Independence Mountains on the north and east, respectively and the Humboldt River on the south. Another hotspot of high concentrations of As in ground water occurs in the Humboldt Sink and the Lovelock Valley, on the south-west corner of the study area. The samples with high concentrations of dissolved As (>0.01 mg/L) within Group-I are located within the known mines of sedimentary-rock hosted gold and polymetallic mineralized zones (Arehart et al., 1993; Wallace et al., 2004). The samples adjacent to or within the known geothermal hot springs, have dissolved As concentrations <0.01 mg/L. The ground water in this group are tapped mostly from the aquifers of Tertiary Volcanic sediments with some Quaternary Alluvial aquifers.

Samples within Group-II are located within the known active and closed mineralized zones (e.g., Lone Tree, Marigold, Twin Creeks), and geothermal hot springs (e.g., Golconda). The samples adjacent to or within the zone of geothermal hot spring and hot wells, concentration of dissolved As is found to be within the range from 0.001 to <0.1 mg/L, and the aquifers for these ground water are Quaternary alluvial aquifers.

On the other hand, the samples within Group-III are located in the Lovelock Valley around the enclosed sub-basins, where the Humboldt River discharges into the Humboldt Sink. In this area, shallow ground water have been extensively used for irrigation (Paul and Thodal, 2003), and potential evaporation predominates

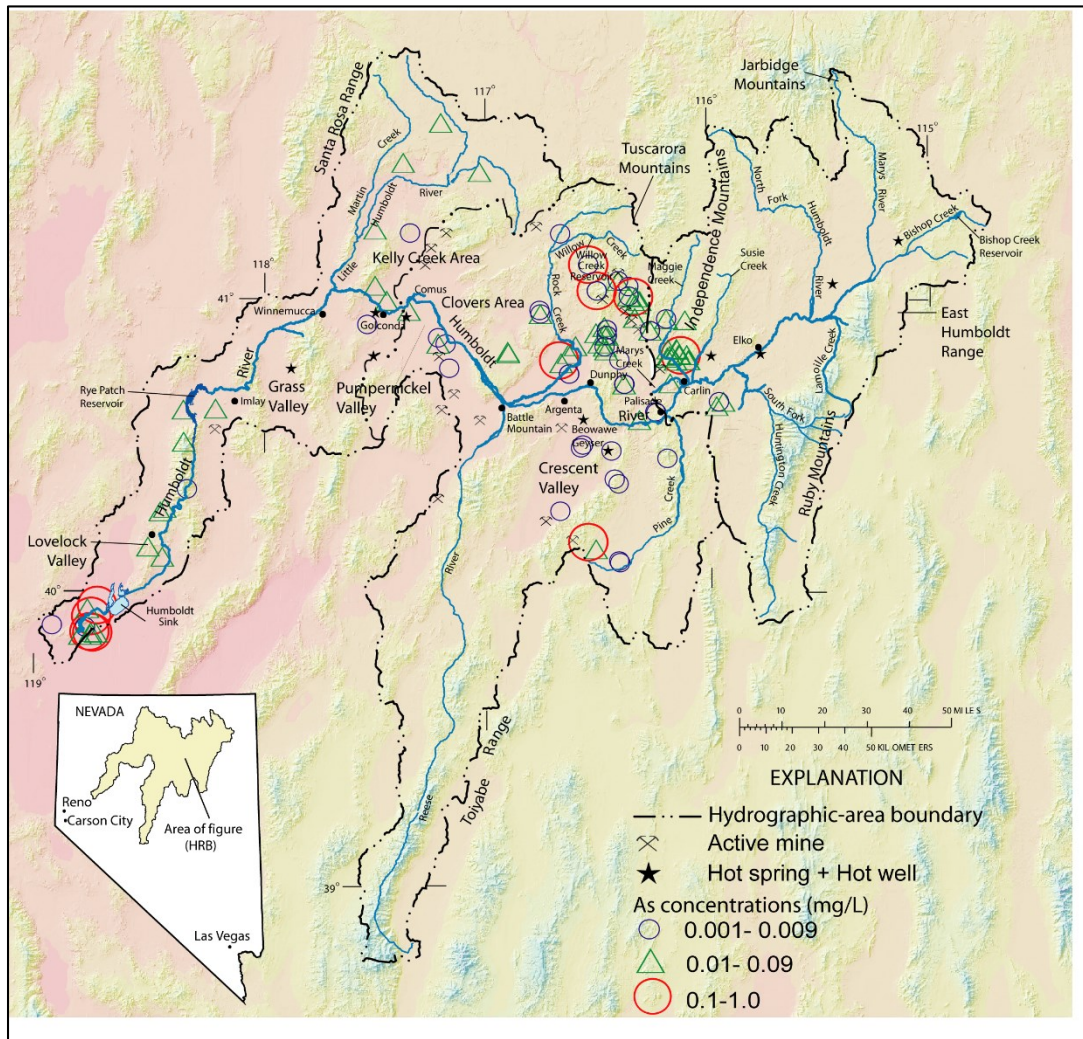


Figure 4.4: Map illustrating spatial distribution of dissolved As concentrations in ground water in mg/L in the HRB area.

(Shevenell, 1996). The high concentrations of dissolved As (>0.01 mg/L) with as much as >0.1 mg/L have been found in these ground water from Quaternary alluvial aquifers and also coincide with the Quaternary playa deposits around the Humboldt Sink.

Similarly, the spatial relationship of As distribution can be visually correlated to the geologic depositional dynamics of the HRB. For example, samples in Group I are associated with the relatively older Tertiary mafic volcanic rocks that make up the valley-fill aquifers, whereas samples from Group-II and III are associated with relatively recent Quaternary alluvial aquifers (Figure 2.2, Chapter 2). The valley-fill Tertiary mafic volcanic rocks were subjected to erosion during the post Miocene erosional activities and were recycled and transported downstream of the HRB and deposited in the MHR and LHRB during the Quaternary Period (Wallace et al., 2008).

4.4.2. Chemical composition of water samples

Table 4.1 lists selected chemical parameters of ground water with arsenic concentrations for each group, and Table 4.2 lists descriptive statistics of each parameters. Overall, the ground water are neutral to strongly alkaline with pH ranging from 6.4 to 9.0. The database used in this study contain only few data for dissolved oxygen but redox potential (i.e., Eh) data; and due to lack of redox couples (i.e., $\text{Fe}^{3+}/\text{Fe}^{2+}$, $\text{Mn}^{4+}/\text{Mn}^{2+}$), it was not possible to determine the exact redox condition of the waters. However, in general, the waters are inferred as aerobic to post-oxic as indicated with the presence of dissolved Fe^{2+} and Mn^{2+} and absence of NO_3 , PO_4 and H_2S in the waters (Appelo and Postma, 1996). The temperature and conductivity of the waters range from 6 to 49 °C and from 86.24 to 3,220 $\mu\text{S}/\text{cm}$ respectively.

Concentrations of As ranges from 0.001 to 0.55 mg/L with an average of 0.043 mg/L and median of 0.015 mg/L, with the highest concentrations occurring in the waters in Group-III.

Group-I waters

The water samples in Group-I are dominantly Ca-Na-HCO₃-type waters with some Ca-Mg-HCO₃ and Na-Ca-HCO₃-SO₄-types of waters (Figure 4.5). The pH in this group shows neutral to alkaline waters with a range from 6.4 to 8.5 (Table 4.2). The temperature and conductivity ranges from 10 to 49 °C and from 86 to 1040 μS/cm, respectively. Concentrations of dissolved As range from 0.001 to 0.4 mg/L. Concentrations of dissolved Fe and Mn range from 0.004 to 3.37 mg/L and 0.0002 to 0.53 mg/L respectively. Concentrations of dissolved SiO₂ and SO₄ range from 5.3 to 73 mg/L and 6.3 to 300 mg/L respectively. No mixing trend is observed in the Piper diagram for this group of waters (Figure 4.5).

Group-II waters

The water samples in Group-II are dominantly Na-HCO₃-type waters with some Na-Cl-type waters (Figure 4.5). The pH in this group shows alkaline waters with a range from 7.5 to 8.45 (Table 4.2). The temperature and conductivity ranges from 6 to 19 °C and from 339 to 3220 μS/cm respectively. The concentrations of As range from 0.003 to 0.07 mg/L. Concentrations of dissolved Fe and Mn range from 0.01 to 0.31 mg/L and 0.001 to 0.94 mg/L respectively. Concentrations of dissolved SiO₂ and SO₄ range from 21 to 67 mg/L and 26 to 320 mg/L, respectively. A mixing trend is observed in the Piper diagram for this group of waters (Figure 4.5) between two end-members (Na+K)-Cl water and (Na+K)-Ca-HCO₃-water in this group.

Group-III waters

The water samples in Group-III are dominantly Na-Ca-HCO₃-type waters with some Na-Cl types of waters (Figure 4.5). The pH in this group shows neutral to highly alkaline waters with a range from 7 to 9 (Table 4.2). The temperature and conductivity ranges from 12.8 to 21°C and from 367 to 2450 μS/cm, respectively. The concentrations of As range from 0.002 to 0.55 mg/L. Concentrations of dissolved Fe and Mn range from 0.003 to 1.23 mg/L and 0.001 to 1 mg/L respectively. Concentrations of dissolved SiO₂ and SO₄ range from 21 to 65 mg/L and 4.6 to 290 mg/L respectively. Two mixing lines are observed in the Piper diagram (Figure 4.5) between the end-members (Na+K)-Cl water and (Na+K)-HCO₃-water, and between Ca-HCO₃ and (Na+K)-Cl water in this group.

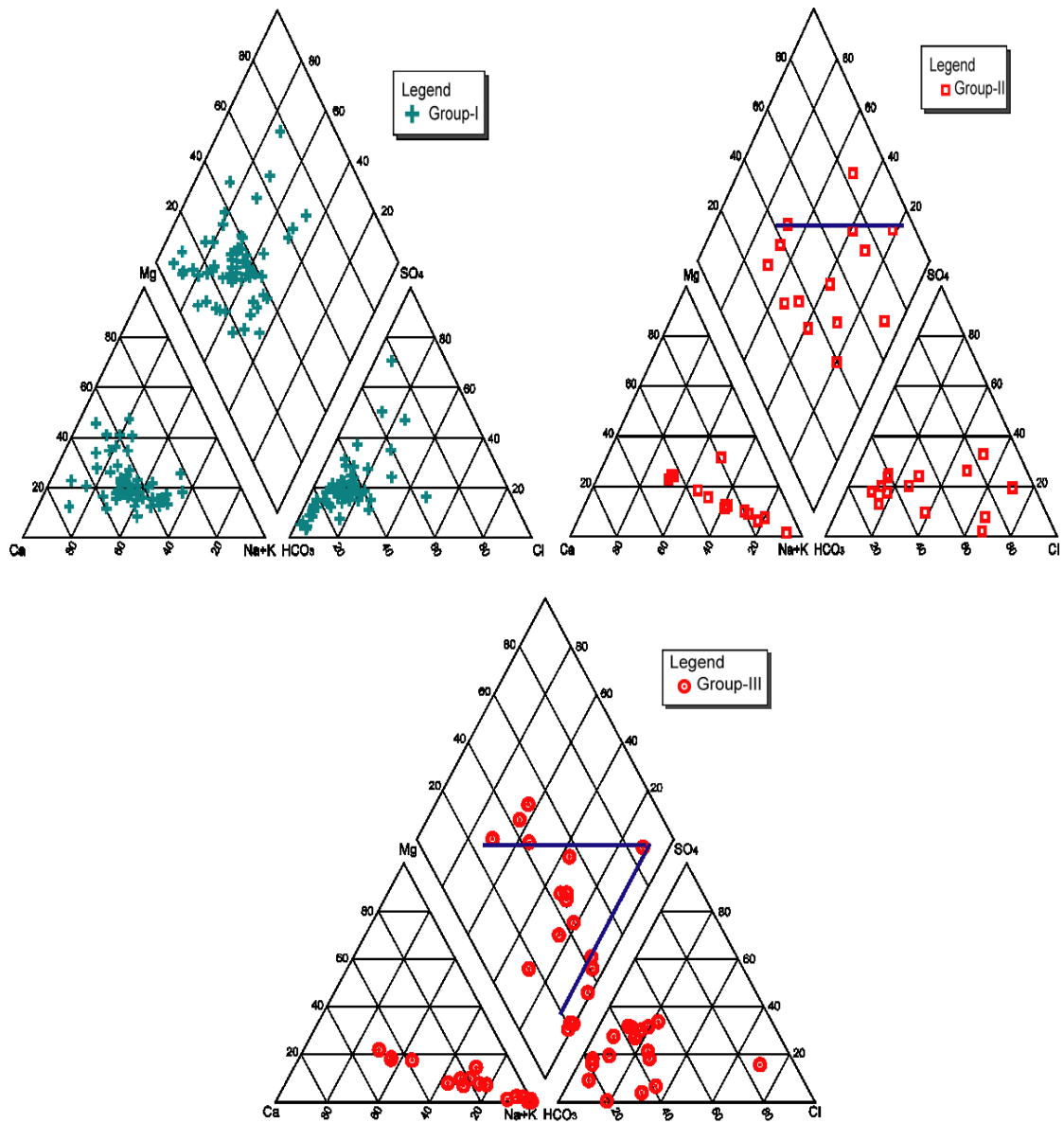


Figure 4.5: Piper diagrams for different groups of ground water illustrating ground water types.

4.4.3. Relationship of arsenic and chemical parameters

The relationships between dissolved As and various chemical parameters including temperature, conductivity, pH, and dissolved ions in each group of water samples have been investigated using bivariate correlations. The bi-variate correlations between dissolved As and other chemical constituents were determined using non-parametric Spearman's rho test. The correlation coefficients for dissolved As with chemical parameters are listed in Table 4.3. The cutoff value of the correlation coefficient 0.75, and the terms, "strong" "moderate" and "weak" as applied to r values, refer to range of >0.75 , $0.75-0.5$, and $0.5-0.3$, respectively. These values are also consistent with the cutoff values of factor loadings used in statistical factor analyses of the data. These relationships between dissolved As and chemical parameters are described in each group of water samples.

The correlations between dissolved As and temperature, bicarbonate and iron are significant, whereas the correlation between dissolved As and pH is negative (Table 4.3) in the waters from Group-I. No significant correlations were found in waters from group-II, whereas, only significant correlation were found between dissolved As and F in group-III waters. The lack of significant correlations between dissolved As and other chemical constituents in water samples from Group-II and III imply occurrences of multiple processes for As and other chemical heterogeneities including mixing with deep ground water, and surface waters as discharge from streams. Similarly, the lack of conclusive correlations between dissolved As and other chemical constituents also indicate underlying uncertainties of the database, and therefore, simple correlations cannot be used for such a large area with limited

Table 4.3: Spearman's rho correlation coefficients for dissolved As and chemical parameters of the ground waters used in this study. Statistics for each pair of variables are based on all the cases with valid data for that pair.

Group	Group-I			Group-II			Group-III		
	Spearman's rho	Correlation Coefficient	Sig. (2-tailed)	N	Correlation Coefficient	Sig. (2-tailed)	N	Correlation Coefficient	Sig. (2-tailed)
Temp	0.275*	0.05	53	0.31	0.38	10	-0.04	0.86	19
pH	-0.296*	0.01	74	0.18	0.53	14	0.11	0.67	19
Bicarb	-0.348**	0.00	74	0.15	0.60	14	0.23	0.35	19
Cond	-0.11	0.37	74	-0.06	0.85	14	0.15	0.55	19
TDS	-0.10	0.40	74	0.07	0.80	14	0.15	0.55	19
As	1.0	.	74	1.00	.	14	1	.	19
B	-0.27	0.37	13	0.21	0.59	9	0.72	0.10	6
Ba	0.00	0.99	66	0.20	0.75	5	-0.14	0.65	13
Br	-0.14	0.66	13	n.d.	n.d.	0	-0.08	0.76	17
Ca	0.01	0.96	74	-0.20	0.49	14	-0.10	0.68	19
Cl	0.02	0.86	74	0.05	0.88	14	-0.01	0.95	19
F	0.09	0.47	74	-0.24	0.42	14	0.660**	0.00	19
Fe	0.248*	0.03	74	-0.01	0.97	14	0.21	0.40	18
K	0.07	0.58	74	0.12	0.68	14	-0.03	0.92	19
Li	-0.01	0.96	45	n.d.	n.d.	1	0.21	0.74	5
Mg	0.10	0.40	74	-0.18	0.54	14	-0.05	0.84	19
Mn	0.01	0.96	74	0.14	0.62	14	0.39	0.10	19
Na	-0.01	0.94	74	0.01	0.98	14	0.13	0.59	19
SiO₂	-0.08	0.50	74	0.25	0.40	14	0.26	0.28	19
SO₄	0.13	0.25	74	0.23	0.43	14	-0.15	0.55	19

Temp: Temperature; Cond: Conductivity; Bicarb: Bicarbonate; n.d.: No data.

* Correlation is significant at the 0.05 level (2-tailed)

** Correlation is significant at the 0.01 level (2-tailed)

4.4.4. Factor analyses results

Factor analyses were performed on the total elemental (and ion) concentrations and various chemical parameters to demonstrate the relationships between As and chemical parameters.

Factor analyses results for Group-I waters

The water samples from Group-I reflect four factors with factor 1 and 2 representing 45% and 36% of the variances respectively (Table 4.4). Factor 1 demonstrates high positive loadings of temperature, bicarbonate, B, F, Li, Mg, Na and SO₄ (0.94, 0.78, 0.95, 0.86, 0.93, 0.81, 0.86, and 0.94, respectively), and negative high loading of As and pH (-0.02, and -0.83, respectively) (Table 4.4). Because of the recognized association of elevated concentrations of dissolved B, F and Li in northern Nevada geothermal waters (Shevenell et al.,2008), the ground water in Factor 1 may suggest the influence of thermal waters for water chemistry with high loadings of temperature, B, F and Li, followed by weathering of sulfides and silicate rocks that contain Na and Mg-minerals such as albite, and biotite with high loadings of SO₄, Na and Mg, respectively. However, As is not associated with these waters because of the negative loading of As.

Factor 2 with about 36% variance demonstrates moderate loading of As (0.68) with high loadings on Ba, Fe, and K (0.96, 0.76, and 0.78, respectively), but negative high loadings on Br, Ca, and Cl (-0.83, -0.90, and -0.89, respectively) (Table 4.4).

Table 4.4: Factor analyses results of total elemental concentrations of the ground water data for group-I. The numbers in the rows represent factor loadings for each component, and marked bold typefaces represent the values of factor loadings of over 0.75. Statistics are based on cases with no missing values for any variable used. Extraction method: Principal Component Analysis (PCA).

Component	Factor 1	Factor 2	Factor 3	Factor 4	Communalities
Temp.	0.94	0.32	0.10	-0.07	1
pH	-0.83	0.35	-0.14	0.42	1
Bicarb.	0.78	-0.53	-0.24	-0.25	1
Cond.	0.72	-0.69	-0.03	-0.01	1
TDS	0.72	-0.69	-0.03	-0.01	1
As	-0.02	0.68	0.73	-0.11	1
B	0.95	0.23	-0.04	0.21	1
Ba	0.24	0.96	0.16	0.02	1
Br	0.14	-0.83	0.51	0.16	1
Ca	0.34	-0.90	-0.24	-0.13	1
Cl	0.10	-0.89	0.41	0.19	1
F	0.86	0.50	-0.06	-0.09	1
Fe	0.12	0.76	0.47	-0.44	1
K	0.58	0.78	0.14	0.19	1
Li	0.93	0.26	-0.18	0.19	1
Mg	0.81	-0.10	0.29	-0.50	1
Mn	0.71	0.50	-0.26	0.43	1
Na	0.86	-0.22	0.37	0.27	1
SiO ₂	-0.07	-0.36	0.86	0.35	1
SO ₄	0.94	0.16	-0.25	0.16	1
Initial eigenvalues	9.07	7.12	2.50	1.31	
Percentage of variance	45.3	35.6	12.5	6.6	
Cumulative % of variance	45.3	81.0	93.4	100	
Total Communalities					20
Proportion of the total variation explained by the factors					1

Note: Temp: Temperature (°C); Bicarb: Bicarbonate (HCO₃); Cond: Conductivity (μS/cm).

Factor 2 with high loadings in Ba, Fe, and K, but moderate loading in As, Mn, and weak loading in temperature, and pH may suggest water-rock reactions involving dissolution of As-bearing Fe and Mn oxy-hydroxides followed by minor dissolution of biotite which contains both K and Fe. The redox reactions under post-oxic conditions are evidenced by high loadings of dissolved Fe and moderate loading of Mn (Appelo and Postma, 1996). The negative high loadings of dissolved Ca and moderate loading of HCO_3 also suggest precipitation of calcite.

Factor 3 with only 12.5% variances reveals high loading of dissolved SiO_2 (0.86) and moderate loading of As, and Br (0.73 and 0.51, respectively) with weak and/or negative loading of temperature, conductivity, B, Cl, F, and Li indicating little or negligible influence of geothermal water but minor influence of dissolution of silicates. Factor 4 with 6.6% variances with no significant loading for any constituents can be neglected.

In summary in Group-I waters, although sulfide dissolution and geothermal mixing contributes to major proportion of waters, As is not significant in those waters, and moderately associated with dissolution of Fe and Mn-oxy-hydroxides and biotite.

Factor analyses results for Group-II waters

The results of factor analyses for water samples in Group-II reveal five factors (Table 4.5), where the factors 1, 2, 3, 4 and 5 represent 40%, 22%, 13%, 11% and 6% of the variances respectively. Factor 1 has negative loading on As (-0.28) with high loadings on conductivity, TDS, Ca, Cl, Na, and SO_4 (0.98, 0.98, 0.93, 0.96, 0.91, and 0.92, respectively), with moderate loadings on B, Mg (0.58, and 0.61 respectively) (Table 4.5). Factor 1 may suggest the water chemistry influenced by mixing with

Table 4.5: Factor analyses results of total elemental concentrations of the ground water data for group-II. The numbers in the rows represent factor loadings for each component, and marked bold typefaces represent the values of factor loadings of over 0.75. Statistics are based on cases with no missing values for any variable used.

Extraction method: Principal Component Analysis (PCA).

Component	Factor 1	Factor 2	Factor 3	Factor 4	Factor 5	Communalities
Temp.	-0.36	0.55	-0.15	0.31	-0.53	0.84
pH	0.32	0.14	0.83	0.23	0.12	0.87
Bicarb.	-0.14	0.14	-0.41	0.84	0.09	0.93
Cond.	0.98	0.15	0.01	-0.02	-0.08	0.99
TDS	0.98	0.16	-0.01	0.06	-0.05	0.99
As	-0.28	-0.33	0.64	0.38	-0.04	0.74
B	0.58	0.48	0.05	0.55	0.26	0.93
Ca	0.93	-0.01	0.14	-0.17	-0.08	0.93
Cl	0.96	0.18	0.06	-0.15	-0.13	1.00
F	0.25	0.84	-0.12	-0.03	-0.16	0.81
Fe	-0.32	0.83	-0.04	-0.37	0.18	0.96
K	-0.40	0.74	-0.05	0.25	0.45	0.97
Mg	0.61	-0.45	-0.34	-0.21	0.47	0.95
Mn	-0.16	0.82	-0.13	-0.41	0.10	0.88
Na	0.91	0.28	0.02	0.10	-0.23	0.97
SiO ₂	-0.05	0.33	0.84	-0.16	0.15	0.86
SO ₄	0.92	-0.16	-0.22	0.17	0.18	0.99
Initial eigenvalues	6.801	3.761	2.202	1.835	1.002	
Percentage of variance	40.008	22.126	12.952	10.797	5.897	
Cumulative % of variance	40.008	62.134	75.086	85.883	91.779	
Total Communalities						15.6
Proportion of the total variation explained by the factors						0.92

Note: Temp: Temperature (°C); Bicarb: Bicarbonate (HCO₃); Cond: Conductivity (μS/cm).

geothermal or brine waters with high concentrations of Na, Cl, B, and higher TDS and conductivity. Carbonate rock dissolution with predominantly limestone dissolution over dolomite can be deduced from high dissolved Ca ions and moderate Mg ions, whereas dissolution of sulfate salts such as gypsum can be deduced from moderate high loadings of both Ca and SO_4 ions in the waters.

Factor 2 (Table 4.5) has negative loading on As (-0.33), and high loadings on F, Fe, and Mn (0.84, 0.83, and 0.82, respectively), with moderate loadings on B, and K (0.48, and 0.74, respectively) may suggest dissolution of Fe and Mn-oxyhydroxides and silicate weathering with dissolution of K-feldspars.

Factor 3 with only 13% of the variances and moderate loading on As (0.64) with high loadings on pH and dissolved SiO_2 (0.83 and 0.84, respectively), represent a minor fraction of water as a result from pH-dependent desorption where pH driven by dissolution of silicates. Factor 4 has only high loading on HCO_3 (0.84) with weak loading on As (0.38) may suggest minor carbonate dissolution or decay of organic matters (which breaks down into HCO_3), but not important for As. Factor 5 with only 6% variances can be neglected because of no significant loadings.

In summary, mixing of geothermal waters and/or dissolution of carbonate rocks along with dissolution of Fe and/or Mn-oxy-hydroxides are not significant for dissolved As in these waters, which represent Factor 1 and Factor 2. However, a minor proportion of water (13%) is associated with As derived from pH-dependent desorption.

Factor analyses results for Group-III waters

The water samples in Group-III reveal four factors representing 43%, 25%, 21% and 10% of the variances for factors 1, 2, 3, and 4 respectively (Table 4.6).

Factor 1 has high loadings on HCO_3 , conductivity, TDS, Mn, and SO_4 (0.93, 0.92, 0.92, 0.97, 0.88, and 0.77, respectively), with moderate loadings on As, Ba, Ca, Cl, and Mg (0.61, 0.7, 0.65, 0.68, and 0.71, respectively), with weak loading on Fe (0.48). Factor 1 may suggest water chemistry influenced dominantly by either evaporation or, mixing with brines from deeper aquifers, followed by dissolution of sulfate salts (e.g., barium sulfate, gypsum) with high SO_4 , Ba and Ca and silicate (e.g., biotite) weathering. With moderate loading of As and Fe (0.61 and 0.48) and high loading of Mn (0.88) indicate dissolution of As-bearing Fe and Mn-oxy-hydroxides for As along with silicate (biotite) dissolution.

Factor 2 with 25 % variances has negative loading on As (-0.36) with high loadings on pH, Li, and Na (0.84, 0.95, and 0.86, respectively), and moderate loadings on Br, and K (0.65 and 0.67, respectively) (Table 4.6). This may suggest that 25% of the waters may have been influenced by mixing with Li and Na enriched high-alkaline waters, but these waters do contribute to As.

Factor 3 with 21% variances has high loadings on F and Fe (0.90 and 0.81, respectively), with moderate loadings on As, and Cl (0.69, and 0.72, respectively), may suggest minor contribution of As from mixing with geothermal waters enriched in F, and Cl. Factor 4 with 10% variances has high loading on SiO_2 (0.75) with moderate loadings on temperature, and Br (0.76, and 0.69, respectively) and negative

Table 4.6: Factor analyses results of total elemental concentrations of the ground water data for group-III. The numbers in the rows represent factor loadings for each component, and marked bold typefaces represent the values of factor loadings of over 0.75. Statistics are based on cases with no missing values for any variable used.

Extraction method: Principal Component Analysis (PCA).

Component	Factor 1	Factor 2	Factor 3	Factor 4	Communalities
Temp.	-0.56	-0.27	0.19	0.76	1
pH	-0.47	0.84	0.26	-0.07	1
Bicarb.	0.93	0.33	-0.14	0.12	1
Cond.	0.92	0.39	-0.06	0.04	1
TDS	0.92	0.39	-0.06	0.04	1
As	0.61	-0.36	0.69	-0.17	1
B	0.97	-0.01	0.09	0.22	1
Ba	0.70	-0.58	-0.41	-0.09	1
Br	-0.20	0.65	-0.26	0.69	1
Ca	0.65	-0.47	-0.60	0.05	1
Cl	0.68	0.09	0.72	-0.09	1
F	0.39	-0.15	0.90	-0.09	1
Fe	0.48	-0.33	0.81	-0.02	1
K	0.46	0.67	-0.32	-0.50	1
Li	0.27	0.95	-0.11	-0.11	1
Mg	0.71	-0.45	-0.51	0.18	1
Mn	0.88	-0.47	0.02	0.10	1
Na	0.32	0.86	0.40	0.01	1
SiO ₂	0.49	0.25	0.36	0.75	1
SO ₄	0.77	0.27	-0.58	0.05	1
Initial eigenvalues	8.68	5.08	4.19	2.05	
Percentage of variance	43.39	25.42	20.95	10.24	
Cumulative % of variance	43.39	68.81	89.76	100	
Total Communalities					20
Proportion of the total variation explained by the factors					1

Note: Temp: Temperature (°C); Bicarb: Bicarbonate (HCO₃); Cond: Conductivity (μS/cm).

loading on As (-0.17) may suggest that a small amount of water (10%) may have been influenced by geothermal water that are high in silica-geothermometer do not contribute to dissolved As significantly.

In summary, with moderate loading of As and Fe and high loading of Mn suggest that dissolution of As-bearing Fe and Mn-oxy-hydroxides along with silicate (biotite) dissolution for dissolved As in these waters. Mixing with brine from deeper aquifers or evaporative enrichment of the surface waters that discharges to ground water could be important for water chemistry, but lesser significant for As enrichment.

4.5. Discussion

4.5.1. Relationship of arsenic and geochemical processes

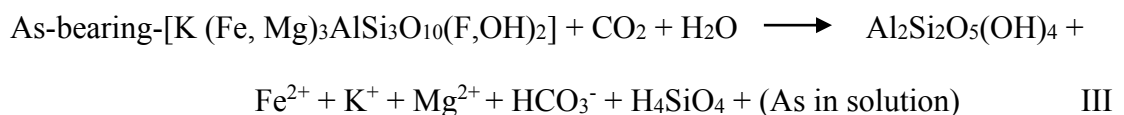
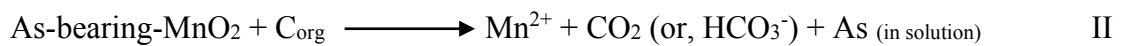
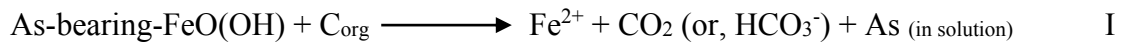
The relationships of dissolved As and other chemical parameters demonstrate that multiple geochemical processes are occurring in all groups of waters at different scales or magnitudes.

Group-I waters

The results from the Piper diagram (Figure 4.5) suggest that the waters in Group-I are mainly Ca-Na-HCO₃-type waters with some Ca-Na-SO₄-type. The results from correlations and factor analyses (Table 4.3 and 4.4), suggest that while oxidation of sulfide minerals may be important for dissolved SO₄ concentrations in many of these ground water; it is not important for dissolved As concentrations. Similarly mixing with geothermal waters or brine from deeper aquifers may be important for elevated concentrations of B, F, Li, Na, Mg, but is not important for elevated As concentrations. This also conforms to the results from spatial mapping of dissolved

As (Figure 4.4), where dissolved As has been <0.01 mg/L adjacent to or within the known geothermal hot springs and hot wells. In contrast, higher elevated As concentrations >0.01 mg/L adjacent to or within the known mineralized zones (Figure 4.4) and factor analyses results (Table 4.4) suggest that As may be locally released from dissolution from sulfides, but most likely released from dissolution of Fe and Mn-oxy-hydroxides and dissolution of ferromagnesian minerals such as biotite containing As.

The relatively high loadings of Fe, K, and moderate loadings of As, and Mn, (Table 4.4, Factor 2) with pH neutral to moderately alkaline conditions imply reductive dissolution of Fe-oxy-hydroxides and Mn-oxides along with dissolution of ferromagnesian biotite and resultant release of dissolved As from As-bearing Fe-oxy-hydroxides and/or Mn-oxides and biotite due to change in redox conditions from dominantly oxic to post oxic conditions:



where, C_{org} is organic matter.

Group-II waters

The Piper diagram (Figure 4.5) for water samples in Group-II indicates that the waters are dominantly Na-Ca-HCO₃-type waters with some Na-Cl-types, with a alkaline pH ranging from 7.5 to 8.45 (Table 4.1). The results from factor analyses (Table 4.5) suggest that the majority of the waters in Group-II can be deduced as

result of mixing with geothermal waters or brine from deeper aquifer followed by minor silicate weathering. However, due to negative loading of As with these factors, and because of low concentrations of dissolved As in these waters suggest that mixing with geothermal water or brine may have contributed to elevated level of conductivity, TDS, Cl, F, and other constituents, and As is likely to be contributed at a lesser magnitude. The moderate concentrations of dissolved As (0.001 to 0.01 mg/L) is most likely contributed due to pH-dependent desorption.

Group-III waters

The Piper diagram (Figure 4.5) for water samples in Group-III indicates that the waters are dominantly Na-HCO₃-Cl-type waters with some Na-Ca-HCO₃-Cl types with a strong alkaline pH ranging from 7 to 9 (Table 4.1). Factor analyses results (Table 4.6) indicate that the majority of these waters can be deduced from ferromagnesian silicate weathering, followed by mixing with brine or mixing with evaporated enriched discharges from the surface waters that contributes to ground water recharge in the alluvium in enclosed basins and playa deposits. Moderate loading of As and Fe and high loading of Mn suggest that dissolution of As-bearing Fe and Mn-oxy-hydroxides along with silicate (biotite) dissolution for dissolved As in these waters.

In summarizing, ground water geochemistry in all groups are influenced by water-rock interactions involving sulfide dissolutions locally in the mineralized zones in Boulder Valley and its surroundings, followed by mixing with geothermal waters or brine from deeper aquifers in areas of Group-III and evaporated enrichment of the river discharge that recharges to shallow alluvial ground water locally in the lower HRB. In overall, dissolution of iron oxy-hydroxides and Mn-oxides along with

dissolution of ferromagnesian silicates play an important role for dissolved As followed by a minor release from pH-dependent desorption.

4.5.2. Conceptual release mechanism of arsenic

Robertson (1989) in a similar semi-arid alluvial basin with oxidizing ground water in Arizona suggested that adsorption of arsenate ions on smectite or iron oxy-hydroxide was one of the major controls on arsenic in ground water. In another similar environmental setting, Ryu et al (2002) suggested desorption was an important processes for arsenic enrichment in the shallow ground water of Dry Owens Lake. On the other hand, in a study of the Southern High Plain ground water in Texas, Scanlon et al. (2009) suggested that As mobilization at the regional scale was due to counter ion effect associated with the change in water chemistry from Ca- to Na-rich water as a result of upward movement of high Na ground water from underlying aquifers.

In the study area, the ground water in Group-II and III have high salinity and moderate to strong alkaline pH, and therefore, desorption of As from the adsorbed iron oxy-hydroxides and/or Mn-oxides under high saline and alkaline conditions may play an important role in further enrichment of arsenic; however, this needs to be examined with batch experiments, mineralogic profiling, and geochemical modeling studies. Similarly, mixing with Na-rich deep brine ground water with overlying Ca-rich ground water in the shallow aquifers can be speculated on the basis of progressive change in water chemistry from Ca-rich in Gropu-I to Na-rich waters in Group II and III; however, this hypothesis needs to be examined for the HRB waters in future studies.

The spatial distribution of dissolved As in ground water reveals relationship between sedimentation depositional dynamics and As concentrations with As released from the older source rocks of Tertiary volcanic rocks in the upper and middle reaches

of the HRB, but becomes less significant in the lower HRB. Therefore, weathering of Tertiary volcanic rocks and oxidation of As-bearing sulfides may be the primary source rocks of As in the region, the secondary source of As (e.g., weathering of As-bearing biotite, and dissolution of As-bearing oxy-hydroxides) becomes significantly important for regional ground water-As in shallow aquifers in the lower-middle and lower HRB area.

In this study it is found that major proportion of As (83%) is within the residual silicate phases followed by iron oxy-hydroxides phases (13%) in the stream sediments of the Humboldt River. The XRD and SEM analyses of the stream sediments of the HR system revealed abundance of muscovite, biotite and smectite-illite clay minerals, and iron-oxides. Therefore, the most plausible explanation for the source of As in regional shallow ground water in our study area could be weathering of As-bearing ferromagnesian minerals (i.e., biotite) (Foster et al., 2000; 2001; Ahmed et al., 2004; Chakraborty et al., 2007; Seddique et al., 2008) and dissolution of As-bearing iron oxy-hydroxides as illustrated in equations (I) and (III).

Dissolution of As-bearing iron oxy-hydroxides and/or Mn-oxides appears to be important where post-oxic redox conditions exist. Iron oxides also play as sinks for As in predominantly oxic environment, and are known to occur in the sediments of the shallow alluvial aquifer sediments and stream flood-plain sediments (Folger 2000; Welch et al. 2000). Although we do not have data about organic matter (C_{org}), or DIC (dissolved inorganic carbon) in the water samples used in this study, circumstantial geological evidence indicate that organic matter was incorporated in the sediments at the time of deposition during Miocene-Pleistocene (Benson et al. 1998; Davis and Moutoux, 1998; Retallack, 2001; Wallace et al., 2008).

Finally, statistical factor analyses and qualitative geochemical analyses alone cannot substantiate conclusive results and therefore future studies are required with respect to sedimentologic and mineralogical profiling of the aquifers, geochemical reaction path modeling and interactions between surface water and ground water.

4.6. Conclusions and future studies

Distribution of arsenic in the ground water of shallow alluvial and basin-fill aquifers in different catchment areas of the HRB have been investigated to determine the factors that control the occurrence of arsenic. Our study has determined that release of arsenic into the ground water in the study area is the likely result of coupled geochemical processes with further enrichment of the element as follows:

- 1) Oxidation of sulfide mineral is important for dissolved SO_4 in the waters that are in contact with sulfide horizons in the mineralized area in the vicinity of Boulder Valley and its surroundings.
- 2) Reductive dissolution of As-bearing iron oxy-hydroxides and Mn-oxides may have played an important role in releasing As into the regional shallow alluvial ground water.
- 3) Dissolution of As-bearing ferromagnesian minerals such as, biotite also play important roles in releasing dissolved As into the regional shallow alluvial ground water.
- 4) Mixing with deep geothermal water has been inferred for localized enrichment of As within the known area of geothermal hot springs in the vicinity of Golconda.

- 5) Evaporative enrichment of As in the surface waters that discharges into the alluvium is inferred from the geochemical and statistical analyses in Lower HRB area.

Future studies are required with depth profiling of the samples, well-logging data, mineralogical profiling of the aquifer materials, batch experiments, ground water-surface water interactions, and geochemical modeling studies to quantify the various geochemical processes involved in enrichment of arsenic into shallow alluvial ground waters.

CHAPTER 5

Statistical and Geochemical Analyses of Arsenic Distribution in the Waters and Sediments of the Humboldt River System, North-Central Nevada

ABSTRACT: The Humboldt River, with an area of approximately 43,700 km² drains through largely Quaternary alluvium and lacustrine sediments, several hydrothermally altered rocks and epithermal and pluton-related mineral deposits. Several geothermal hot springs also drain into the river. Concentrations of dissolved arsenic (As) in the waters range from 0.012 to 0.06 mg/L, with an average of 0.032 mg/L. The water in the river system is alkaline (pH ranges from 8.4 to 9.3), oxic (average 12 mg/L of dissolved O₂, and +139 mV of ORP), and saline with an average of 1000 μ S/cm of specific electrical conductivity. It is also highly enriched in B (average 0.77 mg/L), Li (average 0.15 mg/L), Cl (average 158 mg/L), and SO₄ (average 178 mg/L). Factor analyses of river waters and sediments -suggest several physical and geochemical processes operating at variable scales in three sub-regions: upper, middle and lower reaches of the river. Arsenic is primarily released into the water from dissolution of weathered As-bearing minerals in the upper reach of the river. Mixing of shallow ground water and geothermal waters affect As concentrations in a localized area in the transition area between middle and lower Humboldt River. Further enrichment of As occurs along the flow path of the river by evaporation in the lower reach of the river and in the terminal sink followed by secondary release of As due to desorption from the river-bed sediments with the increase in pH and alkalinity in the lower reach of the river. Results of sequential extraction analyses of the river-bed sediments suggest that concentration of As in river sediments is controlled by partitioning onto clay minerals and Fe-oxy-hydroxides.

Key-words: Arsenic; Humboldt River, Nevada, Evaporation, Geochemistry.

5.1. Introduction

Natural sources of arsenic (As) in streams and rivers primarily include geothermal springs, ground water, wind-blown dust, and drainage from the weathering of sulfides and other As-bearing minerals (Henke, 2009). Arsenic concentrations in rivers and other surface waters depend on several factors, including (1) the geochemical composition of any underwater sediments and rocks, and the rocks surrounding the source of tributaries and springs; (2) inputs from geothermal sources or high As-ground waters; (3) biological activities; (4) change in pH, Eh, temperature, or chemical conditions because of storms and seasonal changes; and (5) human induced activities such as drainage through mined waste rocks containing As-bearing minerals (Ballantyne and Moore, 1988; Webster et al., 1994; Nimick et al., 1998; Welch and Lico, 1998; Tempel et al., 2000; Smedley and Kinniburgh, 2002; Earman and Hershey, 2004; Mohammad and Tempel, 2007; Henke, 2009).

Elevated concentrations of As have been detected in several river waters including Carson River (5-175 $\mu\text{g/L}$) and Walker River (<2-135 $\mu\text{g/L}$) (Johannesson et al., 1997) in west-central Nevada, and North Fork-Humboldt River (4-12 $\mu\text{g/L}$) (Earman and Hershey, 2004) in the north-central Nevada. Concentrations of As in the Carson River and Walker River have been accounted for by weathering of geologic materials and hydrothermal sources (Johannesson et al., 1997). Concentrations of As in the North Fork-Humboldt River have been accounted for by drainage through mined waste rocks containing As-bearing sulfides and other As-minerals (Earman and Hershey, 2004). The North Fork River is a tributary of the Humboldt River located in the upstream reach of the study area (Figure 5.1). However, there have been no

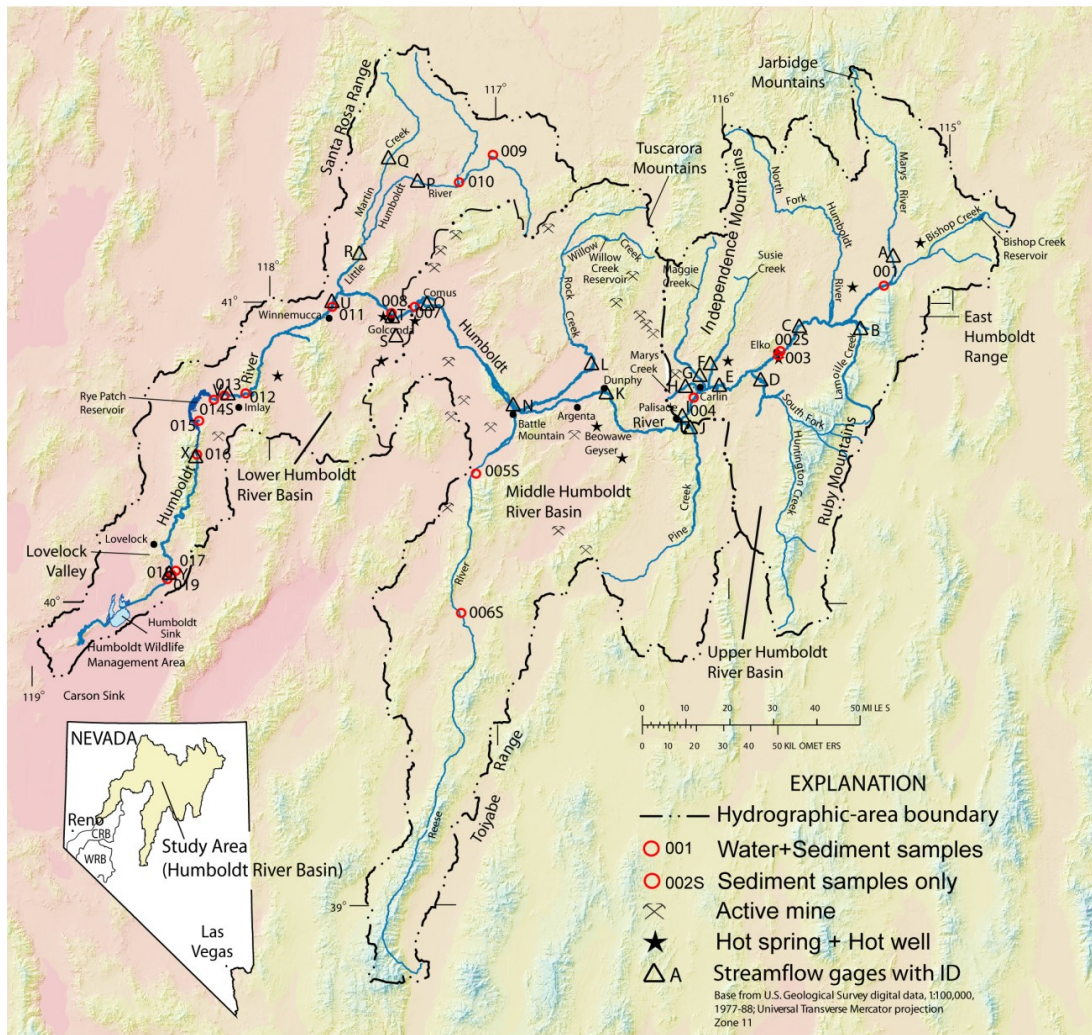


Figure 5.1: Map of the Humboldt River Basin (HRB) in northern Nevada showing the Humboldt River and locations of sampling points of river water and sediments. The inset map shows the study area with locations of Carson River Basin (CRB), Walker River Basin (WRB) on the south-west of the HRB.

comprehensive studies to understand As enrichment and redistribution in the surface waters of the Humboldt River and its sediments.

The Humboldt River system is one of the most diverse hydrographic systems in the US West. It is an internally drained river that is characterized by complex geological and sedimentation dynamics along with numerous metallic-sulfide ores and geothermal systems. The Humboldt River system plays an important role in maintaining wildlife habitats and wetlands, irrigation, and water storage in Rye Patch reservoir, and Humboldt Sink, where it terminates. Irrigation is the predominant use of water in the HRB, which accounts for 98% of the total (Desert Research Institute, 1994). Because of the widespread use of the Humboldt River water for irrigation and numerous mining industries, and because of its importance in supporting wildlife habitats, an understanding of the processes that control As mobilization and enrichment in water and sediments is essential. The objective of this study is to assess the concentrations and sources of As enrichment in the river waters and understand the processes controlling distribution of As in the sediments and waters of the basin as part of our broader objective to assess the cycling of As in the Humboldt River Basin.

5.2. Study area

5.2.1. Humboldt River System

The Humboldt River is the largest of three internally drained river systems in northern Nevada. The river system includes the Little Humboldt River in Elko and Humboldt Counties, the Reese River in Lander County, and the main Humboldt River and its many tributaries that flow westward and then south-westward into the Humboldt Sink (Figure 5.1). The hydrographic basin formed by the Humboldt River and its tributaries encompasses approximately 43,700 km² (16,872 mi²), and it

forms a substantial part of the larger Great Basin (Yager and Folger, 2003). The river drains through or near several geothermal hot springs, hydrothermal alteration zones, and epithermal and pluton-related mineral deposits, including those of silver, copper, and arsenic-rich gold. As a result, the source rocks for sediments in the Humboldt River system are highly enriched in many elements besides arsenic.

The water of the Humboldt River is not only limited in quantity, but is of poor quality due to high salinity and high concentrations of dissolved trace metals, including As. The chemical composition of the Humboldt River water is strongly influenced by the inflow of tributaries that flow through several thermal springs and areas of known mineral deposits. The high salinity in the water has been related to a combination of inflow of ground water, mixing with geothermal and deep brine water, and the intense evaporation that occurs in this semi-arid to arid region.

Hydrology of the Humboldt River

The average monthly mean river discharge data obtained from the US Geological Survey public domain database (<http://waterdata.usgs.gov/nv/nwis/sw>) indicate that the river is in low-flow condition during September, 2007 (Figure 5.2), when the samples for this study were collected, which is also consistent with previous studies (Cohen, 1963; Eakin and Lamke, 1966; Prudic et al., 2006.) Table 5.1 lists the average daily discharge in September, 2007 at various river gage stations along the Humboldt River and its tributaries. The river gains 0.22 m³/s and 0.54 m³/s of daily discharge from Elko (0.034 m³/s) to Carlin (0.25 m³/s), and to Palisade (0.79 m³/s), respectively. The river loses from Palisade towards Dunphy (0.42 m³/s), and continue to lose in Battle Mountain (0.05 m³/s) and Comus (0.01 m³/s). The river continues to lose near Golconda (0.02 m³/s) until it gains at Winnemucca (0.78 m³/s). The river

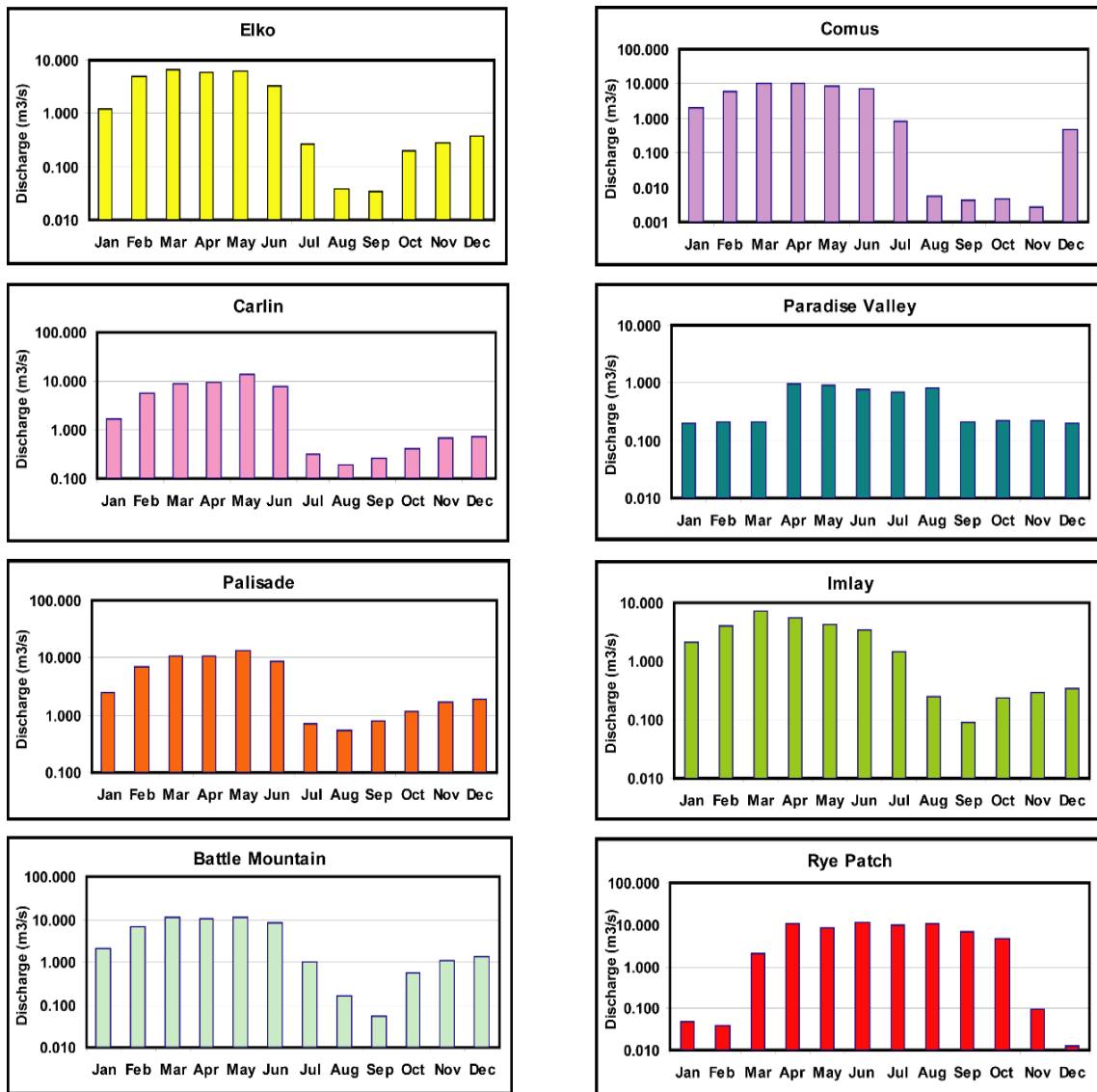


Figure 5.2: Histograms showing average of monthly mean discharge in 2007 of the Humboldt River at different stations.

Table 5.1: Average daily discharge of the Humboldt River during September, 2007 recorded at various stream gages. Data source: <http://wdr.water.usgs.gov/nwisgmap/>. Locations of stream flow gages are given in Figure 5.1 with abbreviated IDs.

Abbreviated ID	USGS Station ID	Stream Gage Location Name	Discharge¹ (m³/sec)
A	10315600	MARYS RV BLW TWIN BUTTES NR DEETH	0.00
B	10316500	LAMOILLE CREEK	0.09
C	10318500	HUMBOLDT RV NR ELKO	0.03
D	10320000	SOUTH-FORK-HUMBOLDT RIVER	0.14
E	10321000	HUMBOLDT RV NR CARLIN	0.25
F	10321590	SUSIE CK AT CARLIN	0.00
G	10322000	MAGGIE CK AT CARLIN	0.26
H	10322150	MARYS CK AT CARLIN	0.10
I	10322500	HUMBOLDT RV AT PALISADE	0.80
J	10322980	COLE CK NR PALISADE	0.00
K	10323425	HUMBOLDT RV AT OLD US 40 BRG AT DUNPHY	0.42
L	10324500	ROCK CREEK	0.01
M	10324700	BOULDER CREEK	0.00
N	10325000	HUMBOLDT RV AT BATTLE MOUNTAIN	0.05
O	10327500	HUMBOLDT RV AT COMUS	0.01
P	10329000	LITTLE HUMBOLDT RIVER	0.21
Q	10329500	MARTIN CREEK NR PARADISE VALLEY	0.17
R	10329000	HUMBOLDT RIVER NR PARADISE VALLEY	0.21
S	10328000	POLE CREEK NR GOLCONDA	0.01
T	10327800	HUMBOLDT RV NR GOLCONDA	0.02
U	10330900	HUMBOLDT RV NR WINNEMUCCA	0.78
V	10333000	HUMBOLDT RV NR IMLAY	0.09
Y	10336000	HUMBOLDT RV NR LOVELOCK	0.59

¹Average mean daily discharge in September, 2007

its flow at Imlay ($0.09 \text{ m}^3/\text{s}$) followed by a gain at Lovelock (0.59). Despite the flows in Little Humboldt River and Martin Creek near Paradise Valley, these waters are lost to subsurface alluvium before reaching Winnemucca (Prudic and Herman, 1996), where the last updated flow in fall of 1963 was $0.78 \text{ m}^3/\text{sec}$ (<http://wdr.water.usgs.gov/nwisgmap/>). The flow in the Humboldt River near Winnemucca during the low-flow season is due to ground water movement towards the river (Eakin and Lamke, 1966). The flow rates in the Humboldt River from Elko to Rye Patch Reservoir show seasonal variations with peak flow occurring during snowmelt runoff at the end of the wet season. The annual runoff from the drainage above the town of Carlin is dominated by snowmelt runoff from the Ruby, Jarbidge, and Independence Mountains and the East Humboldt Range. In contrast, most of the snowmelt runoff from the Tuscarora Mountains, and Santa Rosa and Toiyabe ranges is lost to irrigation diversions, natural evapotranspiration, and infiltration into the alluvium prior to reaching the Humboldt River (Prudic et al., 2006). The increase in annual runoff from Elko to Carlin and from Carlin to Palisade occurs as a result of tributary inflows to the channel. The variations in mean annual runoff or discharge from upstream to downstream also reflect the variations in topography and river morphology. During the low-flow season (e.g., late summer to fall), gains and losses are caused largely by the interchange of water between the river and the ground water reservoir (Cohen, 1963). In addition to ground water-surface water interactions, increases in base flow of the Humboldt River during the fall and winter results from seasonal reductions of evapotranspiration loss (Cohen, 1963).

The average annual precipitation ranges from 15 to 110 cm in the range from 15 to 30 cm in the valleys and floodplain areas. Precipitation generally is greater at

higher elevations in the mountains than in the adjacent valleys and occurs mostly during the wet season from late November to May (Prudic et al., 2006). The average annual precipitation map prepared by the Division of Water Resources (NDWR) of State of Nevada-Department of Conservation and Natural Resources (<http://water.nv.gov>) indicates annual average precipitation with a range of 10-20 cm in the western Humboldt River Basin area with a low annual average of less than 10 cm near Humboldt Sink area. Shevenell (1996) reported potential evaporation greater than precipitation at several weather stations within the Humboldt River Basin. For example, at Imlay station, north of Rye Patch Reservoir, monthly potential evaporation ranges from 0 cm in December and January to 32.75 cm in July, whereas monthly precipitation ranges from 0.53 cm in July to 2.38 cm in May with the average annual potential evaporation and precipitation of 12.42 cm and 1.6 cm, respectively (Shevenell, 1996).

5.2.2. Ground water movement and interaction

Shallow ground waters in the alluvial aquifers of Quaternary and Tertiary sedimentary deposits are closely associated with the flow of the Humboldt River. Details of ground water occurrence in the HRB have been described in Chapter 2, and the interactions between ground water and Humboldt River is presented here. The shallow ground waters in the HRB occurs under water-table conditions during most of the year, with some artesian conditions occur locally where the saturated unit is overlain by impermeable clay units, for example in Grass Valley area (Cohen, 1963). Several thermal springs also occur in relatively small areas locally, where water occurs under artesian conditions. For example, a ground water mound of thermal water occurs along the East Range fault just west of Golconda (Cohen, 1963).

Previous studies indicate that direct infiltration of precipitation probably contributes only a small part of the average annual ground water recharge, and the source of the most ground water is seepage of stream flow, where the ultimate source of the stream flow is precipitation (Cohen, 1963; Eakin and Lamke, 1966). Figure 5.3 illustrates contours of ground water elevation constructed from the ground water data available in Nevada State Engineer's public domain database (<http://water.nv.gov/>). The water-level contours based on largely on the altitude of water levels in wells that penetrate only the upper few hundred feet of the zone of saturation in late September to early October of 2007, and accordingly, the map do not necessarily indicate the precise direction of the ground water movement because of data gaps in some of the catchment basins. However, the general direction of the horizontal component of the ground water movement in the shallow aquifers is consistent with previous studies (Cohen, 1963, Eakin and Lamke, 1966). Thus, the gross direction of ground water movement in September, 2007 as shown in Figure 5.3 is towards the Humboldt River from the higher elevated topography, and then westward and southwestward roughly parallel to the river.

Ground water discharges into the river, where the hydrostatic head in the ground water reservoir adjacent to or beneath the Humboldt River is higher than the stage of the river. Table 5.1 shows that on the average the flow of the Humboldt River is increased between Carlin and Palisade despite zero flow in Susie Creek, and very low flows in Maggie Creek and Mary's River during low-flow condition. In as much as virtually no surface water discharged into this reach of the river, nearly the entire

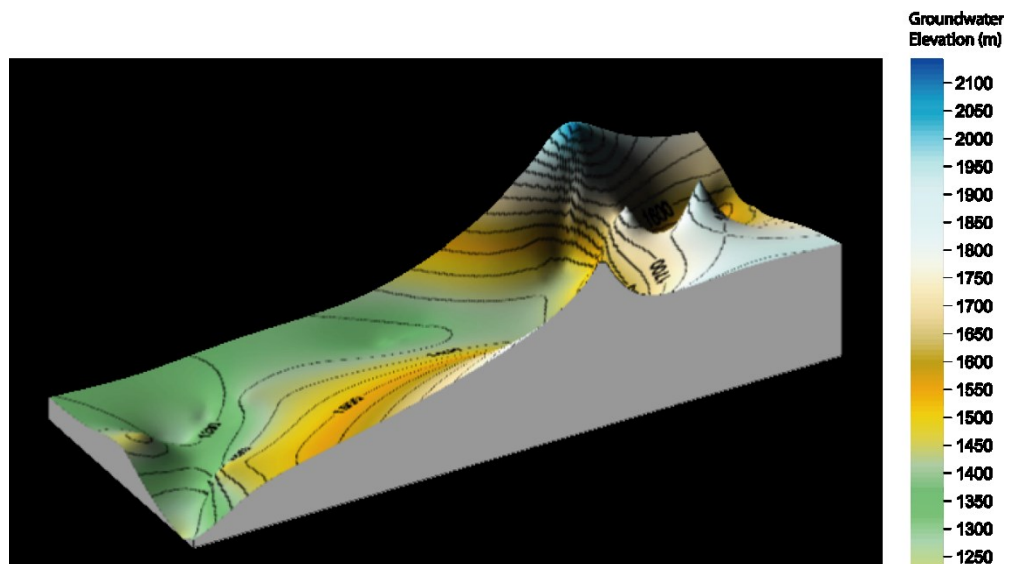
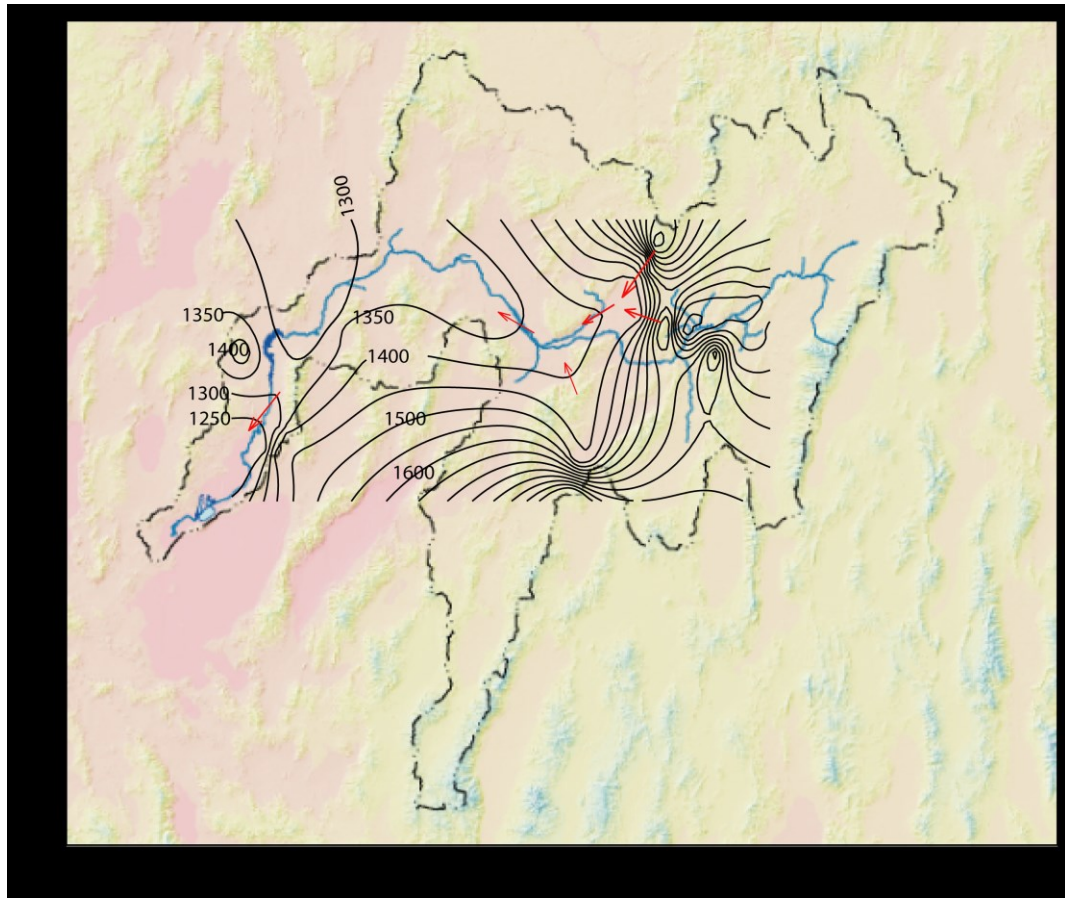


Figure 5.3: Top: Map illustrating contours of ground water elevation (meters above sea-level) and movement indicated by arrows around the HRB flood plains; bottom: 3-D schematic diagram showing ground water elevation with contours.

increase in the flow during this low flow period was the result of ground water discharging into the river. Similarly, with virtually no flow at Comus, the increase in flow at Imlay can be attributed to subsurface inflow of ground water discharging into the river, which is also evidenced in previous study between Comus and Rose Creek, which just north of Imlay (Cohen, 1963). Cohen (1963) also reported that a small part of the increase in flow may have been the result of subsurface inflow to the river of thermal water from the hot spring system near Golconda.

5.2.3. Morphology and geologic setting

The Humboldt River has been divided in this study into three geographic subdivisions on the basis of morphology and geology of the area: Upper Humboldt River (UHR), Middle Humboldt River (MHR), and Lower Humboldt River (LHR) (Figure 5.1 and Table 5.2). Figure 5.4 illustrates schematic surface geology of the area. The UHR extends from its sources at the base of the East Humboldt Range, Ruby Mountains, and Jarbidge Mountains to the confluence of Susie and Maggie Creeks near Carlin (Figure 5.1). The tributaries cut through sedimentary rocks, mafic volcanic (calc-alkali andesitic) and felsic volcanic (high-silica rhyolitic) rocks with some Paleozoic and Mesozoic carbonate rocks. Miocene volcanic and sedimentary rocks with some pre-Tertiary volcanic rocks are widespread along the river in this area; however, the Quaternary sediments are relatively lacking in this segment of the HRB (Figure 5.4).

The MHR comprises the area between Carlin and Comus just upstream of Golconda. The Humboldt River flows westward from Carlin towards Battle Mountain and then north-westwards towards Comus, where river flow is diverted at the Iron

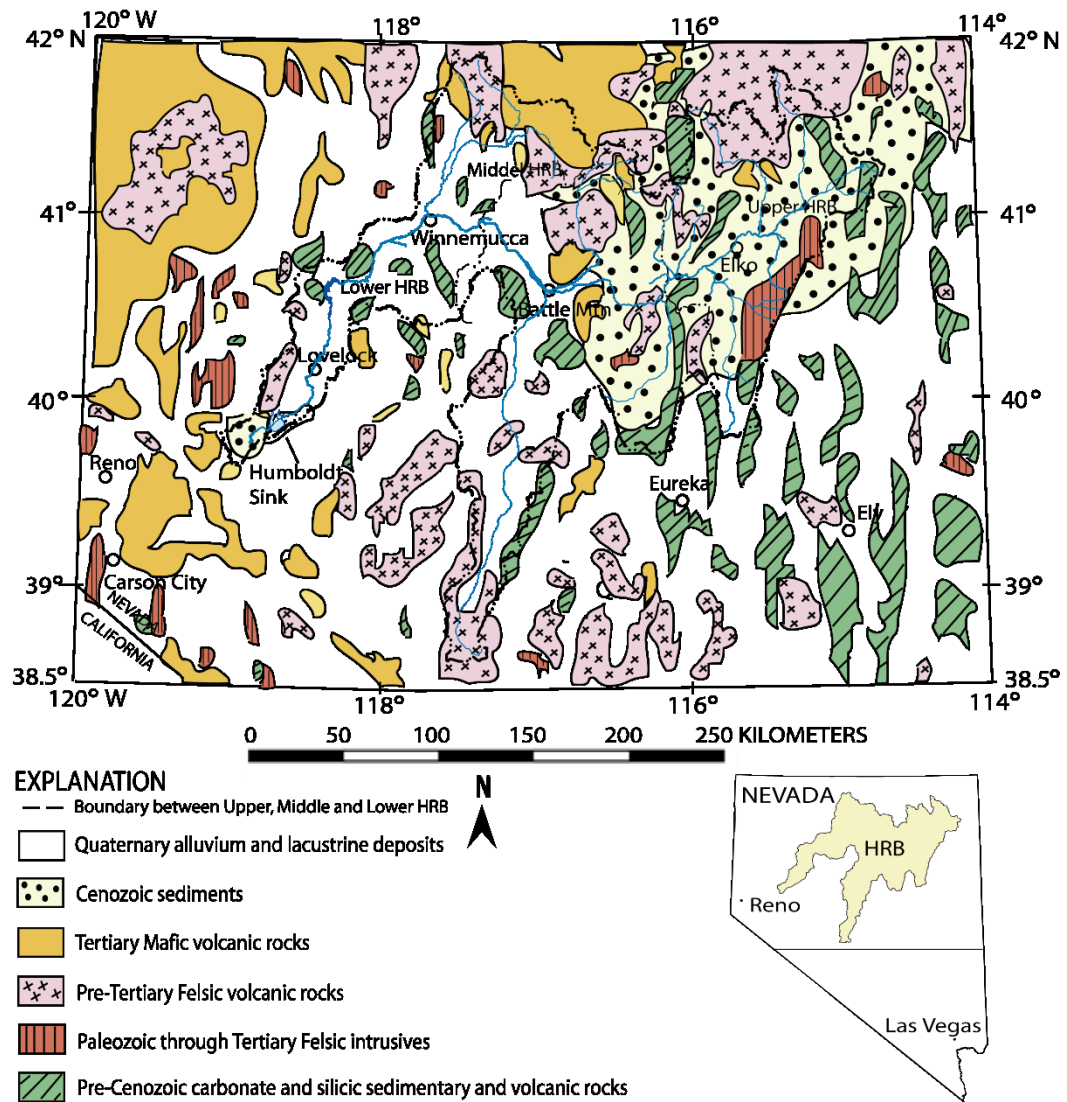


Figure 5.4: Schematic geologic map of HRB and northern Nevada (modified after Prudic et al., 2006; Wallace et al., 2004).

Table 5.2: Generalized summary of hydrologic sub-units of the Humboldt River Basin with schematic geologic settings in northern Nevada (modified after Plume 1995; and Maurer et al. 1996).

Hydrologic sub-units	Geologic characteristics
Upper Humboldt	<p>Relatively lacking of Quaternary flood-plain deposits.</p> <p>Few alluvial-fan deposits of boulders, gravel, sand, silt, clay, and intermittent beds of limestone and rhyolitic ash.</p> <p>Predominantly Cenozoic sedimentary rocks, mafic volcanic (calc-alkali andesitic) and felsic volcanic (high-silica rhyolite) rocks with some Paleozoic and Mesozoic carbonate rocks.</p> <p>Widespread Miocene volcanic and sedimentary rocks with some pre-Tertiary volcanic rocks.</p> <p>Carlin-type gold deposits at Carlin Trend, Independence Mountains, and Cortez near Crescent valley.</p>
Middle Humboldt	<p>Some Quaternary flood-plain deposits of sorted to poorly sorted boulders, gravel, sand, silt, and clay.</p> <p>Intermittent presence of Tertiary volcanic and Cenozoic sedimentary rocks.</p> <p>Widespread older basin-filled deposits of inter-bedded sediments and volcanic rocks deposited in lakes and streams including siltstone, clay, shale, limestone, conglomerate, and sandstone, with some tuff, and ash.</p> <p>Epithermal gold deposits at Midas, and sedimentary rock-hosted disseminated gold deposits at Lone Tree near Golconda.</p>
Lower Humboldt	<p>Widespread presence of Quaternary alluvium and lacustrine deposits of sorted to poorly sorted boulders, gravel, sand, silt, and clay.</p> <p>Sparse presence of pre-Tertiary sedimentary and volcanic rocks.</p> <p>Presence of evaporate minerals in the Quaternary alluvium, playa, and lacustrine deposits.</p>

Point relief canal and Hering Slough (Figure 5.1). This segment of the HRB is characterized by relatively widespread presence of Tertiary volcanic and Cenozoic sedimentary rocks in the drainage east of Battle Mountain, and widespread Quaternary alluvium and lacustrine deposits in the drainage west of Battle Mountain (Figure 5.4).

The LHR lies downstream of the MHR from Comus to the Humboldt Sink (Figure 5.1). The widespread presence of Quaternary alluvium and lacustrine deposits along with sparsely pre-Tertiary sedimentary and volcanic rocks characterize this section (Figure 5.4). The presence of evaporite minerals in the Quaternary alluvium; playa, and lacustrine deposits characterize the geological environment of this area.

5.2.4. Ore deposits, mining and geothermal activities

There are three major classes of mineral deposits in the HRB area: 1) pluton-related polymetallic deposits; 2) sedimentary rock-hosted gold-silver deposits (including Carlin-type and distal-disseminated gold-silver deposits); and 3) gold-silver deposits that formed in relatively shallow, epithermal environments (Wallace et al., 2004). The mining activities for pluton-related deposits are occurring at Battle Mountain, Copper Canyon, and Copper Basin, in the HRB area (Figure 5.1). Sedimentary rock-hosted gold-silver deposits in the HRB contribute the vast majority of the gold mined in the region. Many of the deposits are mined from deep, extremely large open pits, and exploitation of these deep ores has required extensive dewatering of adjacent aquifers (Wallace et al., 2004). In many cases, the fluids produced by dewatering are put back into the Humboldt River after treatment (Prudic et al., 2006). Besides Carlin-type deposits, distal disseminated deposits of gold-silver are being mined at Lone tree, Trenton Canyon, and Bald Mountain regions of the HRB. The

Great Basin region also contains the largest number of geothermal power plants in the US (Duffield and Sass, 2003), and the HRB has a few power plants that exploit geothermal energy (Shevenell and Garside, 2005; Shevenell et al., 2008) (Figure 5.1).

5.3. Methods

Sampling of river water and bottom sediments was performed in late September 2007, which is the low-flow season for Humboldt River. Because of the large extent of the area and limited accessibility of some locations, sampling was undertaken at the intersection points of highway and the river where it was accessible along the Humboldt River and the main tributaries. Location of sampling points was also limited by the availability of flowing water in the river because river flow in the fall typically is low. Samples were only collected at the sites where both river water and sediment samples could be obtained. However, a few samples of sediment-only were collected where flowing water was not present in the river. Because of dry river beds in the MHR section between Dunphy and Comus, two sediment-only samples were collected from the bed of Reese River, which is a tributary of the Humboldt River. Samples 009 and 010 for both water and sediments were collected from the Little Humboldt River in its upper reach. The location of water and sediment sampling sites is shown in Figure 5.1. A total of 15 river water and 18 sediment samples were collected to represent the entire area along the Humboldt River. The water samples that were collected from the river and tributaries were grab samples. The river bed sediment samples were collected using an extensional hand auger from the river bed at depths of 1.5 to 2 meters beneath the river bed.

5.3.1. Water analyses

The pH, oxidation reduction potential (ORP), conductivity, alkalinity, and temperature were measured in situ. Sample collection, handling, storage and preservation were undertaken following the U.S. Geological Survey sampling protocol (Shelton, 1994) to ensure the data quality and consistency. Water samples were filtered at 0.45 μm and subsets of samples for trace metal analysis were acidified with concentrated reagent-grade HNO_3 until pH reached approximately 2 standard units. Major cations and trace elements including As were analyzed by Inductively Coupled Plasma-Mass Spectrometer (ICP-MS). Another subset of filtered but not acidified samples was analyzed for major anions by Ion Chromatography (IC). Data quality was ensured by analyses of replicates, filled blank solutions, and certified reference solutions. All analytical procedures were done in the Acme Analytical Laboratories. Charge balance computed by the EQ3NR (Wolery and Jarek, 2003) computer program was $\leq 5\%$ for all samples. This program was also used for speciation and equilibrium calculation. The physico-chemical parameters and chemical components of water from the Humboldt River are shown in Table 5.3.

Stable isotope analysis

Stable isotope analyses of δD (deuterium) and $\delta^{18}\text{O}$ (oxygen-18) were performed using a Micromass IsoPrime stable isotope ratio mass spectrometer. Water- δD analyses were performed using the method of Morrison et al. (2001). δD results are reported in units of ‰ against the VSMOW standard. Water- $\delta^{18}\text{O}$ analyses were performed using the $\text{CO}_2\text{-H}_2\text{O}$ equilibration method of Epstein and Mayeda (1953).

Table 5.3: Summarized physical parameters and some important chemical components of waters from the Humboldt River. Concentrations are in mg/L unless otherwise stated. Samples were collected in late September, 2007.

Sample ID	pH	ORP (mV)	Cond. (μ S)	Temp ($^{\circ}$ C)	Ca	Mg	Na	K	Cl	SO ₄	Alk. ¹	B	Li	Fe	Mn	SiO ₂	As	$\delta^{18}\text{O}$	δD	$\delta^{34}\text{S}$
U 001	8.77	125.6	1240	14.7	75.9	70.03	252	18.47	61.5	565.1	525.82	2.13	0.11	<0.01	0.01	15.9	0.066	-14.5	-114	4.7
H 003	8.64	134.5	760	18.5	125	57.12	301.3	17.54	151.4	566.3	440.42	0.84	0.29	<0.01	0.37	20.7	0.012	-15.1	-125	9.8
R 004	8.85	10	720	17.6	49.1	20.38	47.99	10.53	24.3	59.3	264.74	0.24	0.11	0.02	0.06	14.8	0.013	N.S.	N.S.	10.3
007	8.85	105	980	13.6	57.9	29.35	173.7	11.91	120.6	144.1	420.9	0.52	0.10	0.04	0.00	15.2	0.021	-9.4	-98	12
008	8.85	105.4	920	16.2	47.7	19.19	146.4	11.76	75.1	104.6	347.7	0.64	0.17	0.03	0.00	18.2	0.037	-11.6	-105	N.S.
009	8.91	143.4	680	14.6	37.3	6.99	50.01	10.88	24	28.9	195.2	0.20	0.03	0.03	0.01	17.3	0.015	-9.2	-92	N.S.
010	8.44	162.6	660	17.4	29.2	5.68	63.21	13.04	26.7	32.4	195.2	0.22	0.04	0.01	0.01	40.4	0.012	-15.7	-125	N.S.
L 011	8.55	156.1	780	13.8	67.8	20.67	139.4	10.05	88.8	124.8	418.46	0.51	0.09	0.01	0.46	22.9	0.017	-13.9	-115	N.S.
H 012	8.96	192.4	830	9.9	43	24.05	114.4	8.92	108.7	132.1	276.94	0.69	0.08	0.03	0.01	14.9	0.019	-12.6	-110	N.S.
R 013	8.95	168	840	11.4	38.7	26.95	133	10.76	123	146.9	235.46	0.80	0.08	0.01	0.00	12.4	0.022	-11.1	-103	N.S.
015	9.13	139.3	1020	17.8	37.4	22.68	168.4	18.17	134.1	124.8	342.82	0.54	0.17	0.02	0.00	16.0	0.048	-7.5	-85	7.2
016	9.25	125	980	17.6	37.9	21.46	148.6	15.68	111.6	98.6	323.3	0.47	0.13	0.01	0.00	15.8	0.037	-8.5	-89	N.S.
017	9.04	145.2	1080	14.5	46.2	20.73	307.6	26.33	332.1	141.5	409.92	1.22	0.30	0.02	0.00	18.5	0.048	-9.6	-95	N.S.
018	8.92	136.1	1160	13.9	42.6	21.55	422.6	27.98	508.6	162.6	427	1.29	0.26	0.03	0.00	19.4	0.053	-9.6	-94	N.S.
019	8.93	119.2	1280	14.5	43.7	21.53	417.9	28.32	481.5	159.3	392.84	1.23	0.26	0.03	0.00	20.2	0.052	-9.7	-94	N.S.

ORP: Oxidation-Reduction Potential; ¹Alk.: Alkalinity as HCO₃⁻; Stable isotopes in ‰; N.S.: Not Sampled. NO₂, NO₃, and PO₄ were below detection limit.

The results of $\delta^{18}\text{O}$ are reported in units of ‰ against the VSMOW standard, where an uncertainty of $\pm 0.1\text{‰}$ was recommended.

Dissolved sulfate- $\delta^{34}\text{S}$ (sulfur-34 of dissolved sulfate) analyses were performed by precipitating dissolved sulfate as BaSO_4 after the method of Carmody et al. (1998), followed by stable isotope analyses performed using a Eurovector elemental analyzer interfaced to a Micromass IsoPrime stable isotope ratio mass spectrometer, after the method of Giesemann et al. (1994) and Grassineau et al. (2001). V_2O_5 was added to BaSO_4 samples as a combustion aid. $\delta^{34}\text{S}$ results are reported in units of ‰ against the VCDT standard, where an uncertainty of $\pm 0.1\text{‰}$ was recommended.

The isotopes were analyzed in the Nevada Stable Isotope Laboratory at the Mackay School of Earth Sciences and Engineering at the University of Nevada, Reno. The results of isotope values are listed in Table 5.3.

5.3.2. Analytical methods for river sediments

Sequential extraction methods

The river-bed sediment samples were dried at room temperature, disaggregated and crushed with acetone-washed porcelain pestle and mortar, and then sieved through a nylon 80 mesh ($<170\mu\text{m}$). These screened sediment samples were used for sequential extraction analysis for As and other cations and trace elements to determine the mineral phases associated with these elements. The sequential extractions were performed under oxic conditions in constantly agitated 50 ml centrifuge tubes, with a sample size of 1 g following methods modified after Tessier et al. (1979) and Li et al. (1995). After each extraction stage, supernatant was separated from the residue by centrifugation, and was stored into polypropylene

bottles for analysis. The residue was rinsed twice with deionised water, hand shaken and separated by centrifugation. The sequential extraction separated in order: exchangeable metals, carbonate-bound metals, amorphous Fe-Mn-oxide metals, organic metals, and residual fractions. Finally, total metals were extracted by digesting 400 mg of samples with 8 ml aqua-regia to determine the initial content of each element in the sample. All extracted fractions were analyzed using ICPMS for concentrations of total elements at the Mackay School of Earth Sciences and Engineering at the University of Nevada, Reno. The sum of elemental concentrations in each fraction and the inaccessible residual fraction are equal to initial content within the experimental error range of $\pm 3\%$.

XRD and SEM analyses

Selected samples that showed highest and lowest concentrations of arsenic in the sequential extraction were further analyzed by X-ray powder diffractometry (XRD) and Scanning Electron Microscopy (SEM) to determine the mineralogical association of arsenic in the sediments. XRD analysis was conducted using a Cu $K\alpha$ radiation and a graphite monochromator on a Philips® vertical diffractometer, stepped at 0.03, from 2° to 60° diffraction angle (2θ). Identification of the minerals in the samples was conducted using PC-APD® Diffraction software of Philips Analytical with search/match of the reference mineral database and generated powder patterns.

SEM analyses were conducted using energy dispersive spectra (EDS) on the same samples analyzed for XRD. SEM analysis was done using Hitachi S-4700 Field-emission scanning electronic microscope at the Department of Chemical and Metallurgical Engineering at the University of Nevada, Reno.

5.3.3. Data analysis

Factor analysis

The data obtained by analyses of waters and sediments were evaluated using factor analysis to identify simple correlations between chemical parameters. Factor analysis is a method of sorting and displaying complex relationships among many variables (Usunoff and Guzman, 1989; Guler et al. 2002); in our case, the variables are chemical parameters. Factor analysis can be used to determine the major processes that may control the distribution of hydrochemical variables as a function of geography and geology (Stuben et al., 2003; Wang et al., 2007; Dongarra et al., 2009; Jang, 2010). These analyses were performed using Principal Component Analysis (PCA) extraction method by means of the Statistical Package for Social Sciences (SPSS) software package. Details about the factor analyses and its limitations and assumptions have been described in chapter 2.

Because of the lack of adequate data in each three geographic areas of the basin (Figure 5.1), simple correlation and comparison analyses were non-representative, and therefore, factor analyses were performed for both river waters and river-bed sediments to determine the underlying complex relationships among many variables (i.e., dissolved As with ions and chemical parameters). The sediment samples 005S and 006S, and river water samples 009 and 010 (Figure 5.1) were not included in the factor analyses because: 1) samples 005S and 006S were only two sediment samples without water samples, collected from the middle Humboldt River Basin and represent the samples from Reese River, a tributary of the Humboldt River; 2) samples 009 and 010 represent samples from Little Humboldt River and Martin Creek, the waters from which do not contribute to the Humboldt river in low-

flow season (Prudic and Herman, 1996). For sediments, factor analyses were performed on the total elemental concentrations obtained from ICP-MS analyses of the solutes from aqua-regia-digested sediment samples. Factor analyses for river waters were performed on the analytical results of water chemistry and physical parameters that include pH, temperature, and electrical conductivity (EC).

5.4. Results

5.4.1. Chemistry of water

In general, the river waters are alkaline with a pH ranging from 8.64 to 9.13, and oxidizing with ORP ranging from 10 mV to 192.4 mV, with a wide range of conductivity ranging from 720 to 1280 $\mu\text{S}/\text{cm}$. Concentrations of dissolved As range from 0.01 mg/L to 0.07 mg/L with an average of 0.03 mg/L and standard deviation of 0.017 (Table 5.3). The water is predominantly (Na+K)-SO₄ type in the UHR, and (Na + K)-HCO₃ type in the northern LHR, with changing to (Na + K)-Cl type around the Lovelock Valley (Figure 5.5). Figure 5.6 illustrates stiff diagrams showing changes in major chemical constituents of the water samples along the flow-path of the river.

Arsenic concentrations in the water analyses are total As (Table 5.3), and speciation modeling results indicate that more than 99% of As species are As (V) [HAsO₄⁻]. Arsenic concentrations range from 0.12 mg/L to 0.066 mg/L with the highest (0.066 mg/L) and the lowest (0.012 mg/L) concentrations in the UHR.

Stable isotopes of ¹⁸O and H (deuterium) of Humboldt River water samples range from -7.5‰ to -15.7‰ for ¹⁸O and from -85‰ to -125‰ for deuterium (Table 5.3 and Figure 5.7). In the plot of $\delta^{18}\text{O}$ versus δD isotopes (Figure 5.7), it can be observed that the overall water has δD and $\delta^{18}\text{O}$ values that systematically shift from

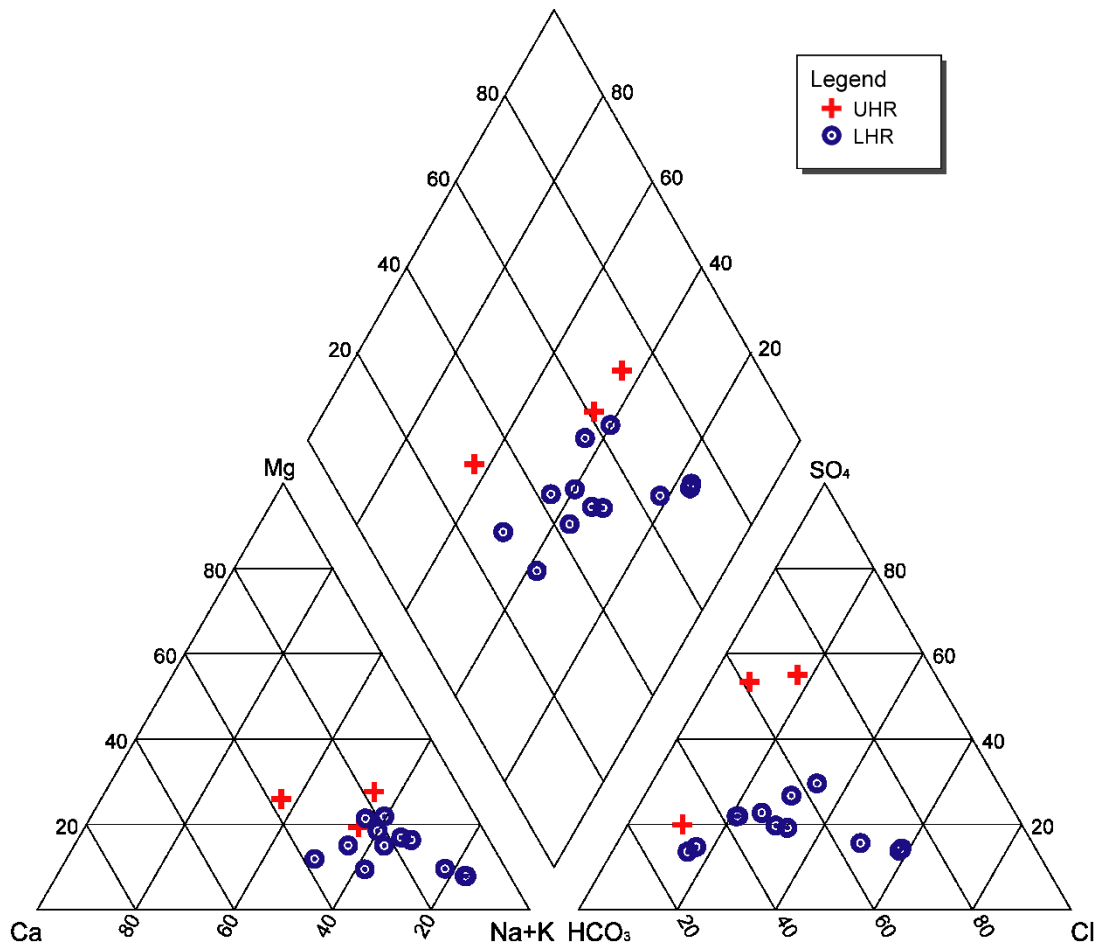


Figure 5.5: Piper diagram showing hydrochemical phases for river waters of the upper, middle and the lower Humboldt River.

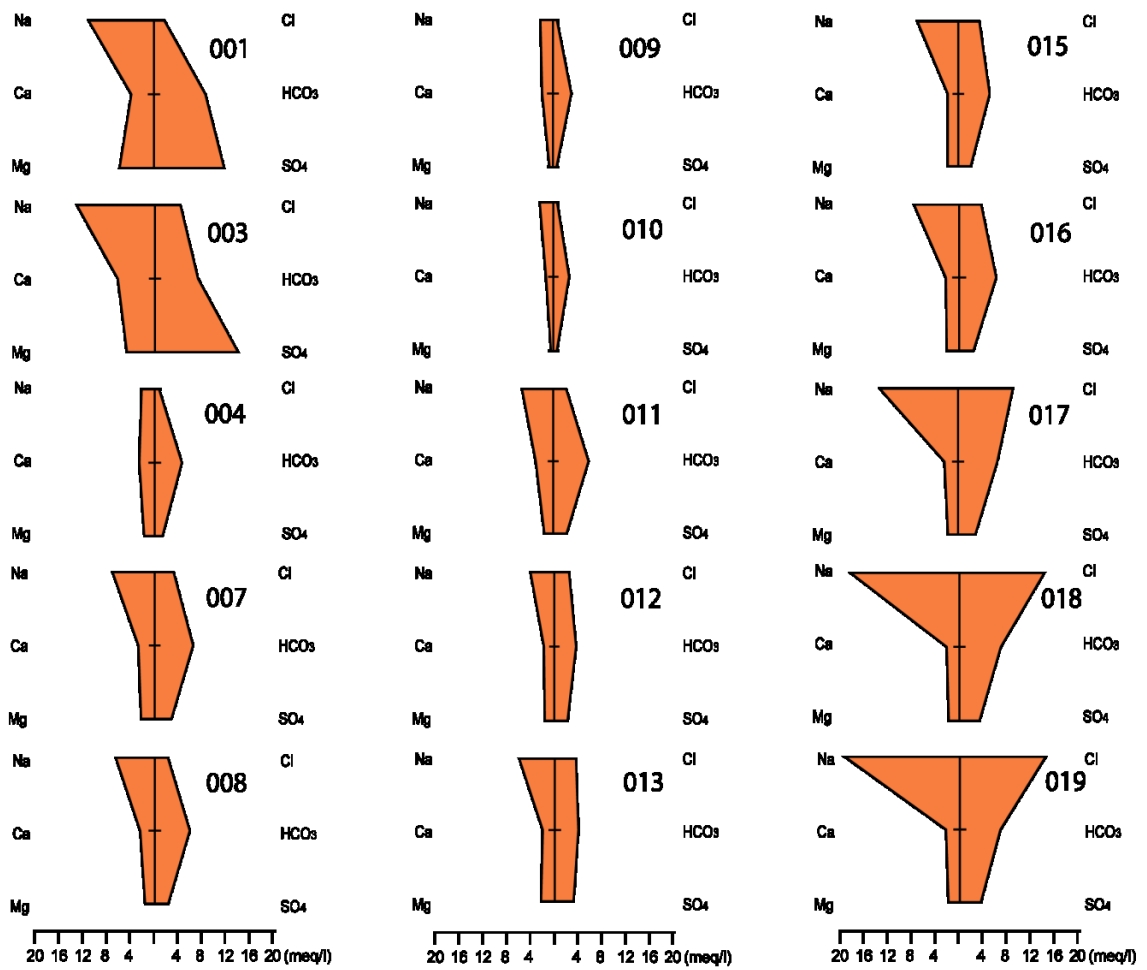


Figure 5.6: Stiff diagrams of river water samples (sample numbers on right of each diagram) showing differences in major chemical composition. Samples from the UHR (001 and 003) have high contents of Na-SO₄; samples from 004 to 016 illustrate almost similar composition with Na-HCO₃, whereas samples from 017 to 019 illustrate higher contents of Na-Cl.

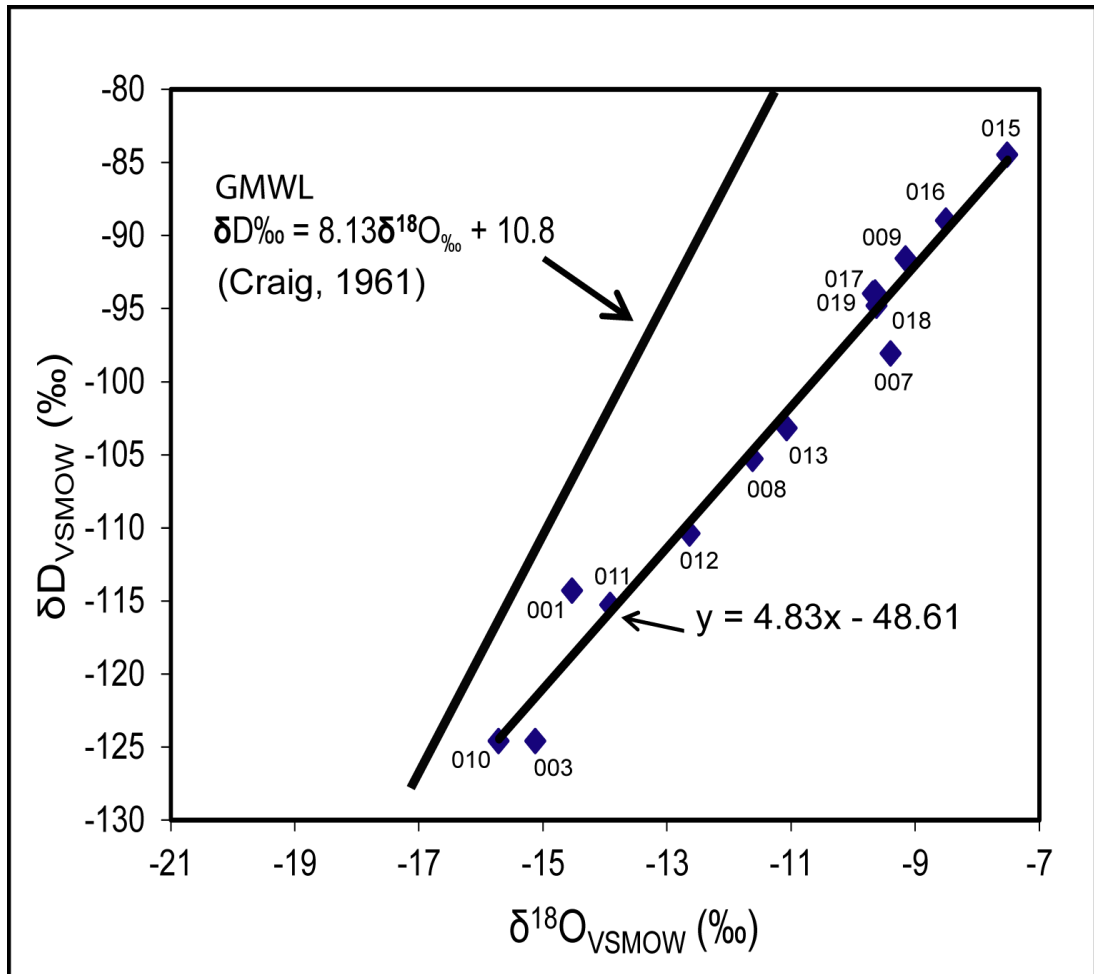


Figure 5.7: Relationship between oxygen and hydrogen isotope data of surface water samples collected from the Humboldt River and its tributaries.

the GMWL towards the right with a slope of about 4.8, indicating that evaporation is occurring (Clark and Fritz, 1997; Sueker, J.K., 2003). Sulfur isotopes of dissolved sulfate range from +4.7‰ to +12‰ with an average of +8.8‰ and standard deviation of +2.6‰ (Table 5.3), indicating oxidation of sulfide minerals for the source of dissolved SO₄ as supported by similar results found by Tuttle et al (2003) in the waters of the Copper Basin near Battle Mountain.

5.4.2. Mineralogy and chemistry of river-bed sediments

The XRD analyses of sediments indicate the most abundant minerals to be quartz, orthoclase feldspar, calcite, and muscovite. No As-mineral phases (e.g., realgar, orpiment, arsenopyrite, etc.) were identified by XRD analysis. SEM analysis of the sediments further identified silicate and detrital aluminum silicate-clay minerals in the river-bed sediments along with minor amounts of iron-oxide/hydroxides (Figure 5.8). For example, sediment samples 006 and 007 (Figure 5.8 A&B) illustrate typical flaky texture of detrital smectite clay on the surface quartz grains; samples 012 and 015 (Figure 5.8 C&D), illustrate smectite-illite growth; with typical flaky smectite clay minerals on the surface of partially dissolved feldspar; samples 016 and 019 (Figure 5.8 E&F) illustrate detrital flaky smectite clays on the surface of partially dissolved feldspar minerals.

The scattered presence of ferrihydrite, which was expected to be more common in the river-bed sediments, is confirmed by the EDS analysis of the sediments. SEM analysis also revealed minor amounts of carbonates with insignificant amounts of sulfur and trace elements including titanium, copper, and barium in some of the sediment samples.

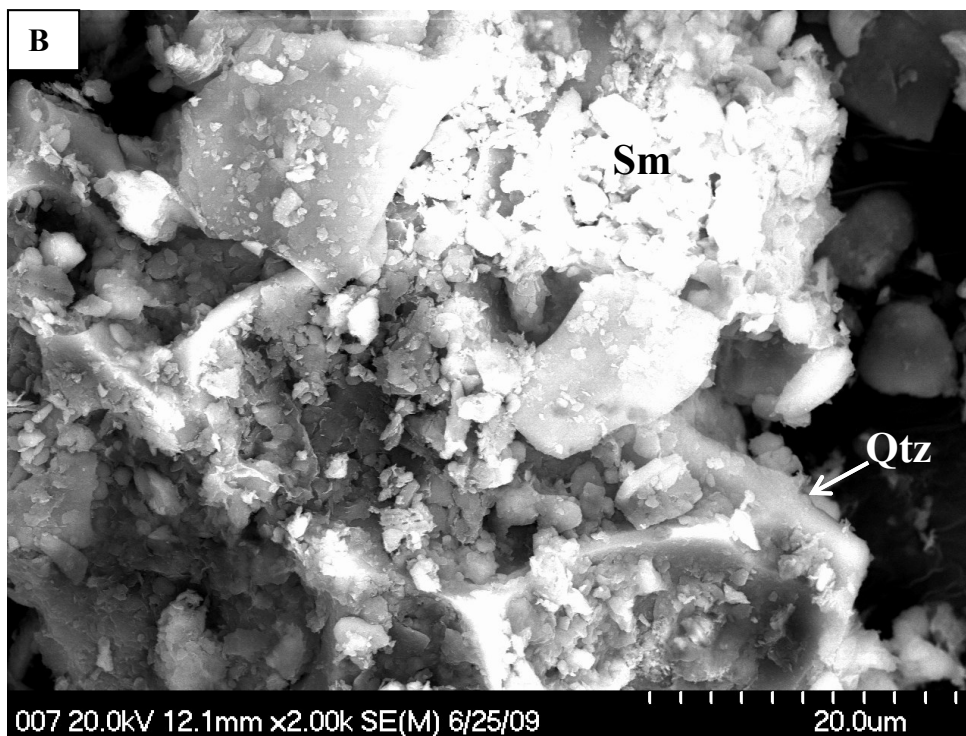
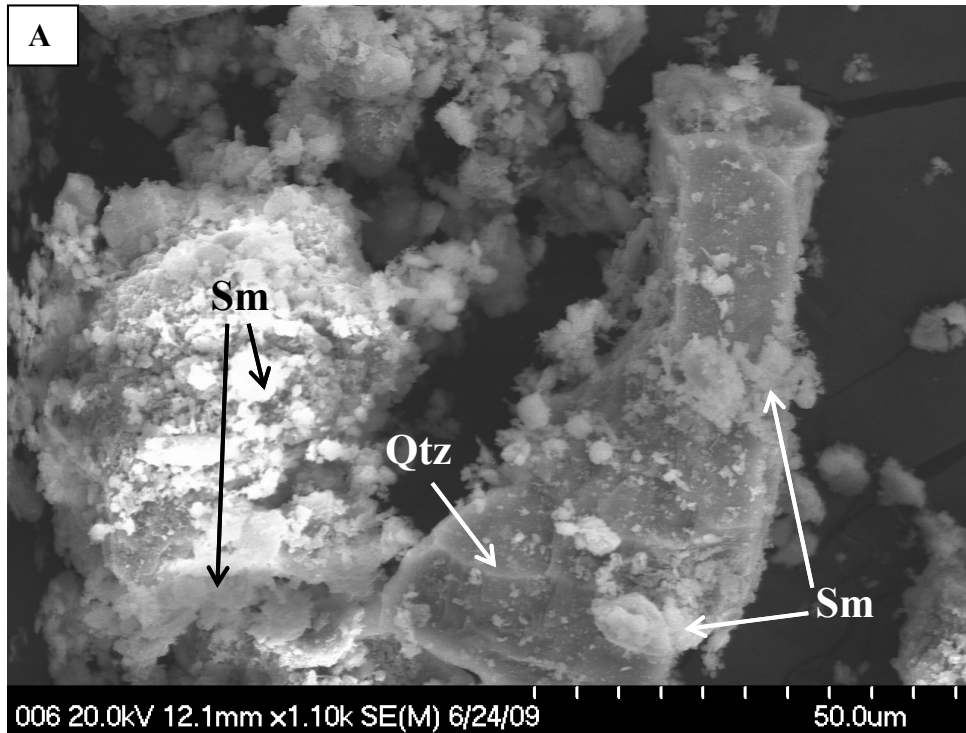


Figure 5.8: Photomicrographs of river-bed sediments: A) sample 006, illustrating typical detrital smectite clay (Sm) on the surface quartz (Qtz) grains; B) sample 007, illustrating typical flaky nature of smectite (Sm) clay minerals on the surface of quartz (Qtz) grains.

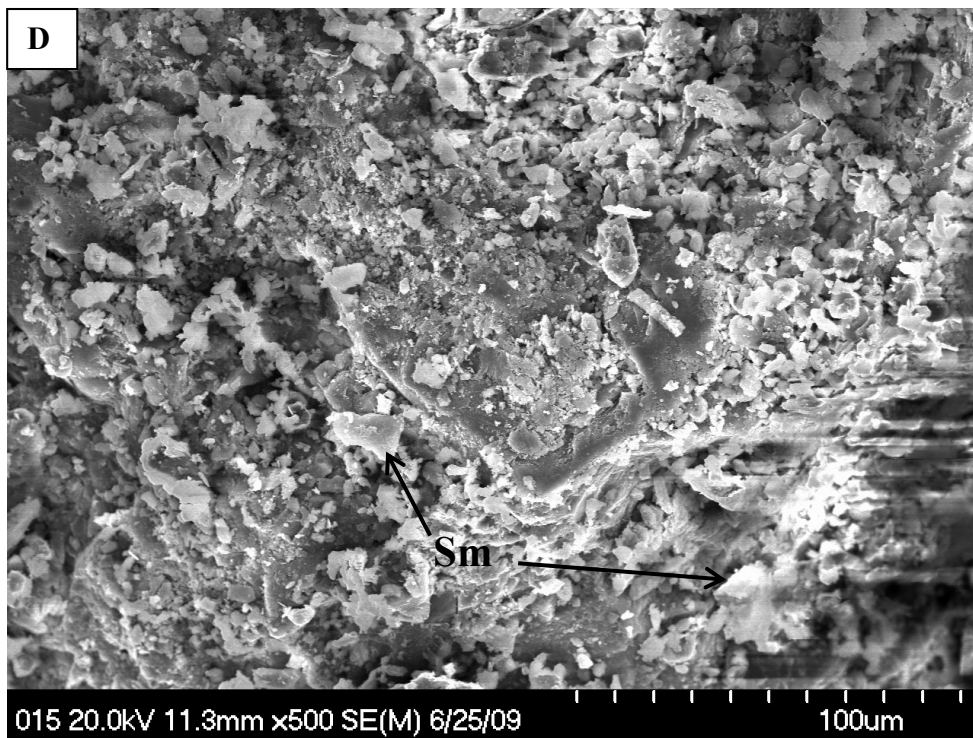


Figure 5.8: Photomicrographs of river-bed sediments: C) sample 012, illustrating smectite-illite (Sm/III); D) sample 015, illustrating typical flaky nature of smectite (Sm) clay minerals on the surface of partially dissolved feldspar.

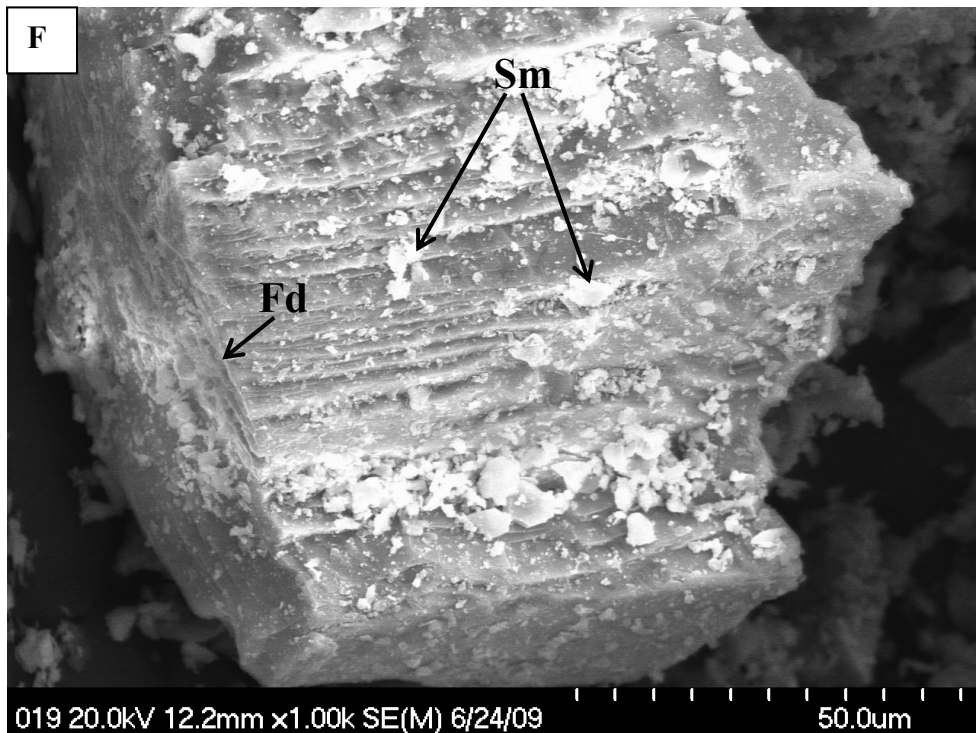
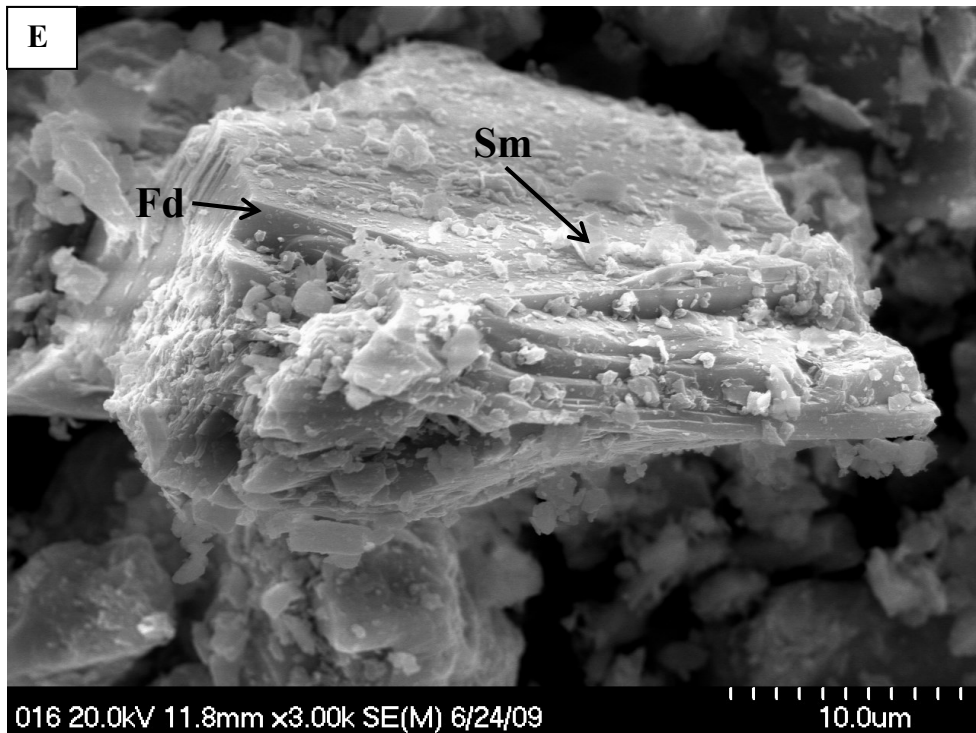


Figure 5.8: Photomicrographs of river-bed sediments: E) sample 016, illustrating detrital flaky smectite clays (Sm) on the surface of feldspar (Fd); F) sample 019, illustrating typical flaky nature of smectite (Sm) clay minerals on the surface of partially dissolved feldspar (Fd).

Table 5.4: Concentrations (mg/kg) of As, and other elements in the river-bed sediment samples in different fractions obtained from sequential extraction analyses. Note: ND: Not Detected.

Element	Fractions	Sample ID																	
		UPPER			MIDDLE									LOWER					
		001	002	003	005	006	007	008	009	010	011	012	013	013b	014	015	016	017	019
Al	Exchangeable	11.6	46.8	2.3	16.0	120	36.3	12.0	21.7	91.2	50.3	41.2	37.5	13.5	22.2	19.8	55.6	94.2	5.0
	Carbonates	215	567	158	244	225	246	346	910	377	312	1620	1535	11.4	207	1310	958	202	74.8
	Organic -metals	526	430	1223	1210	1202	835	1135	1077	1073	633	634	266	1124	1052	397	222	1426	219
	Fe-Mn-Oxides	12.2	4.9	19.6	5.1	14.8	4.3	6.8	1.1	12.6	0.0	9.4	2.8	10.2	4.6	8.4	0.0	4.5	0.0
	Residual	2182	2172	1861	3132	2215	3512	2262	1535	1937	2695	1634	2419	3889	3299	2967	3158	3584	3613
	Total	2978	3322	3323	4706	3876	4734	3862	3644	3592	3782	4038	4361	5147	4684	4802	4492	5410	4009
As	Exchangeable	0.44	0.28	0.23	0.09	0.26	0.26	0.03	0.05	0.05	0.04	0.02	0.02	0.02	0.10	ND	0.00	0.09	ND
	Carbonates	0.21	0.20	0.19	0.40	0.27	0.35	0.45	0.24	0.27	0.25	0.94	0.28	0.47	0.44	0.78	0.21	0.66	0.37
	Organic -metals	1.13	0.94	1.96	4.12	3.09	2.59	4.17	2.38	1.42	1.38	3.76	0.34	3.85	2.29	2.18	0.24	9.73	0.46
	Fe-Mn-Oxides	6.64	3.75	7.46	43.41	21.95	21.13	13.58	2.06	6.37	15.89	31.96	14.01	34.75	30.46	32.18	2.83	45.43	8.91
	Residual	88	89	97	152	131	143	142	47	75	57	121	104	162	75	194	121	150	71
	Total	100	97	111	202	159	171	164	53	87	78	160	122	203	112	233	126	208	83
B	Exchangeable	ND	ND	ND	ND	ND	ND	ND	ND	ND	ND	ND	ND	ND	ND	ND	ND	ND	ND
	Carbonates	1.16	1.08	0.68	1.21	0.83	1.03	1.11	0.36	0.67	0.59	0.75	0.80	0.02	0.55	1.00	0.64	0.98	0.24
	Organic -metals	0.22	0.01	0.91	5.90	1.37	0.00	1.56	0.43	0.29	0.06	0.45	0.00	2.80	0.10	0.33	0.00	17.5	0.25
	Fe-Mn-Oxides	1.16	0.00	0.08	1.19	0.15	0.07	0.14	0.00	0.34	0.07	0.13	0.09	0.32	0.37	0.20	0.02	1.73	0.24
	Residual	504	362	587	300	643	310	670	147	598	47	503	257	740	455	773	132	946	95
	Total	516	372	597	320	654	322	684	157	610	49	514	266	755	465	784	143	977	105
Ca	Exchangeable	288	168	171	113	227	214	138	186	248	186	124	120	166	393	41	82	277	47
	Carbonates	10072	7743	7814	18954	12228	17104	24293	9906	13268	10562	22920	11656	24345	25436	25395	7785	21995	16639
	Organic -metals	617	586	687	4004	2333	983	1770	695	737	675	5674	208	2540	1518	1394	148	15343	356
	Fe-Mn-Oxides	ND	ND	ND	ND	ND	ND	ND	ND	ND	ND	ND	ND	ND	ND	ND	ND	ND	ND
	Residual	36439	44420	44187	51794	41224	50092	29863	28877	36764	43412	29753	51157	47533	40520	39747	57073	38650	40921
	Total	47429	52927	52871	74878	56023	68408	56072	39675	51030	54848	58479	63149	74591	67879	69591	65101	78276	57974

Continued to next page

Element	Fractions	Sample ID																	
		UPPER			MIDDLE			LOWER											
		001	002	003	005	006	007	008	009	010	011	012	013	013b	014	015	016	017	019
Cd	Exchangeable	ND	ND	ND	ND	ND	ND	ND	ND	ND	ND	ND	ND	ND	ND	ND	ND	ND	ND
	Carbonates	0.10	0.03	0.05	0.02	0.05	0.09	0.06	0.03	0.06	0.10	0.03	0.06	0.08	0.13	0.02	0.00	0.08	0.00
	Organic -metals	22.5	24.9	24.2	24.3	23.4	23.5	24.2	23.1	22.3	23.0	21.4	23.3	22.8	22.4	25.8	25.3	26.4	24.8
	Fe-Mn-Oxides	0.23	0.19	0.27	0.75	0.39	0.42	0.31	0.15	0.21	0.30	0.48	0.24	0.63	0.63	0.42	0.03	0.91	0.14
	Residual	16.2	12.3	19.3	7.8	18.7	11.6	23.0	5.6	16.5	2.7	16.4	8.4	20.8	13.4	19.8	4.7	23.1	3.4
	Total	16.8	13.0	20.1	8.2	19.4	12.4	23.8	6.1	18.0	2.9	17.0	9.0	22.8	14.4	20.9	4.8	23.7	3.6
Co	Exchangeable	ND	ND	ND	ND	ND	ND	ND	ND	ND	ND	ND	ND	ND	ND	ND	ND	ND	ND
	Carbonates	0.34	0.29	0.32	0.22	0.28	0.32	0.27	0.60	0.52	0.48	0.42	0.42	0.39	0.36	0.36	0.42	0.33	0.42
	Organic -metals	0.7	0.24	1.38	2.01	0.84	1.24	2.45	2.76	1.42	0.73	0.92	0.16	2.00	0.76	0.89	0.08	5.07	0.27
	Fe-Mn-Oxides	ND	1.77	0.56	0.03	0.95	0.05	0.12	0.82	2.44	0.22	0.14	0.39	0.55	0.17	0.15	0.16	0.98	0.42
	Residual	33	41.9	44.0	38.2	39.5	53.5	48.1	42.6	63.0	27.8	34.9	36.7	56.7	61.4	41.5	25.6	69.9	19.0
	Total	36	46	47	42	42	56	53	48	68	31	38	39	61	64	44	28	77	22
Cu	Exchangeable	ND	ND	ND	ND	ND	ND	ND	ND	ND	ND	ND	ND	ND	ND	ND	ND	ND	ND
	Carbonates	ND	ND	ND	ND	ND	ND	ND	ND	ND	ND	ND	ND	ND	ND	ND	ND	ND	ND
	Organic -metals	5.7	7.06	17.13	11.63	6.17	10.21	15.69	19.42	6.00	5.30	3.70	1.43	14.65	8.58	2.40	1.37	20.34	0.87
	Fe-Mn-Oxides	0.21	1.23	0.67	1.19	0.89	0.89	0.90	0.43	1.67	0.79	0.85	1.16	1.44	2.61	0.78	0.26	0.98	0.42
	Residual	82	83	81	91	74	134	87	59	110	63	81	86	114	227	89	64	126	30
	Total	89	94	101	105	82	148	105	82	121	72	89	90	133	240	95	68	149	32
Fe	Exchangeable	ND	ND	ND	ND	ND	ND	ND	ND	ND	ND	ND	ND	ND	ND	ND	ND	ND	ND
	Carbonates	97.1	214	66	63	46	101	136	197	52	72	436	391	13	44	296	203	66	25
	Organic -metals	ND	ND	ND	ND	ND	ND	ND	ND	ND	ND	ND	ND	ND	ND	ND	ND	ND	ND
	Fe-Mn-Oxides	486	485	718	398	174	524	318	384	227	254	312	324	110	123	315	84	147	371
	Residual	1810	1986	1938	3258	2737	3031	2511	2160	2490	2404	2270	2549	3870	3467	2852	2866	3951	2116
	Total	2492	2786	2822	3820	3056	3757	3066	2840	2868	2829	3119	3363	4092	3733	3562	3252	4265	2612

Continued to next page

Element	Fractions	Sample ID																			
		UPPER			MIDDLE		LOWER														
		001	002	003	005	006	007	008	009	010	011	012	013	013b	014	015	016	017	019		
Mo	Exchangeable	ND	ND	ND	ND	ND	ND	ND	ND	ND	ND	ND	ND	ND	ND	ND	ND	ND	ND	ND	
	Carbonates	0.16	0.02	0.02	0.02	0.02	0.07	0.03	ND	0.02	0.03	ND	ND	0.02	0.00	ND	ND	0.01	ND	ND	
	Organic -metals	0.62	0.10	0.23	0.15	0.16	0.20	0.37	0.24	0.15	0.11	0.22	0.02	0.32	0.12	0.04	0.02	0.48	0.00	ND	ND
	Fe-Mn-Oxides	0.08	0.15	0.11	0.55	0.26	0.22	0.17	0.05	0.12	0.14	0.41	0.15	0.37	0.32	0.30	0.03	0.48	0.11	ND	ND
	Residual	14.6	10.1	14.7	5.87	15.6	7.58	17.6	3.85	15.4	2.31	11.8	7.51	17.1	9.84	15.0	4.57	15.5	2.89	ND	ND
	Total	17.0	10.9	16.6	7.26	17.6	9.57	19.7	5.22	16.19	2.69	13.9	7.82	18.7	11.8	15.9	4.69	17.0	3.12	ND	ND
Ni	Exchangeable	ND	ND	ND	ND	ND	ND	ND	ND	ND	ND	ND	ND	ND	ND	ND	ND	ND	ND	0.03	
	Carbonates	0.29	0.38	0.25	0.17	0.31	0.39	0.32	0.35	0.69	0.43	0.75	0.66	0.16	0.24	0.62	0.37	0.22	0.13	ND	ND
	Organic -metals	2.53	1.27	11.7	14.3	8.72	4.89	16.4	12.7	3.22	2.91	4.61	1.37	17.6	3.05	2.26	0.57	28.4	1.26	ND	ND
	Fe-Mn-Oxides	1.65	2.21	2.94	1.84	1.07	2.00	1.49	1.63	3.52	1.34	1.67	1.78	1.18	1.03	1.31	0.49	2.80	1.70	ND	ND
	Residual	402	462	465	467	424	594	470	364	536	348	412	461	608	655	431	359	686	213	ND	ND
	Total	415	477	489	495	443	612	498	390	554	362	430	476	638	668	446	370	728	222	ND	ND
U	Exchangeable	0.00	0.00	ND	0.00	0.00	0.00	0.00	ND	0.00	ND	0.00	0.00	ND	ND	0.00	0.00	0.01	ND	ND	
	Carbonates	0.02	0.01	0.00	0.02	0.01	0.00	ND	ND	0.03	0.00	0.07	0.08	0.00	0.00	0.08	0.01	0.00	ND	ND	
	Organic -metals	0.44	0.23	0.46	0.62	0.53	0.33	0.42	0.35	0.26	0.20	0.34	0.10	0.52	0.33	0.17	0.03	1.02	0.08	ND	ND
	Fe-Mn-Oxides	0.05	0.02	0.02	0.44	0.16	0.06	0.02	ND	0.07	0.02	0.11	0.07	0.06	0.09	0.10	0.02	0.20	0.06	ND	ND
	Residual	14.6	9.86	10.6	23.0	18.0	14.1	11.4	5.35	9.86	5.88	10.0	12.5	14.8	10.8	12.0	7.87	20.3	3.87	ND	ND
	Total	15.6	10.6	11.5	25.6	19.2	15.0	12.3	5.83	10.7	6.22	10.7	13.35	16.7	11.5	12.9	8.39	22.0	4.09	ND	ND

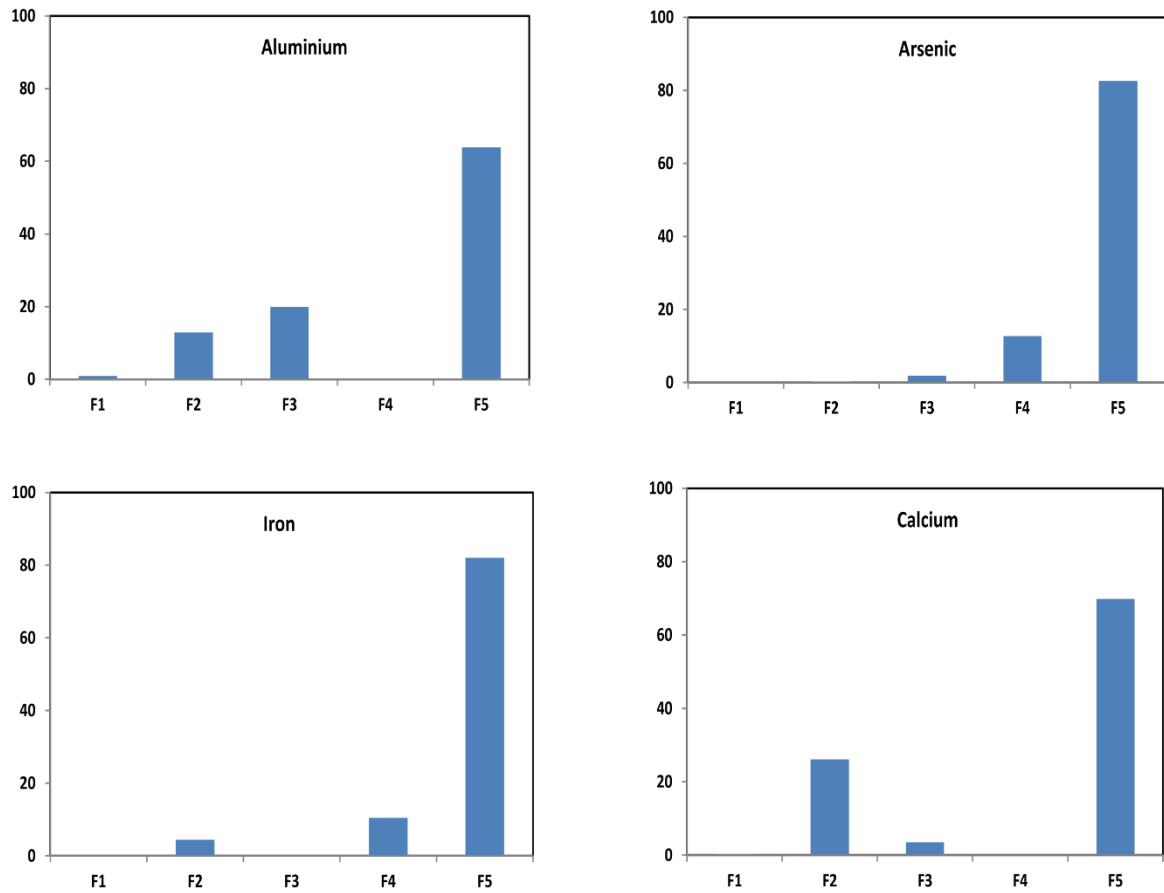


Figure 5.9 : Elemental concentrations (%) of some key-elements in the river-bed sediments obtained from sequential extraction analyses. F1: Exchangeable fraction; F2: Carbonate-bound fraction; F3: Organic metal fraction; F4: Fe-Mn Oxide and hydroxide fraction; F5: Residual fraction.

Results of sequential extraction analysis for As and other elements in the river-bed sediment samples are provided in Table 5.4. Figure 5.9 illustrates the elemental concentrations of As, Al, Fe, and Ca in percentage to total concentrations of elements in the river-bed sediments. On average about 83% of total As is extracted from the residual fraction, which corresponds to silicate and clay minerals followed by 13% from the Fe-Mn-oxide fraction. Arsenic in the organic metal fraction, carbonates, and exchangeable fractions are very low, averaging 1.8%, 0.29% and 0.094%, respectively. Very low percentages of As from the exchangeable fraction (0.094%) indicates that an insignificant amount of As is readily available for exchange.

As expected, the strongly hydrolyzing element Al is measured almost exclusively (about 64%) in the residual fraction, being one of the major constituents of clay minerals, and feldspars. The amount of Al detectable in carbonates (13%) and organic matter (20%) fractions actually corresponds to Al bound to carbonates and organic matter.

About 82% of total iron (Fe) is bound to the residual fraction, followed by about 10% in the Fe-Mn oxide fraction, and about 4% to carbonate-bound metal fractions.

Predominance of Ca (about 70% of total Ca) in the residual fraction occurs in silicate phases such as plagioclase feldspar and smectite clay minerals, followed by 26% in the carbonate fractions indicating carbonate minerals (e.g., calcite) which have been identified by XRD and SEM analyses.

The relative dominance of Al (64%), Ca (70%), and Fe (82%) in the residual fraction can be accounted for by silicate (e.g. feldspars) and clay minerals, such as smectite, and Fe-bearing illite, which have also been identified by XRD and SEM

analyses. A relatively, lesser amount of Fe (about 10%) in Mn-Fe-oxide and hydroxide fraction can be accounted for by Fe partitioned in amorphous and poorly crystalline hydroxides, as expected from SEM and XRD analyses.

5.4.3. Relationship of arsenic with chemical parameters

Factor analyses results for river-bed sediments

The results of factor analyses on total elemental concentrations for river-bed sediments are listed in Tables 5.5 (A, and B). In UHR sediments (samples 001 to 003), two factors have been identified (Table 5.5A). Factor 1 has strong positive loadings on Al, Ca, Co, Cu, Fe, Ni and weak loading on As (0.3) that represents 64% of the total variance. Factor 2 has strong positive loadings on B, Cd, and Mo, and negative loadings on As (-0.95), that represents 36% of the total variance. Results suggest that As is weakly associated with Co, Cu, Fe and Ni in majority of the sediment samples, whereas As is not associated with B, Cd, and Mo.

In LHR sediments (samples 007 to 019), two factors have been identified (Table 5.5B). Factor 1 has strong positive loadings on Al, As, B, Ca, Cd, Co, Fe, Mo, Ni, and U with moderate loading on Cu that represents 75% of the total variance. Factor 2 has negative loading on As (-0.41), and poor loading on Cu that represents 13% of the total variance. Results suggest that the number of elements that are associated with As is increased in the LHR sediments from that of the UHR sediments.

Table 5.5A: Factor analyses results of total elemental concentrations of the upper Humboldt River-bed sediments (samples from 001 to 003) that were digested in aqua-regia. Statistical results were obtained by applying Principal Component Analysis (PCA). The numbers in the rows represent factor loadings for each component, and marked bold typefaces represent the values of factor loadings of over 0.75. Statistics are based on cases with no missing values for any variable used.

Component	Factor 1	Factor 2	Communalities
Al	1.00	0.05	1
As	0.30	-0.95	1
B	-0.10	1.00	1
Ca	1.00	-0.07	1
Cd	0.01	1.00	1
Co	1.00	-0.04	1
Cu	0.83	0.55	1
Fe	1.00	0.04	1
Mo	-0.51	0.86	1
Ni	1.00	0.10	1
U	-0.98	0.21	1
Initial eigenvalues	6.99	4.01	
Percentage of variance	63.5	36.5	
Cumulative % of variance	63.5	100	
Total Communalities			11
Proportion of the total variation explained by the factors			1

Table 5.5B: Factor analyses results of total elemental concentrations of the lower Humboldt River-bed sediments (samples from 007 to 019) that were digested in aqua-regia. Statistical results were obtained by applying Principal Component Analysis (PCA). The numbers in the rows represent factor loadings for each component, and marked bold typefaces represent the values of factor loadings of over 0.75. Statistics are based on cases with no missing values for any variable used.

Component	Factor 1	Factor 2	Communalities
Al	0.85	0.33	0.83
As	0.82	-0.41	0.84
B	0.89	-0.41	0.96
Ca	0.85	0.32	0.83
Cd	0.86	-0.49	0.97
Co	0.94	0.14	0.90
Cu	0.69	0.45	0.67
Fe	0.94	0.29	0.97
Mo	0.82	-0.52	0.94
Ni	0.91	0.28	0.91
U	0.94	0.02	0.89
Initial eigenvalues	8.30	1.43	
Percentage of variance	75.45	13.02	
Cumulative % of variance	75.45	88.47	
Total Communalities			9.73
Proportion of the total variation explained by the factors			0.88

Factor analyses results for river waters

Factor analyses of the upper and lower HR waters indicate the relative importance of geographic regions in water chemistry and arsenic concentrations in river water. Table 5.6 (A & B) presents the results of factor analyses for river waters.

In the UHR waters, dissolved As is moderately associated (0.41) in factor 1 which represents the majority (62%) of the total variance with strong loadings on ORP, alkalinity, Ca, Cl, Cu, K, Mg, Na, and SO₄ (Table 5.6A). The results represented by factor 1 probably reflect oxidation of sulfides with strong positive loading of SO₄ (0.99) and ORP (1.0).

In the LHR, dissolved As is not significant with negative factor loading (factor loading of -0.93) for factor 1 that represents 44% of the variances with strong positive factor loadings on conductivity, B, Ba, Ca, Fe, K, Mg, and Na (Table 5.6B). The evolved water chemistry in the LHR probably reflects the multiple processes including evaporation and mixing with geothermal waters with moderate loading on Cl and high loadings on conductivity, Na, K, Mg, Ca, Ba, and B because of known geothermal waters with high contents of abovementioned elements near Golconda (Table 5.7). Factor 2 with 19% of the variances have high factor loadings on Al, dissolved SiO₂ and SO₄, which probably reflects dissolution of silicates and sulfate salts. Factor 3 with 14% of the variances have moderate loading on As with high loading on Cl and negative high loading on temperature, probably reflects the water chemistry from evaporative enrichment. Factor 4 with 11% of the variances have moderate loading on As with high loading on Li probably reflects the water chemistry influenced by mixing with geothermal water as Li has been known as a tracer for geothermal waters in this region (Coolbaugh et al., 2010).

Table 5.6A: Factor analyses results of total elemental concentrations of the upper Humboldt River-waters (samples from 001 to 004) that were digested in aqua-regia. Statistical results were obtained by applying Principal Component Analysis (PCA). The numbers in the rows represent factor loadings for each component, and marked bold typefaces represent the values of factor loadings of over 0.75. Statistics are based on cases with no missing values for any variable used.

Component	Factor 1	Factor 2	Communalities
pH	-0.84	0.55	1
ORP ¹	1.00	0.02	1
Cond ²	0.49	0.87	1
Temp ³	-0.21	-0.98	1
Alk ⁴	0.92	0.40	1
Al	0.57	-0.82	1
As	0.41	0.91	1
B	0.69	0.73	1
Ba	0.16	0.99	1
Ca	0.82	-0.57	1
Cl	1.00	0.08	1
Cu	1.00	0.08	1
Fe	-1.00	-0.08	1
K	0.98	0.19	1
Li	0.57	-0.82	1
Mg	0.94	0.33	1
Mn	0.47	-0.88	1
Na	1.00	-0.10	1
SiO ₂	0.71	-0.71	1
SO ₄	1.00	0.08	1
Initial eigenvalues	12.4	7.64	
Percentage of variance	61.8	38.2	
Cumulative % of variance	61.8	100	
Total Communalities			20
The proportion of the total variation explained by the factors			1

¹ORP: Oxidation-reduction Potential; ²Cond: Conductivity; ³Temp: Temperature; ⁴Alk: Alkalinity.

Table 5.6B: Factor analyses results of total elemental concentrations of lower Humboldt River-waters (samples from 007 to 019) that were digested in aqua-regia. Statistical results were obtained by applying Principal Component Analysis (PCA). The numbers in the rows represent factor loadings for each component, and marked bold typefaces represent the values of factor loadings of over 0.75. Statistics are based on cases with no missing values for any variable used.

Component	Factor 1	Factor 2	Factor 3	Factor 4	Communalities
pH	0.25	-0.86	-0.31	0.02	0.90
ORP ¹	-0.40	-0.16	0.45	-0.64	0.80
Cond ²	0.95	-0.10	-0.03	0.09	0.92
Temp ³	0.29	-0.04	-0.90	0.26	0.96
Alk ⁴	0.56	0.73	-0.10	0.29	0.93
Al	-0.30	0.91	0.10	0.17	0.96
As	-0.33	-0.26	0.64	0.52	0.86
B	0.96	0.14	0.19	-0.12	0.98
Ba	0.97	-0.02	-0.03	-0.16	0.98
Ca	0.93	0.08	0.27	-0.20	0.99
Cl	0.56	0.11	0.78	-0.03	0.93
Cu	0.55	0.09	0.22	0.22	0.40
Fe	0.91	-0.19	-0.33	-0.06	0.97
K	0.83	0.00	0.36	-0.35	0.95
Li	0.23	0.30	0.04	0.78	0.75
Mg	0.92	-0.18	-0.03	0.12	0.90
Mn	0.33	-0.03	0.35	0.60	0.60
Na	0.94	0.03	-0.15	-0.18	0.93
SiO ₂	-0.39	0.82	-0.10	-0.30	0.92
SO ₄	0.38	0.83	-0.26	-0.27	0.97
Initial eigenvalues	8.75	3.77	2.78	2.29	
Percentage of variance	43.8	18.9	13.9	11.5	
Cumulative % of variance	43.8	62.6	76.5	88.0	
Total Communalities					17.6
The proportion of the total variation explained by the factors					0.88

¹ORP: Oxidation-reduction Potential; ²Cond: Conductivity; ³Temp: Temperature; ⁴Alk: Alkalinity.

Table 5.7: Water quality data from Golconda hot spring system (see next page for source and location information).). Concentrations are mg/L. COND: Conductivity ($\mu\text{S}/\text{cm}$), Temp: Temperature ($^{\circ}\text{C}$). The stable isotopes are reported in ‰.

ID	Temp	pH	COND	Na	K	Ca	Mg	Li	SiO ₂	Cl	F	HCO ₃	SO ₄	As	B	Ba	Br	Fe	Mn	δD	$\delta^{18}\text{O}$	TDS
1942	43	7.03	942	159	24.3	47	7.8	0.527	40	27	2.9	528	56.7	0.0009		0.46		0.79	0.096			626
1945	64.5	8.2	845	146	23	35	8.4		59	20	2	448	56		1.3							571
1946	74		810	130	22	33	6.8	0.36	66	18	1.8		56	0.02	1.1			0.22	0.1	-126	-15.6	548
1947	68			130	20	34	6.6	0.39	145	20.5			48	0.025	1.45	0.31		0.03	0.01			560
1949	60	7	870	150	23	36	7.6		57	23	2.3	440	60									570
2709	65							0.0541														
2710	26.6	7.7	811	126	22	40	6.8		80	20		434	50									558
2711	81.5																					
2712	64.5	8.2	845	146	23	35	8.4	1.7	59	20	2	448	56		1.3							571
2713	65.5		849	180		33	7.7			21		444	108		1.4							570
2714	63.5	7.8		141	22	34	7.8	0.2	57	21	2.3	441	54		1.3				0			557
2715	43	7	942	159	24	47	7.8		40	27	2.9	528	57	0		0		0.79	0			625
2716	61.7																					
3456	74	6.5	810	130	22	33	6.8	0.08	66	18	1.8	429	56	0	1.1		0	0.22	0	-125.5	-15.65	547
3457	18.7	6.7	856	148	22	33	7.8		59	2	2	4	51	0	1.5		1		0			328
3487	27		818	134	19	38	7.8		59	20	1.8	430	53									544
4263																						
4264	74	6.7	856	148	22	33	7.8	0.5	59	20	2	452	51	0.01	1.5		0.5					
4265	60	7.4	818	134	19	38	7.8		59	20	1.8	430	53									
4266	74.5	6.53	810	130	22	33	6.8	0.36	66	18	1.8		56	0.018	1.1		0.02	0.22	0.095	-126	-15.7	
4268	74	6.5		130	22	33	6.8	0.08	66	18	1.8	429	56		1.1			0.22		-125.5	-15.65	547
4281	61.7																					
7882	46.6	6.01	483											0.0408	2.95	0.232				-129.9	-16.62	
7883	61	6.5	850											0.0282	1.4	0.298				-128.4	-16.49	
Average	57.51	6.77	1577	240	20.1	66.4	49.9	0.84	65.4	74.8	2.81	420.6	543.1	0.01	2.04	0.26	0.76	0.36	1.14	-113.1	-12.4	551.7
Median	62.60	6.85	845	143	22.0	34.0	7.80	0.36	59.0	20.0	2.00	440.0	56.0	0.01	1.35	0.30	0.50	0.22	0.01	-126.0	-15.5	559.0

Continued to next page

ID	Location Name	Sample Date	REFERENCE
1942	070 N36 E40 32 1 Golconda Hot Springs	2/20/1974	USGS - NWIS 2001. http://water.usgs.gov/nv/nwis/qw
1945	070 N36 E40 29D 1 Hot Sp near Golconda	12/2/1961	USGS - NWIS 2001. http://water.usgs.gov/nv/nwis/qw
1946	070 N36 E40 29D 1 Hot Sp near Golconda	1/1/1974	USGS - NWIS 2001. http://water.usgs.gov/nv/nwis/qw
1947	070 N36 E40 29D 1 Hot Sp near Golconda	1/1/1978	USGS - NWIS 2001. http://water.usgs.gov/nv/nwis/qw
1949	070 N36 E40 29 2 Hot Spring	5/5/1977	USGS - NWIS 2001. http://water.usgs.gov/nv/nwis/qw
2709	GOLCONDA HOT SPRINGS	6/2/1980	GEO THERM; WHITE 1955A
2710	GOLCONDA AREA WELL	1/6/1947	GEO THERM; COHEN 1962
2711	GOLCONDA AREA WELL		GEO THERM; GARSIDE AND SCHILLING 1979
2712	GOLCONDA AREA-SPRING	1/1/1972	GEO THERM; COHEN 1962; WARING 1965
2713	GOLCONDA HOT SPRINGS		GEO THERM; MILLER AND OTHERS 1953; PENROSE 1893
2714	GOLCONDA HOT SPRINGS	7/23/1954	GEO THERM; WHITE D. USGS. MENLO PARK
2715	GOLCONDA HOT SPRINGS	10/7/1971	GEO THERM; SAND ERSAND MILES 1974; WARING 1965
2716	GOLCONDA TUNGSTEN MINE DRILL HOLE 302		GEO THERM; GARSIDE AND SCHILLING 1979
3456	UNNAMED HOT SPRING NEAR GOLCONDA		GEO THERM; MARINER AND OTHERS 1974 1975
3457	UNNAMED HOT SPRING NEAR GOLCONDA	1/1/1959	GEO THERM; WHITE D. USGS. MENLO PARK
3487	UNNAMED SPRING	9/18/1952	GEO THERM; WHITE D. USGS. MENLO PARK
4263	Golconda Hot Spring	8/4/1982	Robert Mariner USGS; hand entered in summer 2001 from hard copy data sheets.
4264	Golconda Hot Springs		Robert Mariner USGS; hand entered in summer 2001 from hard copy data sheets.
4265	Golconda Hot Springs	10/20/1958	Robert Mariner USGS; hand entered in summer 2001 from hard copy data sheets.
4266	Golconda Hot Springs	6/16/1972	Robert Mariner USGS; hand entered in summer 2001 from hard copy data sheets.
4268	UNNAMED HOT SPRING NEAR GOLCONDA		Garside 1994; MARINER AND OTHERS 1974 1975
4281	GOLCONDA TUNGSTEN MINE DRILL HOLE 302		Garside 1994; GARSIDE AND SCHILLING 1979
7882	Golconda	9/10/2002	USGS - NWIS 2002. http://water.usgs.gov/nv/nwis/qw
7883	Golconda	9/10/2002	USGS - NWIS 2002. http://water.usgs.gov/nv/nwis/qw

5.5. Discussion

5.5.1. Arsenic in river sediments

The results of sequential extractions shows that the highest amount of solid-phase As (83%) is found in the insoluble residual fraction, i.e., silicate and aluminum silicate clay minerals, followed by Fe-Mn oxide phases (13%) in all sediment samples from upper to lower reaches of the river (Figure 5.9, Table 5.4). The results of XRD and observation of quartz, feldspar, partially dissolved feldspar, illite, and smectite in SEM analyses (Figure 5.8) show that these minerals compose the residual fraction.

The results of the sequential extraction analyses of the sediments are fairly consistent with the results of separate factor analyses conducted on the total elemental concentrations of the upper and lower HR bed-sediments (Table 5.5 A, and B) as evidenced by moderate to strong loadings of As with Al, Ca, and Fe in the UHR, and LHR (Table 5.5). The factor analyses results along with sequential extraction analyses results of the sediments suggest that As in silicate mineral phases and iron oxy-hydroxide minerals control the distribution of As in river-bed sediments.

Although iron oxides have been reported in hallow alluvial aquifer sediments and stream flood-plain sediments in the HRB by Folger (2000) and Welch et al. (2000), occurrence of As in silicate minerals have also been reported in other study areas (Breit et al., 2001; Chakraborty et al., 2007; Seddique et al., 2008). For example, As occurs variably in rock forming minerals, and ferromagnesian (Fe-Mg-bearing) minerals, such as biotite and amphibole appear to be the most enriched in As in high temperature (igneous) minerals (Smedley and Kinniburgh, 2002). Saunders et al. (2000) demonstrated that biotite is the most likely source of As due to weathering of

typical igneous and metamorphic rocks. Biotite not only contains significant amounts of As, but it is one of the fastest weathering silicate minerals.

5.5.2. Arsenic in river waters

Seasonal variation

The water samples that were collected for this study were collected in late September, 2007 during low-flow season for the Humboldt River. Therefore, to investigate any seasonal variation of As concentrations in the Humboldt River waters, additional water quality data from NDEP (Nevada Division of Environmental Protection) were used. The data were filtered for the year of 2007 for As and other chemical parameters. The months from March to July is high flow season, and from August to December is low flow season. Table 5.8 lists these data with sample dates.

Although concentrations of Cl, SO₄, and TDS vary to a moderate degree, concentrations of As in general varies very little at various stations (Table 5.8). For example, in the Maggie Creek (HS 14 in Table 5.8) in the UHR, As concentrations change from 0.013 mg/L in high flow season to 21 mg/L in low flow season. However, concentration of As remains same and so does for pH and Cl, but concentration of SO₄ increases from high flow to low-flow season for HS 15 station in the UHR (Table 5.8). On the other hand, no significant change is observed in pH, As, Cl and SO₄ concentrations in stations HS 2B and HS 3A for North-Fork-Humboldt River and South-Fork-Humboldt River in the UHR. Concentrations of As change from 0.007 mg/L to 0.015 mg/L from high flow to low flow season for HS 4 at Humboldt River near Cosino upstream of Elko. Although no data were reported for the year of 2007 in station H1 (not reported here, see Appendix 1 and 2) at the Humboldt River upstream of Elko, the historical data from 1968 to 1975 show no

Table 5.8: Water quality data of the Humboldt River waters at various stations for the year of 2007 (see next page for source and location information). Blank spaces represent no data reported.

Station	Sample	DO	Temp	pH	EC	Ca	Na	Mg	HCO ₃	Cl	SO ₄	As	Ba	B	F	Fe	Mn	TDS
ID	Date	mg/L	C	Field	µS/cm	mg/L	mg/L	mg/L	mg/L	mg/L	mg/L	µg/L	µg/L	µg/L	µg/L	µg/L	µg/L	mg/L
H6	4/23/2007	9.55	9.7	8.61	870				284	78	73	27	50	500	900	620	30	542
H6	8/21/2007	6.44	20.9	8.4	940				286	97	84	22	50	500	1100	500	20	603
H6	8/22/2007																	
HS1	4/23/2007	9.45	10.6	7.95	160				86	5	7	3	70	100	200	630	40	117
HS12	4/23/2007	4.3	10.9	8.51	5000				394	1400	240	52	110	4100	1100	1600	90	2978
HS12	8/21/2007	6.42	22.4	8.58	2000				330	360	130	39	90	1700	1400	1600	60	1225
HS12	8/22/2007																	
HS12	12/3/2007	11.76	1.6	8.61	3000				414	680	190	59	100	2900	1700	280	40	1818
HS14	4/23/2007	9.05	15.2	8.73	540				218	14	56	13	90	100	400	270	20	349
HS14	8/21/2007	13.31	24.7	8.6	630				259	18	63	15	100	300	600	50	20	425
HS14	12/3/2007	11.94	14	8.53	560				242	13	55	21	100	200	600	140	20	342
HS15	8/22/2007	10.77	10.6	7.92	390				183	5	50	4	130	100	100	170	40	245
HS15	12/4/2007	9.29	7.3	7.36	460				178	5	97	4	120	100	100	110	50	289
HS22	10/10/2007	11.9	12.3	8.5	330				154	9	19	7	50	100	700	90	180	201
HS2B	4/23/2007	8.75	12	8.46	330				128	9	41	7	110	100	200	760	50	224
HS2B	12/3/2007	13.63	0.1	8.23	380				163	13	35	10	90	100	400	340	30	249
HS3A	4/24/2007	10.04	9	8.16	340				172	11	17	4	60	100	200	210	50	209
HS3A	8/21/2007	11.59	19.1	7.95	510				283	12	22	8	130	100	600	50	20	320
HS3A	12/4/2007	8.82	10.4	7.77	500				265	12	23	8	120	100	500	50	20	302
HS4	4/23/2007	9.54	10.3	8.4	470				203	15	41	7	100	100	400	1600	80	304
HS4	8/21/2007	8.09	25.7	8.5	650				212	41	84	8	100	200	600	70	70	451
HS4	12/3/2007	14.65	3.2	8.22	590				234	26	56	15	110	400	1400	990	60	382
HS5	8/22/2007	5.55	21.6	8.44	440				191	18	30	9	100	200	600	410	100	271
HS5	12/4/2007	13.05	3.4	8.21	760				287	36	89	11	120	400	800	100	20	480
HS6	4/23/2007	9.85	11.3	8.46	480				203	16	44	8	90	100	400	810	50	311
HS6	8/21/2007	9.46	22	8.31	550				204	30	59	8	90	200	700	50	40	358
HS6	12/3/2007	14	3.4	8.25	650				272	25	67	13	120	300	600	130	20	404
HS8	4/23/2007	9.59	9.2	8.53	530				213	25	50	10	120	100	400	2200	100	344
RPR5A	5/17/2007	9.4	17.3	8.1	920				280	89	78							567
RPRa	5/17/2007	8.3	13.3	8	920				277	89	78							567
SFR3e	5/16/2007	9.1	17.5	8	270				132	8	12							152
SFR3h	5/16/2007	6	9.9	7.8	280				144	9	12							159

Continued to next page

Station Id	Station Name	Water Body Name	HRB Geography	Source
H6	Humboldt River Below Rye Patch Reservoir	Humboldt River	LHR	NDEP
HS1	Mary's River	Marys River	UHR	NDEP
HS12	Humboldt River Above Humboldt Sink	Humboldt River	LHR	NDEP
HS14	Maggie Creek @ SR 221	Maggie Creek	UHR	NDEP
HS15	North Fork Humboldt River @ North Fork Ranch	Humboldt River, North Fork	UHR	NDEP
HS22	South Fork Humboldt River below Dam @ Gage	Humboldt River, South Fork	UHR	NDEP
HS2B	North Fork Humboldt River @ I-80	Humboldt River, North Fork	UHR	NDEP
HS3A	South Fork Humboldt River below Dixie Creek	Humboldt River, South Fork	UHR	NDEP
HS4	Humboldt River @ Osino Cutoff	Humboldt River	UHR	NDEP
HS5	Humboldt River @ Carlin	Humboldt River	UHR	NDEP
HS6	Humboldt River @ Palisade	Humboldt River	UHR	NDEP
HS8	Humboldt River @ Comus	Humboldt River	MHR	NDEP
RPR5A	Rye Patch Reservoir North - Surface	Rye Patch Reservoir	LHR	NDEP
RPRA	Rye Patch Reservoir near Dam - Surface	Rye Patch Reservoir	LHR	NDEP
SFR3e	South Fork Reservoir near Dam - Surface	South Fork Reservoir	UHR	NDEP
SFR3h	South Fork Reservoir near Dam - Bottom	South Fork Reservoir	UHR	NDEP

variations for Cl concentrations (see Appendix 1 and 2 for these additional data). No significant change is observed in As concentration for HS 5 at Humboldt River at Carlin between August and December. With these limited data information, it is inconclusive to infer that concentrations of dissolved SO₄, Cl, and As other chemical parameters do not change significantly for the other UHR stations.

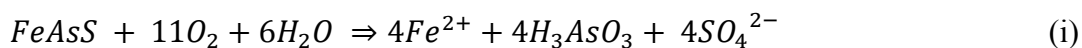
Significant changes in concentrations of dissolved Cl, SO₄, and hence TDS can be observed in different seasons in station HS 12, which is Humboldt River above Humboldt Sink in LHR. For example, dissolved Cl concentration changes from 1400 mg/L in April to 130 mg/L in August, and then to 680 mg/L in December. However, As concentrations do not change significantly in this station. The higher Cl concentration in April is due to additional runoff from the nearby agricultural farmlands and ranches with the addition of snowmelt waters during this time of the year. However, more data are required for each stations for a comprehensive time-series analyses of As and other chemical parameters. With the data currently available, it can be inferred that Cl concentrations in LHR may be affected by seasonal effects and stream flow conditions, As concentrations are affected in a lesser significance.

5.5.3. Processes in the Upper Humboldt River (UHR)

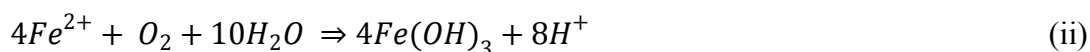
Sulfide oxidation

The strong positive loading of dissolved SO₄ (0.997) and ORP (1.00) with moderate loading of As (0.41) (Table 5.6A) in the UHR waters suggest oxidative dissolution of As-bearing sulfide minerals present in the Cenozoic ore deposits is the primary source for As in waters. These minerals typically undergo significant amounts of oxidation when exposed to the oxygen-rich environment in the river-bed

sediments. For example, arsenopyrite, the most common As-bearing sulfide mineral is oxidized in a series of reactions under near neutral pH conditions as described by Walker et al. (2006):



where, the reaction (i) represents starting of arsenopyrite oxidation by oxygen at near neutral pH, resulting in As(III) as the uncharged ion H_3AsO_3 and dissolved SO_4^{2-} in the solution. The subsequent secondary oxidation of Fe^{2+} released from the above reaction (i) yields protons to solution followed forming iron oxyhydroxides as shown in reaction (ii):



Further oxidation of arsenite [As (III)] produced in reaction (i) results in the formation of arsenate [As (V)] in the solution as shown in reactions (iii) and (iv):



Although the extent of oxidation of the aforementioned species depends on several factors such as, time of contact with the atmosphere, flow rate, oxidant concentration, and photochemical reactions, pH, site hydrologic and biogeochemical conditions (Walker et al., 2006), the reactions above are consistent with the geologic distribution of As-bearing sulfide minerals and/or rocks (e.g., pyrite, arsenopyrite) (Theodore et al., 2003) in the catchment areas of the UHR. The importance of oxidation of sulfide minerals and/or rocks is best displayed in the plot of dissolved SO_4 versus Cl concentrations in the river waters (Figure 5.10). The excess of SO_4 with

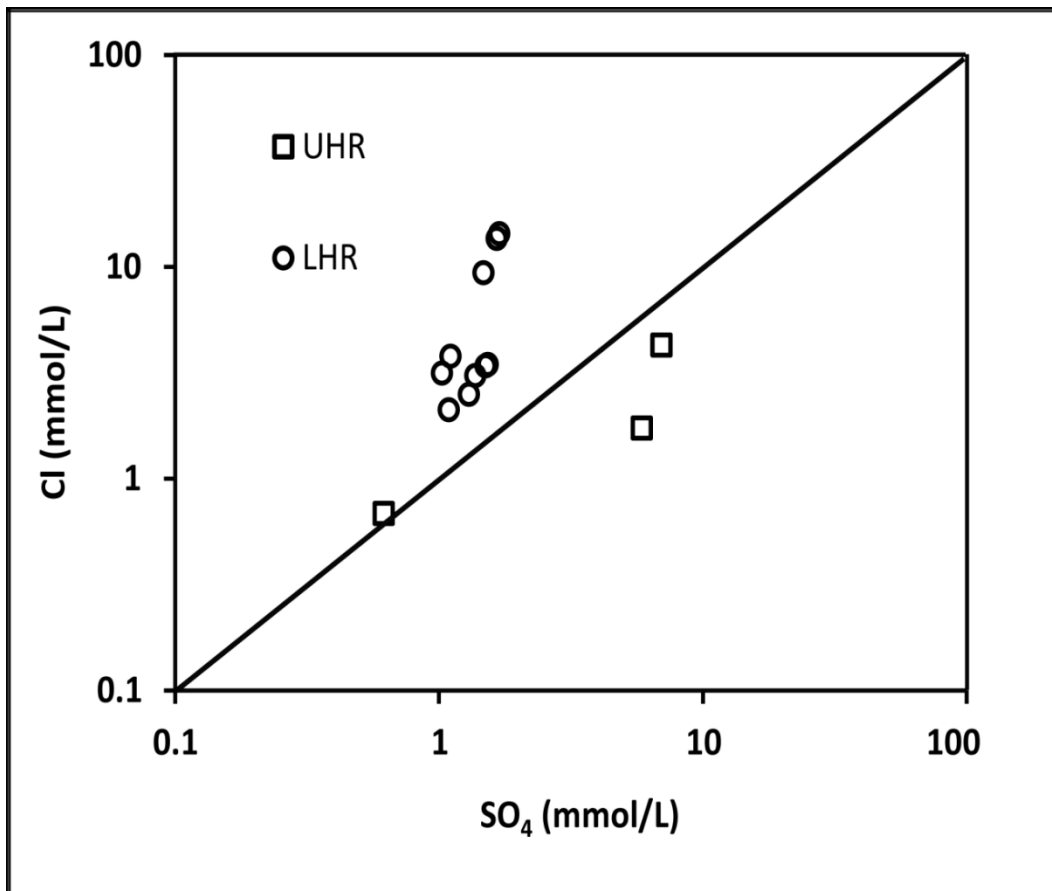


Figure 5.10: Sulfate concentrations (in mmol/L) vs. Cl concentrations (mmol/L) for the water samples from the Humboldt River.

respect to Cl in the UHR waters at samples 001 and 003 can be directly attributed to oxidation of sulfide minerals.

The data of sulfur isotopic signatures ($\delta^{34}\text{S}$ of SO_4) also support the oxidation of sulfide minerals as the source of dissolved SO_4 in the upstream area. The two upstream samples (001 and 003) with high concentrations of dissolved SO_4 (565 mg/L and 566 mg/L respectively) with +4.7‰ and +9.8‰ of $\delta^{34}\text{S}$ respectively, are indicative of localized sulfide oxidation (Ostlund et al., 1995; Stuben et al., 2003) in the upstream area. Similar results were found by Tuttle et al (2003) in the waters of the Copper Basin near Battle Mountain, where the source of dissolved sulfate was suggested as the porphyry deposits of metallic-sulfide minerals.

The moderate correlation between dissolved As and SO_4 in the UHR waters could be due to several reasons: 1) that sulfide oxidation is a localized effect in this area; 2) the correlation coefficient is lower because only three samples were analyzed, where one sample (sample 001) contains a very high concentration of SO_4 (566 mg/L) and low concentration of As (0.012 mg/L); and 3) SO_4 concentration in sample 004 of the UHR water is low because of dilution as a result of mixing with the South Fork River, a tributary to the Humboldt River water (Figure 5.1). The mean daily discharge of South-Fork-Humboldt River during the sampling in low-flow season was 0.14 m^3/sec (Table 5.1), which could be due to a considerable fraction of water released later in the season from the dam on the South-Fork River.

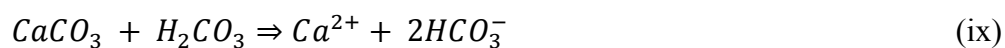
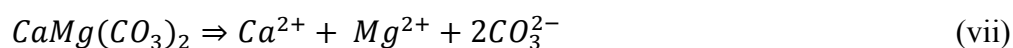
With the zero discharge at Mary's River (Table 5.1 and Figure 5.1) during the time of sampling, it is imperative that the sampled water downstream of the confluence of Mary's River and Humboldt River represents either ground water discharging to Humboldt River (Figure 5.3) because of the gradient from

topographical highs towards the topographical lows in the Humboldt River flood plain, or runoff from irrigation as the sample 001 was collected from the river adjacent to a ranch. Similarly, with very low mean daily discharge of 0.03 m³/sec at Humboldt River near Elko (Table 5.1) upstream of sample 003, the sampled water at this location (sample location 003, Figure 5.1) represents ground water discharging to Humboldt River. The water quality data from surface waters at the South-Fork-Humboldt River (Appendix 1 and 2) also suggest that the water is relatively dilute with very low concentrations of As, Cl and SO₄. The average mean daily discharge during the sampling in the Humboldt River at Palisade was 0.8 m³/sec, which is higher than the sum of the flows from Carlin, Susie Creek, Maggie Creek, and Mary's Creek upstream of sample 004 near Palisade (Table 5.1) implying a fraction of water is contributed from ground water discharge during the low-flow season.

Carbonate dissolution

The relatively high loadings of dissolved Ca, and Mg, with alkalinity (as HCO₃) in the UHR waters explains the dissolution of carbonate rocks containing limestone and dolomite in the country rocks in the UHR region as follows. As the rainwater passes through the atmosphere, it picks up atmospheric CO₂ to form carbonic acid (H₂CO₃) [Equation (v)], which dissolves limestone (CaCO₃) resulting in the release of Ca and CO₃ ions in the water [Equation (vi)]. Similarly, dolomite [CaMg(CO₃)₂] dissolves resulting in the release of Ca, Mg, and CO₃ ions in the water [Equation (vii)] followed by formation of HCO₃ ions in the water [Equation (viii) and (ix)].





This is consistent with the occurrence of Pre-Cenozoic Carbonate rocks containing limestone and dolomite in north-eastern and northern part of the UHR region (Figure 5.2). In a similar study of North Fork watershed, a tributary of the Humboldt River in the UHR region, Earman and Hershey (2000) reported high concentrations of dissolved As (0.016 mg/L) and SO₄ (370 mg/L) in the waters and suggested that oxidation of mined-waste rocks containing As-bearing sulfide minerals were the reason for high dissolved As and SO₄ in the waters followed by in situ acid neutralization because of dissolution of carbonate host rocks. The study area of Earman and Hershey (2000) is located around an abandoned gold mine named, Big Spring Project, approximately 105 km north of Elko in the northern part of the Independence Mountains (Figure 5.1). The water samples 001 and 003 from this study are located downstream of the confluence between the North Fork-Humboldt River and the main stream of the Humboldt River.

Dilution

The change in dissolved sulfate concentrations from sample 003 (566.3 mg/L) to sample 004 (59.3 mg/L) in the upstream area can be explained by the effect of dilution along the flow-path, where sample 004 is located in the downstream of the confluence of South Fork-Humboldt River and the Humboldt River (Figure 5.1). The sharp reduction in dissolved SO₄ accompanied by sharp reduction in ORP from 134

mV to 10 mV along with increase in Fe concentration from <0.01 mg/L to 0.019 mg/L from sample 003 to sample 004 (Table 5.3), mixing with a localized reduced ground water can be inferred as evidenced by ground water movement (Figure 5.3) and stream-flow data (Table 5.1). Dissolved Fe is increased in waters because of higher solubility of Fe²⁺ than Fe³⁺ due to change from highly oxidizing conditions to relatively less oxidizing conditions. Therefore, the decrease in concentrations of dissolved As and SO₄ from sample 001 and 003 to 004 is due to dilution as a result of mixing with South-Fork-Humboldt River and other tributaries with the Humboldt River water and mixing with reduced ground waters, where the river on average gains mean annual discharge of 1.68 m³/s between Elko and Carlin, and 2.48 m³/s of mean annual discharge between Elko and Palisade (<http://waterdata.usgs.gov/nv/nwis/sw>).

5.5.4. Processes in the Lower Humboldt River (LHR)

Geothermal water mixing

In the LHR, dissolved As is not significant with negative factor loading (factor loading of -0.93) for factor 1 that represents 44% of the variances with strong positive factor loadings on conductivity, B, Ba, Ca, Fe, K, Mg, and Na (Table 5.6B), and the evolved water chemistry in the LHR reflects coupled processes of evaporation and mixing with geothermal waters. Factor 2 with 19% of the variances have high factor loadings on Al, dissolved SiO₂ and SO₄, which reflects dissolution of silicates and sulfate salts because of mixing with geothermal waters and evaporative enrichment, respectively. Mixing of geothermal hot spring water for As enrichment as the major factor in the northern part of LHR water is inferred, because 1) several geothermal hot springs such as Beowawe Geyser near Battle Mountain, Midas hot spring, Hot spring

system at Golconda (Table 5.7), are active in that region; and 2) high concentrations of dissolved B ions are also known to occur in the geothermal hot springs located in this area (Shevenell et al., 2008; Coolbaugh et al., 2010). Additionally, mixing with geothermal waters has been reported by Cohen (1963) near Golconda during the low-flow season. This is also evidenced with the discharge data at locations near sample 007 and 008 near Comus and Golconda, respectively along the ground water movement (Figure 5.3). The average mean daily discharge during the sampling period (i.e. low-flow season) was 0.01 m³/sec and 0.02 m³/sec for Comus and Golconda, respectively (Table 5.1). However, with low concentrations of dissolved As (mean and median 0.01 mg/L) in the Golconda Hot spring system, and concentrations of 0.021 mg/L and 0.037 mg/L for sample 007 and 008 near Golconda Hot spring system therefore infer additional input from non-thermal ground water discharge to the Humboldt River along with evaporation. Evaporation and ground water discharging the Humboldt River during the low-flow season has been reported by Cohen (1963), and Eakin and Lamke (1966), and additionally, ground water movement is evidenced in our ground water-surface water interaction analysis (Figure 5.3). Contribution of additional dissolved As could also be due to mine discharge from Lone Tree Mine upstream of sample 007 and 008. However, it is inconclusive whether these mine discharges have contributed a significant fraction of As-enriched waters to the Humboldt River, because the Lone Tree Mine was closed in the summer of 2007 (Source: NDEP) just before sampling in late September of 2007.

Evaporation

In the southern LHR region, evaporation is predominant with the location of terminal sink and positive correlations between As and Cl (Table 5.6 B). Because with evaporation, enrichment of dissolved elements occurs with proportional increment of dissolved Cl, evaporation is more likely than mixing with geothermal waters, because of no known geothermal hot springs in the southern LHR. However, additional increment of Cl and other dissolved ions are also possible via agricultural runoffs from the irrigated farmlands in the Lovelock Valley, where Humboldt River water and shallow ground waters are extensively used for irrigation (Seiler et al., 1993; Paul and Thodal, 2003).

Statewide potential evaporation data reported by (Shevenell, 1996) suggest that average annual potential evaporation rates are higher than precipitation in Imlay, north of Rye Patch Reservoir (Figure 5.1), where concentrations of dissolved As and Cl at sample 012 increases slightly (Table 5.3) from upstream location at 011. Concentrations of dissolved As increases from 0.02 mg/L at sample 013 (near Imlay) to 0.048 mg/L at sample 015 (near Rye Patch reservoir Dam) along with increases in dissolved Cl. This increases in Cl and As can be inferred due to evaporation where average daily discharge at the time of sampling was very low ($0.09 \text{ m}^3/\text{sec}$) at Imlay. However, concentrations of Cl, SO_4 and As decreases from sample 015 to 016, where average daily discharge during the sampling was high ($6.69 \text{ m}^3/\text{sec}$), which is located downstream of Rye Patch reservoir dam (Table 5.1), and can be explained by additional flow of water from the reservoir. Concentrations of dissolved As incrementally increases downstream of sample location 016 towards sample locations 017, 018 and 019 in the Lovelock Valley, where average daily discharge has been

estimated as 0.59 m³/sec (Table 3.1). This increase in dissolved As along with Cl and other ions are due to progressive evaporative enrichment of the Humboldt River water as well as irrigated shallow ground water used in the area.

The enrichment of stable isotopes of deuterium and O-18 (Figure 5.4) of the sampled waters in the southern part of the LHR (specifically, samples from 015 to 019) also suggest evaporation plays the most important role in subsequent enrichment of As in the southern part of the LHR waters. The importance of evaporation in the LHR can be displayed by plotting the ratio of dissolved SO₄ to Cl along the flow-path of the Humboldt River (Figure 5.11), where the ratio of SO₄ to Cl is very high in the UHR, which is because of excess of dissolved SO₄ with respect to Cl as a result of oxidation of sulfide minerals, but gradually becomes less than one (<1) in the LHR because of gradual increase of Cl due to evaporation and addition from irrigation runoffs.

Effect of pH and desorption

In many oxidizing systems such as in Carson Sink (which is located in the vicinity of Humboldt Sink) in Western U.S. (Welch et al., 1988), and in Arizona of Southwest U.S. (Robertson, 1989), pH is positively correlated with dissolved As, and elevated concentrations of As has been linked to pH-dependent desorption. The pH of the Humboldt River water ranges from 8.44 to 9.25 indicating very alkaline conditions. At alkaline pH, mineral surfaces become increasingly negatively charged, thus promoting arsenic desorption (O'Shea, 2006). With almost parallel observational trends of pH and As concentrations with few exceptions (Figure 5.12), the effect of pH can be inferred to play a secondary role in As enrichment. However, the lack of

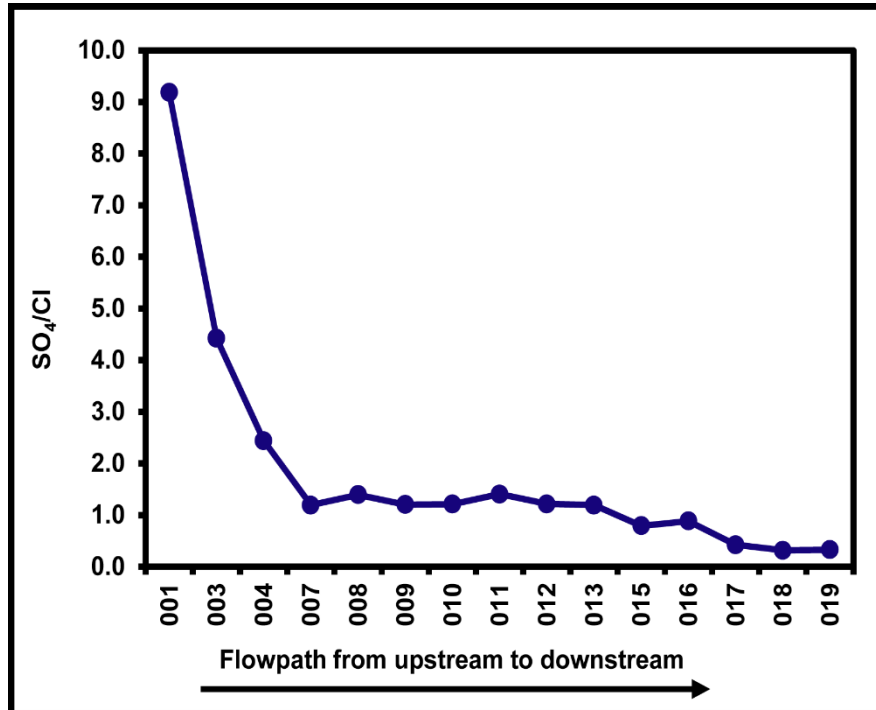


Figure 5.11: Ratio of dissolved sulfate to chloride in the waters along the flow-path of the Humboldt River. Ratio of sulfate to chloride gradually decreases in the LHR.

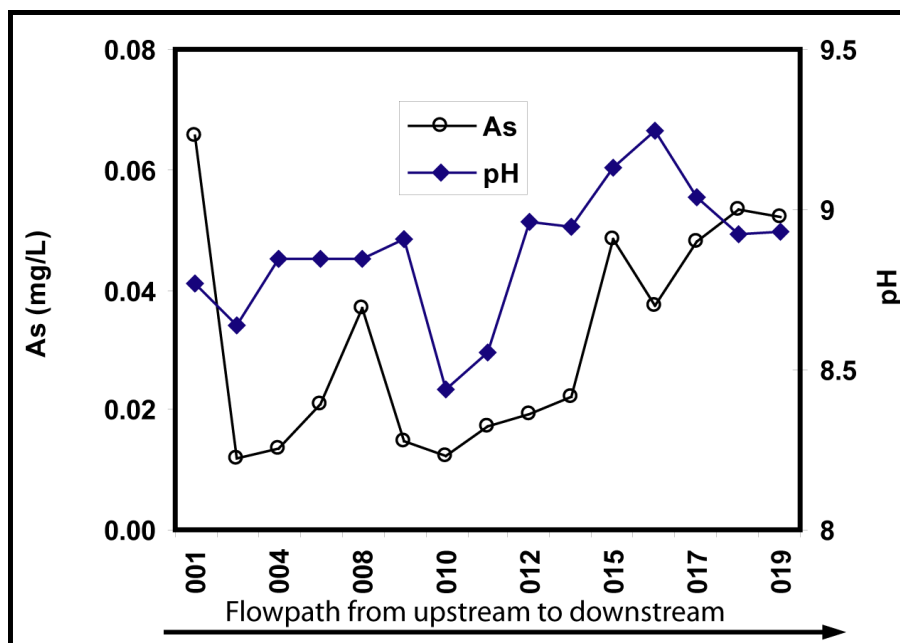


Figure 5.12: Relationship of pH with As concentrations in the Humboldt River waters.

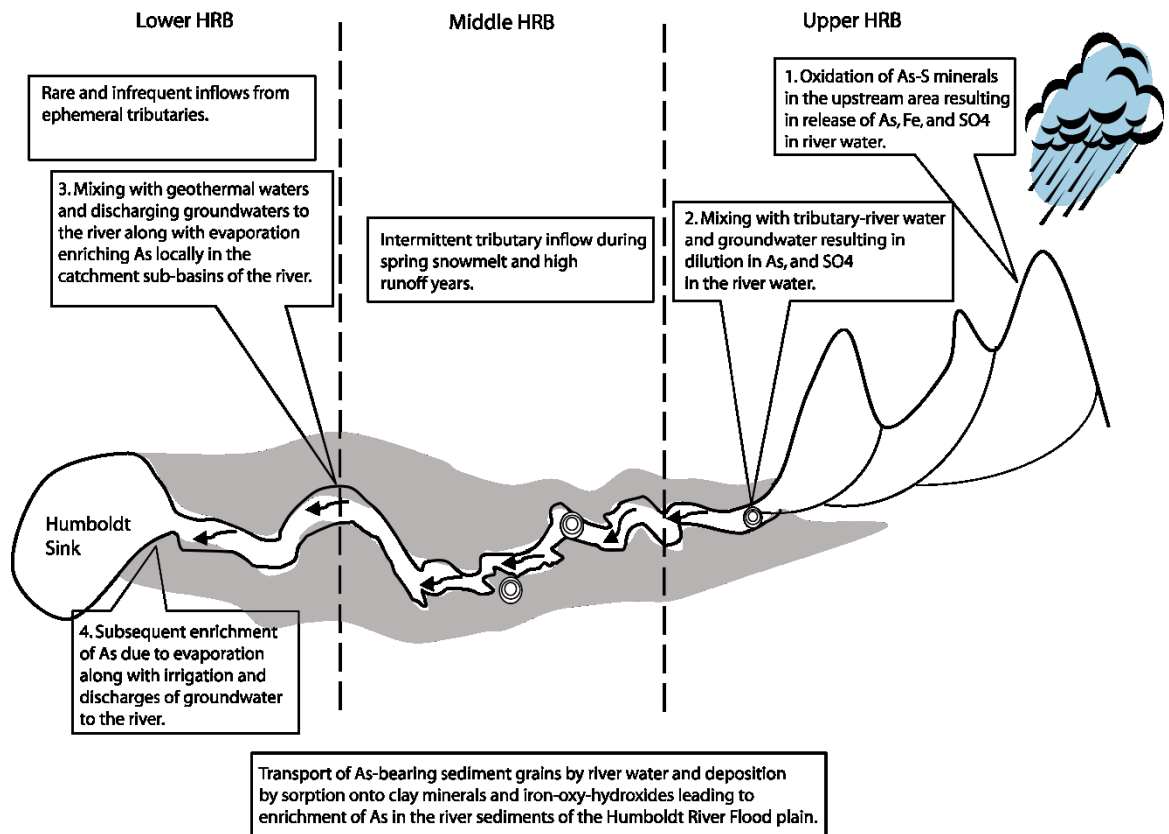


Figure 5.13: Schematic conceptual model showing arsenic mobilization and transportation pathways along the Humboldt River waters and its sediments from upper to lower reaches.

strong correlations observed from factor analyses in all waters from UHR to LHR (Table 5.6), the effect of pH in secondary As enrichment remains inconclusive.

5.5.5. Conceptual model

With the data collected in this study and based on geo-hydrologic settings of the area, we propose a conceptual model for arsenic enrichment and distribution in the Humboldt River water and its sediments (Figure 5.13).

The primary source of aqueous As in the area is believed to be As-rich sediments, derived from Cenozoic rocks in the upstream areas including the Tertiary volcanic rocks and Tertiary metal-ore deposits that contains As-bearing-sulfide minerals. Oxidative dissolution of these As-bearing sulfide minerals over prolonged residence times is the primary source of As in river waters of the UHR.

The As-bearing sediments as a result of weathering of As-bearing source rocks in the upstream area have been transported down the Humboldt River since the late Miocene to be deposited in oxic playa environments and, in the sub-oxic lake-bottom sediments in a semi-humid environment during the Plio-Pleistocene time. Arsenic is sorbed and attached on the surfaces of clay minerals and iron oxy-hydroxides in the river-bed and lake-bottom sediments. The process continues today with sediments in the upstream transported downstream during the periods of high runoffs and then deposited in intermittent shallow lakes.

Mixing of geothermal water contributed to enrichment of dissolved As in the northern part of the LHR region, which appears to be a localized effect along with minor effect of evaporation. Subsequent enrichment of As occurred by evaporative enrichment of solutes in the lower reaches of the Humboldt River. With the increase in alkalinity and pH, arsenic concentrations subsequently increased by desorption

from iron oxy-hydroxides to the river waters. However, pH-dependent desorption remains inconclusive compared to the prevalent evaporation in the LHR regions including the Humboldt Sink area. In addition, irrigation using shallow ground water which are enriched in As (Mohammad and Tempel, 2011A, in prep) also contribute to As and other dissolved ions such as Cl in the southern part of the LHR. The results of factor analyses of waters from upper, middle and lower HR regions indicate that the source of As from oxidation of As-bearing sulfide minerals in the upstream region becomes less significant in the lower Humboldt River, and mixing of geothermal waters becomes an important factor in northern part of the LHR. With the temperate and arid climate, evaporation becomes increasingly significant factor in enriching dissolved As concentrations in the lower HR waters.

In a similar study with semi-arid climatic conditions, Romero et al. (2003) presented several factors for As enrichment in the Rio Loa River waters in Chile, which are high evaporation, extreme arid conditions, and the lack of low-As tributaries. Unlike As-rich effluents from the water treatment plants to contribute additional source of As in Rio Loa River, irrigation of As-rich shallow ground water and ground water-surface water interaction plays additional roles in our study area.

5.6. Conclusions

Our analytical data of water chemistry and isotopes, mineralogy and chemistry of river-bed sediments obtained from XRD, SEM and sequential extraction analyses of sediments, and factor analyses of data from both water and river-bed sediments indicate that concentrations of As in the Humboldt river waters and sediments are controlled by several geochemical and hydrological processes. The findings from this study are summarized below.

- 1) Tertiary volcanic rocks and metal-ore deposits containing As-bearing sulfides are the primary source of As in sediments and river water.
- 2) Sorption of As onto silicate and clay minerals, and iron oxy-hydroxide mineral surfaces affects the mobilization of As into river waters and controls the distribution of As in river sediments.
- 3) Oxidation of As-bearing sulfide minerals contributes to As concentrations in the waters of the upper Humboldt River.
- 4) Dilution of dissolved As occurs in the upper Humboldt River as result of mixing with diluted waters from the South-Fork-Humboldt River and ground water inflows towards the river during low-flow season.
- 5) Localized effect of geothermal mixing has been inferred in the waters of the northern part of the lower Humboldt River near Golconda from statistical factor analyses.
- 6) Subsequent enrichment of As concentrations occurs from evaporative enrichment of the solutes because of the favorable arid and temperate climate and terminal sink in the lower Humboldt River.
- 7) Desorption is inconclusive in secondary mobilization of dissolved As in the waters of the lower Humboldt River.

Results reported in this study represent only a segment of the year and do not consider seasonal variations. Therefore, future studies are required with respect to temporal variations of As in river waters with respect to variations in discharge. Geochemical modeling studies are required to quantify the various processes involved in mobilization and enriching As concentrations along the flow path of the river.

CHAPTER 6

Geochemical Modeling of Processes Controlling Arsenic Enrichment in the Waters of the Humboldt River, Northern Nevada.

ABSTRACT: The water chemistry and dissolved arsenic (As) concentrations in the waters of the Humboldt River (HR) drainage are controlled by hydrological and geochemical processes: oxidation of sulfides, dilution of water by mixing with tributaries and groundwater, mixing with geothermal water, and evapotranspiration at various magnitudes along the flow path. These processes have been evaluated by quantifying each of the processes using geochemical reaction path modeling codes EQ3/6 and PHREEQC. The results of modeling indicate that oxidation of As-bearing sulfide minerals plays one of the important roles for high concentrations of As (0.07 mg/L) and SO₄ (565 mg/L) in the upstream region, which is characterized by Cenozoic and Tertiary volcanic rocks and sediments deposits containing sulfide minerals. The primary source of As is less significant in the middle and lower Humboldt River, where mixing with geothermal water and groundwater locally controls the distribution of dissolved As. Evapotranspiration (modeled as evaporation) plays the most important role in the lower HR for further enriching dissolved As along with secondary enrichment from desorption.

KEY WORDS: Humboldt River; Nevada; Arsenic; Geochemical modeling; sulfides; geothermal; evaporation.

6.1. Introduction

Elevated concentrations of arsenic (As) in natural water exceeding the drinking water standard of $10\mu\text{g/L}$ (WHO, 2001; EPA, 2003) is one of the major threats to human health in many parts of the world. Although high concentrations of arsenic in natural waters are often associated with mine tailings, geothermal springs, and As-rich rocks and minerals, mobilization of As is affected by a combination of natural processes, including weathering reactions, adsorption-desorption, redox conditions, solubility of minerals, geo-microbiological activities and volcanic emissions, as well as through a range of anthropogenic activities (Smedley and Kinniburgh, 2002). The objective of this paper is to quantify processes on As-enrichment in the Humboldt River (HR) waters by applying a geochemical reaction path modeling approach to the problem. We believe that quantification of processes leads to a better understanding of As behavior in a natural system.

In general, a reaction path model traces how a fluid's chemistry evolves and which minerals precipitate or dissolve over the course of geochemical processes. Construction of geochemical models for metals reactivity at near-surface conditions requires the inclusion of mineral surface complexation theory (Dzombak and Morel, 1990) to account for metal adsorption and desorption, because the mobility of As in the natural environment is commonly controlled by adsorption/desorption, and precipitation/dissolution reactions (Lengke and Tempel, 2005). However, in an open system-surface environment (river, lakes, etc.), various physical processes such as conservative mixing (i.e., without reaction) of fluids (for example, between tributaries

and/or springs, between thermal and non-thermal fluids, etc.) and evapotranspiration in the semi-arid environment also control concentrations of As and other ions by either dilution or enrichment of dissolved As in the water (Tempel et al., 2000; Sracek et al., 2004; Scanlon et al., 2009). Biological processes, specifically geo-microbiologic processes have been proven as one of the most important processes for cycling of As between different phases in certain geologic settings, where organic matters are abundant, most likely in estuarine and floodplain environment. Bacterial reduction of arsenic containing iron-oxy-hydroxides triggered by iron-reducing bacteria has been reported in many recent research works, namely in Ganges Delta and other similar geologic settings, where the prerequisite for abundant organic matters in the sediments have been substantiated by flooding and/or sea level changes during the Quaternary and Pleistocene age (Smedley and Kinniburgh, 2002; Saunders et al., 2005). This study is limited with respect to geochemical aspects of arsenic cycling.

Despite several studies on geochemical modeling on As-cycling in surface water and groundwater (Stollenwerk, 2003; Lengke and Tempel, 2005; Lee et al., 2005; Balistrieri et al., 2006; Postma et al., 2007; Polizzotto et al., 2008; Sharif et al., 2011), no studies have been undertaken for As-cycling in the surface waters of the HR system. Arsenic concentrations as high as 0.066 mg/L (median 0.02 mg/L) have been found in the surface waters of the HR. It has been hypothesized that concentrations of dissolved As are controlled by several physical hydrological processes (i.e., dilution, mixing with geothermal springs and evapotranspiration), coupled with geochemical processes (i.e., desorption). Quantifying these various processes controlling As concentration along the flow-path of the HR system is important because, the HR system not only is an integral

part to agriculture and irrigation, it also provides critical wet-land ecosystem for wildlife habitat and accommodates discharges from mining activities, and industries and recharge for groundwater.

6.2. Background

6.2.1. Study area

The HR with its many tributaries and springs constitute the largest internally drained river system in northern Nevada. The HR Basin (HRB) encompasses approximately 43,700 km² (Yager and Folger, 2003). The river flows westward from its source region in the northeastern Nevada during periods of well above normal runoff (1983-84, 1997-98 and 2005, Prudic, D.E., personal communication, 2011) water exits the sink and flows south into the adjacent Carson Sink (Figure 6.1). The river drains through or near several geothermal hot springs, hydrothermal alteration zones, and epithermal and pluton-related mineral deposits, including those of silver, copper, and arsenic-rich gold. As a result, the source rocks for sediments in the HR are highly enriched in many elements including arsenic.

6.2.2. Geology and mineralogy

Geology

The HR has been divided into three geographic subdivisions as previously done by others (Prudic et al., 2006) based on morphology and geology of the drainage basin or watershed: Upper HR (UHR), Middle HR (MHR), and Lower HR (LHR) (Figure 6.1).

Figure 6.2 illustrates schematic surface geology of the area. The UHR extends from its sources at the base of the East Humboldt Range, Ruby Mountains, and Jarbidge Mountains to Palisade. The drainage area is comprised mostly of Cenozoic sedimentary rocks, Tertiary mafic volcanic (calc-alkali andesitic) and Pre-Tertiary felsic volcanic (high-silica rhyolitic) rocks with some Paleozoic and Mesozoic carbonate rocks.

The MHR comprises the area from Palisade to upstream of Golconda. The course of the river is generally northwest (Figure 6.1). The drainage area of the MHR is characterized by relatively widespread presence of Tertiary volcanic and Cenozoic sedimentary rocks north and east of Battle Mountain, and widespread Quaternary alluvium and lacustrine deposits south and west of Battle Mountain (Figure 6.2).

The LHR lies downstream of the MHR and includes the drainage downstream of the confluence with the Little Humboldt River near Winnemucca southwest to the Humboldt Sink. The drainage is comprised mostly of Quaternary alluvium and lacustrine deposits in the valleys and alluvial fans along with pre-Tertiary sedimentary and volcanic rocks in the Mountains (Figure 6.2). Extensive thick salt deposits of non-marine evaporite deposits (halite, anhydrite, and gypsum) from the Cenozoic have been reported in the area around Lower Humboldt River Basin (Faulds et al., 1997; Price et al., 2005).

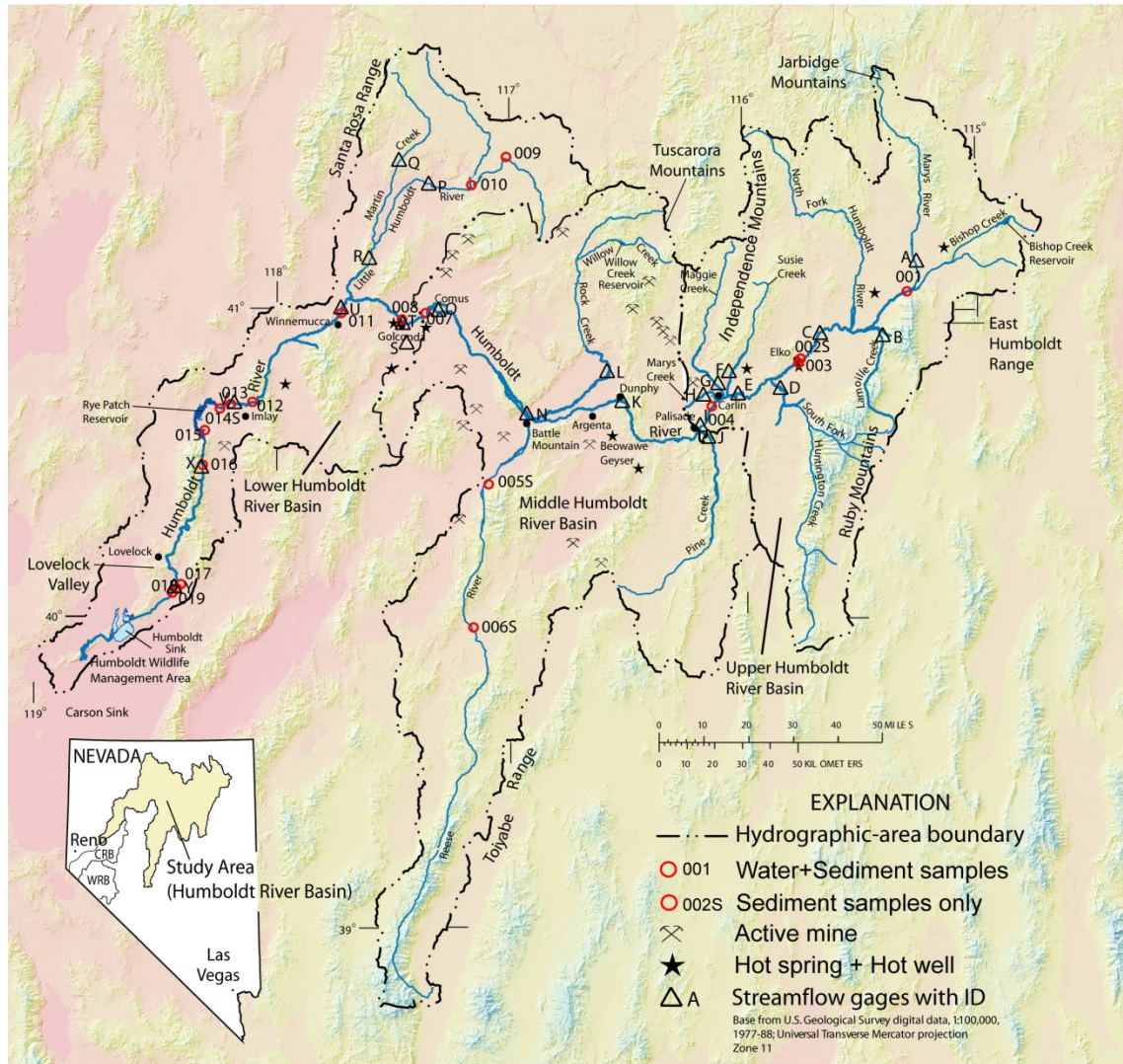


Figure 6.1: Location map of the Humboldt River Basin (HRB) in northern Nevada showing the locations of active mines, hot springs and hot wells (modified after Prudic et al., 2006), and sampling points of stream water and sediments used in this study.

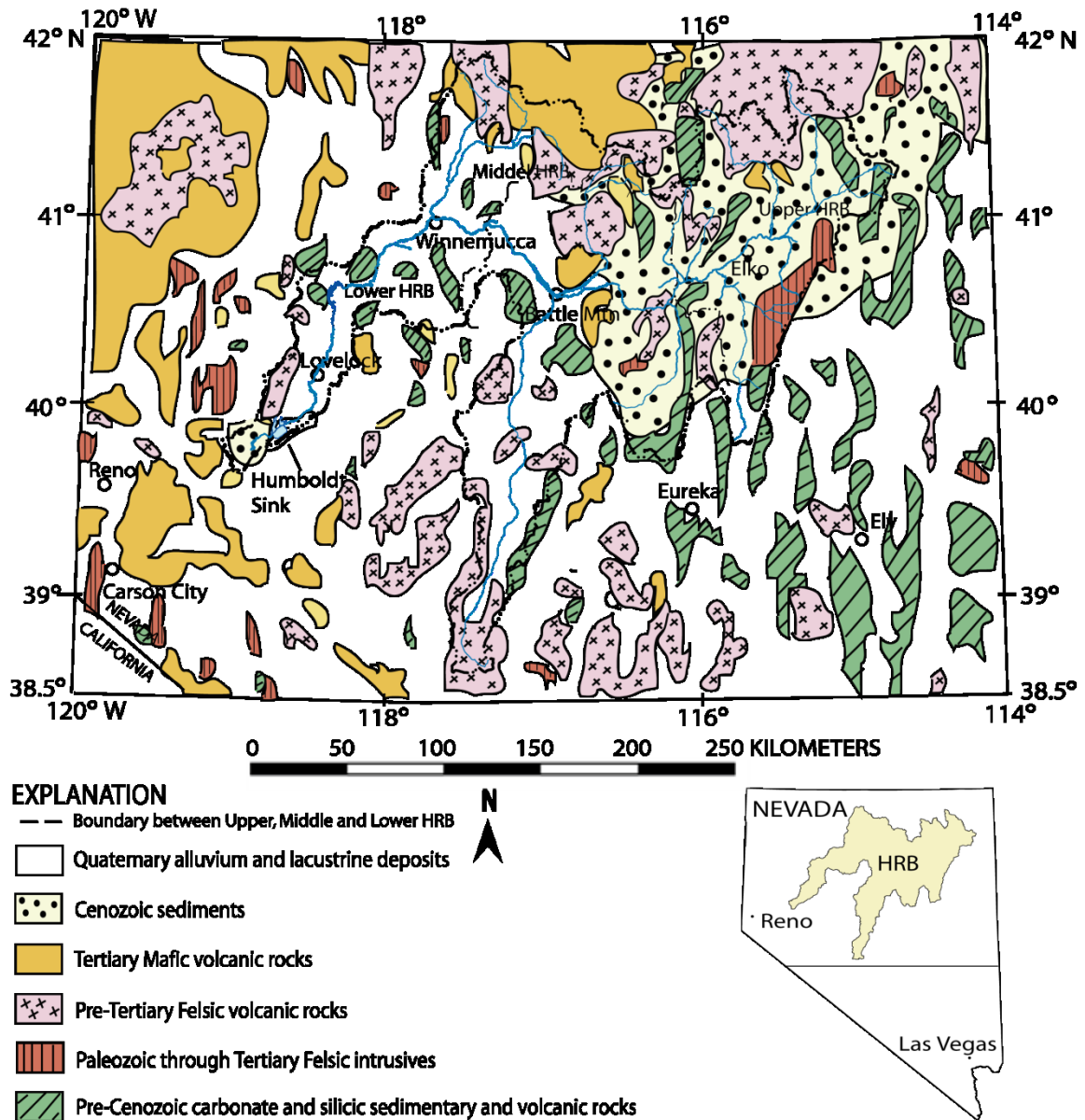


Figure 6.2: Schematic generalized geologic map of the HRB and northern Nevada illustrating broad lithologic distribution of major rock formations (modified after Wallace et al., 2004).

Mineralogy

The Tertiary mafic volcanic rocks are primarily plagioclase, biotite, and Fe-oxide minerals. The Pre-Tertiary felsic volcanic rocks are primarily quartz, albite, K-feldspars, some biotite, rhyolite (some clay-altered and some containing glass shards and/or small crystals of biotite), and muscovite. Tertiary volcanic and sedimentary rocks of Carlin Formation contain quartz, K-feldspars, muscovite, some biotite and welded and non-welded white tuff commonly weathered to clay (illite and smectite) along with some glass shards. The Pre-Cenozoic carbonate rocks consist primarily of calcite and dolomite. The Quaternary alluvium and lacustrine deposits consist primarily of quartz, feldspars, muscovite, biotite, and Fe-oxides, whereas the playa deposits in the LHR regions contain primarily evaporite minerals and salts. (Sherlock et al., 1996; Theodore et al., 2003)

X-ray Powder Diffraction (XRD) and Energy-Dispersive (EDS) Scanning Electron Microscopy (SEM) analyses of riverbed sediments along the HR indicate that the most common minerals are quartz, albite, anorthite, K-feldspar, calcite, muscovite, smectite, illite, montmorillonite, and Fe-oxides (Mohammad and Tempel, 2013B, in prep.) with minor occurrences of pyrite in the UHR near mineralized zones (Theodore et al, 2003). Earman and Hershey (2004) reported that waste rocks produced from the abandoned “Big Spring” mine, which is located near the upper end of the North Fork Humboldt River (Figure 6.1) in the UHR region contain pyrite, marcasite, and arsenopyrite as most abundant minerals.

Ore deposits, mining and geothermal activities

Sedimentary rock-hosted metal deposits in the HRB contribute the vast majority of the gold, silver, copper, lead and other metals mined in the region. These metal deposits are typically associated with sulfides and As-bearing sulfide minerals such as pyrite, chalcopyrite, arsenopyrite, marcasite, orpiment, and realgar in the sediments (Arehart et al., 1993; Theodore et al., 2003; Wallace et al., 2004). Many of these deposits are mined from deep, extremely large open pits, and exploitation of these deep ores has required extensive dewatering of adjacent aquifers (Wallace et al., 2004), and in several cases, the fluids produced by dewatering are put back into the HR after treatment (Prudic et al., 2006). The Great Basin region and the HRB area has a number of hot springs and hot wells, some of which are being used for power plants (Shevenell and Garside, 2005; Shevenell et al., 2008).

6.2.3. Hydrology of the Humboldt River Basin

The precipitation ranges from 15 to 110 cm annually and most commonly in the range of 15 to 30 cm in the valleys and floodplain areas. Precipitation generally is greater at higher elevations in the mountains than in the adjacent valleys and occurs mostly during the wet season from late November to May (Prudic et al., 2006). The average annual precipitation map prepared by the Division of Water Resources (NDWR) of State of Nevada-Department of Conservation and Natural Resources (<http://water.nv.gov/>) indicates annual average precipitation with a range of 10-20 cm in the western HR Basin with an annual average of less than 10 cm near the Humboldt Sink.. Shevenell (1996) reported monthly potential evaporation at several weather stations in the valleys and low

lands of the HRB that exceeded monthly precipitation. For example, at Imlay, north of Rye Patch Reservoir, monthly potential evaporation ranges from 0 to 32.75 cm, whereas monthly precipitation ranges from 0.53 to 2.38 cm. Monthly potential evaporation is even greater near the Humboldt Sink (Shevenell, 1996).

A previous study on the measurements of river discharge data indicate the river gains flow from Elko to Palisade, and then loses flow most years from Battle Mountain to Rye Patch Reservoir (Prudic et al., 2006). The flow rates in the HR from Elko to Rye Patch Reservoir show seasonal variations with peak flow occurring during snowmelt runoff at the end of the wet season. The annual runoff from the drainage above the town of Carlin is dominated by snowmelt runoff from the Ruby, Jarbidge, and Independence Mountains and the East Humboldt Range. In contrast, most of the snowmelt runoff from the Tuscarora Mountains, and Santa Rosa and Toiyabe ranges downstream of Carlin is lost to irrigation diversions, natural evapotranspiration, and infiltration into the alluvium prior to reaching the HR (Prudic et al., 2006). The increase in discharge in the HR from Elko to Palisade occurs as a result of tributary inflows from the South-ForkHumboldt River (SFHR) and Susie, Maggie, and Mary's Creek along with groundwater discharge between Carlin and Palisade (Maurer et al., 1997; Prudic et al., 2006). The interactions between groundwater and surface waters are described in more detail in section 2.1.2 in Chapter 3.

The HR plays an important role in maintaining wildlife habitats and wetlands, irrigation, and water storage in Rye Patch reservoir, and Humboldt Sink, which is located in the LHR. Approximately, 67% of all water used in the HRB is from the river or its

tributaries (Earman and Hershey, 2004). Irrigation is the predominant use of surface water in the HRB (Desert Research Institute, 1994).

6.2.4. Hydrogeochemistry of the Humboldt River

Table 6.1 lists physical and hydro-chemical data of the water samples of the HR. Details of the sample collection and analytical methods can be found in Chapter 4 and 5. The Piper diagram and Stiff diagram analyses of the waters (Figures 5.5 and 5.6 in Chapter 5) show that water chemistry changes from predominantly-sulfate water [(Na+K)-SO₄] in the UHR, to bicarbonate water [(Na + K)-HCO₃] in the MHR and northern LHR, and finally to chloride-water [(Na + K)-Cl] around the Lovelock Valley in the downstream.

6.3. Modeling methods

Geochemical reaction path modeling techniques were utilized to test our preliminary hypotheses that oxidation of As-bearing sulfide minerals is the primary source of As in the UHR region of the HR system, and concentrations of dissolved As in the water are affected by several physical processes such as mixing with shallow groundwater and geothermal water, and evaporation along the flow-path of the HR from upstream to downstream. For this, a conceptual model was first developed to illustrate the relationships and interactions of processes. Input to the model included petrographic and mineralogic data, fluid composition (composition of precipitation and observed river water composition) for geochemical reaction path modeling. However, quantifying the

Table 6.1: Summarized physical parameters and some important chemical components of waters from the Humboldt River. Concentrations are in mg/L unless otherwise stated. Samples were collected in late September, 2007.

Sample ID	pH	ORP (mV)	Cond (μ S)	Temp ($^{\circ}$ C)	Ca	Mg	Na	K	Cl	SO ₄	Alk. ¹	B	Li	Fe	Mn	SiO ₂	As	$\delta^{18}\text{O}$	δD	$\delta^{34}\text{S}$
U 001	8.77	125	1240	14.7	75.9	70.0	252	18.5	61.5	565	526	2.13	0.11	<0.01	0.01	15.9	0.07	-14.5	-114	4.7
H 003	8.64	134	760	18.5	125	57.1	301	17.5	151	566	440	0.84	0.29	<0.01	0.37	20.7	0.01	-15.1	-125	9.8
R 004	8.85	10	720	17.6	49.1	20.4	47.9	10.5	24.3	59.3	265	0.24	0.11	0.02	0.06	14.8	0.01	N.S.	N.S.	10.3
007	8.85	105	980	13.6	57.9	29.3	174	11.9	120	144	421	0.52	0.10	0.04	0.01	15.2	0.02	-9.4	-98	12
008	8.85	105	920	16.2	47.7	19.2	146	11.7	75.1	104	348	0.64	0.17	0.03	0.01	18.2	0.04	-11.6	-105	N.S.
009	8.91	143	680	14.6	37.3	6.9	50.1	10.8	24	28.9	195	0.20	0.03	0.03	0.01	17.3	0.01	-9.2	-92	N.S.
010	8.44	163	660	17.4	29.2	5.7	63.2	13.0	26.7	32.4	195	0.22	0.04	0.01	0.01	40.4	0.01	-15.7	-125	N.S.
L 011	8.55	156	780	13.8	67.8	20.7	139	10.0	88.8	124	418	0.51	0.09	0.01	0.46	22.9	0.02	-13.9	-115	N.S.
H 012	8.96	192	830	9.9	43	24.0	114	8.92	109	132	277	0.69	0.08	0.03	0.01	14.9	0.02	-12.6	-110	N.S.
R 013	8.95	168	840	11.4	38.7	26.9	133	10.7	123	146	235	0.80	0.08	0.01	0.01	12.4	0.02	-11.1	-103	N.S.
015	9.13	139	1020	17.8	37.4	22.7	168	18.2	134	125	343	0.54	0.17	0.02	0.01	16.0	0.05	-7.5	-85	7.2
016	9.25	125	980	17.6	37.9	21.5	149	15.7	111	98.6	323	0.47	0.13	0.01	0.01	15.8	0.04	-8.5	-89	N.S.
017	9.04	145	1080	14.5	46.2	20.7	308	26.3	332	141	409	1.22	0.30	0.02	0.01	18.5	0.05	-9.6	-95	N.S.
018	8.92	136	1160	13.9	42.6	21.5	423	27.9	508	163	427	1.29	0.26	0.03	0.01	19.4	0.05	-9.6	-94	N.S.
019	8.93	119	1280	14.5	43.7	21.5	418	28.3	482	159	393	1.23	0.26	0.03	0.01	20.2	0.05	-9.7	-94	N.S.

ORP: Oxidation-Reduction Potential; ¹Alk.: Alkalinity as HCO₃⁻; Stable isotopes in ‰; N.S.: Not Sampled. NO₂, NO₃, and PO₄ were below detection limit.

various physical processes such as mixing, dilution, and evapotranspiration in the reaction path modeling depends on the availability of the water. Therefore, the conceptual model also incorporates a simplified hydrologic analysis for different pathways of the study area.

6.3.1 Conceptual model

A simplified conceptual hydrologic model was developed based on the flow data of the HR acquired by USGS, and previous studies involving precipitation, evapotranspiration and groundwater –surface water flow in different parts of the study area. The simplified water balance of the basin is:

$$\delta S = P - E + R + GW_i = GW_o$$

where, δS is the change in storage in the river water, P = precipitation, E = evaporation, R = surface runoff, GW_i = groundwater inflow to the river, GW_o = groundwater outflow.

Groundwater outflow may include discharge as springs, discharge to surface water bodies, groundwater outflow to outside the system boundary, and pumping for domestic, agricultural, industrial and mining uses. However, due to a larger study area with discontinuous sub basins and catchments, and due to broad nature of this study, detailed hydrologic water balance was not within the scope of this study. The major factors for this: 1) distance from one sampling location to another with at least 30 to 50 km apart; 2) the water samples were collected during the dry season and hence the water from one location to another location in most cases were not interconnected. Additionally, site specific evaporation data, precipitation data, and groundwater inflow data for each pathways along the HR do not exist for a detailed hydrologic model. Therefore, a

simplified conceptual model was adopted using base flow analysis of the stream flow data for each river gages and sampling locations. Base flow is the portion of stream flow that comes from groundwater or other delayed sources (Tallaksen, 1995). A simple web based base flow analysis method called WHAT (Web Based Hydrograph Analysis Tool; <https://engineering.purdue.edu/~what/>) was used to determine the fractions of direct runoff and groundwater inflows from the stream flow data with justifiable assumptions that the streams are intermittent with porous aquifer, and the total stream flow equals the summation of direct runoff and base flow, where direct runoff equals the rainfall excess (direct runoff = rainfall – losses), where, losses = interception, infiltration, depression storage, etc. also known as basin recharge; and rainfall excess or direct runoff = overland flow. Because of the “relatively” dry season, there was very little rainfall to no rainfall at some places, and therefore, the resultant analysis indicates majorities of flows were due to base flow for some stations. For example, at locations near sample 001 and 003 (Figure 6.5), the base flow was 100%, and 97% respectively (Table 6.2). The average precipitation during September ranges from 1.4 cm to 1.7 cm in the UHR region, and 1.0 cm to 1.1 cm in the HR and LHR regions (Table 6.5).

The ratio of total base flow to discharge is base flow index (BFI). The WHAT method uses the automated base flow separation technique and offers a convenient tool to calculate BFI for multiple watersheds having different size and geology, or for a single watershed in multiple years having different meteorological forcing or land use practice (Kyoung J. Lim et al., 2005). Here two-parameter digital-filter algorithm (Eckhardt, 2005) with default value of $\alpha = 0.98$, and BFI_{max} of 0.80 has been used to separate the base flow and determine the BFI. Because the samples were collected during late

September of 2007, the calculated BFI during the summer of 2007 has been used to determine the fraction of shallow groundwater inflows at each stations. Table 6.2 lists the results of base flow analysis based on the available stream flow data in different stream gages. Table 6.3 lists the historical groundwater quality data collected by NDEP.

Potential evapotranspiration (PET) was estimated from an empirical study by Shevenell, (1996), where PET was estimated on a 1 km grid for each of the 12 months of the year for state of Nevada. A coefficient factor of 0.7 has been used for open water evaporation as commonly used in northern Nevada (Shevenell, 1996). Table 6.4 lists average evaporation data in northern Nevada obtained from various NDEP stations. The average monthly evaporation for shallow open water is 4.1 to 4.5 inches (10.4 to 11.4 cm) in the UHR and MHR regions in northern Nevada, and about 4.6 to 5 inches (11.6 to 12.7 cm) around Imlay, Winnemucca, Rye Patch reservoir and Lovelock area in the LHR region in relatively southern part of the HRB. The higher rates of evaporation in the LHR reflects the comparatively more surface area of the open water and availability of water than to UHR area.

Table 6.5 lists the precipitation data for northern Nevada collected from National Climatic Data Center. Average annual precipitation ranges from 21 to 35 cm, and average September precipitation ranges from 1 to 2 cm in northern Nevada.

The 10-year average chemical composition of precipitation from Lehman Cave's station in Ely, NV, was used for the purpose of modeling to reflect the chemical composition of precipitation within the study area. This location represents similar terrain and topography in the south-east of the HRB. The chemical composition of precipitation does not include dryfall (dust) data because the concentration of dissolved Cl in dry fall

Table 6.2: Average daily base flow of the Humboldt River during August - September, 2007 recorded at various stream gages. Data source: <http://wdr.water.usgs.gov/nwisgmap/>

Abbreviated ID*	USGS Station ID	Stream Gage Location Name	Total Flow (m ³ /sec)	Direct Runoff (m ³ /sec)	Base Flow (m ³ /sec)	BFI
A	10315600	MARYS RV BLW TWIN BUTTES NR DEETH	0.02	0.00	0.02	1.00
B	10316500	LAMOILLE CREEK	7.03	2.29	4.74	0.67
C	10318500	HUMBOLDT RV NR ELKO	2.24	0.06	2.18	0.97
D	10320000	SOUTH-FORK-HUMBOLDT RIVER	6.45	2.43	4.02	0.62
E	10321000	HUMBOLDT RV NR CARLIN	13.85	4.91	8.95	0.65
F	10321590	SUSIE CK AT CARLIN	3.61	1.49	2.13	0.40
G	10322000	MAGGIE CK AT CARLIN	11.01	4.47	6.54	0.59
H	10322150	MARYS CK AT CARLIN	6.03	2.14	3.89	0.65
I	10322500	HUMBOLDT RV AT PALISADE	41.55	14.98	26.56	0.64
AVERAGE		UPPER HUMBOLDT RIVER	10.20	3.64	6.56	0.69
K	10323425	HUMBOLDT RV AT OLD US 40 BRG AT DUNPHY	21.14	8.16	12.98	0.61
L	10324500	ROCK CREEK	0.36	0.23	0.12	0.35
M	10324700	BOULDER CREEK	4.60	2.57	2.03	0.44
N	10325000	HUMBOLDT RV AT BATTLE MOUNTAIN	6.80	3.72	3.08	0.45
AVERAGE		MIDDLE HUMBOLDT RIVER	8.22	3.67	4.55	0.46
O	10327500	HUMBOLDT RV AT COMUS	0.31	0.11	0.19	0.64
P	10329000	LITTLE HUMBOLDT RIVER	31.98	11.90	20.08	0.63
Q	10329500	MARTIN CREEK NR PARADISE VALLEY	9.83	3.50	6.33	0.64
V	10333000	HUMBOLDT RV NR IMLAY	10.73	4.31	6.43	0.60
X	10335000	HUMBOLDT RIVER NR RYE PATCH RESERVOIR	527.38	204.38	322.99	0.61
AVERAGE		LOWER HUMBOLDT RIVER	116.05	44.84	71.21	0.62

*See Figure 6.1 for locations of the Station.

BFI: Base flow Index: Ratio of total base flow to total flow.

Table 6.3: Groundwater quality data for groups-I, II, and III corresponding to Upper Humboldt, Middle Humboldt, and Lower Humboldt River basins, respectively.

	Group-I				Group-II				Group-III			
	Min.	Max.	Mean	Std. Dev.	Min.	Max.	Mean	Std. Dev.	Min.	Max.	Mean	Std. Dev.
TEMP	10	49	17.27	8.04	6	19	11.76	3.66	12.80	21.00	15.87	3.02
COND	86.24	1040	466.4	206.8	338.8	3220	762.89	806.09	367	2450	963.08	537.2
pH	6.40	8.50	7.42	0.40	7.50	8.45	7.94	0.26	7	9	7.94	0.55
TDS _c	56	916.7	319.5	155.4	220	1940.1	580.8	472.09	238.3	1590.9	625.4	348.8
K	0.87	24.4	5.98	5.64	1.30	16	6.43	4.47	1.70	34	7.31	7.86
Na	5.11	144	32.04	23.19	25.80	530	85.36	133.92	27	590	146.5	128.8
Ca	6.28	112.4	43.74	22.72	22	100	41.15	21.75	0.36	110	17.19	34.76
Mg	1.74	59.2	11.97	9.12	6.16	72	12.67	16.70	0.11	30	4.30	8.13
SiO ₂	5.30	73	38.27	14.51	21	67	44.94	14.43	21	65	38.42	12.87
As	0.001	0.40	0.02	0.06	0.003	0.07	0.01	0.02	0.002	0.55	0.04	0.15
Ba	0.003	0.20	0.07	0.04	0.06	0.09	0.07	0.01	0.01	0.58	0.06	0.15
Cl	2.06	114	18.38	20.86	17.80	730	67.57	201.39	7.36	360	56.31	98.68
F	0.07	1.98	0.49	0.45	0.20	1.50	0.46	0.32	0.30	2.50	0.70	0.53
Fe	0.004	3.37	0.04	0.55	0.01	0.31	0.05	0.08	0.003	1.23	0.01	0.29
HCO ₃	34	573	188.3	99.8	129	308	197.4	47.98	108	1280	318.8	254.5
Mn	0.0002	0.53	0.01	0.08	0.001	0.94	0.02	0.26	0.001	1	0.03	0.33
SO ₄	6.30	300	38.19	50.16	26	320	65.25	96.55	4.60	290	61.31	78.21

Note: TEMP: Temperature (°C); COND: Conductivity (µS/cm); Min: Minimum; Max: Maximum; Std. Dev: Standard Deviation.

Group-I represents groundwater from UHR basin; Group-II represents groundwater from MHR basin, and Group-III represents groundwater from LHR basin.

Table 6.4: Average evaporation data (inches) of various stations in northern Nevada. Data source: State of Nevada Department of Conservation & Natural Resources. http://water.nv.gov/mapping/et/et_stations.cfm.

Station	Station Name	Basin Name	Start Year	End Year	No. Years Avg.	Ref Et	Shallow Open Water
260691	BATTLE MTN AP	Lower Reese River Valley	1974	2006	30	4.3	4.5
260795	BEOWAWE	Crescent Valley	1976	2006	30	4.3	4.5
260800	BEOWAWE U OF N RCH	Grass Valley	1973	2007	28	4.2	4.4
261630	CENTRAL NEVADA FLD LAB	Upper Reese River Valley	1966	1985	13	4.5	4.7
261740	CLOVER VALLEY	Clover Valley	1926	2007	30	4	4.2
261975	CORTEZ GOLD MINE	Crescent Valley	1969	1979	10	4.1	4.3
262570	ELKO	Elko Segment	2000	2007	6	3.9	4.1
262573	ELKO RGNL AP	Elko Segment	1978	2007	30	4	4.2
263101	GEYSER RCH	Lake Valley	1972	2002	19	4.5	4.7
263245	GOLCONDA	Winnemucca Segment	1970	2005	30	4.6	4.8
263957	IMLAY	Imlay Area	1964	2007	30	4.5	4.7
264700	LOVELOCK DERBY FLD	Lovelock Valley	1970	2005	30	4.7	4.9
266746	REESE RIVER	Upper Reese River Valley	1973	2006	26	4.3	4.5
267192	RYE PATCH DAM	Imlay Area	1973	2007	30	4.8	5
267690	SOUTH FORK SP	Dixie Creek - Tenmile	1994	2007	8	4.3	4.5
268988	WELLS	Marys River Area	1975	2004	30	4	4.2
269168	WINNEMUCCA #2	Grass Valley	2000	2007	6	4.4	4.7
269171	WINNEMUCCA MUNI AP	Winnemucca Segment	1978	2007	30	4.7	4.9

Table 6.5: Average annual and September precipitation data of northern Nevada.
Data source: National Climatic Data Center.

Average annual precipitation			
Days	Place/Station	Inches	cm
81	Elko	9.9	25.2
81	Mountain City	12.5	31.7
88	Ruby Lake	13.9	35.3
53	Rye Patch Reservoir Dam	8.6	21.7
71	Winnemucca	8.3	21.0
Precipitation totals for September			
Days	Place/Station	Inches	cm
4	Elko	0.6	1.4
4	Mountain City	0.7	1.7
5	Ruby Lake	0.8	2.1
3	Rye Patch Reservoir Dam	0.4	1.0
3	Winnemucca	0.4	1.1

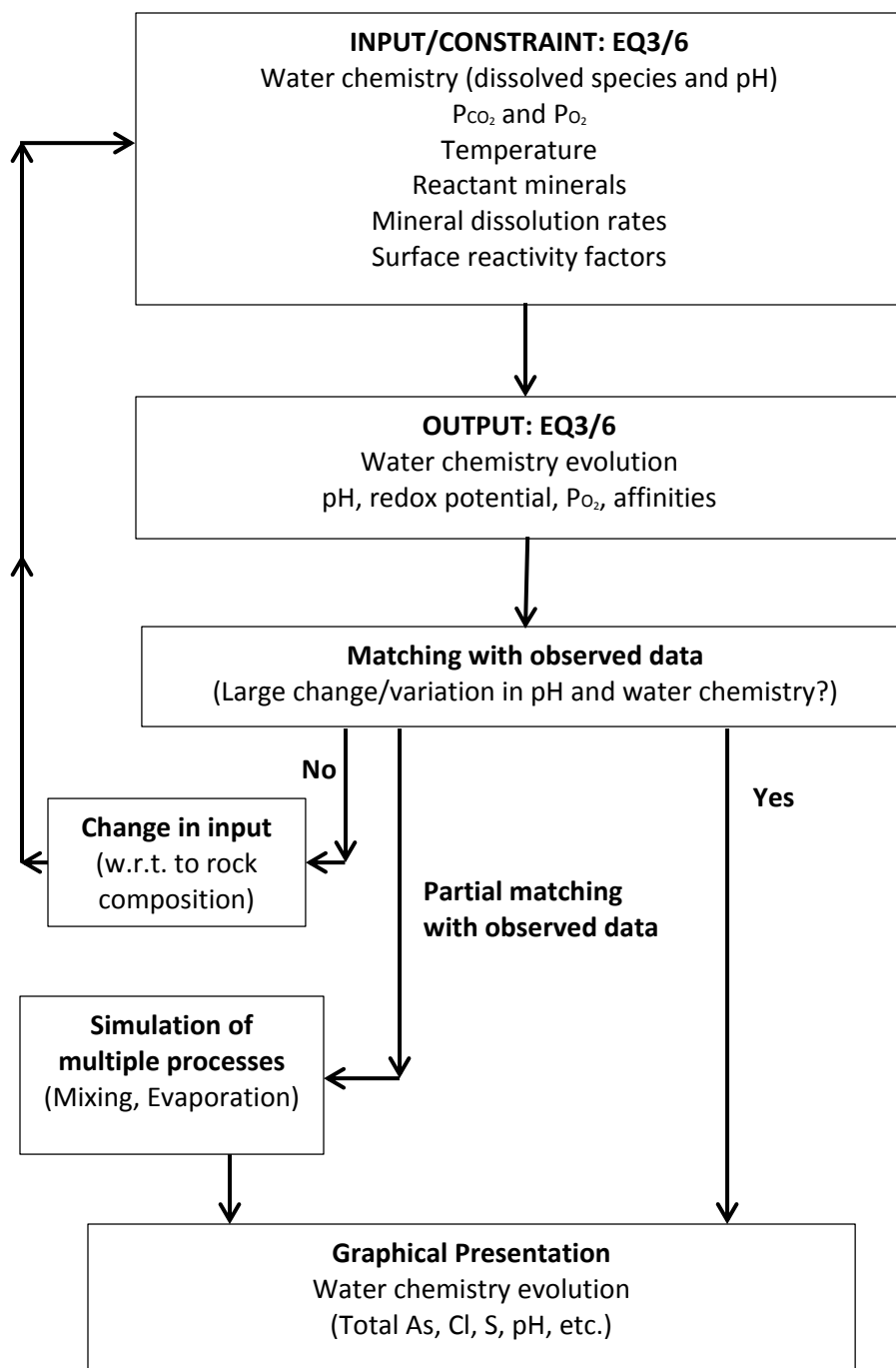


Figure 6.3: Flow chart showing procedure used to combine reaction path calculations with mineral and water chemistry data in EQ3/6 computer codes (modified after Lengke and Tempel, 2005).

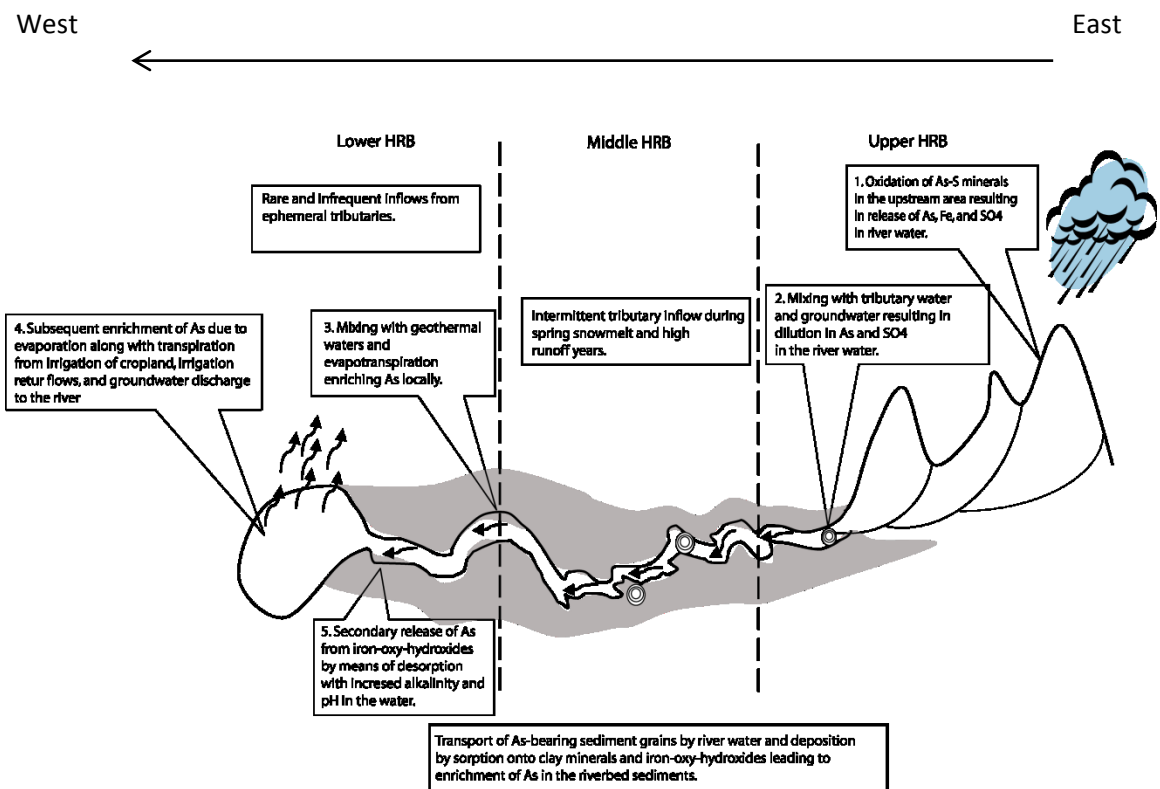


Figure 6.4: Schematic diagram showing different path-ways used in the conceptual model.

Table 6.6: Water chemistry data that were used in the simulations for different pathways along the flow-path of the Humboldt River.

	Sample ID	pH	Temp C	Cond µS/cm	Ca mg/L	Mg mg/L	Na mg/L	K mg/L	Cl mg/L	SO ₄ mg/L	HCO ₃ mg/L	SiO ₂ mg/L	As mg/L
Pathway 1													
Initial Comp.	Rainwater ^{a1}	5.39	-	-	1.32	0.03	0.1	0.03	0.12	0.54	b	-	-
	Groundwater near Mary's River ⁴	8.5	-	-	59.3	59.2	144	12.6	58	300	512	18.3	0.060
Pathway 2													
Initial Comp.	HR 003 at Elko	8.64	18.50	760	125.0	57.1	301	17.5	151.0	566	440	20.7	0.010
	Groundwater at SFHR ²	8.45	11.16	458	45.5	10.7	36.3	6.53	8.2	13.9	238	14.6	0.010
	Groundwater at Palisade ⁵	7.42			43.7	12.0	32.0	6.98	8.4	12.2	188	18.3	0.015
Measured Comp.	HR 004 at palisade	8.85	17.6	720	49.1	20.4	48.0	10.5	24.3	59.3	265	14.8	0.013
Pathway 3													
Initial. Comp.	HR 007 near Comus	8.85	13.6	980	57.9	29.4	174	11.9	121	144	421	15.2	0.021
	Groundwater near Golconda ⁶	7.94			41.15	12.67	105.4	6.43	47.57	75.25	297	22.94	0.038
	Geothermal water ³ (GEO)	7	63.5	845	34	7.8	141	22	20	78	440	59	0.020
Measured Comp.	HR 008 at Golconda	8.85	16.2	920	47.7	19.2	146	11.8	75.1	105	348	18.2	0.037
Pathway 4													
Initial Comp.	HR 012 at Imlay	8.96	9.9	830	43.0	24.1	114	8.9	109	132	277	14.9	0.019
	Groundwater near Imlay ⁷	8.20			27.2	26.8	147	9.8	124	148	254	12.9	0.020
Measured Comp.	HR 013 at Upstream Ryepatch reservoir	8.95	11.4	840	38.7	27.0	133	10.8	123	147	235	12.4	0.022
Pathway 5													
Initial Comp.	HR 013 at Upstream Ryepatch reservoir	8.95	11.4	840	38.7	27.0	133	10.8	123	147	235	12.4	0.022
	HR 015 at downstream Ryepatch												
Measured Comp.	Reservoir	9.13	17.8	1020	37.37	22.68	168.4	18.17	134.1	125	343	16.0	0.048
Pathway 6													
Initial Comp.	HR 017 at Lovelock Valley	9.04	14.5	1080	46.2	20.7	308	26.3	332	142	410	18.5	0.048
	Groundwater at Lovelock Valley ⁸	8.70			34.8	15	392	24	462	144	294	20.5	0.040
Measured Comp.	HR 019 at upstream Humboldt Sink	8.93	14.5	1280	43.7	21.5	418	28.3	482	159	393	20.2	0.052

a: Assumed to be equilibrium with atmospheric O₂ (Atm. O₂ = 21% = 0.21); i.e., Log (0.21) = -0.678 ; i.e., Log fO₂ = -0.678

b: Assumed to be in equilibrium with atmospheric CO₂ (Atm. CO₂ = 0.035% = 3.5 X10⁻⁴); i.e., Log (3.5 X 10⁻⁴) = -3.456

HR: Humboldt River; SFHR: SouthFork_Humboldt River Comp.: Composition

1: Average (1997-2007) rainwater composition from Lehman's Cave, Ely, NV(Data Source: Annual Data for Site: NV05;

Great Basin National Park-Lehman Caves; ; <http://nadp.sws.uiuc.edu/nadpdata/annualReq.asp?site=NV05>)

2: Average (1997-2007) of South Fork-Humboldt River water Chemical composition (Data source: NDEP)

3: Geothermal hot spring water from Golconda Hotspring system [Great Basin Groundwater Geochemical Database]

4, 5, 6, 7, 8: Representative ground water [NDEP and Great Basin Groundwater Geochemical Database]

does not vary significantly and can be justified for the purpose of geochemical reaction path modeling, where the objective is to demonstrate the effect of water-rock interactions for dissolved As and sulfate in the water.

Figure 6.4 illustrates the relationship of processes along the flow path of the HR, and Figure 6.5 shows the calculations steps of the EQ3/6 computer code used in this study. Table 6.6 lists the water chemistry data that have been used for simulations along the flow path. The conceptual geochemical model for each the flow paths are described as follows.

Pathway 1: Water-rock reactions involving oxidative dissolution of As-bearing sulfide minerals resulting in dissolved sulfate and arsenic, followed by in-situ acid neutralization by carbonate host rocks resulting in increased pH of the water in the UHR. The water is further mixed with shallow groundwater inflow followed by evaporation at this flow path near Mary's River and Humboldt River (Table 6.6 and Figure 6.5).

Pathway 2: Concentrations of dissolved As and other solutes decrease from the upstream to downstream in this flow path between Elko and Palisade because of mixing with shallow groundwater inflows at the South Fork Humboldt River and at Palisade (Table 6.6 and Figure 6.5).

Pathway 3: Shallow groundwater inflows followed by evaporation results in increased concentrations of dissolved As in the water between Comus and Golconda (Table 6.6 and Figure 6.6). Localized mixing with geothermal water is also inferred because of the location of sampling points near Golconda, where the Golconda hot

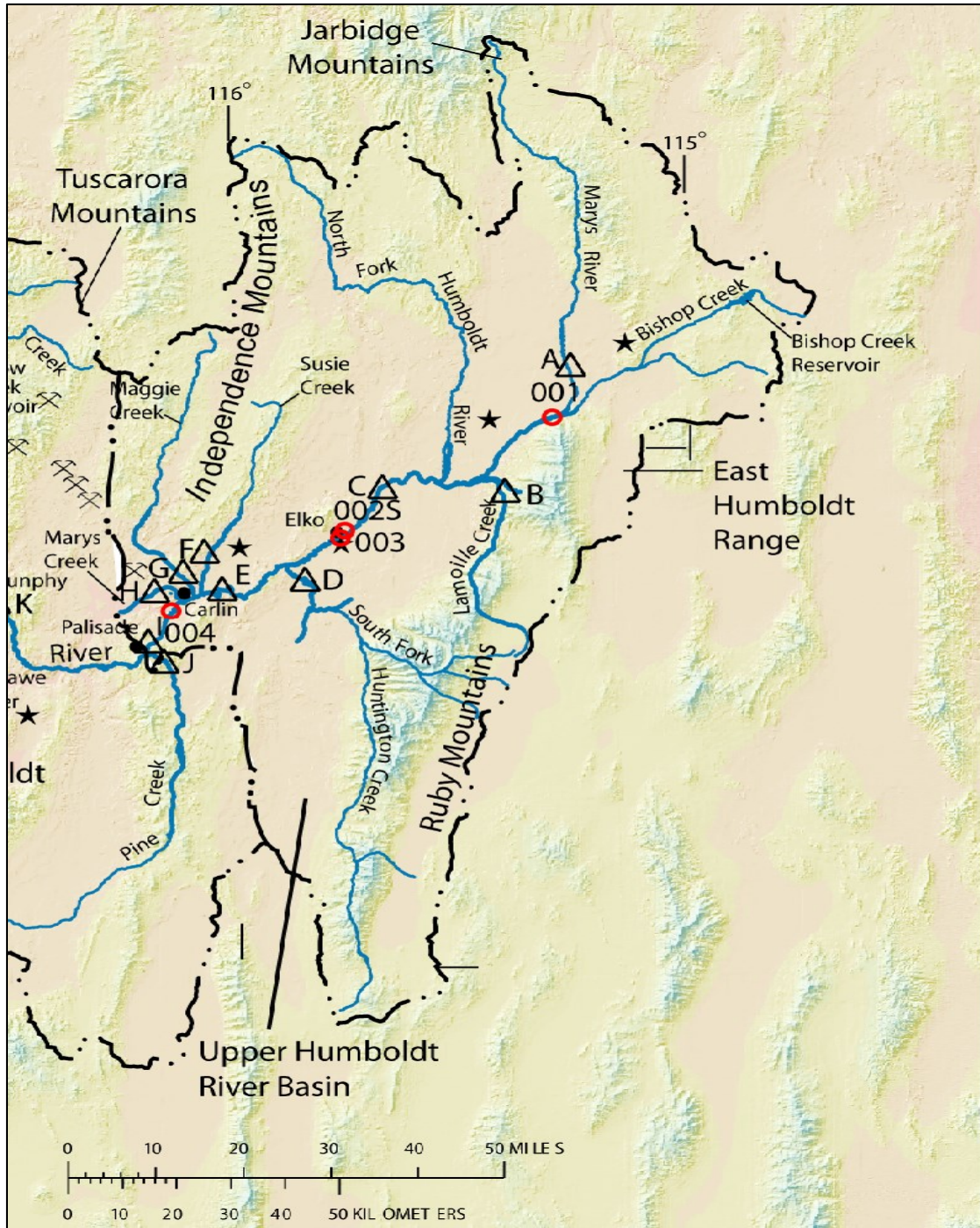


Figure 6.5: Location of samples used in modeled pathways 1 and 2 (sample 001, and sample 003 to 004) in the Upper Humboldt River.

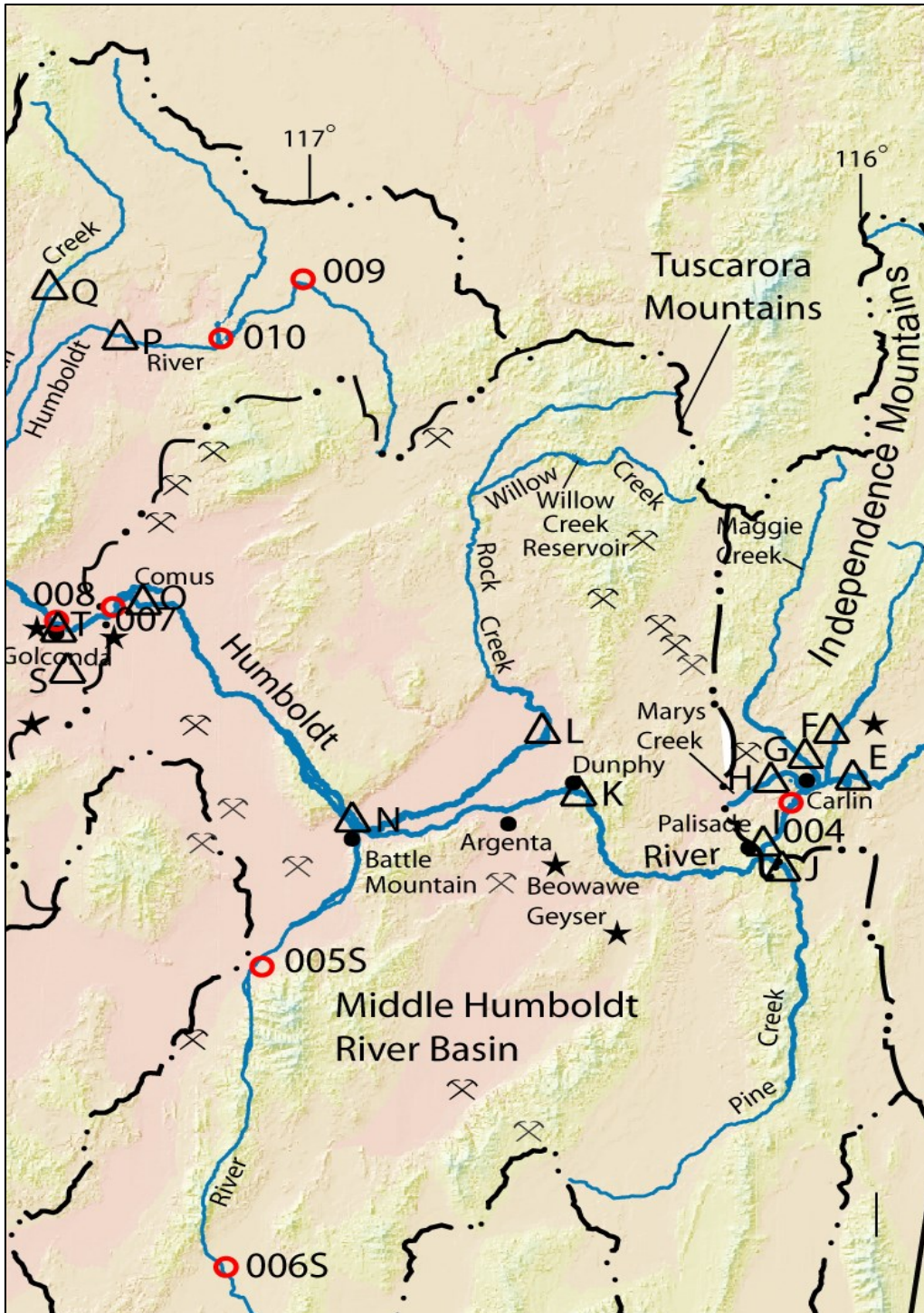


Figure 6.6: Location of samples used in modeled pathway 3 (sample 007 to 008) in the Middle Humboldt River.

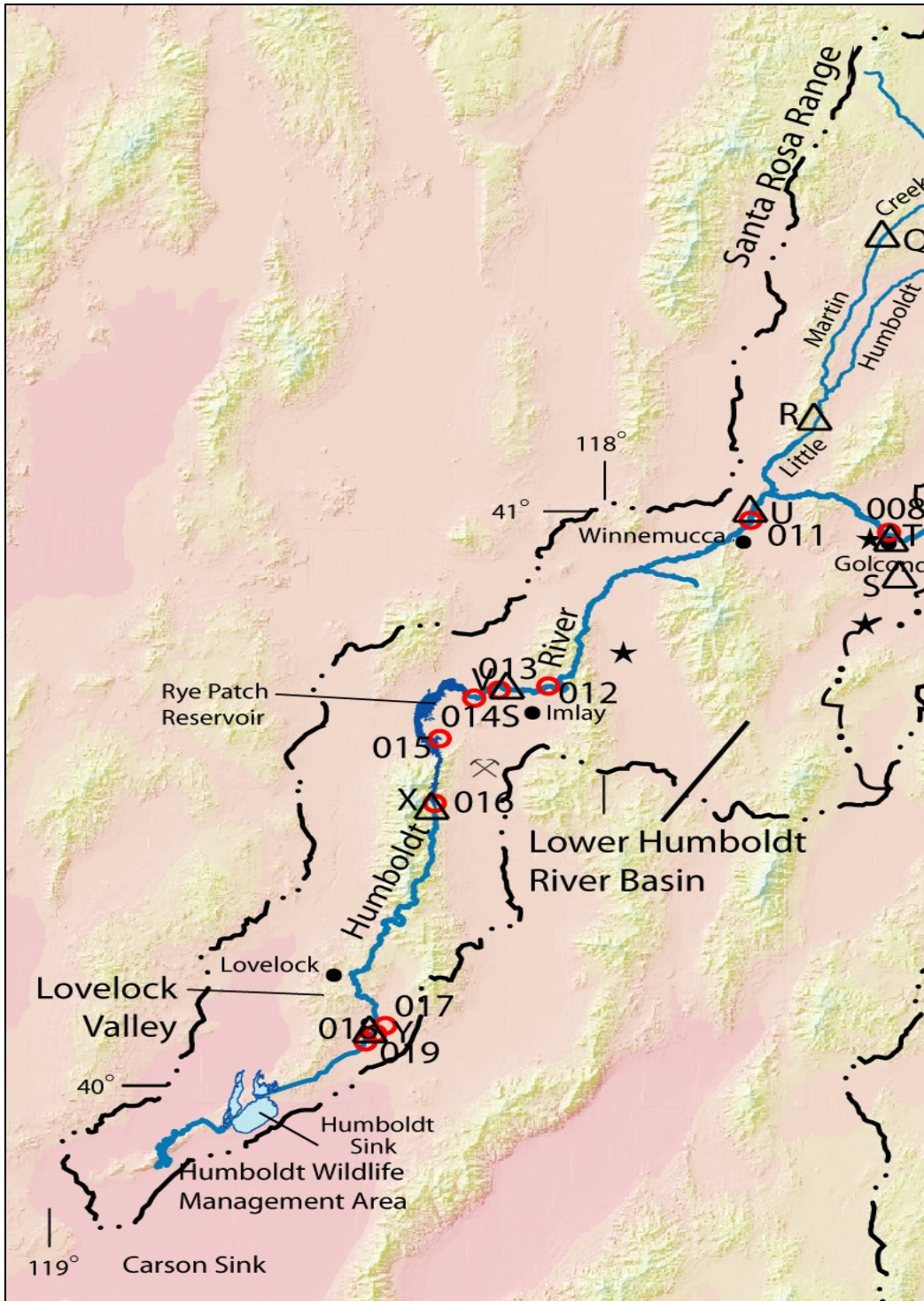


Figure 6.7: Location of samples used in modeled pathways 4, 5 and 6 (sample 012 to 013; 015 to 016; and 017 to 019) in the Lower Humboldt River.

springs with dissolved As and other trace elements has been reported by Cohen (1963) and Shevenell et al. (2008).

Pathway 4: Dissolved As concentrations increase from sample 012 to 013 near Imlay because of groundwater inflow followed by evaporation (Table 6.6 and Figure 6.7).

Pathway 5: Desorption of from As-bearing iron oxy-hydroxides from the river bed sediments may play an additional role in As distribution in the HRB. Simulations were performed to evaluate the role of desorption in the LHR because of the potential effect of alkaline pH on As desorption (Table 6.6 and Figure 6.7). Desorption was simulated for only LHR waters because desorption of arsenate from iron-oxide surfaces is preferentially favored under alkaline pH (Fuller and Davis, 1989; Dzombak and Morel, 1990).

Pathway 6: Finally, evaporation is simulated to explain the progressive increase in As and Cl, and other dissolved ions in the LHR near Lovelock Valley because of increased evapotranspiration near the Humboldt Sink (Table 6.6 and Figure 6.7).

6.3.2. Thermodynamic modeling calculations

All modeling calculations were performed using the reaction path code EQ3/6 (Wolery and Jarek, 2003). EQ3 is a speciation code, which calculates the equilibrium state of fluid at a given temperature. EQ6 is a reaction path code which allows system temperature and composition to be varied over a defined reaction path. Another computer code PHREEQC (Parkhurst and Appelo, 1999) was used to determine the role of desorption in enriching As concentrations in the water.

Fluid equilibration and single point calculations

The waters used in this study were equilibrated using EQ3 at the corresponding temperatures that were recorded during the sample collection. The output of equilibration yields chemical characteristics of the waters including pH, aqueous speciation and mineral saturation states. Because the waters in the HR are relatively dilute with low ionic strength, the B-dot equation, an extension of Debye-Huckel equation is used for simulations (Wolery and Jarek, 2003).

Single-point calculations were performed using EQ6 at the corresponding temperatures to model open-space precipitation in the river bed sediments. A single point calculation simply allows supersaturated minerals to precipitate from an equilibrated fluid analysis by determining which minerals are the most thermodynamically likely to precipitate (Wolery and Jarek, 2003).

6.3.3. Model constraints

Water-rock reaction simulation

Mineralogic and rock geochemistry data have been constrained from published geochemical and mineralogic data of rocks and river sediments (Mohammad and Tempel, 2013B; Sherlock et al., 1996; Theodore et al., 2003; Earmann and Hershey, 2004). Because of the lack of unreacted spring water data from the study area, we used published rainwater composition (<http://nadp.sws.uiuc.edu/nadpdata/>) from the region that represents similar terrain and weather conditions. It does not however include the concentrations of dryfall (dust) that falls in the basin between periods of rain or snow,

and can be justified because of no significant effect on dissolved ions. For simplicity, it is assumed that snow-melt spring water that has not reacted with rocks is similar to the composition of rain water. The results from simulations were then matched to observed water chemistry at sample 001. Here, simulation of water-rock interaction demonstrates the magnitude of water-rock interaction with rocks containing As-bearing sulfides, silicates and carbonates. Water composition that results from the modeled water-rock reactions with rain water and country-rocks is compared with sample composition for pathway -1.

Reactant minerals used in the oxidative dissolution model in pathway-1 are quartz, anorthite, K-feldspar, calcite, dolomite, muscovite, illite, smectite, pyrite, and arsenopyrite that represent various lithologies and the proportions of those lithologies in the country-rocks in the UHR. These minerals have been observed in a previous study (Mohammad and Tempel, 2013B, in prep.) and published by others from the same region (Theodore et al., 2003; Earman and Hershey, 2004). Table 6.7 lists these reactant minerals and percentage of country rock composition.

Mineral dissolution and oxidation rates

Table 6.8 lists kinetics rates of mineral dissolution used in the reaction path calculation, and the references from which the rate data were obtained. The extent of water-rock reaction that takes place during the residence time of rain water/snow-melt water (which is a year-round process) is important and can be constrained by assigning appropriate mineral dissolution and oxidation rates of country-rock minerals in the model. The quartz dissolution rate is chosen as a reference rate because quartz is the most

Table 6.7: Values used to calculate the amounts of reactant minerals titrated into the fluid over the course of the reaction path when modeling reaction of rainwater with country rocks.

Minerals	Volumetric Ratio (v%)	Molar vol.¹ (cm³/mol)	Moles of Reactants (mol/kg)
Quartz	30	22.7	4.635
Albite	8	100	0.280
Anorthite	2	101	0.070
K-feldspar	8	109	0.258
Muscovite	5	141	0.125
Annite	3	154	0.068
Illite	8	500	0.056
Smectite-high Fe-Mg	8	139	0.202
Calcite	13	36.9	1.234
Dolomite	5	64.4	0.272
Pyrite	5	23.9	0.732
Arsenopyrite	5	26.4	0.663

1: Molar Volumes were taken from LLNL database in EQ3/6 (Wolery and Jarek, 2003)

Table 6.8: Kinetics rates used in mineral dissolution in the water-rock reaction simulation in EQ3/6. Dissolution rates are given as mol/m²/s. Relative rate for quartz was set to 1 to allow complete dissolution because quartz is the most abundant reactant mineral. All other relative rates were calculated relative to quartz.

Reactant minerals	Mol % country rock	Log rate (mol/m ² /s)	Relative rate (X Quartz rate)	References
<i>Silicates</i>				
Quartz	30	-13.39	1	Rimstidt and Barnes, 1980
Albite	8	-12.26	1.3X10 ¹	Burch et al., 1993
Anorthite	2	-8.55	6.9X10 ⁴	Fleer, 1982
K-Feldspar	8	-12.50	7.8	Schweda, 1989
Muscovite	5	-13.07	2.1	Lin and Clemency, 1981
Annite	3	-13.07	2.1	assumed muscovite rate
Illite ¹	8	-13.07	2.1	assumed muscovite rate
Smectite ²	8	-13.07	2.1	assumed muscovite rate
<i>Carbonates</i>				
Calcite	13	-6.00	2.5X10 ⁷	Plummer et al., 1978; Svensson and Dreybrodt, 1992
Dolomite	5	-8.00	2.5X10 ⁵	Busenburg and Plummer, 1987
<i>Sulfides</i>				
Pyrite	5	-9.40	9.8X10 ³	Williamson and Rimstidt, 1994
Arsenopyrite	5	-10.14	1.8X10 ³	Walker et al., 2006

¹Rate for illite is assumed to be the same as that for muscovite

²Rate for smectite is assumed to be similar to that for illite

abundant reactive mineral and dissolves slowest of any of the minerals used in the model, and the rates of dissolution for other minerals are assigned relative to the quartz dissolution rate. Oxidation rates for pyrite, and arsenopyrite and others were chosen accordingly with the consistent value of pH in our waters. Using relative dissolution and oxidation rates provides a convenient alternative to using absolute dissolution rates in geochemical reaction path code EQ3/6, where it can eliminate or minimize convergence problems (Tempel et al, 2000; Wolery and Jarek, 2003). Although mineral dissolution rates can be affected by pH, the dissolution rates in the calculations are assumed to be constant over the range of geochemical conditions observed in the UHR to maintain the simplicity, which is also reasonable because the pH of the waters consistently ranges from 8.64 to 8.77 in the UHR region.

Mixing simulation

Mixing models were only performed within the same pathways and sub basins (e.g., between samples in the Upper Humboldt River basin), where the samples represented the two end members of the continuous pathway. Mixing simulations have also been done between shallow groundwater and the river waters, where groundwater inflows are evident. For example, groundwater is mixed with the water resulted from water-rock reactions near Mary's River at sample location 001 (Figure 6.5). In all mixing simulations, ratios have been based on the results of base flow analysis (Table 6.2). The matched sample water from pathway-1 is not used as input for the next step (Pathway-2), because of the discontinuity and lack of flowing water between these two stations. Pathway-2 simulates mixing between HR 003 waters and groundwater at the

South Fork-Humboldt River followed by groundwater at Palisade. For Pathway-3, mixing between geothermal hot spring water near Golconda, and sample HR 007 was simulated followed by subsequent mixing with groundwater and matched with HR 008 adjacent to Golconda.

In mixing simulations, the proportions of end member waters were determined by assuming that Cl behaves as a conservative element along the flow-path of the river (i.e., no Cl is gained from or lost to solid or gas phases from reactions). For the mixing simulation with geothermal spring water, the Golconda Hot Springs data (Table 6.6) from the Great Basin Center for Geothermal Energy have been used. The public domain groundwater quality data from the NDEP and Great Basin Geochemical Database have been used for groundwater composition. Table 6.3 shows the summarized statistics of representative groundwater quality data, and Table 6.6 shows all input data for simulations.

Evaporation simulation

Evaporations were modeled using EQ3/6 by allowing the minerals to precipitate that were actually observed and reported. These minerals are calcite, quartz, albite, muscovite, illite, smectite, pyrite and arsenopyrite. The amount of moles removed due to evaporation of 1kg of water is determined from the percentage of evaporation assuming 55.51 moles in 1 kg of water. The percentage of evaporation for shallow open water was estimated based on the available Evaporation data (Table 6.4), and the area of drainage for each sub basins along with the results from previous studies.

Desorption simulation

Desorption was simulated using PHREEQC computer code (Parkhurst and Appelo, 1999) to determine its role in enriching As concentrations in the LHR water. The WATEQ database was used because this database contains the necessary thermodynamic data for As. The Log K values for the reactions between As species and hydrous ferric oxide mineral surface (Table 6.9) were obtained from Dzombak and Morel (1990). Input files were set up using the elemental chemistry data obtained from the sequential extraction of the river sediments.

For the desorption, the surface species of hydrous ferric oxides (FeOOH) were estimated following the method by Parkhurst and Appelo (1999) with iron concentrations extracted from sequential extraction analyses. For example, at sediment sample 013 near Imlay, solid-phase Fe concentration in Fe-oxide fraction was 324 mg/kg which corresponded to 5.79×10^{-3} moles of Fe per kg solution. Using surface site density of 0.2 mole sites per mole of Fe, a total of 1.58×10^{-3} mols of sites was used in the calculations. A gram formula weight of 89 was used to estimate the mass of hydrous ferric oxides (FeOOH) as 0.513 g. The specific surface area of $600 \text{ m}^2/\text{g}$ was taken from Dzombak and Morel (1990).

6.3.4. Modeling assumptions

Redox potential of the rain water is assumed to be constrained by equilibrium with O_2 in the atmosphere. Although biological activity may also contribute to redox conditions, these processes have not been quantified and are not included in these simulations.

Table 6.9: Surface parameters of ferrihydrite (HFO) and equilibrium constants used in the desorption modeling.

<i>HFO surface parameters</i>	
Stoichiometry: FeO ₃ .H ₂ O; 89 g HFO per mole Fe	
Surface area: 600 m ² /g	
Surface site density: 0.2 mole sites per mole Fe	
<i>Adsorption reactions</i>	<i>LogK</i>
Hfo_wOH + H ⁺ = Hfo_wOH ₂ ⁺	7.29
Hfo_wOH = Hfo_wO ⁻ + H ⁺	-8.93
Hfo_wOH + AsO ₄ ⁻³ + 3H ⁺ = Hfo_wH ₂ AsO ₄ + H ₂ O	29.31
Hfo_wOH + AsO ₄ ⁻³ + 2H ⁺ = Hfo_wHAsO ₄ ⁻ + H ₂ O	23.51
Hfo_wOH + AsO ₄ ⁻³ = Hfo_wOHAsO ₄ ⁻³	10.58

The pH of the rain water is assumed to be in equilibrium with atmospheric O₂ (10^{-0.7} atm.) and CO₂ (10^{-3.5} atm.) since the reaction is taking place at the surface and in an open system environment. To represent such conditions, the fixed fugacity option was used in EQ3/6 (Wolery and Jarek, 2003). The simulations including water-rock reactions, mixing and evaporation all were simulated under an open-system condition consistent with redox conditions of the waters in HR.

It was assumed that both rain and snow-melt waters are similar in composition before reacting with rocks. Concentrations of dissolved ions likely vary with seasonal fluctuations of flow in the river water, which depends on recharge from rain and snow-melt during the wet season and on groundwater discharging to the river during the base-flow or low-flow conditions.

Because the samples were collected during late September of 2007, during low flow season, and because the river flow was lost from Palisade to Comus during summer (see Chapter 3, Section 2.1.1 and 2.1.2), sample 004 was not used as the initial composition for mixing with geothermal water near Golconda. Instead, sample 007 was used as the initial composition before mixing with geothermal water near sample 008 at Golconda. Simulations of evaporation were performed on the water samples from LHR at sample 012 near Imlay. Sample 011 was not used in the simulation because the distance between 011 and 012 is about 40 miles, and the discharge data (Table 3.1, Chapter 3) indicate that most of the water from Winnemucca is lost at the point of sample 012 near Imlay. Sample 009 and 010 represent samples from Little Humboldt River and Martin Creek, which do not contribute to the Humboldt River, and therefore were not included in the modeling. Samples 017, 018 and 018 represent the same area within a span of about

0.5 mile from each other, and therefore only one sample (017) is included in the model from these three samples.

Simulations in this study were conducted to demonstrate the physical and geochemical processes that occur in the HR during one season. However, the magnitude of these processes may vary with season due to changes in flow conditions. Therefore, sensitivity analyses were performed with respect to various flow conditions and other variables.

6.4. Modeling results

6.4.1. Speciation and mineral saturation calculations

In the aqueous speciation model using EQ3, the dominant aqueous species in solution are listed in Table 6.10. Note that As and Fe are present in their oxidized forms [As(V) and Fe(III)] in all water samples at equilibrium. Other cations and anions are predominantly present as free ions (i.e., Ca^{2+} , Mg^{2+} , Na^+ , K^+ , Fe^{2+} , Cl^- , etc.). Although, no speciation data are available for redox sensitive ions to test the degree of redox disequilibrium in the system, the system is a fairly oxidized system with oxidation-reduction potential values ranging from 10 mV to 192 mV (Table 6.1).

The saturation indices that were calculated using EQ6-single point calculations and the minerals that were observed in the sediments are given in Table 6.11. At ambient temperatures, the river waters are supersaturated with respect to the minerals quartz, smectite clays, dolomite, goethite, and hematite (Table 6.10). Other mineral phases are theoretically supersaturated in the waters; however, none of these have been determined

or reported in published studies. Single point calculations were used to determine the actual minerals that were thermodynamically likely to precipitate in the existing conditions. The resultant product mineral assemblage included calcite, muscovite, Casaponite, Ca-nontronite, Mg-nontronite, and annite, and is consistent with the observed and previously reported mineral assemblages.

The results of each of the modeled processes described by the conceptual model for distribution of dissolved As concentrations are shown in Table 6.12.

6.4.2. Sensitivity analysis

Sensitivity analyses to change flow conditions were conducted by increasing or decreasing mixing ratios of the contributing tributary waters and geothermal waters. These analyses show that model results will vary with season to some extent with variable mixing ratios. However, while total dissolved ions may change with season, proportions of ions in modeled and measured waters remain largely unchanged (Chapter 3, Table 3.8) because they reflect water-rock interactions with the local and regional geology which does not change with season. Alternatively, physical processes modeled in this study will show seasonal variability (i.e. mixing ratios, extent of evaporation), but geochemical processes are independent of season because they result from water-rock interactions that are governed by kinetic rate laws. Factors that may affect kinetic rate laws are temperature, pH, and dissolved oxygen. Temperatures do change with season, but the range of temperature change within the HR would be considered negligible within the larger scope of water-rock interactions.

Table 6.10: Speciation results showing dominant species resulted from EQ3 speciation modeling for Humboldt River sample waters.

Component	Dominant Species	Percent of Total														
		Sample ID														
		001	003	004	007	008	009	010	011	012	013	015	016	017	0180	019
Br ⁻	Br ⁻	99.97	99.96	99.99	99.98	99.98	99.99	99.99	99.98	99.98	99.98	99.98	99.98	99.96	99.95	99.95
Ca ⁺⁺	Ca ⁺⁺	73.24	76.3	83.99	79.88	81.07	87.33	92.03	84.8	82.9	83.8	73.33	70.82	76.58	73.28	80.35
	CaSO ₄ (aq)	12.93	13.05	2.66	4.75	3.96	1.55	1.87	4.59	5.08	5.59	4.14	3.3	4.08	12.42	4.37
	CaCO ₃ (aq)	10.1	7.56	10.74	11.76	11.8	8.95	3.77	6.64	9.32	8.28	19.87	23.48	16.07	11.22	12.06
	CaHCO ₃ ⁺	3.56	3.02	2.57	3.52	3.07	2.12	2.31	3.9	2.58	2.17	2.54	2.28	3.02	2.92	2.96
Cl ⁻	Cl ⁻	99.77	99.75	99.92	99.85	99.87	99.94	99.94	99.87	99.88	99.87	99.86	99.87	99.8	99.76	99.75
Fe ⁺⁺	Fe(OH) ₃ (aq)	84.54	87.58	68.89	82.45	82.73	81.67	91.9	89.85	79.52	79.84	72.38	66.7	75.92	80.21	79.84
	Fe(OH) ₄ ⁻	14.47	11.15	13.42	16.51	16.38	18.03	6.88	8.97	20.26	19.92	27.46	33.19	23.86	19.4	19.68
	FeCO ₃ (aq)			10.93	0.49											
H ₂ AsO ₄ ⁻	HAsO ₄ ²⁻	99.11	98.96	99.14	99.16	99.15	99.18	98.24	98.68	99.24	99.23	99.19	99.12	99.22	99.21	99.21
	H ₂ AsO ₄ ⁻		0.08					1.68	1.2							
HCO ₃ ⁻	HCO ₃ ⁻	89.47	88.96	90.73	90.47	91.05	92.07	95.81	93.29	90.8	90.6	86.43	83.68	88	89.99	89.33
	CO ₃ ²⁻	3.06	2.51	3.37	3.31	3.44	3.5	1.33	1.69	3.72	3.81	6.58	8.24	5.33	4.26	4.34
K ⁺	K ⁺	98.13	98.19	99.73	99.42	99.55	99.85	99.83	99.48	99.42	99.37	99.46	99.57	99.44	98.19	99.4
Li ⁺	Li ⁺	98.48	98.53	99.78	99.53	99.63	99.88	99.86	99.58	99.53	99.49	99.57	99.65	99.54	98.53	99.5
Mg ⁺⁺	Mg ⁺⁺	70.3	71.17	87.03	82.02	83.6	90.49	92.55	85.03	84.38	84.45	78.66	78.09	80.42	71.11	82.35
	MgSO ₄ (aq)	20.99	22.33	4.83	7.95	7	2.63	3.27	7.51	7.73	8.71	7.87	6.41	7.16	20.05	7.53
	MgCO ₃ (aq)	5.01	3.52	5.45	6.23	6.08	4.66	1.85	3.42	5.05	4.38	10.51	12.77	8.68	5.68	6.4
	MgHCO ₃ ⁺	3.46	2.86	2.63	3.6	3.15	2.15	2.28	3.89	2.6	2.17	2.71	2.5	3.18	2.86	3.06

Continued to next page

Component	Dominant Species	Percent of Total														
		Sample ID														
		001	003	004	007	008	009	010	011	012	013	015	016	017	0180	019
	Mn ⁺⁺	21.31	29.75	26.15	20.36	22.54	28.01	51.51	32.09	21.96	25.34	14.5	12.15	15.87	19.26	20.7
	MnSO ₄ (aq)	6.22	8.59	1.39	1.99	1.84	0.82	1.76	2.86	2.17	2.75	1.38	0.95	1.4	5.38	1.86
Na ⁺	Na ⁺	97.25	97.55	99.11	98.47	98.75	99.3	99.33	98.55	98.7	98.78	98.65	98.74	98.44	97.39	98.44
SO ₄ ²⁻	SO ₄ ²⁻	82.31	80.47	87.22	86.34	88.14	91.6	92.32	86.86	88.55	87.93	88.56	88.89	88.04	88.33	87.25
	MgSO ₄ (aq)	10.28	8.9	6.56	6.4	5.07	2.52	2.26	4.92	5.56	6.32	5.66	5.52	4.15	3.36	4.02
	CaSO ₄ (aq)	4.16	6.9	5.28	4.58	4.33	4.8	4.04	5.98	3.96	3.53	2.97	3.04	3.19	2.5	2.87
	NaSO ₄ ⁻	3.09	3.57		2.57	2.33	0.94	1.2	2.12	1.84	2.1	2.62	2.38	4.36	5.56	5.59
SiO ₂ (aq)	SiO ₂ (aq)	92.88	93.74	93.18	92.58	92.37	92.96	97.21	96.31	92.25	91.86	85.42	82.16	86.83	88.65	88.27
	HSiO ₃ ⁻	4.97	4.25	6.26	5.57	6.01	6.39	2.49	2.91	6.22	6.39	11.25	14.1	8.46	6.51	6.75

Table 6.11: Saturation Indices calculated from water samples of the Humboldt River using EQ3/6 computer codes.

Mineral phases	Log Q/K values of samples*															Observed
	001	003	004	007	008	009	010	011	012	013	015	016	017	0180	019	
Calcite	1.47	1.55	1.30	1.43	1.33	1.11	0.62	1.25	1.22	1.11	1.45	1.53	1.46	1.27	1.31	X
Dolomite (ordered)	4.26	4.11	3.60	3.92	3.65	2.87	1.90	3.33	3.52	3.41	4.08	4.22	3.96	3.60	3.69	
Dolomite (disordered)	2.64	2.52	2.00	2.29	2.04	1.24	0.30	1.70	1.86	1.76	2.48	2.62	2.33	1.97	2.07	
Quartz	0.62	0.65	0.52	0.62	0.64	0.66	0.98	0.81	0.71	0.59	0.51	0.49	0.66	0.70	0.71	X
K-Feldspar	2.47	2.40	1.89	2.68	2.33	2.45	3.68	2.87	2.66	2.32	2.08	2.27	2.79	3.73	2.94	X
Albite	0.62	0.71	-0.39	0.83	0.47	0.12	1.43	1.01	0.69	0.36	0.11	0.31	0.86	1.90	1.12	X
Anorthite	-5.72	-5.43	-5.89	-5.12	-5.73	-5.69	-4.53	-5.23	-5.64	-5.92	-6.14	-5.57	-5.79	-4.24	-5.74	X
Illite	2.04	1.95	1.20	2.61	1.73	1.78	3.95	2.85	2.32	1.84	0.93	1.40	1.89	4.00	2.18	X
Kaolinite	0.57	0.54	0.00	1.15	0.35	0.44	2.36	1.51	0.86	0.49	-0.61	-0.27	0.15	2.07	0.45	
Muscovite	2.75	2.58	1.79	3.52	2.35	2.51	5.03	3.69	3.04	2.57	1.38	1.96	2.55	5.33	2.92	X
Goethite	4.26	4.37	4.56	4.83	4.78	4.77	4.40	4.25	4.56	4.18	4.63	4.47	4.53	4.68	4.76	X
Hematite	9.45	9.69	10.1	10.6	10.5	10.5	9.73	9.43	10.0	9.29	10.2	9.88	9.98	10.3	10.4	X
Smectite clays:																X
Smectite (high-Fe-Mg)	2.08	2.07	2.60	2.76	2.29	1.58	2.23	1.77	1.63	1.26	1.81	2.20	2.02	3.15	2.49	
Smectite (low-Fe-Mg)	2.77	2.75	2.75	3.29	2.82	2.35	3.33	2.78	2.62	2.19	2.37	2.72	2.77	3.91	3.14	
Ca-Saponite	7.99	7.73	7.53	7.60	7.52	6.60	5.28	6.07	7.65	7.54	9.08	9.74	8.36	7.77	7.89	
Ca-Nontronite	13.5	13.8	13.7	14.7	14.6	14.6	15.1	14.2	14.5	13.2	13.8	13.5	14.1	14.9	14.8	
Ca-Beidellite	0.66	0.73	-0.06	1.35	0.48	0.60	3.15	1.95	1.07	0.50	-0.72	-0.30	0.29	2.53	0.66	
Ca-Montmorillonite	2.67	2.71	2.01	3.12	2.51	2.51	4.45	3.55	3.03	2.49	1.72	2.07	2.50	4.04	2.75	

*Log Q/K values are not directly comparable to each other minerals, because the Log Q/K value is dependent upon the size of the formula unit used in the calculations. For example, the Log Q/K for pyrite expressed as F_2S_4 would be twice that of FeS_2 . Because of this effect, phyllosilicates and other aluminosilicates tend to have large absolute values of Log Q/K, while minerals with very simple formulas, such as quartz (SiO_2) have proportionately smaller Log Q/K values

Table 6.12: Simulation results for various parameters and As concentrations for all modeled pathways. Concentrations are in mg/L.

Parameters		pH	Ca	Mg	Na	K	Cl	SO ₄	HCO ₃	SiO ₂	As
Pathway-1											
Initial comp.	Rainwater ^{a1}	5.39	1.32	0.03	0.10	0.03	0.12	0.54	^b	-	-
	Groundwater near Mary's River ⁴	8.5	59.3	59.2	144	12.6	58.0	300	512	18.3	0.06
Simulation step-1	Water-rock (WR) reactions	8.67	66.2	66.0	164	16.3	0.12	486	506	12.7	0.053
Simulation step-2	Groundwater inflow @ 92%	8.51	59.9	59.7	146	12.9	53.4	315	512	17.8	0.059
Simulation step-3	Evaporation of step-2 water @ 10%	8.80	65.9	65.7	160	14.2	58.7	346	563	19.6	0.065
Measured	HR 001 at Mary's River	8.77	75.9	70.0	252	18.5	61.5	565	526	15.9	0.066
Pathway-2											
Initial Comp.	HR 003 at Elko	8.64	125.0	57.1	301	17.5	151.0	566	440	20.7	0.010
	Groundwater at SFHR ²	8.45	45.5	10.7	36.3	6.53	8.2	13.9	238	14.6	0.010
	Groundwater at Palisade ⁵	7.42	43.7	12.0	32.0	6.98	8.4	12.2	188	18.3	0.015
Simulation step-1	Groundwater inflow at SFHR @ 62%	8.52	75.7	28.3	136.9	10.70	62.5	167.1	359	16.9	0.010
Simulation step-2	Groundwater inflow at Palisade @ 64%	7.65	53.7	17.3	67.0	8.10	26.6	64.6	242	17.4	0.013
Measured	HR 004 at Palisade	8.85	49.1	20.4	48.0	10.5	24.3	59.3	265	14.8	0.013

Continued to next page

a: Assumed to be equilibrium with atmospheric O₂ (Atm. O₂ = 21% = 0.21); i.e., Log (0.21) = -0.678 ; i.e., Log fO₂ = -0.678b: Assumed to be in equilibrium with atmospheric CO₂ (Atm. CO₂ = 0.035% = 3.5 X10⁻⁴); i.e., Log (3.5 X 10⁻⁴) = -3.456

HR: Humboldt River; SFHR: SouthFork_Humboldt River Comp.: Composition

1: Average (1997-2007) rainwater composition from Lehman's Cave, Ely, NV(Data Source: Annual Data for Site: NV05; Great Basin National Park-Lehman Caves; ; <http://nadp.sws.uiuc.edu/nadpdata/annualReq.asp?site=NV05>)

2: Average (1997-2007) of South Fork-Humboldt River water Chemical composition (Data source: NDEP)

3: Geothermal hot spring water from Golconda Hotspring system [Great Basin Groundwater Geochemical Database]

4, 5, 6, 7, 8: Representative ground water [NDEP and Great Basin Groundwater Geochemical Database]

Parameters		pH	Ca	Mg	Na	K	Cl	SO ₄	HCO ₃	SiO ₂	As
Pathway-3											
Initial. Comp.	HR 007 near Comus	8.85	57.9	29.35	173.69	11.91	120.6	144	421	15.15	0.021
	Groundwater near Golconda ⁶	7.94	41.15	12.67	105.36	6.43	47.57	75.25	297	22.94	0.038
	Geothermal water ³ (GEO)	7	34	7.8	141	22	20	78	440	59	0.02
Simulation step-1	Groundwater inflow @ 64%	8.5	47.2	18.7	130	8.4	73.9	100	342	20.1	0.032
Simulation step-2	Mix step-1 water and GEO @ 90-10 ratio	8.35	45.86	17.59	131.06	9.76	68.47	98	351.48	24.02	0.031
Simulation step-3	Mix GEO and HR 007 @ 45-55 ratio	8.66	43.70	19.60	159.00	16.40	75.30	114	387.00	21.69	0.016
Simulation step-4	Evaporation of step-1 mixed water @ 5%	8.93	49.54	19.61	136.46	8.82	77.55	105	351.89	21.14	0.033
Measured	HR 008 at Golconda	8.85	47.7	19.2	146	11.8	75.1	105	348	18.2	0.037
Pathway-4											
Initial Comp.	HR 012 at Imlay	8.96	43.0	24.1	114	8.9	109	132	277	14.9	0.019
	Groundwater near Imlay ⁷	8.20	27.2	26.8	147	9.8	124	148	254	12.9	0.020
Simulation step-1	Groundwater inflow at Imlay @ 60%	8.50	33.5	25.7	134	9.4	118	142	263	13.7	0.020
Simulation step-2	Evaporation of HR water 012 @ 10%	9.86	47.3	26.5	125	9.8	120	145	305	16.4	0.021
Simulation step-3	Evaporation of mixed water at step-1 @ 5%	8.93	35.2	27.0	140	9.9	124	149	277	14.4	0.021
Measured	HR 013 at upstream Ryepatch Reservoir	8.95	38.7	27.0	133	10.8	123	147	235	12.4	0.022

Continued to next page

a: Assumed to be equilibrium with atmospheric O₂ (Atm. O₂ = 21% = 0.21); i.e., Log (0.21) = -0.678 ; i.e., Log fO₂ = -0.678

b: Assumed to be in equilibrium with atmospheric CO₂ (Atm. CO₂ = 0.035% = 3.5 X10⁻⁴); i.e., Log (3.5 X 10⁻⁴) = -3.456

HR: Humboldt River; SFHR: SouthFork_Humboldt River Comp.: Composition

1: Average (1997-2007) rainwater composition from Lehman's Cave, Ely, NV(Data Source: Annual Data for Site: NV05; Great Basin National Park-Lehman Caves; ; <http://nadp.sws.uiuc.edu/nadpdata/annualReq.asp?site=NV05>)

2: Average (1997-2007) of South Fork-Humboldt River water Chemical composition (Data source: NDEP)

3: Geothermal hot spring water from Golconda Hotspring system [Great Basin Groundwater Geochemical Database]

4, 5, 6, 7, 8: Representative ground water [NDEP and Great Basin Groundwater Geochemical Database]

Parameters		pH	Ca	Mg	Na	K	Cl	SO₄	HCO₃	SiO₂	As
Pathway 5											
Initial Comp.	HR 013 at upstream Ryepatch Reservoir	8.95	38.7	27.0	133	10.8	123	147	235	12.4	0.022
Simulation step-1	Desorption	8.95	39.0	27.0	133	11.0	122	147	235	12.4	0.041
Simulation step-2	Evaporation of step-1 water @ 10%	9.13	42.9	29.7	146	12.1	134	162	259	13.64	0.045
Measured	HR 015 at downstream Ryepatch Reservoir	9.13	37.4	22.7	168	18.2	134	125	343	16.0	0.048
Pathway-6											
Input Comp.	HR 017 at Lovelock Valley	9.04	46.2	20.73	307.63	26.33	332.1	141.5	409.92	18.54	0.048
	Groundwater at Lovelock Valley ⁸	8.70	34.8	15	392	24	462	144	294	20.5	0.04
Simulation step-1	Groundwater inflow @ 60%	8.84	39.3	17.3	358	24.9	410	143	340	19.7	0.043
Simulation step-2	Evaporation of step-1 water @ 15%	9.16	45.2	19.9	412	28.7	472	164	391	22.7	0.050
Measured	HR 019 upstream Humboldt Sink	8.93	43.7	21.5	418	28.3	482	159	393	20.2	0.052

a: Assumed to be equilibrium with atmospheric O₂ (Atm. O₂ = 21% = 0.21); i.e., Log (0.21) = -0.678 ; i.e., Log fO₂ = -0.678

b: Assumed to be in equilibrium with atmospheric CO₂ (Atm. CO₂ = 0.035% = 3.5 X10⁻⁴); i.e., Log (3.5 X 10⁻⁴) = -3.456

HR: Humboldt River; SFHR: SouthFork_Humboldt River Comp.: Composition

1: Average (1997-2007) rainwater composition from Lehman's Cave, Ely, NV(Data Source: Annual Data for Site: NV05; Great Basin National Park-Lehman Caves; ; <http://nadp.sws.uiuc.edu/nadpdata/annualReq.asp?site=NV05>)

2: Average (1997-2007) of South Fork-Humboldt River water Chemical composition (Data source: NDEP)

3: Geothermal hot spring water from Golconda Hotspring system [Great Basin Groundwater Geochemical Database]

4, 5, 6, 7, 8: Representative ground water [NDEP and Great Basin Groundwater Geochemical Database]

6.5. Modeling discussion

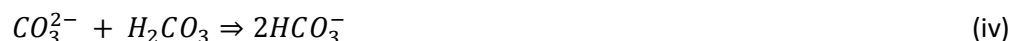
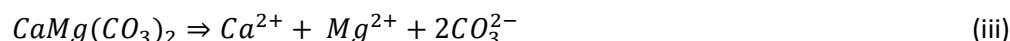
6.5.1. Pathway 1

Water-rock reactions simulation

In general, simulated water-rock reactions between the unreacted rainwater and the reactant mineral assemblage described in methods resulted in a close approximation of the observed mineralogy and water chemistry sampled in the upstream of the HR at the confluence of the UHR and Mary's River in Elko County, with some exceptions, which are discussed later. The degree of water-rock interaction that achieved these results was $\log \xi = -6.42$ which is equivalent to total of 9.92×10^{-1} moles of minerals dissolved per liter of solution. The water-rock reactions simulation yielded a product mineral assemblage of calcite, muscovite (illite proxy), Ca-saponite, Ca-nontronite, Mg-nontronite, and annite. These model results are consistent with petrographic analyses conducted by this study and reported minerals from previous studies (Sherlock et al., 1996; Theodore et al., 2003; Earmann and Hershey, 2004; Mohammad and Tempel, 2013B in prep). Although modeled concentrations of dissolved Ca, Mg, K, SO₄, HCO₃, SiO₂, total As, and pH also matched reasonably well with measured concentrations (Table 6.12), there have been major discrepancy with respect to dissolved Cl concentrations in the simulated water and observed water. This has been discussed in the following section.

Dissolved ions from water-rock reactions simulation

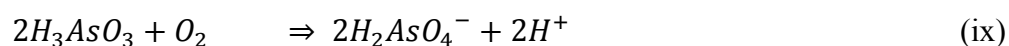
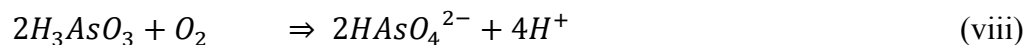
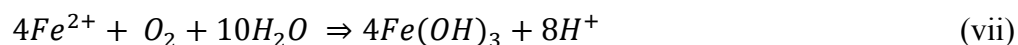
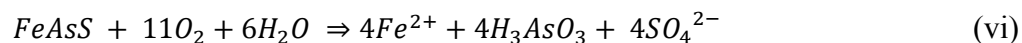
Results from simulation step-1 for pathway-1 (Table 6.12) indicates that modeled concentrations of Ca (66.2 mg/L) and Mg (66 mg/L) were controlled by dissolution of calcite, dolomite and Mg-smectite in the reactant mineral assemblage. These values are a reasonable match for measured concentrations of Ca (75.9 mg/L) and Mg (70.0 mg/L) in the 001 near the confluence of Mary's River and Bishop Creek in Elko County, Nevada. In this region, Pre-Cenozoic limestone and dolomite rocks provide the Ca and Mg to the waters by dissolution as follows:



The modeled concentration of K (16.3 mg/L) is closely matched for measured K concentrations (18.5 mg/L) and is due to the dissolution of K-feldspars and constrained by the precipitation of illitic clays. Modeled silica concentration (12.7 mg/L) is closely matched for the measured concentration (15.8 mg/L) and is due to feldspar dissolution.

Measured HCO_3^- concentration (526 mg/L) is slightly higher than in the modeled water (506 mg/L), but show less than 4% difference and is a reasonable match. Carbonate mineral equilibria are controlling HCO_3^- concentrations both in model calculations and in the HR with calcite found in stream sediments in this study (Mohammad and Tempel, 2013 B, in prep.). Modeled As concentrations (0.053 mg/L) are within 20% agreement with observed dissolved As values (0.066 mg/L) and modeled SO_4 values (514 mg/L) are

less than 9% different than measured SO_4 values (565 mg/L). Hence the agreement between modeled and observed As and SO_4 values is good and results from oxidative dissolution of pyrite and As-bearing sulfides as follows (Walker et al., 006):



where, the reaction (vi) represents initiation of arsenopyrite oxidation by oxygen at near neutral pH, resulting in As (III) [H_3AsO_3] and dissolved SO_4^{2-} in the solution; the reaction (vii) represents the subsequent secondary oxidation of Fe^{2+} released in reaction (vi) to form iron oxyhydroxides; and the reactions (viii) and (ix) represent further oxidation of arsenite [As (III)] produced in reaction (vi) to form arsenate [As (V)].

In model calculations, 3.75×10^{-3} moles of pyrite and 6.89×10^{-7} moles of arsenopyrite were required to be destroyed per liter of solution to increase concentrations of As and SO_4 from rainwater to sampled HR water. These amounts of pyrite and arsenopyrite are small and represent less than 1% of the pyrite and less than 0.001% of the arsenopyrite available to react in the reactant mineral assemblage in the model per liter of solution. Thus, the minor occurrence of sulfide minerals observed in the Cenozoic sediments in the upstream area of the HR (Sherlock et al., 1996; Theodore et al., 2003; Earman and Hershey, 2004) and close agreement between model results and measured concentrations suggests that sulfide mineral oxidation is a likely source for As and SO_4 in pathway-1 near the confluence of Mary's River and Humboldt River (Figure 6.5).

Modeled pH values (8.65) match observed pH (8.77) closely. While sulfide oxidation is the likely source of As and SO_4 in the UHR, the acidity produced by this reaction is buffered by carbonate equilibria in the HRB. Evidence that carbonate equilibria buffers the system can be found in the carbonate minerals that are present in the rocks (Sherlock et al., 1996; Theodore et al., 2003) and sediments (Earman and Hershey, 2004; Mohammad and Tempel, 2013, in prep.) and HCO_3^- concentrations are representative of carbonate terrains (Appelo and Postma, 1996; Drever, 1997; Hershey et al., 2007). Therefore, the initial pH of the modeled rainwater (6.0) is buffered by water-rock interactions to an alkaline pH of approximately 8.7.

Major differences between the modeled and measured concentrations are found in the values of dissolved Na and Cl. Concentrations of Na are 164 mg/L modeled and 252 mg/L measured, and concentrations for Cl are 0.12 mg/L modeled and 61.5 mg/L measured. The unusual low concentration of dissolved Cl in the modeled water is unrealistic for natural waters, and hence evaporation and groundwater inflows have been invoked in the simulation (simulation steps 2 and 3, Table 6.12) for pathway-1. The difference in Na concentrations may be explained by differences in feldspar dissolution kinetic rates and amounts of Na-feldspar between model and natural conditions. While laboratory rate laws derived at 25°C and representative proportions of Na-feldspars were used in model calculations, dissolution rates in the subsurface for groundwater may be higher due to higher temperature gradients in the region. Further, Na-feldspar contents may be locally higher in Pathway-1 which might further yield a higher amount of Na. Additional source of Na could be contributed from evaporative concentration of shallow groundwater discharging to the river during the sampling period. The base flow analysis

results (Table 6.2) indicates that about 92% of the total flow corresponds to shallow groundwater inflow at this sample location of HR 001 near Mary's River and Humboldt River. However, the vast majority of Cl in groundwater in most places with some recharge is simple concentration of rainwater. The plants take up 90-95% of the water in most semi-arid regions, leaving the water that recharges through the soil zone enriched in Cl by a factor of 10 to 20 (Tyler and Walker, 1994), and thus enrich groundwater with 10 to 12 mg/l of Cl from 0.10 mg/L of Cl in rainwater. Therefore, it is not solely evaporation, but an uptake by plants (transpiration) enrichment of the water left behind.

Because simple mixing with un-mineralized alluvium groundwater alone cannot substantiate high TDS with high Na and Cl as evidenced from the groundwater quality data (Table 6.3), where, mean concentrations of Na and Cl are 32 and 18.4 mg/L, respectively; therefore, evapo-concentration followed by groundwater inflow have been invoked in the simulation (simulation steps 2 and 3, Table 6.12) in pathway-1. The results from successive simulation steps of water-rock reactions followed by groundwater inflow at the rate of 92%, evaporation of mixed water at the rate of 10% correspond to the closest match with observed water (Table 6.12).

Therefore, accumulative evapo-concentration of Cl as a result of continuous evaporation of shallow groundwater inflow along with transpiration in the root zones is likely the mechanism for relatively higher concentrations of Cl in sample HR 001 near the confluence of Humboldt River and Mary's River (Figure 6.5). After each evaporation cycle, salts accumulate in the root-zones and on the surface of the lands and successive flushing of salts from the roots and the land-surface during each cycle of irrigation cause high concentrations of Cl. Potential evaporation in this area exceeds ten times higher than

the precipitation during the period from April to October (potential evaporation is 1.65 cm and precipitation is 1.93 cm in September; Shevenell, 1996). This is also supported by previous study by Prudic et al. (2006), that reported an average of 8% of the total mean annual precipitation from 1950-99 was runoff at the gages on the Humboldt River at Elko, Carlin, and Palisade, and the rest of precipitation was lost to evapotranspiration assuming no long term change in groundwater storage.

In summarizing the processes in Pathway 1, carbonate equilibria control pH and HCO_3 concentrations. Specifically, calcite and dolomite dissolution control Ca and Mg concentrations. Concentrations of Si and K are controlled by feldspar dissolution and constrained by clay mineral precipitation. Dissolved As and SO_4 concentrations are controlled by oxidation dissolution of pyrite and As-bearing sulfides. Dissolved As concentrations, and Na and Cl concentrations are further controlled by shallow groundwater inflow that discharges to the river as base flow (Table 6.2) followed by evaporation.

6.5.2. Pathway 2

Dilution between samples 003 and 004 in Pathway-2 is illustrated by simulating two mixing simulations: first between the HR water 003 and groundwater inflow at South Fork-Humboldt River (SFHR) followed by further mixing between groundwater inflows at Palisade based on the base flow analysis (Table 6.2). The results indicate that mixing at the rate of 62% of groundwater inflow at SFHR followed by mixing at the rate of 64% groundwater inflow at Palisade provides the best match for the observed water sample at sample location 004 (Table 6.12). The concentrations of As in modeled water (0.013

mg/L) matches with the observed As concentrations in sample 004 (0.013 mg/L). The concentration of Cl for modeled water (26.6 mg/L) matches fairly to the observed water (24.3 mg/L). The concentrations of other elements such as Ca, Mg, K, C (as in HCO_3), SO_4 and Si (as in SiO_2) consistently match closely with observed water.

The major discrepancy between modeled water and measured water is observed in dissolved Na concentration. The model over-predicted Na concentrations. The excess Na in the modeled water can be explained by the higher amount of Na (301 mg/L) in input water Table 6.12). Similarly, the model slightly over predicted Cl and SO_4 concentrations because of the higher concentrations of dissolved Cl and SO_4 (151 mg/L and 566 mg/L, respectively) in input water. Dissolved SO_4 concentration is reduced (59.3 mg/L) in the measured water at sample location 004 due to localized SO_4 -reduction as evidenced from sharp change in oxidation-reduction potential (ORP) from 134 mV to 10 mV in sample 003 to 004. The latter is also evidenced by increase in Fe and Mn concentrations from sample location 003 to 004 indicating change of redox condition from oxidizing to post-oxic conditions (Appelo and Postma, 1996).

The base flow analysis (Table 6.2) indicates that about 62 % and 64% of the flows are shallow groundwater inflows at the SFHR and Palisades, respectively near sample 004. Mixing with post-oxic ground water is also evidenced from the change in ORP values from oxic to post-oxic, and an increase in dissolved Mn and Fe in sample 004 from upstream samples (Table 6.1).

6.5.3. Pathway 3

Pathway-3 illustrates the effects of groundwater inflows, mixing with geothermal water, and evaporation. Because, localized deep geothermal groundwater has been reported by Lamke and Eakin, (1966), because of the location of Golconda Hot Spring geothermal system near sample 008, mixing with geothermal water was evaluated. The results of mixing simulation between geothermal (GEO) water and the HR water 007 reveals that mixing of geothermal water to HR water at the rate of 45% is required to best match with the measured water sample at 008 near Golconda (simulation step-3, Pathway 3, Table 6.12). The concentrations of Cl for both modeled and measured waters are 75.3 and 75.1 mg/L, and concentrations for dissolved SO₄, Na, K, Mg, SiO₂ match to some extent, between modeled and observed waters.

However, the major discrepancy is noted in dissolved As concentration in the modeled water (0.016 mg/L) and observed water (0.037 mg/L), which is more than 50%. Another discrepancy is noted in HCO₃ concentration, where the model over-predicted HCO₃ (387 mg/L) compared to measured water (348 mg/L). Therefore, mixing with deep geothermal groundwater containing dissolved As, Li, and B may play some roles in enriching As, and other constituents, but falls far short because of the requirement of exceptionally high percentage of geothermal water (about 45%) for the model (Simulation step-3, Pathway-3, Table 6.12), which is unrealistic.

On the other hand, stream flow data and base flow analysis (Table 6.2), and previous studies by Cohen (1963) and Lamke and Eakin (1966) indicate that groundwater in this part of the HR discharges to the river during the low-flow season. However, shallow groundwater from the alluvium, which is naturally un-mineralized, are not likely

to contribute As, Li, and B (Table 6.1) to the river water alone, and hence, inflow of groundwater followed by evapo-concentration has been invoked. Although, mixing with a lower percentage of geothermal water (Simulation step-2, pathway, 3, Table 6.12) provides somewhat close match to the measured water at 008, the lack of reported flow from deep geothermal groundwater to shallow groundwater in this pathway cancel out geothermal mixing. Alternatively, the results from groundwater inflow at the rate of 64% followed by evaporation at the rate of 5% (Simulation steps 1 and 4, pathway-3, Table 6.12) seems more realistic and are in agreement with the base flow analysis, evaporation data (Tables 4.2 and 4.4), and previous studies. The results of 64% inflow groundwater followed by 5% evaporation provides the best match between model results and observed water with respect to dissolved As, Cl, Na, Ca, Mg, SO₄, HCO₃, and other constituents.

6.5.4. Pathway 4

Because of the higher rate of evaporation around Imlay and Rye Patch Reservoir, effect of evaporation was evaluated in Pathway-4 between sample 012 and 013 (Figure 6.7). The groundwater inflow at Imlay is about 60% (Table 6.2) based on the base flow analysis. Therefore, simulations of groundwater inflow at the rate of 60% followed by evaporation at the rate of 5% were evaluated (Simulations steps 1 and 3, Pathway-4, Table 6.12), and compared with evaporation simulation only without invoking groundwater inflow (Simulation step-2). The results indicate that it requires evaporation at the rate of 10% from sample 012 to provide somewhat match among dissolved As and Cl concentrations in the measured water sample at 013, but results in discrepancy in HCO₃ and other constituents. On the other hand, evaporation without invoking groundwater inflow is unrealistic as evidenced from the base flow analysis (Table 6.2).

The results groundwater inflow at rate of 60% followed by evaporation at the rate of 5% provides the best match between modeled water and observed water (Table 6.12). The concentrations of As in the modeled water (0.021 mg/L) match closely with the measured As concentration (0.022 mg/L) at sample 013. Concentration of Cl in the modeled water (124 mg/L) also matches closely with measured Cl concentration (123 mg/L) in sample 013.

The discrepancy in HCO_3 concentrations between the modeled (277 mg/L) and measured waters (235 mg/L) at sample location 013 (Table 6.12). The relatively higher concentration in the modeled water compared to the measured HCO_3 could be due to high HCO_3 in the initial composition at sample 012. Measured HCO_3 at sample 012 may also be higher due to local mineralogical differences (i.e., carbonate content).

6.5.5. Pathway 5

To explain the increased As concentrations in the LHR waters, desorption was simulated using computer code PHREEQC (Parkhurst and Appelo, 1999), which is justified by the prevailing alkaline pH of the water ranging from 8.98 to 9.13 in the LHR waters (Table 6.1). The sediment data that have been used in desorption simulation are provided in Table 3.4 in Chapter 3. Pathway-5 between sample 013 and 015 at Rye Patch Reservoir (Figure 6.7) illustrates the effects of desorption and evaporation because of the alkaline pH that favors desorption and because of higher rate of evaporation at Rye Patch Reservoir (Table 6.4). Results from desorption simulation (Simulation step-1, Pathway-5, Table 6.12) indicates that concentrations of As in the modeled water (0.041 mg/L) of sample HR013 were slightly under-predicted to measured water at sample HR 015 (0.048 mg/L).

The results of desorption simulation indicate that an additional amount of 0.019 mg/L of As (Table 6.12) might have been released from sediment sample located near sample 013, which corresponds to total As concentration of 0.041 mg/L. While desorption only provides a good match for dissolved As between modeled water and observed water at sample 015 (Table 6.12), discrepancies remain for other solutes and elements including dissolved Cl and SO₄. Therefore, evaporation was simulated at the rate of 10% based on the higher rates of evaporation around Rye Patch reservoir (Table 6.4). The results indicate a good match in dissolved Cl and As concentrations between the modeled water and measured water at 015 (Table 6.12) with some exception, and therefore, both evaporation and desorption are important especially in high alkaline pH conditions for enriched As concentrations. The Cl concentration for both modeled water and measured water was exact 134 mg/L, whereas dissolved As concentrations for modeled water (0.045 mg/L) and measured water in sample 013 (0.048 mg/L) indicate a fair match.

The highest discrepancy is measured in concentrations of Na, SO₄, and HCO₃ concentrations (Table 6.12). The modeled water under-predicted HCO₃ which is constrained by calcite precipitation. The increase in SO₄ in the modeled water is due to higher content of SO₄ in the input of the model. The concentration of Na is under-predicted in the modeled water (146 mg/L), and is also constrained by mineral precipitation such as Na-nontronite in the model.

Sensitivity analysis with respect to As content in the sediment indicates that (Figure 6.8), As with 19 mg/Kg in the sediment provides the best match with corresponding pH of 9.13 to reach the target concentration of 0.019 mg/L, which is a

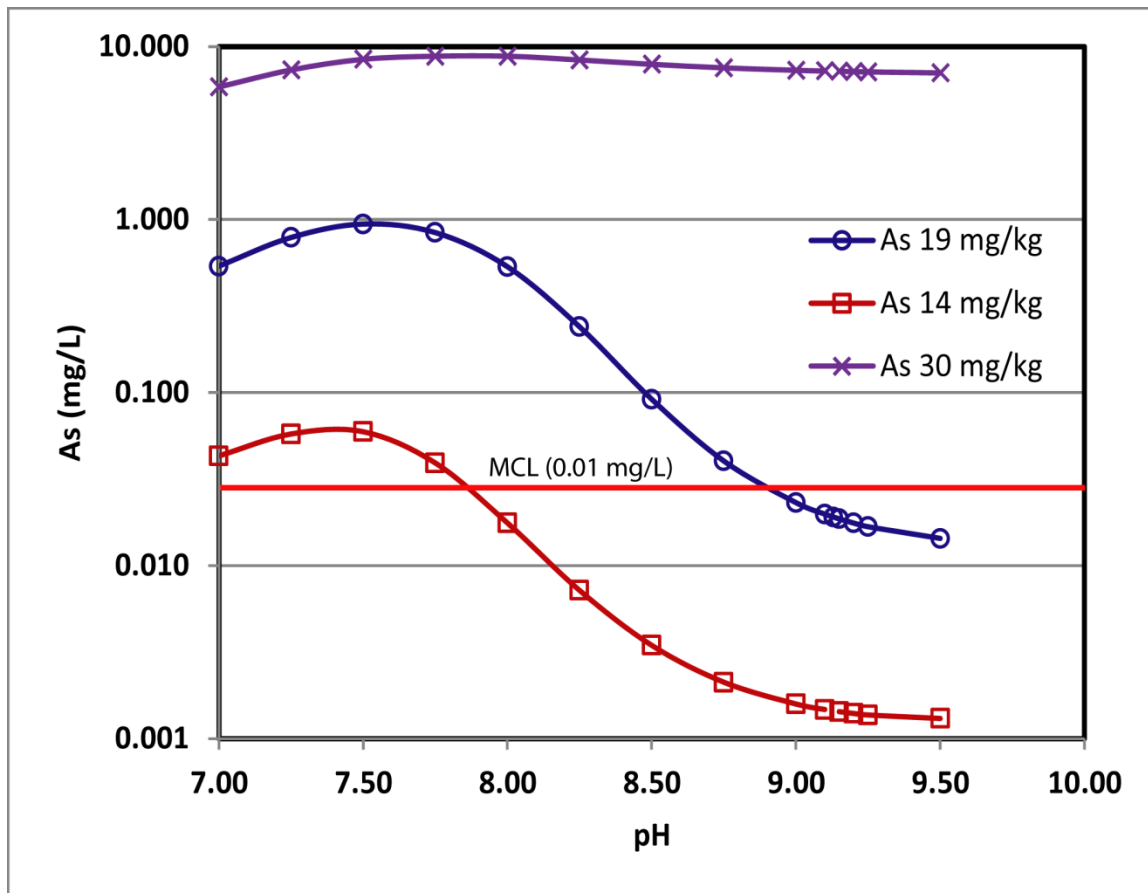


Figure 6.8: Concentrations of dissolved As released as a result of desorption simulations for different concentrations of As in the sediments.

close approximation of average As concentration in sediment samples (Mohammad and Tempel, 2013B, in prep.). Therefore, desorption may explain an additional increase in As in the downstream river water along with evaporation.

6.5.6. Pathway 6

Pathway-6 (Figure 6.7) illustrates the effects of groundwater inflows followed by evaporation because of the increased rates of evaporation around Lovelock (Table 6.4). Evaporation is also evidenced by the progressive deuterium enrichment (Table 6.1) in the LHR samples. Rate of groundwater inflow is based on the average base flow analysis, which indicates average base flow of 62% (Table 6.2) for the LHR.

Although the Cl concentration in the modeled water (472 mg/L) does not match with the measured water (482 mg/L), the As concentrations for modeled water (0.050 mg/L) matches well with the measured water (0.052 mg/L) in sample 019 (Table 6.12).

Evaporation is also supported by the continually increasing concentrations of Na, Cl, HCO₃, SO₄, and As in the Lovelock Valley near the Humboldt Sink, where a previous study by Seiler et al. (1993) reported high concentrations of As (0.057 mg/L near Lovelock and 0.078 mg/L in the Humboldt Lake. Additionally, inflow shallow groundwater at about 60% with relatively high concentrations of dissolved As, Cl, and SO₄ as evidenced from the base flow analysis (Table 6.2) suggest that inflow of shallow groundwater plays an equally important role in enriching As and other trace elements.

6.6. Conclusions

The evolving water chemistry of the HR from its upstream to downstream regions is controlled by hydrological and geochemical processes such as oxidation of sulfide minerals, dissolution of carbonate rocks, mixing with shallow groundwater discharging to the river, and evaporation. These various processes have been evaluated with geochemical reaction path modeling using computer codes EQ3/6 and PHREEQC. The major highlights of this study are:

- 1) High concentrations of dissolved As and SO_4 in the upstream waters of the HR are controlled by oxidation of sulfides and As-bearing sulfide minerals in the Cenozoic volcanic rocks and sediments in the UHR.
- 2) The primary source of As from oxidative dissolution of sulfide minerals is less significant in the MHR and LHR regions, where mixing with groundwater and evaporation become more significant for As and other dissolved ions.
- 3) Groundwater-surface water interaction plays a critical role in water chemistry of the river water, where shallow groundwater discharges to the river as base flow.
- 4) Evaporation plays the most important role in As concentrations and other dissolved ions in the LHR waters because of higher rate of evaporation because of increased surface area and water content.
- 5) Desorption of As from river-bed sediments plays a secondary role in overall water-chemistry compared to the effects of evaporative concentrations of dissolved ions in the LHR regions.

The findings of this study suggest that the HR waters with very high concentrations of dissolved Na, Cl, SO₄, and As from the upstream to downstream regions should be evaluated for potential groundwater and wetland contamination. Future studies should therefore be directed with detailed assessment of shallow groundwater with respect to As concentrations because of their use for irrigation in the HRB area. Risk assessment should be evaluated with respect to public health of the region with a potential risk of As exposure via food-chain from croplands to cattle and/or dairy products. Additionally, effects of mining discharge and linking of geothermal springs to the contamination of HR and shallow groundwater should be evaluated separately.

The results presented in this study is subject to the samples that were collected during dry and low-flow season, and therefore do not represent the year-round processes. The seasonal variations in As concentrations and other dissolved elements because of changes in river flow are likely to affect the overall water chemistry. Therefore, data of river flow (discharge) measurement in conjunction with sampling are essential, and more importantly, sampling of all tributaries at point of confluences are critical. Future studies are required with respect to temporal variations of As in river waters and evaluation of groundwater-surface water interactions to determine the uncertainties associated with seasonal variations, and for changing the water chemistry in the river water respectively.

CHAPTER 7

7. Conclusions and recommendations

7.1. Summary of results

The distribution of As in the shallow alluvial aquifers are spatially related to metallic mineralized zones in the Boulder Valley, and the Quaternary playa deposits of the Lovelock Valley and the Humboldt Sink area. The concentrations of dissolved As in the Humboldt River waters from its upstream to downstream regions is controlled by various hydrological and geochemical processes such as oxidation of sulfide minerals, dissolution of carbonate rocks, mixing with shallow ground water and geothermal water.

Oxidative dissolution of As-bearing sulfide mineral is likely the source for dissolved SO_4 and As in the ground waters that are in contact with sulfide horizons in the mineralized area in the vicinity of Boulder Valley and its surroundings. Dissolution of As-bearing ferromagnesian minerals such as, biotite play additional roles in releasing dissolved As into the regional shallow alluvial ground water. Deep geothermal water has been inferred for localized high enrichment of dissolved As within the known area of geothermal hot springs in the vicinity of Golconda.

Mineralogic and chemical analyses of river-bed sediments obtained from XRD, SEM and sequential extraction analyses of sediments, and factor analyses of data from both water and river-bed sediments indicate that concentrations of As in the Humboldt river waters and sediments are controlled by several geochemical and hydrological processes. Oxidation of As-bearing sulfide minerals contributes to As concentrations in

the waters of the upper Humboldt River. Concentration of dissolved As in the Humboldt River waters is affected as a result of mixing with ground water inflows (i.e., as base flows). Localized effect of geothermal mixing has been inferred in the waters of the northern part of the lower Humboldt River near Golconda from statistical factor analyses. Subsequent enrichment of As concentrations occurs from evapo-transpirative enrichment of the solutes because of the favorable arid and temperate climate and terminal sink in the lower Humboldt River. Sorption of As onto silicate and clay minerals, and iron oxyhydroxide mineral surfaces affects the mobilization of As into river waters and controls the distribution of As in river sediments.

The results of geochemical speciation and reaction path modeling confirm that the high concentrations of dissolved As and SO_4 in the upstream waters of the HR are controlled by oxidation of sulfides and As-bearing sulfide minerals in the Cenozoic volcanic rocks and sediments. The primary source of As from oxidative dissolution of sulfide minerals is less significant in the Middle Humboldt and Lower Humboldt regions, where mixing with shallow groundwater (as inflows to the river) and evapo-transpiration becomes more significant for As and other dissolved ions.

The results of this study suggest that groundwater-surface water interaction plays a major role in water chemistry of the river water where shallow groundwater discharges to the river as base flows, and hence should be addressed in future studies.

7.2. Recommendations for future studies

The findings of this project suggest that the ground waters in the shallow alluvial aquifers, the surface waters and the flood-plain sediments of the Humboldt River Basin

area may possess the risk of contamination with dissolved As concentrations exceeding the US Environmental Protection Agency's Maximum Contaminant Level. The Humboldt River waters with very high concentrations of dissolved Na, Cl, SO₄, and As at various sections from upstream to downstream regions may not be suitable for some of its designated beneficial uses, and land use such as irrigation, ranching and farming near the terminus of the Humboldt Sink should be re-evaluated for possible wetland contamination along the flow-path and in the Humboldt Sink and Humboldt Wildlife Management Area.

Biogeochemical (i.e., transpiration) and seasonal variations in dissolved As, and other trace elemental concentrations in the river waters and other surface waters should be considered to determine their respective roles (i.e., precipitation, snow falls, and evaporation) in distribution of dissolved As between different phases. For a more comprehensive study, well-logging, sampling depth-intervals, and aquifer mineralogy should be considered. These will help to determine the spatial and temporal distribution of As in the ground water and will shed significant insights about any potential roles of local geology, geomorphology, hydrology, sediments (e.g., aquifer materials, hydraulic conductivity, permeability, etc.), geothermal activities, evaporation, or mining activities on As distribution in the area. Further, vigorous geochemical reaction path modeling of the hydro-geochemical reactions which occur at stream bed and at various depths of aquifer under different redox conditions in Humboldt River Basin site should be undertaken. Simulations of this kind will provide significant insights for interpreting the spatial sequence of geochemical reactions in the context of the dynamic evolution of As

and other trace metals in the global cycles. This in turn will help in developing a robust conceptualized model of As-cycling in this type of semi-arid environment.

7.3. Global significance

With the increasing risks of human health hazards with cancer, diabetes, and heart diseases linking to elevated level of dissolved As in drinking water, and being one of the prominent causes of skin-cancer mortality in the world, contamination of ground water and surface waters by naturally occurring As should be considered with extreme importance. Tens to hundreds of million people are exposed to As-contaminated ground water in many parts of the world including Nepal, Vietnam, West Bengal, India and Bangladesh. Contamination of ground waters with high levels As exceeding the EPA-MCL level of 0.01 mg/L have been identified worldwide including western USA, Texas, Alabama, Mexico, Chile, Vietnam, Hungary, Mongolia, China, Taiwan and many more.

This study is an example of how a systematic approach that includes aspects of hydrology, geochemistry, mineralogy, statistics, and geochemical modeling can significantly contribute towards understanding the complex mechanistic processes that are responsible for widespread arsenic release into nature, and will help in predicting arsenic poisoning elsewhere. This study represents examples of various processes operating for As mobilization in both flood-plain sediments and river waters, and shallow alluvial ground waters within a semi-arid environmental conditions. The findings from this research not only would help delineate such potential contamination of waters in northern Nevada, but also globally with similar hydrogeologic and geochemical settings.

8. REFERENCES

- Ahmed, K.M., Bhattacharya, P., Hasan, M.A., Akhter, S.H., Alam, S.M.M., Bhuyian, M.A.H., Imam, M.B., Khan, A.A., and Sracek, O., 2004. Arsenic enrichment in ground water of the alluvial aquifers in Bangladesh: an overview: *Applied Geochemistry: Arsenic in Ground water of Sedimentary Aquifers*, v. 19, p. 181-200.
- Appelo, C.A.J., and Postma, D., 1996. *Geochemistry, ground water and pollution*: Rotterdam, Netherlands, A.A. Balkema, 536 p.
- Arehart, G.B., Chryssoulis S.L., Kesler S.E., 1993. Gold and arsenic in iron sulfides from sediment-hosted disseminated gold deposits-implications for depositional processes. *Economic Geology* (1):171-185.
- Balistrieri, L.S., Tempel, R.N., Stillings, L.L., and Shevenell, L.A., 2006. Modeling spatial and temporal variations in temperature and salinity during stratification and overturn in Dexter Pit Lake, Tuscarora, Nevada, USA: *Applied Geochemistry*, v. 21, p. 1184-1203.
- Ballantyne, J.M., and Moore, J.N., 1988. Arsenic geochemistry in geothermal systems: *Geochimica et Cosmochimica Acta*, v. 52, p. 475-483.
- Benson, L.V., May, H.M., Antweiler, R.C., Brinton, T.I., Kashgarian, M., Smoot, J.P., Lund, S.P., 1998. Continuous Lake-Sediment Records of Glaciation in the Sierra Nevada between 52,600 and 12,500 14C yr B.P. *Quaternary Research*. 50 (2):113-127.
- Berg, M., Tran, H.C., Nguyen, T.C., Pham, H.V., Schertenleib, R., and Giger, W. 2001, Arsenic Contamination of Ground and Drinking Water in Vietnam: A Human Health Threat: *Environmental Science & Technology [ENVIRON. SCI. TECHNOL.]*. v. 35, p. 2621-2626.
- Bhumbla, D.K., and Keefer, R.F., 1994. Arsenic mobilization and bioavailability in soils, *in* Nriagu, J.O., ed., *Arsenic in the Environment, Part I: Cycling and Characterization*, Volume 26: New York, John Wiley & Sons, Inc., p. 51-82.
- Breit, G.N., Foster, A.L., Sanzalone, R.F., Yount, J.C., Whitney, J.W., Welch, A.H., and Islam, M.N., 2001. Arsenic cycling in eastern Bangladesh: the role of phyllosilicates, *Geol. Soc. Am. Abstract Program*. 32, p. A192.
- Brookins, D.G., 1988. *Eh-pH Diagrams for Geochemistry*: Berlin, Springer-Verlag: 176 p.

- Carmody, R.W., Plummer, L.N., Busenberg, E., and Coplen, T.B., 1998. Methods for collection of dissolved sulfate and sulfide and analysis of their sulfur isotopic composition., U.S.Geological Survey Open-file Report 97-234, p. 91.
- Chakraborty, S., Wolthers, M., Chatterjee, D., and Charlet, L., 2007. Adsorption of arsenite and arsenate onto muscovite and biotite mica: *Journal of Colloid and Interface Science*:Elkin 06, International Electrokinetics Conference, June 25-29, Nancy, France, v. 309, p. 392-401.
- Child, D., 2006, *The essentials of Factor Analysis*: London, Continuum International Publishing Group, 180 p.
- Clark, I., and Fritz, P., 1997. *Environmental Isotopes in Hydrogeology*: Boca Raton, Lewis Publishers, 328 p.
- Cline, J.S., 2001. Timing of Gold and Arsenic Sulfide Mineral Deposition at the Getchell Carlin-Type Gold Deposit, North-Central Nevada. *Economic Geology*. 96 (1):75- 89.
- Cohen, P., 1963, An evaluation of the water resources of the Humboldt River Valley near Winnemucca, Nevada, *Water Resources Bulletin N. 24*: Carson City, Nevada, U.S. Geological Survey, p. 104.
- Coolbaugh, M., Lechler, P., Sladek, C., and Kratt, C., 2010. Lithium in Tufas of the Great Basin: Exploration Implications for Geothermal Energy and Lithium Resources: *Geothermal Resources Council Transactions*, v. 34, p. 521-526.
- Crompton, E.J., 1995. Potential hydrologic effects of mining in the Humboldt River Basin, northern Nevada:, U.S. Geological Survey Water-Resources Investigations Report 94-4233, 2 sheets.: Carson City.
- Davis, O.K, Moutoux, T.E., 1998. Tertiary and Quaternary vegetation history of the Great Salt Lake, Utah. *Journal of Paleolimnology*. 19:417-427, doi:10.1023/A:1007959203433.
- Davis, J.C., 2002. *Statistics and Data Analysis in Geology*, John Wiley & Sons. ISBN 978-0-471-17275-8, p. 678.
- Desert Research Institute (DRI), 1994. Evaluation of surface runoff to perennial and ephemeral drainages from mine sites in northern Nevada, 319 (H) Nonpoint Source Workplan: Reno, NV, Water Resources Center, Desert Research Institute.
- Dongarrà, G., Manno, E., Sabatino, G., and Varrica, D., 2009. Geochemical characteristics of waters in mineralised area of Peloritani Mountains (Sicily, Italy): *Applied Geochemistry*, v. 24, p. 900-914.

- Drever, J.I., 1997. The geochemistry of natural water: surface and groundwater environments: Upper Saddle River, New Jersey, Prentice Hall Inc., 436 p.
- Duffield, W., A., and Sass, J.H., 2003. Geothermal energy-Clean power from the Earth's heat: Reston, Virginia, US Geological Survey, p. 1-36.
- Dzombak, D.A., and Morel, F.M.M., 1990. Surface complexation modeling: hydrous ferric oxide: New York, John Wiley & Sons, 365 p.
- Eakin, T.E., and Lamke, R.D., 1966, Hydrologic reconnaissance of the Humboldt River Basin, Nevada: Carson City, Nevada, U.S. Geological Survey, p. 106.
- Earman, S., and Hershey, R.L., 2004. Water quality impacts from waste rock at a Carlin-type gold mine, Elko County, Nevada: Environmental Geochemistry, v. 45, p. 1043-1053.
- Eckhardt, K., 2005. How to Construct Recursive Digital Filters for Baseflow Separation: Hydrological Processes, v. 19 (2), p. 507-515.
- EPA, 2009. List of Drinking Water Contaminants & MCLs. Environmental Protection Agency, USA. URL: <http://water.epa.gov/drink/contaminants/index.cfm>.
- Faulds, J.E., Schreiber, B.C., Reynolds, S.J., Gonzalez, L., and Okaya, D., 1997. Origin and paleogeography of an immense, nonmarine Miocene salt deposit in the Basin and Range (western USA): Journal of Geology, v. 105, p. 19-36.
- Fisher, R.S., and Mullican, I., William F., 1997. Hydrochemical evolution of sodium-sulfate and sodium-chloride groundwater beneath the Northern Chihuahuan Desert, Trans-Pecos, Texas, USA: Hydrogeology Journal, v. 5, p. 4-16.
- Folger, H. W., 2000. Analytical results and sample locations of reanalyzed NURE stream-sediment and soil samples for the Humboldt River Basin mineral-environmental resource assessment, northern Nevada. USGS Open File Report 00-421. US Geological Survey, Reston, Virginia, pp 516.
- Foster, A.L., Breit, G.N., Welch, A.H., Whitney, J.W., Yount, J.C., Islam, M.S., Alam, M.M., Islam, M.K., and Islam, M.N., 2000. In-situ identification of arsenic species in soil and aquifer sediments from Ramrail, Brahmnabaria, Bangladesh: Eos. Trans. Am. Geophys. Union, v. 81, p. F523.
- Fuller, C.C., and Davis, J.A., 1989. Influence of coupling of sorption and photosynthetic processes on trace element cycles in natural waters: Nature, v. 340, p. 52-54, doi:10.1038/340052a0.

- Gieseemann A., Jager H.J., Norman A.L., Krouse H.P. and Brand W.A., 1994. On-line sulfur- isotope determination using an elemental analyzer coupled to a mass spectrometer. *Analytical Chemistry*, 66: 2816-2819.
- Grassineau N.V., Matthey D.P. and Lowry D., 2001. Sulfur Isotope Analysis of Sulfide and Sulfate minerals by Continuous Flow-Isotope Ratio Mass Spectrometry. *Analytical Chemistry*, 73: 220-225.
- Guler, C., Thyne, G.D., McCray, J.E., Turner, A.K., 2002. Evaluation of graphical and multivariate statistical method for classification of water chemistry data: *Hydrogeology Journal*, v. 10 (4), p. 455-474.
- Hem, J.D., 1985. Study and interpretation of the chemical characteristics of natural water. Third Edition: U.S. Geological Survey Water-Supply paper, v. 2254, p. 264.
- Henke, K.R., 2009. Arsenic in natural Environments, *in* Henke, K.R., ed., *Arsenic: Environmental Chemistry, Health Threats and Waste Treatment: West Sussex, U.K., John Wiley & Sons Ltd.*, p. 569.
- Henry, C.D., 2008. Ash-flow tuffs and paleovalleys in northeastern Nevada: Implications for Eocene paleogeography and extension in the Sevier hinterland, northern Great Basin. *Geosphere* 4 (1): 1-35.
- Hershey, R.L., Heilweil, V.M., Gardner, P., Lyles, B.F., Earman, S., Thomas, J.M., and Lundmark, K.W., 2007. Ground-water chemistry interpretations supporting the Basin and Range regional carbonate-rock aquifer system (BARCAS) study, eastern Nevada and western Utah, DHS Publication No. 41230, Desert Research Institute, Nevada System of Higher Education and U.S. Geological Survey, p. 86.
- Hounslow, A.W., 1995. *Water Quality Data: Analysis and Interpretation*: Boca Raton, CRC Press, Inc., 397 p.
- Huerta-Diaz, M.A., and Morse, J.W., 1992. Pyritization of trace metals in anoxic marine sediments: *Geochimica et Cosmochimica Acta*, v. 56, p. 2681-2702.
- Jang, C.-S., 2010. Applying scores of multivariate statistical analyses to characterize relationships between hydrochemical properties and geological origins of springs in Taiwan: *Journal of Geochemical Exploration*, v. 105, p. 11-18.
- Johannesson, K.H., Lyons, W.B., Huey, S., Doyle, G.A., Swanson, E.E., and Hackett, E., 1997. Oxyanion Concentrations in Eastern Sierra Nevada Rivers-2. Arsenic and Phosphate: *Aquatic Geochemistry*, v. V3, p. 61-97.

- Jones, C.A., Inskeep, W.P., Bauder, J.W., and Keith, K.E., 1999. Arsenic solubility and attenuation in soils of the Madison River basin, Montana; impacts of long-term irrigation: *Journal of Environmental Quality*, v. 28, p. 1314-1320.
- Kelly, W.R., Holm, T.R., D.Wilson, S., and Roadcap, G.S., 2005. Arsenic in Glacial Aquifers: Sources and Geochemical Controls: *Ground Water*, v. 43, p. 500–510.
- Kyoung J. Lim, Bernard A. Engel, Zhenxu Tang, Joongdae Choi, Ki-Sung Kim, Suresh Muthukrishnan, Dibyajyoti Tripathy, 2005. AUTOMATED WEB GIS BASED HYDROGRAPH ANALYSIS TOOL, WHAT1: *JAWRA Journal of the American Water Resources Association*, Vol. 41, No. 6. (2005), p. 1407-1416, [doi:10.1111/j.1752-1688.2005.tb03808.x](https://doi.org/10.1111/j.1752-1688.2005.tb03808.x)
- Lee, M.-K., Saunders, J.A., Wilkin, R.T., and Mohammad, S., 2005. Geochemical modeling of arsenic speciation and mobilization: Implications for bioremediation, 2005. O'Day, P.A., Vlassopoulos, D., Meng, X., and Benning, L.G., eds., In *Advances in Arsenic Research: Integration of Experimental and Observational Studies and Implications for Mitigation*, Volume 915: ACS Symposium Series: Washington, D.C., American Chemical Society.
- Le Guern, C., Baranger, P., Crouzet, C., Bodenan, F., and Conil, P., 2003. Arsenic trapping by iron oxyhydroxides and carbonates at hydrothermal spring outlets: *Applied Geochemistry*, v. 18, p. 1313-1323.
- Lengke, M.F., and Tempel, R.N., 2005. Geochemical modeling of arsenic sulfide oxidation kinetics in a mining environment: *Geochimica et Cosmochimica Acta*, v. 69, p. 341-356.
- Li, X., Coles, B.J., Ramsey, M.H., and Thornton, I., 1995. Sequential extraction of soils for multielement analysis by ICP-AES: *Chemical Geology (Analytical Spectroscopy in the Earth Sciences)*, v. 124, p. 109-123.
- Maurer, D.K., Plume, R.W., Thomas, J.M., Johnson, A.K., 1996. Water resources and effects of changes in ground-water use along the Carlin Trend, North-Central Nevada. *Water Resources Investigation Report 96-4134*. Carson City, NV. US Geological Survey, US Department of Interior, p. 146.
- Mohammad, S., and Tempel, R.N., 2007. Occurrence and Distribution of Naturally Occurring Arsenic in the Humboldt River Basin, Northern Nevada, *in* Starrett, S.K., Hong, J., Wilcock, R.J., Li, Q., Carson, J.H., and Arnold, S., eds., *Third International Conference on Environmental Science and Technology*, Volume 2: Houston, Texas, USA, American Science Press, Houston, USA, p. 262-267.

- Morrison J., Brockwell T., Merren T., Fourel F., and A. M. Phillips, 2001. On-line high-precision stable hydrogen isotopic analyses on nanoliter water samples. *Analytical Chemistry*, 73, 3570-3575.
- National Research Council, 2001. *Arsenic in Drinking Water: 2001 Update*: Washington, D.C., National Academy Press, Division on Earth and Life Studies, National Research Council, p. 244.
- Nevada Bureau of Mines and Geology.
<http://www.unr.edu/Geothermal/GeochemDB.htm>.
- Nevada-Department of Conservation and Natural Resources, Division of Water Resources. <http://water.nv.gov/>.
- Nevada Division of Water Planning, 1995. *Nevada State Water Plan: PART 2 - WATER USE AND FORECASTS*, Section 1: Historic and Current Water Use, Carson City. <http://water.nv.gov/programs/planning/stateplan/>.
- Nimick, D.A., Moore, J.N., Dalby, C.E., and Savka, M.W., 1998. The fate of geothermal arsenic in the Madison and Missouri rivers of Montana and Wyoming: *Water Resources Journal*, v. 199, p. 30-56.
- Onishi, H., 1969. Arsenic, *in* Wedepohl, K.H., ed., *Handbook of Geochemistry*, Volume II-2: New York, Springer-Verlag, p. Chapter 33.
- Östlund, P., Torssander, P., Mörth, C.-M., and Claesson, S., 1995. Lead and sulphur isotope dilution during dispersion from the Falun mining area: *Journal of Geochemical Exploration: Heavy Metal Aspects of Mining Pollution and Its Remediation*, v. 52, p. 91-95.
- Parkhurst, D.L., and Appelo, C.A.J., 1999. *User's Guide to PHREEQC (Version 2)--A Computer Program for Speciation, Batch-Reaction, One-Dimensional Transport, and Inverse Geochemical Calculations*, U.S. Geological Survey Water-Resources Investigations Report 99-4259.
- Paul, A.P., and Thodal, C.E., 2003, *Data on streamflow and quality of water and bottom sediment in and near Humboldt Wildlife Management area, Churchill and Pershing Counties, Nevada, 1988-2000.*, U.S. Geological Survey Open File Report 03-335: Carson City, Nevada, U.S. Geological Survey, p. 94.
- Peters, S.C., and Burkert, L., 2008. The occurrence and geochemistry of arsenic in groundwaters of the Newark basin of Pennsylvania: *Applied Geochemistry*, v. 23, p. 85-98.

- Plume, R.W., 1995. Water resources and potential effects of ground water development in Maggie, Marys, and Susies Creek Basins, Elko and Eureka Counties, Nevada, U.S. Geological Survey Water Resources Investigations Report 94-4222, US Geological Survey, U.S. Department of Interior.
- Plume, R.W., 1996. Hydrogeologic framework of the Great Basin region of Nevada, Utah, and adjacent states. Regional Aquifer-System Analysis-Great Basin, Nevada-Utah. US Geological Survey Professional Paper- 1409-B, USGS, Washington.
- Polizzotto, M.L., Kocar, B.D., Benner, S.G., Sampson, M., and Fendorf, S., 2008. Near-surface wetland sediments as a source of arsenic release to ground water in Asia: *Nature*, v. 454, p. 505-508.
- Postma, D., Larsen, F., Minh Hue, N.T., Duc, M.T., Viet, P.H., Nhan, P.Q., and Jessen, S., 2007. Arsenic in groundwater of the Red River floodplain, Vietnam: Controlling geochemical processes and reactive transport modeling: *Geochimica et Cosmochimica Acta*, v. 71, p. 5054-5071.
- Price, Jonathan G., Hess, Ronald H., Fitch Shane, Faulds, James E., Garside, Larry J., Shevenell, Lisa, and Warren, Sean, 2005. Preliminary Assessment of the Potential for Carbon Dioxide Disposal by Sequestration in Geological Settings in Nevada Nevada Bureau of Mines and Geology report 51, p. 21.
- Prudic, D.E., and Herman, M.E., 1996. Groundwater flow and simulated effects of development in Paradise Valley, a basin tributary to the Humboldt River in Humboldt County, Nevada, Regional Aquifer System Analysis-Great Basin, Nevada-Utah, U.S. Geological Survey Professional Paper 1409-F: Carson City, Nevada, U.S. Geological Survey, p. 92.
- Prudic, D.E., Niswonger, R.G., and Plume, R.W., 2006. Trends in streamflow on the Humboldt River between Elko and Imlay, Nevada, 1950-99: Carson City, Nevada, U.S. Geological Survey, p. 58.
- Reiner, S., R., Laczniak, R., J., DeMeo, G., A., Smith, L., J., Elliot, P., E., Nylund, W.E., and Fridrich, C., J., 2002. Ground-Water Discharge Determined from Measurements of Evapotranspiration, Other Available Hydrologic Components, and Shallow Water-Level Changes, Oasis Valley, Nye County, Nevada, Water-Resources Investigations Report 01-4239: Carson City, Nevada, U.S. Department of the Interior, U.S. Geological Survey, p. 65.
- Retallack, G.J., 2001. Cenozoic expansion of grasslands and climatic cooling. *The Journal of Geology*. 109:407-426, doi:10.1086/320791.

- Reyment, R.A., and Joreskog, K., 1993. *Applied Factor Analysis in the Natural Sciences*: New York, USA., Cambridge University Press.
- Robertson, F.N., 1989. Arsenic in ground-water under oxidizing conditions, southwest United States. *Environmental Geochemistry and Health* 11(3-4):171-185.
- Romero, L., Alonso, H., Campano, P., Fanfani, L., Cidu, R., Dadea, C., Keegan, T., Thornton, I., and Farago, M., 2003, Arsenic enrichment in **waters** and sediments of the Rio Loa (Second Region, Chile): *Applied Geochemistry*, v. 18, p. 1399-1416.
- Ryu, J.H., Gao, S., Dahlgren, R.A., Zierenberg, R.A., 2002. Arsenic distribution, speciation and solubility in shallow ground water of Owens dry lake, California. *Geochimica et Cosmochimica Acta*. 66 (17):2981-2994.
- Saunders, J.A., Pritchett, M.A., Lee, M.-K., and Wolf, L.W., 2000. Weathering of biotite in the southern Appalachians as a source of arsenic in the hydrosphere: Implications for the Himalayas and Bangladesh, *American Geophysical Union, Volume 81, EOS Transactions, AGU*, p. F552.
- Saunders, J., Mohammad, S., Korte, N., Lee, M.-K., Fayek, M., Castle, D., and Barnett, M., 2005A. Groundwater geochemistry, microbiology, and mineralogy in two arsenic-bearing holocene alluvial aquifers from the USA., *in* O'Day, P.A., Vlassopoulos, D., Meng, X., and Benning, L.G., eds., *Advances in Arsenic Research: Integration of Experimental and Observational Studies and Implications for Mitigation*, Volume 915: ACS Symposium Series: Washington, D.C., American Chemical Society.
- Saunders, J. A., Lee, M.-K., Uddin, A., Mohammad, S., Wilkin, Richard T., Fayek, Mostafa, Korte, Nic E., 2005B. Natural arsenic contamination of Holocene alluvial aquifers by linked tectonic, weathering, and microbial processes: *Geochemistry, Geophysics, Geosystems*, v. 6 (4), DOI -10.1029/2004GC000803, <http://dx.doi.org/10.1029/2004GC000803>.
- Savage, K.S., Bird, D.K., and Ashley, R.P., 2000. Legacy of the California gold rush; environmental geochemistry of arsenic in the southern Mother Lode gold district: *International Geology Review*, v. 42, p. 385-415.
- Scanlon, B.R., Nicot, J.P., Reedy, R.C., Kurtzman, D., Mukherjee, A., and Nordstrom, D.K., 2009. Elevated naturally occurring arsenic in a semiarid oxidizing system, Southern High Plains aquifer, Texas, USA: *Applied Geochemistry*, v. 24, p. 2061-2071.

- Schreiber, M.E., Simo, J.A., and Freiberg, P.G., 2000. Stratigraphic and geochemical controls on naturally occurring arsenic in groundwater, eastern Wisconsin, USA: *Hydrogeology Journal*, v. 8, p. 161-176.
- Seddique, A.A., Masuda, H., Mitamura, M., Shinoda, K., Yamanaka, T., Itai, T., Maruoka, T., Uesugi, K., Ahmed, K.M., Biswas, D.K., 2008. Arsenic release from biotite into a Holocene ground water aquifer in Bangladesh. *Applied Geochemistry*. 23 (8):2236-2248.
- Seiler, R.L., Ekechukwu, G.A., and Hallock, R.J., 1993, Reconnaissance investigation of water quality, bottom sediment, and biota associated with irrigation drainage in and near Humboldt Wildlife Management Area, Churchill and Pershing Counties, Nevada, Water Resources Investigation Report 93-4072: Carson City, U.S. Geological Survey.
- Sharif, M.S.U., Davis, R.K., Steele, K.F., Kim, B., Hays, P.D., Kresse, T.M., and Fazio, J.A., 2011. Surface complexation modeling for predicting solid phase arsenic concentrations in the sediments of the Mississippi River Valley alluvial aquifer, Arkansas, USA: *Applied Geochemistry: Arsenic and other toxic elements in global groundwater systems*, v. 26, p. 496-504.
- Shelton, L.R., 1994. Field Guide for Collecting and Processing Stream-Water Samples for the National Water-Quality Assessment Program, U.S. Geological Survey Open-File Report 94-455, p. 50.
- Sherlock, M.G., Cox, D.P., and Huber, D.F., 1996. Known mineral deposits and occurrences in Nevada, *in* Singer, D.A., ed., *An analysis of Nevada's metal-bearing mineral resources*: Reno, Nevada Bureau of Mines and Geology Open File Report 96-2.
- Shevenell, L., 1996. Statewide potential evapotranspiration maps for Nevada, Nevada Bureau of Mines and Geology Report 48: Reno, Mackay School of Mines, p. 1-32.
- Shevenell, L., and Garside, L.J., 2005. Nevada Geothermal Resources, Second Edition, Nevada Bureau of Mines and Geology Map 141: Reno, Nevada, Nevada Bureau of Mines and Geology.
- Shevenell, L., Coolbaugh, M.F., Sladek, C., Zehner, R., Kratt, C., Faulds, J.E., and Penfield, R., 2008. Our Evolving Knowledge of Nevada's Geothermal Resource Potential: *Geothermal Resources Council Transactions*, v. 32, p. 169-173.
- Smedley, P.L., and Kinniburgh, D.G., 2002. A review of the source, behaviour and distribution of arsenic in natural water: *Applied Geochemistry*, v. 17, p. 517-568.

- Smith, A.H., Marshall, G., Yuan, Y., Ferreccio, C., Liaw, J., Ehrenstein, O.v., Steinmaus, C., Bates, M.N., and Selvin, S., 2006. Increased Mortality from Lung Cancer and Bronchiectasis in Young Adults after Exposure to Arsenic in Utero and in Early Childhood: *Environmental Health Perspectives*, v. 114, p. 1293-1296.
- SPSS 16.0, Command Syntax Reference, 2007. SPSS Inc., Chicago Ill.
- Sracek, O., Bhattacharya, P., Jacks, G., Gustafsson, J.-P., and Bromssen, M.v., 2004. Behavior of arsenic and geochemical modeling of arsenic enrichment in aqueous environments: *Applied Geochemistry*, v. 19, p. 169-180.
- Stauffer, R.E., and Thompson, J.M., 1984. Arsenic and antimony in geothermal water of Yellowstone National Park, Wyoming, USA: *Geochimica et Cosmochimica Acta*, v. 48, p. 2547-2561.
- Stollenwerk, K.G., 2003. Geochemical processes controlling transport of arsenic in groundwater: a review of adsorption., *in* Welch, A.H., and Stollenwerk, K.G., eds., *Arsenic in Ground Water: Geochemistry and Occurrence*: Boston, MA, Kluwer Academic Publishers, p. 67–100.
- Stüben, D., Berner, Z., Chandrasekharam, D., and Karmakar, J., 2003. Arsenic enrichment in ground water of West Bengal, India: geochemical evidence for mobilization of As under reducing conditions: *Applied Geochemistry: Arsenic Geochemistry-selected papers from the 10th Water-Rock Interaction Symposium, Villasimius, Italy, 10-15 June 2001*, v. 18, p. 1417-1434.
- Tallaksen, L.M., 1995. A review of baseflow recession analysis, *J. Hydrol.*, v. 165, p. 349-370.
- Tempel, R.N., Shevenell, L.A., Lechler, P., and Price, J., 2000. Geochemical modeling approach to predicting arsenic concentrations in a mine pit lake: *Applied Geochemistry*, v. 15, p. 475-492.
- Tessier, A., Campbell, P.G.C., and Bisson, M., 1979. Sequential extraction procedure for the speciation of particulate trace metals: *Analytical Chemistry*, v. 51, p. 844-851.
- Theodore, T.G., Kotlyar, B.B., Singer, D.A., Berger, V.I., Abbott, E.W., and Foster, A.L., 2003. *Applied Geochemistry, Geology, and Mineralogy of the Northernmost Carlin Trend, Nevada*: *Economic Geology*, v. 98, p. 287-316.
- Tuttle, M.L.W., Wanty, R.B., and Berger, B.R., 2003. Environmental Controls on Water Quality: Case Studies from Battle Mountain Mining District, North-Central Nevada, *in* Stillings, L., ed., *U.S. Geological Survey Bulletin 2210-A*.

- Tyler, S. W., and Walker, G. R., 1994. Root zone effects on tracer migration in arid zones, *Soil Sci. Soc. Am. J.*, v. 58, p. 26–31.
- US Geological Survey-NWIS(National Water Information System) database:
<http://water.usgs.gov/nv/nwis/qw>.
- U.S. Geological Surface Water Data for Nevada, URL:
<http://waterdata.usgs.gov/nv/nwis/sw>
- Usunoff, E.J., and Guzman, A.G., 1989. Multivariate analysis in hydrochemistry: An example of the use of factor and correspondence analyses: *Ground water*, v. 27, p. 27-34.
- Walker, F.P., Schreiber, M.E., and Rimstidt, J.D., 2006. Kinetics of arsenopyrite oxidative dissolution by oxygen: *Geochimica et Cosmochimica Acta*, v. 70, p. 1668-1676.
- Wallace, A., Ludington, S., Mihalasky, M.J., Peters, S.G., Theodore, T.G., Ponce, D.A., John, D.A., and Berger, B.R., 2004. Assessment of Metallic Resources in the Humboldt River Basin, Northern Nevada with a section on platinum-group-element (PGE) potential of the Humboldt Mafic Complex by Zientek, Michael L., Sidder, Gary B., and Zierenberg, Robert A., *U.S. Geological Survey Bulletin* 2218, p. 312.
- Wallace, A.R., Perkins, M.E., Fleck, R.J., 2008. Late Cenozoic paleogeographic evolution of northeastern Nevada: Evidence from the sedimentary basins. *Geosphere* 4 (1): 36-74.
- Wang, S.-W., Liu, C.-W., and Jang, C.-S., 2007. Factors responsible for high arsenic concentrations in two ground water catchments in Taiwan: *Applied Geochemistry*, v. 22, p. 460-476.
- Webster, J.G., Nordstrom, D.K., and Smith, K.S., 1994. Transport and natural attenuation of Cu, Zn, As, and Fe in the acid mine drainage of Leviathan and Bryant Creeks, *in* Alpers, C.N., and Blowes, D.W., eds., *Environmental Geochemistry of Sulfide Oxidation*, Volume Series 550, Am. Chem. Soc. Symp., p. 244–260.
- Welch, A.H., Lico, M.S., and Hughes, J.L., 1988. Arsenic in Ground Water of the Western United States: *Ground Water*, v. 26, p. 333-347.
- Welch, A.H., and Lico, M.S., 1998. Factors controlling As and U in shallow ground water, southern Carson Desert, Nevada: *Applied Geochemistry*, v. 13, p. 521-539.

- Welch, A.H., Westjohn, D.B., Helsel, D.R., and Wanty, R.B., 2000. Arsenic in Ground Water of the United States: Occurrence and Geochemistry: Ground Water, v. 38, p. 589-604.
- WHAT (Web Based Hydrograph Analysis Tool), 2004. Purdue University, URL: <http://pasture.ecn.purdue.edu/~what/>.
- WHO, 2001. Arsenic and arsenic compounds. Environmental health criteria. World Health Organization Geneva, pp 224.
- Wolery, T.W., and Jarek, R.L., 2003. Software user's manual. EQ3/6, Version 8.0. Sandia National Laboratories U.S. Dept. of Energy Report.
- Yager, D., B., and Folger, H., W., 2003. Map Showing Arsenic Concentrations from Stream Sediments and Soils Throughout the Humboldt River Basin and Surrounding Areas, Northern Nevada: Denver, CO, USGS Department of the Interior, US Geological Survey.
- Yager, D.B., and Folger, H.W., 2005, A data viewer for stream-sediment and surface-water chemistry, geology, and geography of the Humboldt River Basin, northern Nevada, *in* Stillings, L.L., ed., Geo-environmental investigations of the Humboldt River Basin, northern Nevada: Carson City, U.S. Geological Survey Bulletin 2210-F, p. 9.
- Zheng, Y., Stute, M., van Geen, A., Gavrieli, I., Dhar, R., Simpson, H.J., Schlosser, P., and Ahmed, K.M., 2004. Redox control of arsenic mobilization in Bangladesh groundwater: Applied Geochemistry, Arsenic in Groundwater of Sedimentary Aquifers, v. 19, p. 201-214.